

**Development of Artificial Intelligence-based models for predicting  
soil hydraulic and cracking properties**

Thesis submitted for the award of the degree of

**Doctor of Philosophy**

by

**Insha Wani**



विद्याघनं सर्वधन प्रधानम्

भारतीय प्रौद्योगिकी  
संस्थान जम्मू  
**INDIAN INSTITUTE OF  
TECHNOLOGY JAMMU**

**Department of Civil Engineering**

**Indian Institute of Technology Jammu**

**Jammu-181221**

**June 2022**

## Declaration

---

I hereby declare that the matter embodied in this thesis entitled “**Development of Artificial Intelligence-based models for predicting soil hydraulic and cracking properties**” is the result of investigations carried out by me in the Department of Civil Engineering, Indian Institute of Technology, Jammu, India, under the supervision of Dr. Vinod Kushvaha (IIT Jammu) and Dr. Ankit Garg (Shantou University, China). The thesis has not been submitted elsewhere for the award of any degree or diploma, membership, etc. In keeping with the general practice in reporting the scientific observations, due acknowledgements have been made whenever the work described is based on the findings of other investigators. Any omission that might have occurred due to oversight or error in judgement is regretted. A complete bibliography of the books and journals referred to in this thesis is given at the end of the thesis.

June 2022

Insha Wani

Indian Institute of Technology Jammu

2018RCE0032

*I dedicate my thesis to my parents and my sister  
for their immense love, support, wisdom and  
encouragement to pursue my dreams*

## Abstract

---

Physio-chemical properties of biochar make it a promising material in agriculture, environment and climatic mitigation. However, biochar usage in geoen지니어ing is still in its early stages due to limited research and contradictions in the literature on the influence of biochar on soil properties like hydraulic conductivity and mechanical strength. Research is being carried out to find means and techniques for utilizing biochar as an amendment in the geotechnical engineering infrastructure such as landfills, slope reconstruction, and green covers. Conservation of soil is important because its formation takes hundreds of years, while erosion (landslides, rain, floods, wind) and cracking can cause its destruction in much lesser time. Erosion and cracking of soil are related to the water holding capacity of soil directly or indirectly. The water holding capacity of the biochar is very high due to its porous nature (along with its other properties that add cohesion between the biochar and soil particles). As such, when biochar is added to the soil, the porosity of the biochar soil composite is increased. The unsaturated water retention capacity of biochar and its other cementing properties make it a suitable amendment for soil conservation. Previous studies do not provide a clear understanding of how biochar will impact the water retention capacity of soils with varying grain size distribution. Further, different types of biochar (produced from animal and plant waste) could impact physiochemical properties and the cracking of soil. Such studies will help narrow down the selection of appropriate biochar and its amount to maximise water content and minimise soil cracking.

The objective of the thesis is to explore the influence of biochar in amending the behaviour of soil properties with respect to the water retention capacity, erosion and cracking. The study has been divided into three sub-objectives (1) biochar effect on the water retention capacity of soils with varying grain size distributions, (2) erosion prediction as a function of biochar content, degree of compaction, slope gradient, slope length, and rainfall intensity and (3) Effect of the various soil properties and biochar content on the crack intensity of biochar-amended soil. It was observed that (a) Any increase in the water retention of soil biochar composite depends on the grain size distribution of the soil biochar composite. There is a threshold clay content (6–8%) beyond which any effect of biochar seems less significant. In soils with higher sand content, the influence of biochar in increasing NWC seems more pronounced on the dry side than on the wet side of SWCC, even though a relatively higher amount of biochar (10%) was required to observe changes in the drier side of SWCC, (b) an increase in biochar amendment helped decrease the total erosion rate and water flow rate, and (c) the addition of optimum biochar percentage helped control cracking.

The dissertation's contribution is that the models developed are a way forward for the preliminary design analysis for soil-biochar composite behaviour without conducting laborious, costly and time-consuming experimentation. These models can be used for preliminary designing of the recompacted slopes, landfills, embankments, green rooftops and other related structures in geoen지니어ing. The models developed are very flexible and can be extended to different types of soil, biochar amendment, particle size distribution, slope and rainfall conditions.

## Synopsis

---

Biochar is a black carbon product produced from organic materials by pyrolysis. It is a stable substrate. Biochar increases the pH of the soil, nutrient retention, cation exchange capacity (CEC) and an increase in soil C sequestration. Biochar has other benefits that include improving soil fertility, encouraging seed germination, enhancing vegetative growth of plants, increasing soil resistance to diseases, adsorption of toxic pollutants, improving the water holding capacity (WHC) of the land etc. Besides, biochar can also be used as energy fuel and C sink. Biochar has a high surface area, anion and cation exchange capacity, porosity, and aromatic structure. It acts as a soil conditioner by improving physicochemical and biological properties. Soil's bulk density is more than biochar, so treatment of soil with biochar decreases the bulk density of soil biochar composite, thus increasing porosity. Biochar binds nutrients and cations and improves particle size distribution and soil texture.

Observations have been made that exposure of biochar amended soils (BAS) to freezing and thawing cycles cause changes in soil hydraulic conductivity ( $k$ ), soil water retention and physical degradation of biochar. Treatment of soil with biochar reduces nitrogen loss due to leaching and  $N_2O$  emissions, both with and without plants. Spherically shaped micrometre-sized biochar particles are produced in hydrothermal carbonization with numerous polar oxygenated functionalities from original carbohydrates, making the material more hydrophobic and highly dispersible in water. Together with sequestering C, these soil amending qualities have contributed to a surge in biochar interest. The importance of the biochar, its properties, and its uses can be understood because before 2000, a Google Scholar search of "biochar" returned 595 papers. Between 2000 and 2010, 4,340 papers, and within the past six years, 15,400 papers were published, an almost 2,500% increase from pre-2000 levels. After 2011, there were around 19187 papers published according to the web of science.

From the available literature about the biochar-soil composite, it is understood that the key factors which determine the quality and quantity of biochar depend upon pyrolysis temperature and type of feedstock. Increasing pyrolysis temperature decreases grain size and increases surface area, adsorption capacity, and pH, affecting the oxygen-to-carbon (O/C) and hydrogen-to-carbon (H/C) ratios. The literature suggests that the O/C and H/C ratios influence the stability and hydrophilic nature of the biochar, respectively and help understand the design life of particular biochar and applications. The knowledge of the biochar properties like surface area, O/C and H/C ratio, pH, and production parameters, including yield temperature, is important for its field utilization as any change in physicochemical properties determines its effect in agriculture and engineering applications.

Many researchers pointed out contradictory observations about some basic properties of biochar. Contradictions have been observed in various biochar properties, including biochar's effect on WHC, erosion control, strength, alkalinity, vegetation, water-stable aggregates, and cracking. The factors affecting the landfill slope stability, including compressibility, shear strength, and tensile strength, have not been investigated clearly.

Studies are being carried out to study the benefits of biochar in various areas, including environmental management, agronomy, and geoen지니어ing. The researchers are using modern ways and techniques to analyze the behaviour of different materials, including biochar. Artificial Neural Network (ANN) has been a widely accepted scientific technique for developing models and analyzing soil behaviour. Researchers have determined SWCC using ANN. The study aims at the use of machine learning techniques ANN and Multiple Regression Analysis (MRA) in determining the hydraulic properties of biochar amended soils as mentioned below;

- I. Biochar effect on the water retention capacity of soils with varying grain size distributions,
- II. Prediction of erosion as a function of biochar content, degree of compaction, slope gradient, slope length, and rainfall intensity and
- III. Effect of the various soil properties and biochar content on the crack intensity of biochar-amended soil.

- I. Biochar effect on the water retention capacity of soils with varying grain size distributions,

- *Experimental Methodology:* The experimental data of water content and soil suction required for the determination of the SWCC curve was obtained from the literature to determine the hydraulic properties of biochar amended soils consisting of sand, clay, and silt content: 58% – 98%, 0% – 20% and 2% – 37%, respectively. The biomass used for biochar production was water hyacinth, peanut shell and dairy manure. The biomass had a lignocellulosic nature with 46% cellulose content and 21% hemicellulose. The procedure for biochar production was adopted from the literature. The biomass was cut into pieces of 30–50 mm. The temperature of the pyrolysis process was maintained at 300°C – 500°C for 45 min as per the optimum conditions for water hyacinth species. The biochar was cut using an automatic crusher and sieved through a 2-mm sieve. After achieving the desired torrefaction temperature required for biochar production, the sample was removed and subjected to further analysis. The procedure for establishing SWCC varied among the above studies.
- *ANN Methodology:* Technical analysis was done using ANN for different sets of experimental data from the literature to determine the hydraulic properties of biochar amended soils. For SWCC analysis, the commercially available STATISTICA, version 12 software, was used. The ANN model was developed using seven parameters soil suction, biochar content, sand content, silt content, clay content, fine content (silt and clay), and the ratio of fine to sand content as input for the prediction of Normalized Water Content (NWC). Seven hundred ninety-four data points from 23 soil samples were divided as 80% for training and the balance 20% as test data. The mean percentage deviation of 13.76% and the coefficient of determination of 0.7109 were obtained.

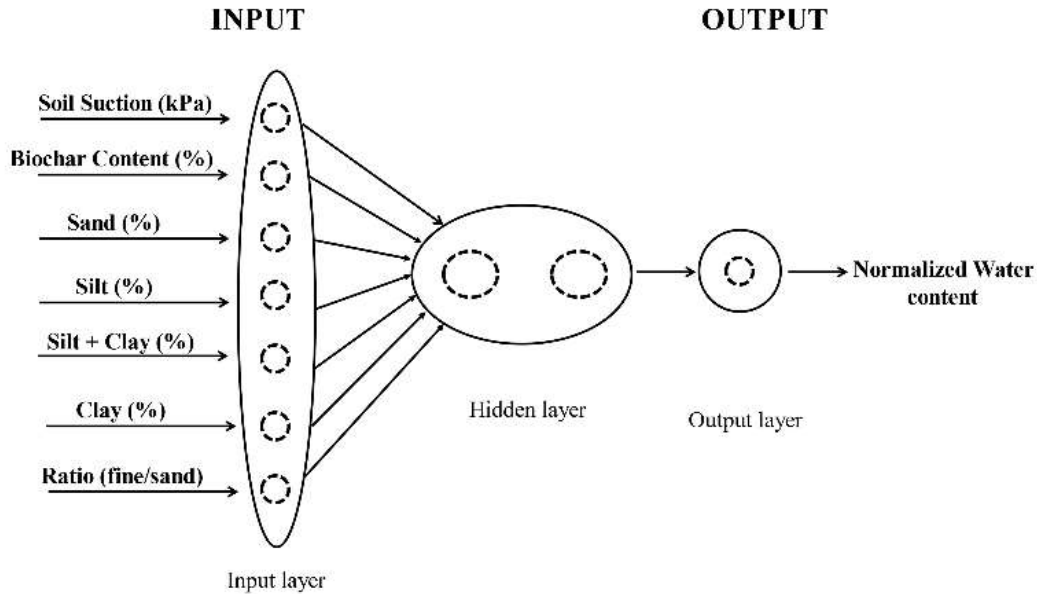


**Figure 1** ANN architecture used for the prediction of Normalized Water Content

- *Results:* For biochar content of 3% with increasing clay content up to 4%, the NWC reduced from 0.9 (wet side) to around 0.6 (dry side). In the case of 6% clay content, the NWC reduced from 0.9 to around 0.32. For clay content beyond 6%, the NWC reduced from around 0.65 to around 0.25. This may be because the fine biochar particles arrange themselves with clay particles to be in a compact position. They create a dense medium and increase the capillarity action at the initial stages. However, when the quantity of fines increases, the pores get clogged, resulting in decreased water retention. For sandy soils, it was observed that the NWC reduced from around 0.6 to around 0.25. The fines percentage addition works well up to 10% biochar amendment in sandy soils (from 0.95 – around 0.6), beyond which it again clogs the pores and decreases water retention. In both cases, the low water retention creates more runoff and can cause erosion, landslides, embankment failures, etc.
- *Observations:* The ANN-based model was found to predict SWCC reasonably well. Based on predictions, it was found that there is a threshold clay content of 6–8%, beyond which any effect of biochar becomes less significant. For soils with higher sand content, there was an increase in normalized water content of SWCC with the presence of biochar, even though a relatively higher amount of biochar is required to cause changes in the drier side of SWCC for sandy soils.

**II.** Prediction of erosion as a function of biochar content, degree of compaction, slope gradient, slope length, and rainfall intensity

- *Experimental Methodology:* Data was also obtained from an in-house flume setup developed containing a 1.50-meter-high rainfall simulator designed to simulate rainfall of 60 mm/hour and 90 mm/hour for measuring hydraulic properties, infiltration and relative erosion. The width of the flume was 0.6 meters, and the length was 2 meters, respectively, as shown in Figure 2.

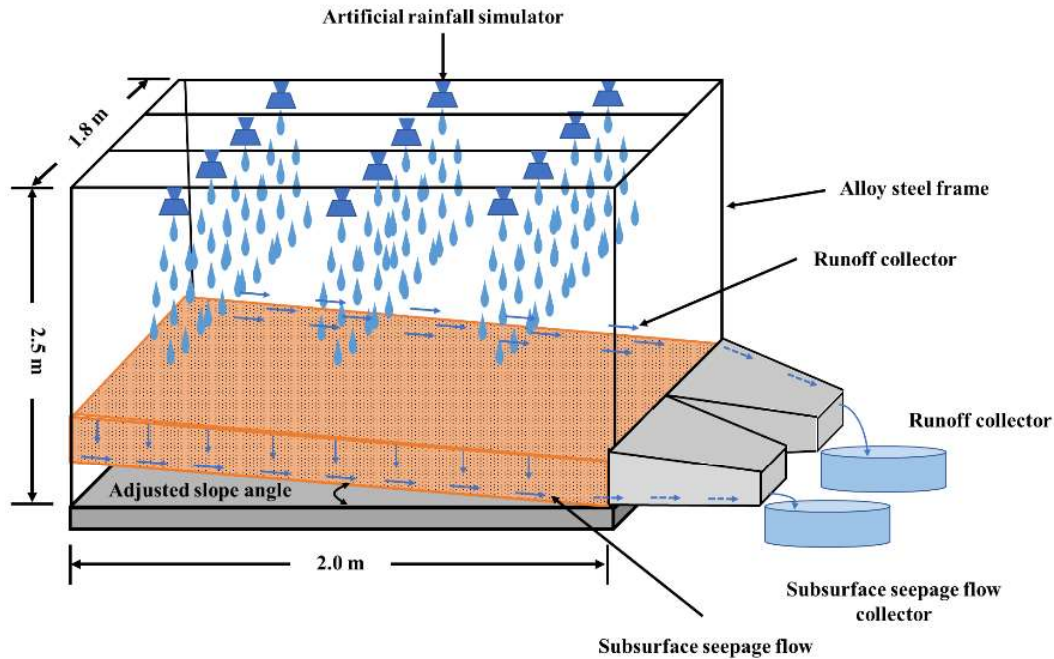


**Figure 2** Flume test

A distilled water-filled tank was installed, and the calibration was done using hydraulic pressure and a pluviograph for recordings at a rate of 0.1 MPa for 60 mm/hour and 0.15 MPa for 90 mm/hour. An alloy steel frame was added to the setup and measured rainfall-induced runoff and subsurface seepage flux—a drainage layer containing geotextile fibre (minimizing soil particle flow). A 6 cm thick gravel layer was placed below the soil layers (Colluvial soil). Biochar was produced from water hyacinth collected from the coastal region of Shantou, China.

- *ANN Methodology:* The other soil property affected by the hydraulic property is erosion. STATISTICA version 12 was used for model development to predict the total erosion rate and total flow rate from the factors slope length and gradient, compaction degree, rainfall rate and biochar percentage. STATISTICA version 12 was used for model development to predict the total erosion rate and total flow rate from the factors slope length and gradient, compaction degree, rainfall rate and biochar percentage.

The model predicted that the slope length influenced the total erosion rate while as total flow rate was influenced by a 5% biochar amendment. The  $R^2$  value for ANN models developed was 0.788 for total erosion rate and 0.939 for total water flow rate, respectively. The error percentage for the total erosion rate was 15%, and total water flow rates were 7%, respectively. ANN model developed for erosion was found to be consistent with the experimental and literature data. The development of such models can help in the preliminary designing of green cover by using the required biochar content under various slope and rainfall conditions.

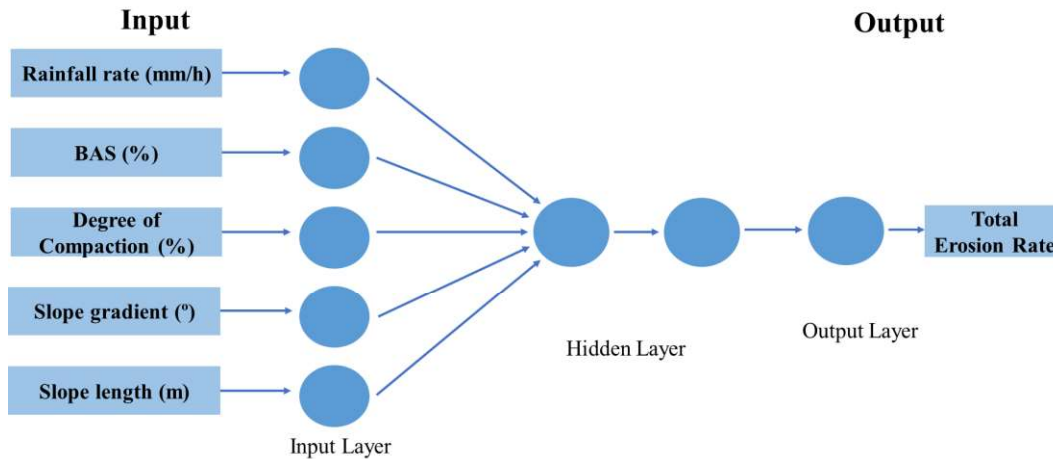


**Figure 3** ANN design model used to predict Total Erosion Rate

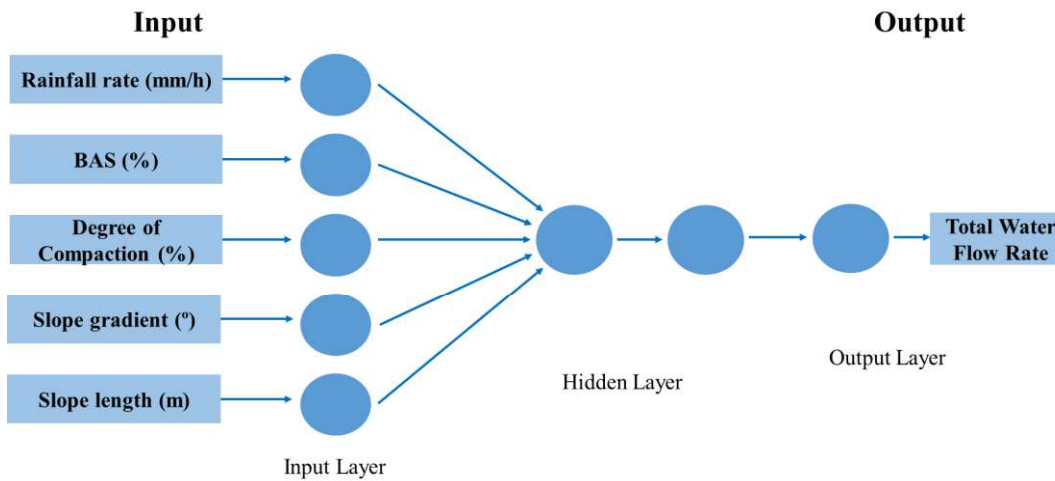


**Figure 4** ANN architecture used for prediction of Total Water Flow Rate

➤ *Results:* Observation was made that the total erosion rate and total water flow rate increased with an increase in compaction. Compaction causes changes in the soil properties like porosity and permeability. Pores become clogged, and water movement is impeded, reducing water availability. However, under prolonged rainfall, there may be an enhancement in water-logging due to decreased permeability which may cause erosion of fine soil and biochar particles present in the upper layers of compacted soil.

The total erosion and water flow rate increase with rainfall intensity. The impact and speed with which the rainfall hits the soil particles detaches it from the soil layers and causes erosion. It was observed that there was a decrease in both the parameters with the slope length. This may be because runoff gets sufficient area and time for infiltration. Biochar addition causes discontinuity and surface roughness and can resist further movement of particles.

It was observed that the erosion rate increased gradually with increasing slope gradient from 7° to 20°. The increase was more significant from slope gradients of 7° to 12°. The water flow rate (i.e., runoff) is enhanced mainly due to the gravity effect.

The observation was that the erosion rate reduces with an increase in amendment ratio from 0 to 10%. The reduction in erosion rate was observed to be minimum between biochar amendments of 0% to 5%. This implies that the biochar effect on erosion is not significant during the lower biochar amendments. The total water flow rate is first enhanced with increased biochar content from 0% to 5% and then decreases beyond it. With increasing biochar content to 10%, the subsurface flow of biochar on erosion rate seems to be more dominant at 10% biochar content. However, higher percentages may increase the alkalinity of the soils.

Slope length was the most influential parameter in determining erosion rate, followed by slope gradient, degree of compaction, biochar amendments percentages, and rainfall rate. Biochar amendment percentage seemed important in determining the total water flow rate, slope gradient, rainfall rate, slope length, and degree of compaction.

- *Observations:* 10% biochar amendment ratio seems more effective in controlling erosion and runoff than lower amendment ratios. Slope length seems to have a more pronounced effect in controlling total erosion rate, followed by the degree of compaction, biochar percentage and rainfall rate. Biochar content seems to be the most influential parameter for total water flow rate, followed by slope gradient and rainfall intensity.

### III. Effect of the various soil properties and biochar content on the crack intensity of biochar-amended soil.

- *Experimental Methodology:* For determining resistance and behaviour of BAS against cracking, animal and plant feedstock-based biochar were produced in-house from pig manure (PM) and wood (W), respectively. They were separately added to soil at 0%, 5%, 10% and 15% with clayey sandy soil under the degree of compaction (DoC) (65% and 80% of MDD). The BAS was then compacted in the Petri dishes. The moulds used for BAS consisted of glass dishes of 10.3 cm diameter and 1.7 cm height in which the soil was subjected to alternate 12 and 15 days of four dryings and three wetting cycles, every 24 hours for 70 days. A high-resolution 8-bit depth camera was used to take images, and analysis was done using open code Image J to obtain crack intensity factor (CIF).
- *MRA Methodology:* The cracking of soils is also dependent on the hydraulic properties of soil. MRA was used to determine crack intensity factor (CIF) from parameters of soil compaction, plastic limit, specific gravity and the biochar content. When the value of  $p$  in the regression analysis for independent variables shall be less than 0.05, the parameters are sufficient to reject the null hypothesis, and the model is considered satisfactory. Otherwise (if the  $p$ -value is more than 0.05), the null hypothesis has a risk factor of more than 5%, and the model needs re-consideration. When the MRA was run for CIF determination using the parameters DoC, Plastic limit, liquid limit, specific gravity and biochar content, the  $R^2$  value

was 0.925. The liquid and plastic limits had  $p$ -values of 0.949 and 0.079, respectively and were not considered. MRA was re-run with three parameters, biochar content, degree of compaction and plastic limit. The new  $p$ -values and  $R^2$  were satisfactory. As such, the model was considered satisfactory. From the model, it was observed that biochar content has the strongest  $p$ -value and, as such, was the most influential parameter.

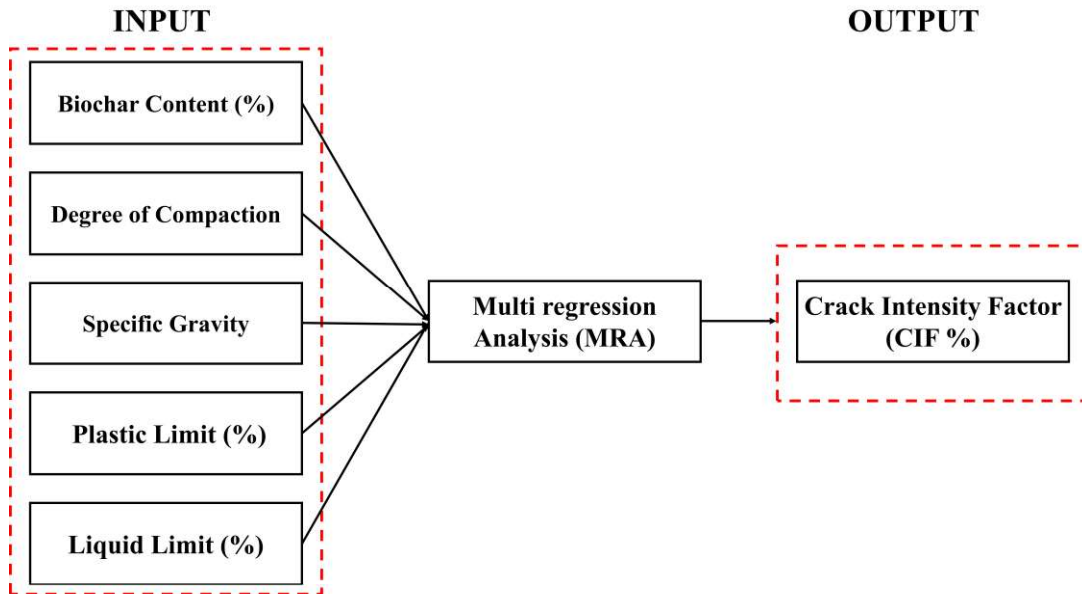


**Figure 5** Framework of MRA approach showing input and predicted parameters

- *Results:* A comparison was made between the measured and predicted CIF with varying biochar content in the BAS at 65% and 80% compaction states of the samples. When the soils were treated with two types of biochar, the intensity of cracks decreased. A drastic reduction was observed in the CIF with increased biochar content, probably due to high intrapores of biochar. Any increase in plastic limit and compaction state decreased the crack intensity factor. Biochar content was the most significant, followed by plastic limit and DoC, with Liquid Limit and specific gravity having the least influence.
  - *Observations:* From the MRA model, it was observed that the biochar content, plastic limit, and DoC influence soil cracking. Wood biochar was more effective in controlling cracking intensity than pig manure biochar, probably due to wood-produced biochar's highly porous nature.
- 
- The ANN models developed show that
    - The efficiency of biochar amendment in water retention in soils seems dependent on grain size distribution.
    - 10% biochar amendment was observed as the most influential in controlling total erosion and water flow rates.
  - The MRA model developed shows that
    - 15% biochar amendment seems optimum for controlling the CIF.

- The models developed can be used for recompacted slopes, landfills, embankments, etc. It can provide a way forward for the preliminary design analysis and soil behaviour on biochar application and save experimental time and money. The models developed can be extended to any type of soil, biochar amendment, slope and rainfall conditions.

## Acknowledgements

---

Praise to the Almighty for his blessings throughout my work to complete my research successfully.

I want to express my gratitude and appreciation to my research supervisor *Dr. Vinod Kushvaha*, Department of Civil Engineering, Indian Institute of Technology (IIT) Jammu. His guidance, support and constant encouragement have been invaluable throughout the research period and have made this journey an inspirational experience for me. His understanding of the research area has helped me significantly improve the dissertation and its contents. I am grateful for his comments, suggestions and constructive criticism throughout the research. The dissertation greatly benefitted from his recommendations and insights.

I want to thank my joint supervisor *Dr. Ankit Garg*, Shantou University, China, for his guidance, painstaking efforts, valuable suggestions, support and encouragement throughout the research. I will be indebted to his constant assistance provided during this period. His vast knowledge of the subject and experience made this research possible and more interesting. I am grateful to him for his instructions, comments, recommendations, suggestions, and insights that proved valuable in improving my knowledge of the work and the dissertation.

It has been an honour to have *Dr. Vinod Kushvaha* and *Dr. Ankit Garg* as my PhD supervisors. I will always be indebted to them for being a saviour whenever any problem has surrounded me.

I want to thank the Department of Civil Engineering faculty members, IIT Jammu, for their support and encouragement. I would also like to express my gratitude to the members of the Student Research Committee, *Dr. Nitin Joshi*, *Dr. Rahul R Salunkhe* and *Dr. Sreedeeep Sekharan*, for their valuable suggestions during work.

I am grateful for the good support system I had to survive and stay sane in grad school. My sincere thanks to *Aanchna* whose constant input and support have been valuable and encouraging for the last seven years. I am also grateful to *Sristi*, *Bhargav* and *Randeep Bali* for their support during my PhD journey. I am also grateful to *Khogesh*, *Abhishek*, *Abdul Haseeb* and *Insha* for the wonderful friends they have been through my PhD and for supporting me in my worst times. I had a delightful time here at IIT Jammu with my PhD batchmates, *Ambreen*, *Suhaib*, *Mehran*, *Ayoub*, *Burhan*, *Hardeep*, *Gaurav*, *Deebha*, *Kamal*, *Murtaza*, *Saima*, and *Farah*.

Lastly, I want to express my deepest gratitude to my family members for the unconditional love, care, sacrifice and blessings throughout my studies. I am blessed with parents, *Fayaz Ahmad Wani* and *Javeda Parveen* and my sister *Nida Wani* who have shown immense confidence and have stood with me through thick and thin. I also want to thank my fiancé, *Asif Iqbal*, for being the most patient and supporting me while pursuing my PhD. I thank them for their understanding, never-ending encouragement, and always being there for me.

# Table of Contents

---

ABSTRACT.....	IV
SYNOPSIS.....	V
LIST OF FIGURES.....	XVI
LIST OF TABLES.....	XVIII
LIST OF ABBREVIATIONS.....	XIX
LIST OF ELEMENTS AND COMPOUNDS.....	XXII
LIST OF SYMBOLS.....	XXIII
<b>CHAPTER 1: INTRODUCTION .....</b>	<b>1</b>
1.1 BACKGROUND.....	1
1.2 OBJECTIVE .....	6
1.3 ORGANIZATION OF THESIS .....	6
<b>CHAPTER 2: LITERATURE REVIEW .....</b>	<b>8</b>
2.1 GENERAL .....	8
2.1.1 <i>Biochar, char and charcoal</i> .....	9
2.1.2 <i>Feedstock</i> .....	10
2.1.3 <i>Major biomass constituents</i> .....	11
2.1.4 <i>Production</i> .....	16
2.1.5 <i>Properties</i> .....	21
2.2 INFLUENCE OF BIOCHAR ON THE WATER HOLDING CAPACITY (WHC) OF VARIOUS SOILS .....	31
2.3 INFLUENCE OF BIOCHAR ON EROSION CONTROL .....	39
2.3.1 <i>Physical Properties of Biochar and Erosion control</i> .....	40
2.3.2 <i>The influence of chemical properties of biochar on erosion</i> .....	66
2.4 INFLUENCE OF BIOCHAR ON CRACKING INTENSITY OF SOILS .....	70
2.5 LIMITATIONS.....	71
2.6 MOTIVATION.....	72
<b>CHAPTER 3: METHODOLOGY .....</b>	<b>73</b>
3.1 BACKGROUND.....	73
<b>CHAPTER 4: EXPLORING THE EFFICIENCY OF BIOCHAR IN ENHANCING WATER RETENTION IN SOILS WITH VARYING GRAIN SIZE DISTRIBUTIONS USING THE ANN TECHNIQUE .....</b>	<b>77</b>
4.1 BACKGROUND.....	77
4.2 INTRODUCTION .....	78

4.3	MATERIALS AND METHODOLOGY .....	79
4.3	RESULTS AND DISCUSSIONS .....	85
4.4	OBSERVATION .....	92
<b>CHAPTER 5: APPLICATION OF ARTIFICIAL INTELLIGENCE FOR PREDICTING EROSION OF BIOCHAR AMENDED SOILS.....</b>		<b>94</b>
5.1	BACKGROUND.....	94
5.2	INTRODUCTION .....	95
5.3	MATERIALS AND METHODOLOGY .....	96
5.4	RESULTS AND DISCUSSIONS .....	104
5.5	OBSERVATION .....	113
<b>CHAPTER 6: MULTIPLE REGRESSION MODEL FOR PREDICTING CRACKS IN SOIL AMENDED WITH PIG MANURE BIOCHAR AND WOOD BIOCHAR .....</b>		<b>115</b>
6.1	BACKGROUND.....	115
6.2	INTRODUCTION .....	115
6.3	MATERIALS AND METHODOLOGY .....	117
6.4	RESULTS AND DISCUSSION.....	121
6.5	OBSERVATIONS .....	130
<b>CHAPTER 7: CONCLUSION .....</b>		<b>132</b>
<b>CHAPTER 8: FUTURE SCOPE.....</b>		<b>134</b>
<b>REFERENCES.....</b>		<b>ERROR! BOOKMARK NOT DEFINED.</b>
<b>LIST OF PUBLICATIONS.....</b>		<b>178</b>

## List of Figures

---

<b>Figure 1</b> ANN architecture used for the prediction of Normalized Water Content	vii
<b>Figure 2</b> Flume test	viii
<b>Figure 3</b> ANN design model used to predict Total Erosion Rate	ix
<b>Figure 4</b> ANN architecture used for prediction of Total Water Flow Rate	ix
<b>Figure 5</b> Framework of MRA approach showing input and predicted parameters	xi
<b>Figure 6</b> Use of biochar in various fields	9
<b>Figure 7</b> Molecular structure of the biochar produced at different pyrolysis temperatures [107]	12
<b>Figure 8</b> Cellulose pyrolysis: Biochar formation mechanism [107]	13
<b>Figure 9</b> Biochar preparation mechanism by decomposition of hemicellulose [107]	14
<b>Figure 10</b> Biochar preparation mechanism by decomposition of lignin [20]	15
<b>Figure 11</b> Biochar surface acidic functional groups [53]	26
<b>Figure 12</b> Biochar surface basic functional groups [53]	26
<b>Figure 13</b> Pyrolysis temperature effect on biochar: (a) amorphous carbon; (b) turbostratic carbon; (c) graphite carbon [53]	27
<b>Figure 14</b> Typical SWCC showing distinct zones of desaturation [283]	31
<b>Figure 15</b> Physicochemical properties of soil	39
<b>Figure 16</b> Factors affecting erosion [312]	40
<b>Figure 17</b> Decomposition of biomass constituents	67
<b>Figure 18</b> ANN Architecture	73
<b>Figure 19</b> Weight and bias	74
<b>Figure 20</b> Conversion of water hyacinth feedstock to biochar [93]	80
<b>Figure 21</b> Experimental setup for measurement of gas permeability [93]	81
<b>Figure 22</b> Setup for conducting tests on soil columns [90]	82
<b>Figure 23</b> Flowchart for ANN modelling	84
<b>Figure 24</b> ANN architecture used for the prediction of normalized water content	85
<b>Figure 25</b> Variation between predicted normalized water content and measured normalized water content ( $R^2$ )	86
<b>Figure 26</b> Comparison of measured and predicted SWCCs corresponding to biochar content of (a) 0%, (b) 5% and (c) 10%	87
<b>Figure 27</b> The soil suction and NWC with varying silt and clay for biochar amendment of 3% and 10%	89
<b>Figure 28</b> Variation of NWC and soil suction at different biochar contents for soil with higher sand content	91
<b>Figure 29</b> Relative significance of parameters affecting SWCC	92
<b>Figure 30</b> Illustrative sketch of flume experiment [481]	98
<b>Figure 31</b> ANN design model used for prediction of (a) Total Flow (b) Flow Rate [481]	100

<b>Figure 32</b> Flowchart for ANN modelling [481]	101
<b>Figure 33</b> Comparison between Experimental and Predicted (a) Total Erosion Rate and (b) Total Water Flow [481]	103
<b>Figure 34</b> Variation of experimental with ANN predicted values for (a) Total Erosion Rate and (b) Total Water Flow Rate [481]	104
<b>Figure 35</b> Graph showing the effect of change in DoC on total erosion and total water flow rate [481]	105
<b>Figure 36</b> Variation of Total Erosion Rate and Total Water Flow Rate with the Rainfall Rate [481]	107
<b>Figure 37</b> Variation of Total Erosion Rate and Total Water Flow Rate with the Slope Length [481]	108
<b>Figure 38</b> Variation of Erosion Total Rate and Total Water Flow Rate with the Slope Gradient [481]	109
<b>Figure 39</b> Variation of Erosion Rate and Total Water Flow Rate with the Biochar Amendment Ratio [481]	111
<b>Figure 40</b> Relative Significance of Various Parameters on (a) Total Erosion Rate, (b) Total Water Flow Rate [481]	112
<b>Figure 41</b> Experimental procedure for determining crack intensity factor (CIF) for biochar amended samples (BAS) [35, 406]	118
<b>Figure 42</b> Graphical representation of linear regression model	120
<b>Figure 43</b> Framework of MRA approach showing input and predicted parameters [35]	121
<b>Figure 44</b> Plot between measured CIF and predicted CIF to demonstrate the performance of the MRA model, including all influencing parameters [35]	122
<b>Figure 45</b> Plot between measured CIF and predicted CIF to demonstrate the performance of the MRA model, including only statistically significant parameters [35]	123
<b>Figure 46</b> Comparison between predicted and measured CIF with different biochar content [35]	125
<b>Figure 47</b> Comparison between measured and predicted CIF for different plastic limits [35]	126
<b>Figure 48</b> Measured and predicted CIF % using proposed MRA model at 65% and 80% DoC for (a) 5%; (b) 10% and (c) 15% biochar amendment [35]	128
<b>Figure 49</b> Framework for MRA approach with input and predicted parameters [35]	130

## List of tables

---

<b>Table 1</b> Difference between Char, Charcoal and Biochar	10
<b>Table 2</b> Different types of thermochemical processes	20
<b>Table 3</b> Preparation of biochar using various biomass and its testing on different soil properties	35
<b>Table 4</b> Literature indication effect of biochar on erosion taking into consideration soil fines	45
<b>Table 5</b> Literature indicating the effect of biochar and soil fines on soil loss and total runoff volumes	60
<b>Table 6</b> Previous studies indicating soil fines, biochar content, water content, critical shear stress and erodibility coefficient	62
<b>Table 7</b> calculated $p$ -values for all influencing parameters	121
<b>Table 8</b> Calculated $p$ values for significant parameters	123

## List of Abbreviations

---

AEV	Air Entry value
ANN	Artificial Neural Network
ASTM	American Society for Testing and Materials
AWC	Available Water Content
BAS	Biochar amended Soils
BC	Biochar
CBR	California Bearing ratio
CEC	Cation Exchange Capacity
CIF	Crack Intensity Factor
DoC	Degree of Compaction
EBC	European Biochar Certificate
FEM	Finite Element Analysis
FTIR	Fourier transform infrared spectroscopy
GWC	Gravimetric Water Content
IBI	International Biochar Initiative
KNN	<i>k</i> -nearest neighbor
LL	Liquid Limit
MAP	Microwave Assisted Pyrolysis
MDD	Maximum Dry Density
WB	Wood Biochar
PMB	Pig manure Biochar

MAPD	Mean Absolute Percentage Deviation
MLRA	Multiple Linear Regression Analysis
MRA	Multiple Regression Analysis
MRM	Multiple Regression Model
NMHC	Non-Methane Hydrocarbon Compounds
NWC	Normalized Water Content
OMC	Optimum Moisture Content
PAH	Polycyclic Aromatic Hydrocarbons
PAW	Plant Available Water
PAM	Polyacrylamide
PWP	Permanent Wilting Point
pH	potential of hydrogen
PL	Plastic Limit
R <sup>2</sup>	Coefficient of determination
RCC	Reinforced Cement concrete
RGB	Red Green Blue
SBC	Soil Biochar Composite
SEM	Scanning electron microscopy
SG	Specific Gravity
SOC	Soil Organic Content
SOM	Soil Organic Mater
SWCC	Soil Water Characteristic Curve
SWR	Soil Water Retention
SWRC	Soil–water characteristic curve

TP	Terra Preta
USEPA	United States Environmental Protection Agency
VWC	Volumetric water content
WHC	Water holding capacity
WHB	Water hyacinth biochar
WRC	Water retention capacity
k	Hydraulic conductivity
$k_g$	Gas permeability
$k_{sat}$	Saturated hydraulic conductivity

## List of Elements and Compounds

---

C	Carbon
Ca	Calcium
Cu	Copper
Fe	Iron
H	Hydrogen
K	Potassium
Mg	Magnesium
N	Nitrogen
O	Oxygen
P	Phosphorus
S	Sulphur
Si	Silicon
Zn	Zinc
C=O	Carbonyl Group
C <sub>6</sub> H <sub>5</sub> -OH	Phenol
CH <sub>4</sub>	Methane
CO	Carbon Monoxide
CO <sub>2</sub>	Carbon dioxide

## List of Symbols

---

%	Percentage
°C	Degree Celsius
cm	Centimetre
cm <sup>3</sup>	Cubic Centimetre
g	Grams
h	Hours
kg	Kilograms
kN/m <sup>3</sup>	Kilo Newton Per Cubic Metre
kPa	Kilo Pascals
$\alpha$	Significance Level
m	Meter
m <sup>2</sup>	Metre Square
min	Minute
ml	Mililitre
mm	Milimetre
MPa	Megapascal
$M_s$	Mass of Solids
$M_w$	Mass of Water
°	Degree
sec	Seconds
$u_a$	Air Pressure

$u_w$	Vapour Pressure
$V_s$	Volume of Solids
$V_v$	Volume of Voids
$V_w$	Volume of Water
$\mu m$	Micro Meter
$\pi$	Osmotic Suction
$\Psi$	Total Suction

# Chapter 1: Introduction

---

## 1.1 Background

Biochar is a black carbonaceous, fine-grained, porous, solid end product produced by thermochemical conversion of a broad spectrum of biomass under a controlled oxygen environment [1–4]. It possesses unique heterogeneous elemental composition, functional groups, textural properties, minerals, and electro-kinetic surface potentials [5–7]. The material has an appearance somewhat similar to charcoal, synthesized from various types of biomass, such as agroforestry residue, animal wastes and remains, animal manures, sewage sludge, seaweeds [8, 9], freshwater macro-algae [5, 10], and invasive plant species [3, 11–13]. As a novel renewable material, biochar is effectively used in agriculture, environmental remediation, climate mitigation, and geoengineering and has proven to be a sustainable waste disposal material.

Burning or decomposing agroforestry wastes in an open environment is not a clean way to eliminate large amounts of solid waste generated from different agricultural and forestry practices. Open burning of crop residues leads to a loss of potential nutrient resources. It also releases air pollutants, which prevent radiative-convective coupling of the Sun-Earth system, significantly contributing to Asian Brown Clouds [14, 15]. The harmful emission includes particulate matter (PM<sub>2.5</sub> and PM<sub>10</sub>) in the form of ash, polycyclic aromatic hydrocarbons (PAH), soot, and non-methane hydrocarbon compounds (NMHCs) [16, 17]. Conversion of this waste into biochar leads to a cleaner environment and advantages of a resource that can further be used for sustainable agronomic, environmental, and engineering purposes.

Various methods of thermochemical conversions, such as pyrolysis, carbonization, hydrothermal treatment, etc., are being used to synthesize biochar [3, 18, 19]. However, pyrolysis is more suitable for preparing biochar on a large scale [20], and the process mainly involves the decomposition of lignocellulosic components thermally in an oxygen-deficient environment [21]. Further, the conventional pyrolysis process can be classified as slow, fast, flash, hydrothermal, or gasification, depending on pyrolyzing temperature, residence time, and heating rate. The yield of biochar and its properties is dependent on the pyrolysis process being used and the composition of feedstock used. The feedstock undergoes a primary decomposition that produces thermally stable solid char [20, 22] and is followed by the secondary decomposition reactions, which convert the unstable, volatile compounds to form gas products [22, 23]. The feedstock type determines the composition and morphology of the biochar. The biochar produced from dense woody feedstocks is of high porosity, surface area, pH, and aromatic composition [24, 25] as compared to biochar derived from animal wastes, which have low surface areas [26] and less porosity [27]. The biochar produced from aquatic raw materials has high nutrient content and functional

groups but has less surface area and organic carbon content [28]. Lei and Zhang [29] observed that the hydraulic conductivity of wood-derived biochar was more than manure-derived biochar.

Biochar increases crop productivity, acts as an instrument for climate mitigation, remediates organic and inorganic pollutants from soil and aqueous medium, and amplifies the soil carbon sequestration [2, 30–35]. The classic example of using biochar for soil fertility and sustainability can be seen in Terra Preta (TP) of Amazon basins, where extensive organic matter deposits have been found [1]. TP is dark-coloured fertile soil interspersed with relatively infertile Amazonian ferrisols [36]. Studies on TP suggest that these soils result from intentional/unintentional anthropogenic efforts that gave rise to the accumulation of large quantities of plant and animal debris, ashes, and bone fire residues and made soil fertile and rich in pyrogenic organic matter. TP contains high concentrations of nutrients such as phosphorus (P), nitrogen (N), potassium (K), calcium (Ca), copper (Cu), and magnesium (Mg) [21] and high percentages of stable organic soil matter [1, 4]. Other examples of biochar in agriculture can be dated back to the beginning of rice cultivation in Asia, when charcoal prepared from rice husks was probably used [37]. Applying biochar to soil alters microbes' population, diversity, activity, and interactions of plants with microbes by cycling nutrients and modifying the habitat. Biochar prepared from weed species *Parthenium hysterophorus* showed an improvement in seedling vigor index of maize, soil dehydrogenase activity, catalase, basal soil respiration, and active microbial biomass carbon. However, soil microbial activity is not adversely affected [11]. Biochar prepared from water hyacinth (*Eichornia crassipes*) at different temperatures (200°C to 500°C) and residence time (30 min to 120 min) also showed increased maize seedling vigor index, alkaline phosphatase, acid phosphatase, fluorescein hydrolases, soil respiration, and active microbial biomass [12].

Biochar has a high surface area, cation and anion exchange capacity, porosity, and aromatic structure. It also has alkaline pH, varied functional groups (hydroxyl, phenolic and carboxyl), and minerals (dolomite, calcite, sylvite, periclase, quartz, and montmorillonite) [30, 38, 39]. It acts as a conditioner to the soil by improving physicochemical and biological properties [40]. The bulk density of soil is more than biochar, so treating the soil with biochar decreases the bulk density of SBC, thus increasing porosity. Biochar primarily binds nutrient cations and improves particle size distribution and soil texture [41]. Biochar has a porous structure, due to which its water holding capacity (WHC) is high. Biochar addition to soil and its effects on freezing and thawing have recently gained attention. It is observed that exposure to freezing and thawing cycles in BAS causes changes in soil hydraulic conductivity ( $k$ ) and SWR. This happens because of biochar's physical degradation by freeze-thaw cycles [42]. Treating soil with biochar reduces nitrogen loss from leaching and  $N_2O$  emissions, both with and without plants [43]. Spherically shaped micrometre-sized particles are produced in hydrothermal carbonization with numerous polar oxygenated functionalities from original carbohydrates, making the material more hydrophobic and highly dispersible in water [4, 43–47]. The physicochemical and functional properties of biochar vary as a function of feedstock and pyrolysis conditions employed during preparation. Hence, complete awareness/information on the effect of feedstock and pyrolysis conditions is essential in designing and modifying biochar for its desirable specific applications. Observations from previous literature show that biochar produced

at the pyrolyzing temperature greater than or equal to 500°C has more surface area, high aromaticity, increased pH, and more ash content, improving other soil physical properties [48–50]. Higher pyrolysis temperature results in a high pH of biochar [51–54], even though some researchers have reported otherwise. For example, studies by Nguyen et al. and Zhang et al. [55, 56] have reported the acidic nature of biochar produced at 350°C to 600°C. Biochar preparation at high temperatures has a high aromatic structure and surface area (making it more water-absorbent), resulting in higher carbon sequestration and environmental remediation [57]. However, an unprecedented increase in pyrolysis temperature resulted in the breakdown of structural and textural properties and decreased surface area [39, 41]. For example, in an investigation, Ramola et al. [39] observed that the maximum surface area was achieved at a temperature of 500°C, but it started to decrease at 700°C. Besides, Ahmad et al. [58] and Ghanim et al. [59] observed that increased pyrolytic temperature increased the C content, whereas N<sub>2</sub>, O<sub>2</sub>, and H decreased due to decarboxylation and dehydration. The O/C and H/C ratios started decreasing with an increase in the pyrolysis temperature due to the condensation of aromatic hydrocarbon structure [60]. The decrease in the O/C ratio indicates loss of polar functional groups and more carbonization, making the biochar more hydrophilic. Dehydration is caused due to removal of hydroxyl groups, and decarboxylation causes the removal of carboxyl and carbonyl groups [61, 62]. Considering novelty and unique inherent characteristics, biochar helps modify soils' physicochemical and biological properties [41, 63]. The porous nature and high surface area of biochar affect the soil's hydraulic conductivity, WHC, porosity, aggregate stability, and bulk density [64]. The decrease in bulk density of soil biochar composite (SBC) is caused due to low bulk density of biochar [63, 65]. However, the authors reported a minor decrease in the second year of the experiment, and in the third year, no decrease was observed in bulk density [65]. Some researchers observe that the biochar amendment to soil increases the formation and stability of aggregates but reduces soil strength [66–68]. The increase in the liquid limit, plastic limit, pH and moisture content of the biochar-treated soil, and decrease in the maximum dry density of ordinary soil was reported by several researchers [69–71].

A few researchers have explored the use of biochar as a construction material. Choi et al. [72] observed that the free water in concrete during mixing could be absorbed by biochar (due to high pH and WHC), which it can release during the hardening of concrete and help in curing [73]. Gupta and Kua [73] illustrated that plastering done during the Ithaka Institute restoration in Switzerland was done with 50% biochar and a balance of 50% with other cementing materials [73]. The properties of low thermal conductivity, high chemical stability, and low flammability make biochar appropriate as a construction material. The insulation provided by biochar plaster is excellent with the required indoor humidity. Few authors have considered biochar an excellent material for humidity control, as biochar is a microporous carbon [73, 74]. The porous structure of biochar acts as insulation and prevents thermal bridging; thus, it helps prevent heat/cold travel from inside to outside or vice versa of a building [73]. Biochar (specially produced at a higher temperature) is chemically stable and helps prevent concrete from chemical attacks whether used as a coating on concrete or mixed with concrete. The addition of 2% biochar to concrete samples increased seven (7) day's strength by 40% [73], whereas when 1% of cement was replaced by biochar, the flexural strength and toughness of concrete increased [73, 75]. Because biochar is less flammable, it can reduce fire in construction [73, 76]. Riera et al. [77] reported an increase of up to 20% in compressive and

tensile strength by amendment of 1–2% of biochar with cement [77, 78] also an increase in early strength and water tightness [77]. Biochar is also considered a possible cheap admixture and alternate modifier in bitumen for road construction [72, 73, 79–82]. Biochar addition of 10% by weight improves viscosity and rutting resistance of asphalt [73, 81], higher resistance to water penetration, and increased durability [73, 79]. However, the literature on biochar as a construction material for buildings or roads is in the infancy stage. The gaps at various levels, especially testing standards for durability, water penetration, humidity control, strength, CO<sub>2</sub> sequestration, and use of an optimal percentage of biochar and field data, have been noticed in research. The effects of cost-effectiveness, a life of RCC given its CO<sub>2</sub> content, and other technical issues need to be investigated as the researchers are still not clear about these important aspects.

From the literature, it has been observed that there are no preliminary guidelines for using biochar in the construction sector. Future research jointly with the industry is needed to promote its usage in construction. However, different biochar initiatives/guidelines are available for biochar production and application in the agriculture sector. These initiatives include EBC, IBI, etc. The basic criteria for biochar production, feedstock, and constituents are almost similar. Some of the important guidelines summarized from EBC (effective from 1st January 2012) certified by q-inspecta for biochar production in Europe are summarized as under:

1. Biochar in Europe shall be provided from local forestry-based organic material feedstock (with a proper record) free from contaminants and proof of sustainable forest management.
2. The pyrolysis temperature and composition of biochar produced shall not fluctuate more than 20° and 15%, respectively. After one year (or any interruption), the sampling process should be repeated.
3. Either 2.25 Liter biochar samples have to be obtained from 1 day's production properly mixed (as per EBC guidelines), or 100-gram samples taken randomly every 30 min and sent to the laboratory for testing. Also, random sampling by the controlling inspector has to be sent to the laboratory.
4. To guarantee protection from negative environmental impacts and avoid uneconomical physicochemical characterization, EBC has marked limits for different constituents of biochar among which some are C-Content > 50% of dry mass C—content; molar H/C<sub>org</sub> < 0.7; molar O/C<sub>org</sub> < 0.4; Pb < 150 g/t dry mass; Cu < 100 g/t dry mass; PAH < 12 mg/kg dry mass.
5. Pyrolysis (production process) shall preferably avoid the use of fossil fuels. Gases produced shall not be allowed to escape into the atmosphere. No less than 70% of heat, which remains in the pyrolysis gas, shall be effectively used.
6. Fire and dust protection safety measures (including personal protection equipment), feedstock transportation in a moist form and self-declaration of workers shall be obligatory.

Biochar has been proven as a substance with multidimensional applications. However, its use in geotechnical engineering infrastructure is relatively new. Geotechnical engineering mainly deals with soil engineering properties such as shear strength, compressibility, hydraulic conductivity, and bearing capacity. These properties are mainly governed by soil particle size, WRC, and porosity. The reinforcing techniques of soil stabilization are formed by mixing soil with reinforcing agents like cementitious, synthetic, metallic, or fibrous

materials. The design criteria for a stable landfill cover system depend upon its compressibility and shear strength [70, 83–85], which the authors believe, can be achieved using biochar as a reinforcing agent. In their study, Pardo et al. [86] observed that the fine biochar particles form a thin layer around the soil/ sand particles that get thicker over 30 days afterwards. It was found that the biochar particles around the sand particles minimize the movement of sand particles, due to which there is less contraction in the mixture. The mixture's shear strength increases due to negative capillary water pressure and water film around the particles [86]. In their study, Zong et al. [87], using three biochars, woodchips, straw, and wastewater sludge, observed that tensile strength decreased from 466 kPa to 233, 164 and 175 kPa at 6% biochar amendment, respectively. The cohesion and angle of friction, the basis for the shear strength, are affected by aggregation's bonding mechanism. The study reported that the cohesion decreased (significantly for wood chips), whereas no effect was noticed on the angle of friction. The study concludes that shear and tensile strength decrease with biochar amendment. Wallace et al. [88], in their study on two biochars (softwood and hemp), noticed that Young's modulus of elasticity and hardness were sufficient to use biochar as a composite filler material.

Similarly, GuhaRay et al. [89] studied 5% and 10% biochar amendment to the soil. They found that CBR and UCS increased, which they attributed to the increased shear strength due to increased cohesive bonding between the particles by adding biochar [89]. In another study by Reddy et al. [70] on silty soil and biochar, the values of compressibility were 0.054 cm and 0.027 cm after 24 h; cohesion was 6.62 kPa and 51.71 kPa, and the angle of friction was 24.9° and 42.8°; hydraulic conductivity  $4.3 \times 10^{-9}$  and  $1.2 \times 10^{-2}$  /second respectively [70]. The biochar composite soil was accordingly found to have low compressibility, high hydraulic conductivity, and shear strength, increasing the biochar amendment percentage. The general DoC of soils used in agriculture is 65%, and that of soils used for geotechnical applications is around 80% to 95% [1, 90–93]. For biochar prepared from wood feedstock (pine wood, fir wood, aged wood chips, and wood pellets), the factor of safety for slope covers increased to about two times when used in drained soil [94]. This was attributed to increased cohesion values, shear strength and angle of friction of BAS. Biochar derived from water hyacinth feedstock was used to treat soils to increase water retention capacity and decrease gas permeability [93]. The authors observed that gas permeability decreased by 50–65% when adding 5% to 10% biochar to the soil. This may be due to increased soil suction in BAS, thereby demonstrating an increase in soil stability. The increase in soil stability can be correlated with the biochar's surface area [24].

From the above discussion, it is observed that even though the researchers observed an increase in shear strength, tensile strength, and reduced compressibility, there are researchers that report otherwise [95]. These contradictory results highlight the knowledge gap about the strength parameters of biochar amendments in various soil types under different testing conditions. Future systematic research is required to understand the efficiency of biochar in enhancing strength properties under different testing conditions, including stress paths.

Similarly, keeping in view various research and the requirements of geotechnical engineering, it is observed that biochar acts as a reinforcement material for soil when considered as an agent for soil stabilization. As reinforcement material's function is to increase strength and decrease compressibility, the biochar selected

should possess these desirable functional properties for engineering purposes. It shall also help reduce water infiltration in soil slopes and landfill covers. Studies demonstrate that water retention capacity increased from  $29.5 \pm 0.89\%$  to  $48.45 \pm 0.59\%$  for bare soil and soil amended with 15% water hyacinth biochar. This was attributed to biochar's fine-grained and porous textural properties prepared from water hyacinth. A reduction in CIF was observed from 7 to 2.8%. The authors observed that the decrease in crack intensity would reduce infiltration in slopes [90]. Studies also suggested that biochar intrapores retain water in BAS, reducing gas permeability [93]. Huang et al. [96] stated that soils could be made impermeable by compacting BAS to 95% suitable for engineering applications.

Many studies have been put forth in agriculture, environmental sciences, and energy resource conservation regarding biochar and optimization of pyrolysis conditions. However, it is observed that relatively less literature is available on the production and use of biochar in geotechnical engineering. There is a lack of studies considering the mechanical aspects (i.e., shear strength, tensile strength and compressibility) and the adverse effects of biochar and BAS. It is observed that the geotechnical applicability of BAS has not been done to its optimum use, especially for the stabilization and reinforcement of soil slopes. The availability of feedstock and its cost-effectiveness is a primary concern. Its scale and cost of production, applicability in a specific field, and properties are significant factors. As far as the authors are aware, very little research seems to have been done in this field and needs a thorough discussion. More research is needed for the validation of biochar benefits in geoenvironmental engineering.

## 1.2 Objective

The principal objective of the research is to explore the efficiency of biochar in affecting the hydraulic properties of BAS by developing and using AI-based models. The sub-objectives as detailed below:

1. Exploring the biochar efficiency in improving the water retention capacity of soils with varying grain size distributions.
2. Erosion prediction as a function of biochar content, degree of compaction, slope conditions, and rainfall intensity.
3. Effect of the various soil properties and biochar content on the cracks intensity of biochar-amended soil.

## 1.3 Organization of Thesis

This thesis has been presented in eight chapters: Chapter 2 involves a general introduction and provides a brief description of biochar, raw materials from which it is produced, various methods for production, general properties and uses. Chapter 2 also includes a literature review. In this part, a brief description of previous work

done in various connected parameters like properties of biochar, the influence of properties of biochar on soil or any other medium in which it is added like concrete, road construction.

Chapter 3 involves the methodology adopted for the study and gives a brief description of ANN and MRA used for the model developed in the study.

Chapters 4, 5 and 6 consist of the studies presented to achieve the objectives using ANN and MRA. In this part, AI models have been developed to predict results, compare results obtained by different models with the experimental results, and discuss the accuracy of results obtained by different check systems.

Chapter 7 presents conclusions that have been observed from chapters 4<sup>th</sup>, 5<sup>th</sup>, and 6<sup>th</sup>. Chapter 8 presents the future scope and recommendations of the work.

## Chapter 2: Literature Review

---

### 2.1 General

Agriculture, forestry, animal and aquatic materials, residues and wastes are organic materials. They form raw materials for biochar production, known as feedstocks or biomass [3, 5, 8, 10–13]. Biomass or feedstock is subjected to thermochemical degradation under controlled conditions of air, heat and temperature. The end products obtained in the process include biochar (solid), bio-oil (liquid) and syngas (gas). The quantity and quality of these three end products are governed by the parameters of thermal degradation (temperature, heat, and air supply) and the type of feedstock. Biochar obtained is solid, black in colour, porous in nature, and light in weight, with carbon (C) constituting a major part [2, 4, 24, 35, 91, 96]. This solid material, biochar, resembles charcoal in colour to a large extent. It is composed of different constituents [6] with a carbon content of around 44%–93.7% depending on the type of raw material used, manufacturing process, and parameters [97, 98]. Carbon percentage from less than 1% to greater than 80% has been reported by some researchers, again depending on the biomass type and the methods of preparation [99, 100].

Biochar is considered a new, modern, unconventional material and has a life span of thousands of years [97, 98]. It has emerged as a soil modifier for crop production, a novelty material in environmental remediation, and a carbon sequester [1, 6, 101, 102]. It has made its way in agriculture, environmental remediation, climate mitigation, and geoengineering and provides scientific and profitable disposal of all bio-wastes. The Amazonian Tera Preta (TP) soils provide a typical example of agricultural use of biochar [1]. These soils are dark in colour, probably produced by human or natural activities resulting in huge quantities of organic debris and, in turn, making the soil fertile. Terra Preta soils are dark-coloured fertile soils interspersed with relatively non-fertile Amazonian ferrisols [36]. The constituents in addition to carbon present in biochar include nitrogen (N), calcium (Ca), phosphorus (P), potassium (K), magnesium (Mg) and copper (Cu) [103] and higher amounts of stable organic soil matter [1, 4].

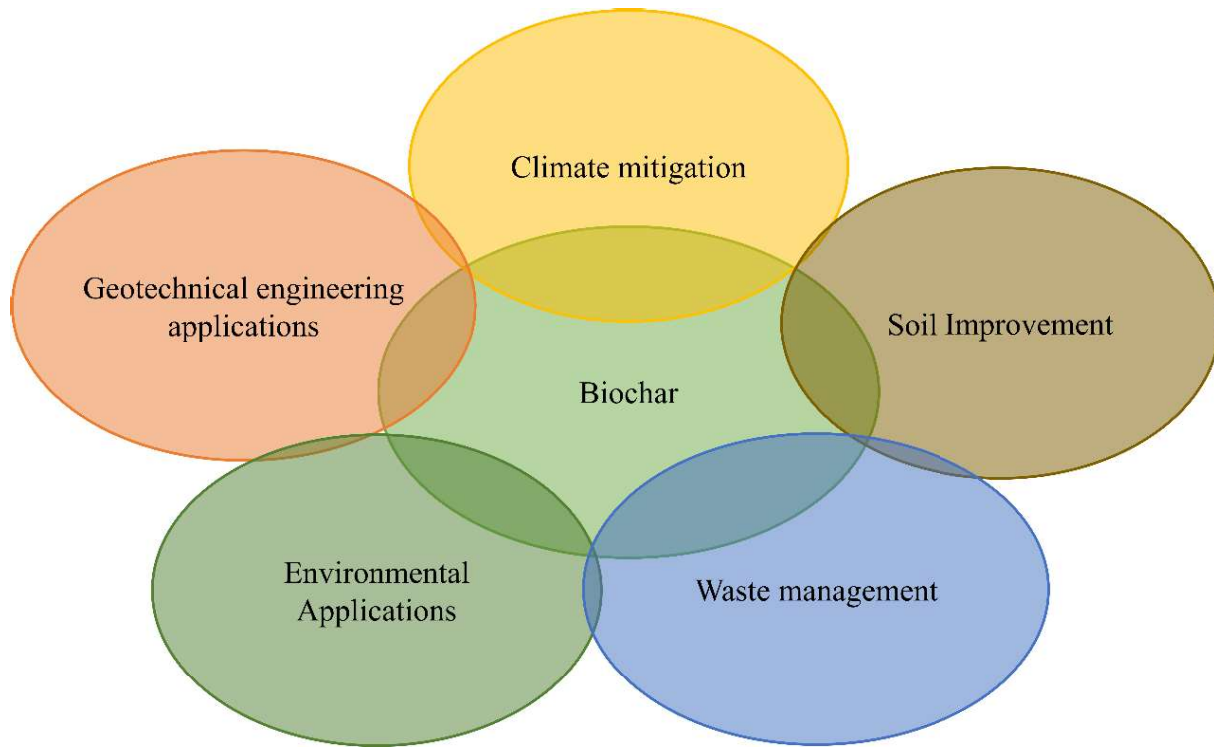


**Figure 6** Use of biochar in various fields

### 2.1.1 *Biochar, char and charcoal*

Biochar includes the application of charred organic matter apart from agricultural and environmental applications, such as promoting its use for soil remediation and geo-environmental and geoengineering purposes.

Char and charcoal differ in that char can be obtained by charring a raw material to a lesser extent than charcoal [104]. The terms burning, charring and pyrolysis are altogether different processes. Burning is the complete or incomplete combustion of any material in an open-air supply into ashes where no char or charcoal is left behind. The charring process produces char or charcoal with limited or no oxygen supply. On the other hand, pyrolysis is used for scientific procedures to examine the organic chemistry of organic substances [105] and for bioenergy systems that capture the off-gases emitted during charring and produce hydrogen syngas bio-oils, heat or electricity [106]. Sometimes, some traces of char or biochar in the ashes affect ash properties in technology and the environment. Burning, charring and pyrolysis also differ from each other in terms of gaseous produce.

**Table 1** Difference between Char, Charcoal and Biochar

Char	Charcoal	Biochar
<ul style="list-style-type: none"> <li>• It is obtained by partially burning organic raw material in an open-air supply.</li> <li>• It is similar to charcoal in appearance but has less carbon content, is less porous and has lesser nutritional properties than charcoal.</li> </ul>	<ul style="list-style-type: none"> <li>• Black solid porous material consists of an amorphous form of carbon. We can obtain this material as a residue when wood, bone, or other organic matter is burned without air.</li> <li>• It is produced using biomass by burning in the limited supply of oxygen at lower temperatures, usually up to 300°C</li> <li>• Due to the low production temperatures, charcoal is less porous, less stable and holds less water and nutrients</li> <li>• During the production, a major portion of harmful gases are produced, which are released into the atmosphere causing environmental pollution</li> </ul>	<ul style="list-style-type: none"> <li>• Carbon-rich solid derived from biomass (organic matter) produced using pyrolysis at higher temperatures above 400°C.</li> <li>• High production temperature leads to high porosity and stable structure.</li> <li>• Biochar has a half-life of more than 500 years</li> <li>• During the production of biochar, bio-oil and syngas are produced, which can be further used as fuels</li> </ul>

### 2.1.2 Feedstock

Biomass is a heterogeneous material. Its availability is so huge globally that, if exploited, these raw materials can provide about 10%-20% of the world's fuel demand. The available biomass can reduce the demand for fossil energy sources and thus help conserve energy. The amount and quality of the biochar obtained rely on the structure and type of biomass used to prepare biochar to a large extent. The cellulose, hemicellulose, lignin, and a considerable moisture content form the main components of the plant material and inorganic species [107].

- i) Cellulose constitutes about 40% - 60% of the plant material (depending upon the biomass quality) and is a common form of carbon in biomass. The glucose (six-carbon sugar) forms a complex sugar polymer (polysaccharide) and is resistant to hydrolysis due to its crystalline structure. The polysaccharide is obtained from the fermentable sugars in the chemical reaction.
- ii) Hemicellulose, another carbon source, constitutes about 20% - 40% of the plant material. It is a complex polysaccharide made from a variety of five and six-carbon sugars. It is easy to hydrolyze into simple sugars but undergoes difficulty in fermentation.

iii) Lignin accounts for about 10% to 24% of plant material, providing structural stability to the plant. It is not composed of sugars but is a complex polymer and is left behind as a residue during the sugar conversion process. When burnt, it can produce good heat energy.

The thermal decomposition of hemicellulose occurs in the temperature range of 200°C - 260°C, for cellulose between 240°C - 350°C, for lignin usually at 280 - 500°C, whereas evaporation of moisture takes place between 100°C - 120°C [1, 5, 34, 107–110]. Biomass is usually cut into predetermined small sizes and pre-treated as per the requirements of thermochemical conversion techniques [111]. Dense raw materials like dense wood produce biochar of high porosity, surface area, pH, and aromatic composition [24, 25] as compared to biochar derived from animal wastes, having low surface areas [26] and less porosity [27]. Biochar produced from aquatic raw materials has high nutrient content and functional groups but a low surface area and organic carbon content [28]. Lei and Zhang (2013) observed that the hydraulic conductivity of wood-derived biochar was more than that of manure biochar [29].

### 2.1.3 Major biomass constituents

Biomass has a complex structure and consists mainly of cellulose, hemicellulose, lignin, and moisture content. Percentages of these biopolymers vary in dissimilar biomass sources. The degree and rate at which the components decompose depend on the temperature, oxygen provision, heating rate, residence time, particle size, reactor type, etc., used for biochar preparation processes. Hemicellulose decays at 200°C to 260°C, followed by the cellulose breakdown at 240°C to 350 °C and finally, at a temperature between 280°C and 500°C, decompositions of lignin occur (**Figure 7**) during pyrolysis [34, 107, 109, 110, 112].

Cellulose, hemicellulose, and lignin are the principal sub-components of biomass, some inorganic elements [107] and other nutrient-based constituents. The composition of these constituents in specific biomass establishes the nature of the product formed. A brief characterization of these constituents has been discussed in the following sections.

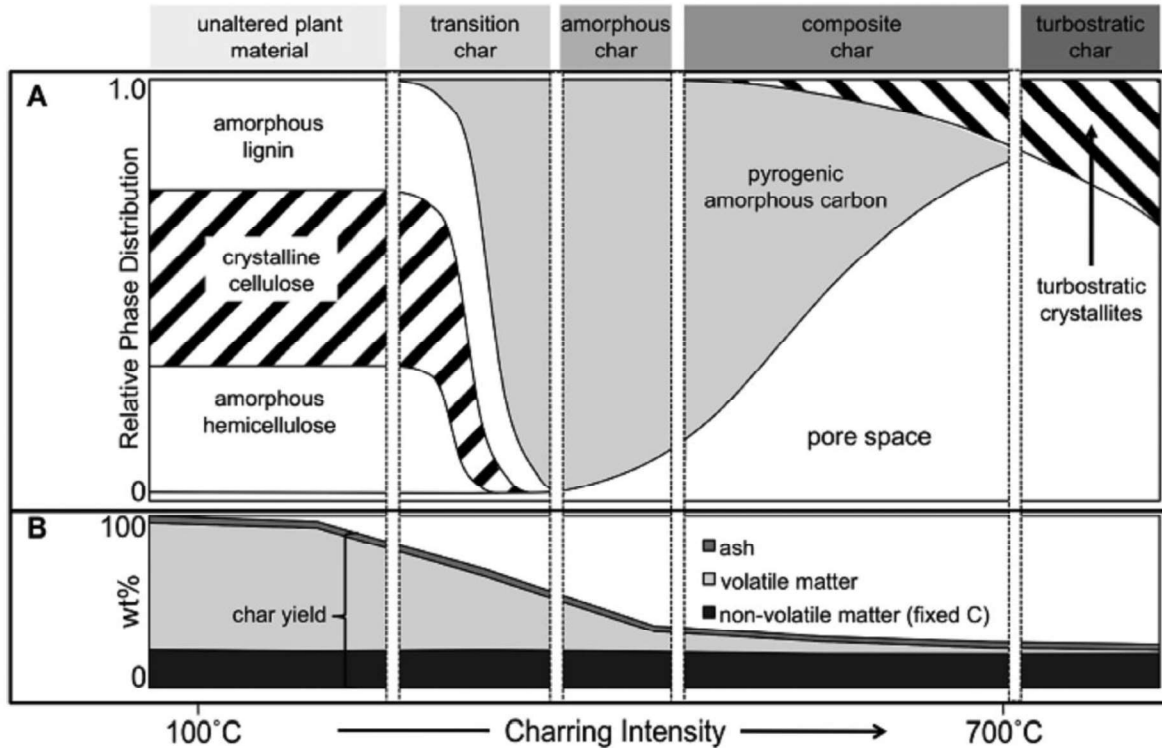


**Figure 7** Molecular structure of the biochar produced at different pyrolysis temperatures [107]

The decomposition at low heat and temperature causes cellulose polymerization (slow pyrolysis). However, levoglucosan is formed by volatilization by fast pyrolysis. Initial cellulose depolymerization causes the formation of oligosaccharides. Further cleavage of glucosidic bond produces de-glucopyranose. More molecular rearrangement leads to the formation of levoglucosan. Levoglucosan undergoes a series of intermolecular rearrangements and dehydration, forming hydroxyl- methyl furfural, producing volatile bio-oil and syngas on further decomposition. Alternatively, levoglucosan undergoes dehydration, producing levoglucosenone. Biochar is produced due to polymerization, aromatization, and intermolecular condensation reactions of levoglucosenone (**Figure 8**) [51, 107, 113–121]. The yield of charcoal is good at high pressure in the case of feedstock with higher moisture content [62–66]. For biochar production, initially, the moisture content evaporates from the feedstock as white smoke and is then followed by pyrolysis.

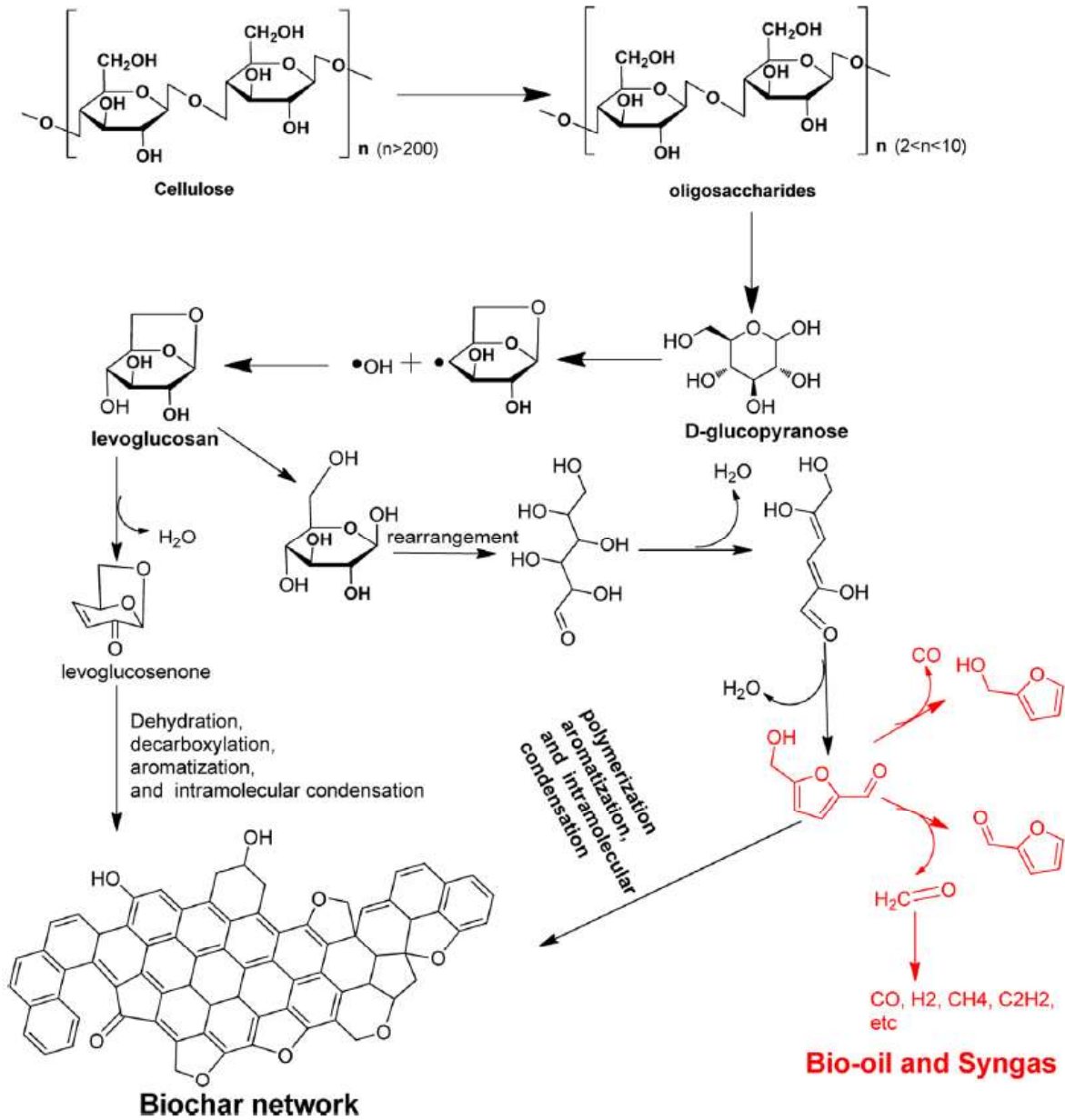


**Figure 8** Cellulose pyrolysis: Biochar formation mechanism [107]

The hemicellulose pyrolysis mechanism begins with depolymerization, resulting in oligosaccharides' formation (**Figure 9**). Cleavage of glycosidic linkage of xylan chain and rearrangement of oligosaccharides' depolymerized molecules produces 1,4-anhydro-D-xylopyranose. It undergoes various pathways, decomposition, decarboxylation, aromatization, and intermolecular condensation to form solid biochar or decomposing compounds with low molecular weights, bio-oil, and syngas [107, 118, 122–129].

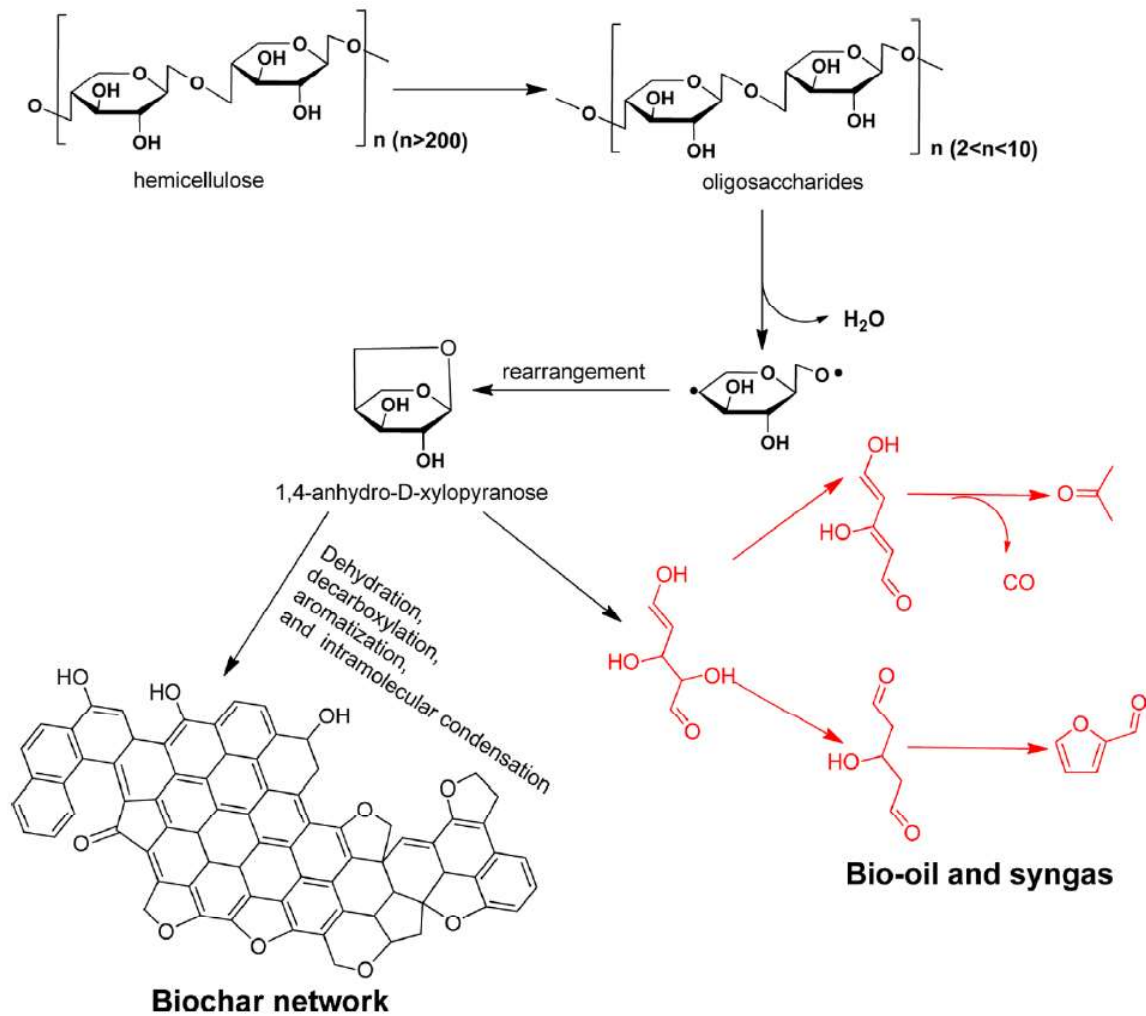


**Figure 9** Biochar preparation mechanism by decomposition of hemicellulose [107]

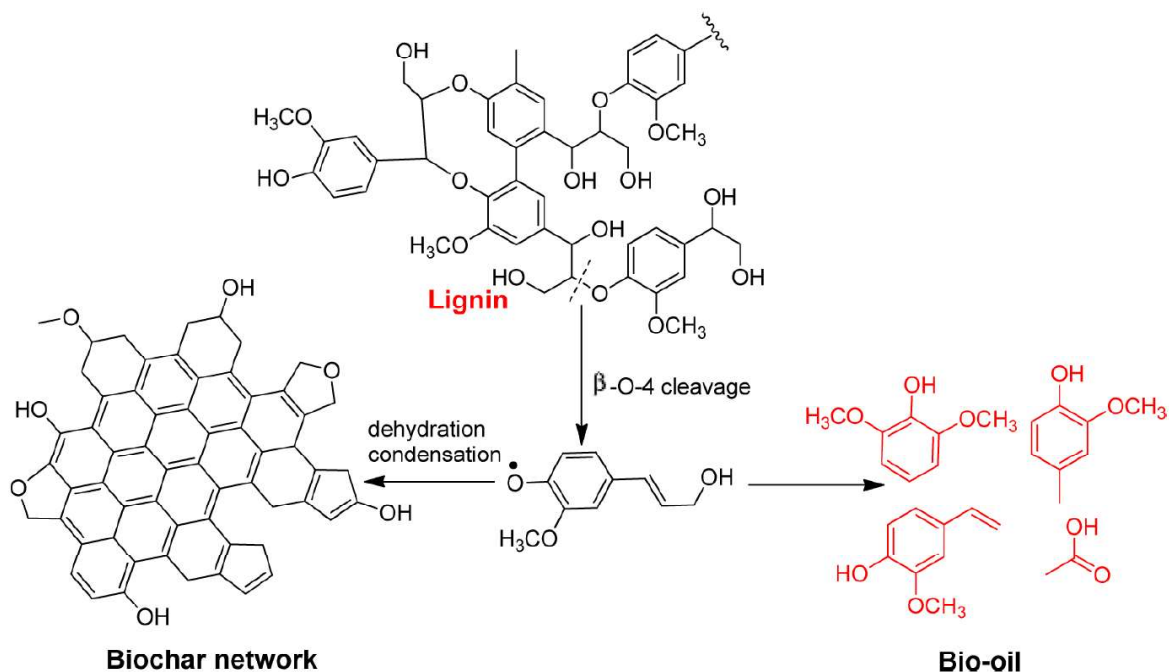


**Figure 10** Biochar preparation mechanism by decomposition of lignin [20]

Lignin works as a bonding agent between the other two constituents, cellulose and hemicellulose, provides mechanical support to the plant, helps in a water transport mechanism, and prevents degradation by microorganisms. Its percentage varies between different plant species. The feedstock with high lignin content can produce more charcoal yields [130]. Lignin composition is complex compared to cellulose and hemicellulose and forms a complex mechanism of decomposition (**Figure 10**). The free radical reaction of lignin pyrolysis is also a complex but important mechanism. The breakage of  $\beta$ -O-4 linkages are considered an initial move in the free radical chain reaction. The protons of other species with weak C-H and O-H bonds (e.g.,  $C_6H_5-OH$ ) are captured by the radicals and result in decomposed products, e.g., vanillin and 2-methoxy-4-methyl phenol. A chain propagation is obtained by passing the reaction to other species for a further reaction, which terminates by forming stable compounds due to collision among two radicals. The observation of free radicals is complicated in the pyrolysis process. The exact lignin pyrolysis mechanism is challenging to clarify [107, 131–135].

The presence of high moisture content in the feedstock is suitable for preparing biochar. Higher moisture content improves the charcoal yield at higher pressures [136–140]. Biochar preparation involves two processes, drying and pyrolysis. In the initial stages of carbonization, water evaporation occurs in the form of white smoke. Temperature control is vital for optimizing product yield as it influences pressure, heating rate, and contact time parameters between solid and gaseous phases. The liquid yield is higher at a temperature of 400°C –500 °C, beyond which the condensable vapour decomposes (secondary reactions), resulting in lesser liquid fractions. Minimizing the degree of secondary reactions requires rapid

heating and cooling, reducing liquid products, but the quality of biochar may not be satisfactory [141]. Pyrolysis conditions increase the contact between primary vapour and hot char, favouring char formation with lower liquid yield [142, 143].

#### 2.1.4 Production

Pyrolysis is the thermochemical degradation of organic raw materials under controlled conditions. It is the main process for biochar production. In the process, temperature, pressure and oxygen supply are the basic parameters provided under a controlled environment. Pyrolysis process starts with the evaporation of moisture, followed by volatilization, depolymerization and degradation of feedstock. Some secondary and tertiary reactions occur during the formation of the end products [144]. Many pyrolysis processes are described per the limits of parameters like temperature, heating rate, time, and feedstock adopted. Mainly the process of pyrolysis has been classified as conventional (slow, fast, flash), gasification, hydrothermal [18, 19], solar [145–147], microwave, catalytic [145, 148, 149], and vacuum [145, 150] methods. In pyrolysis, thermal cracking or the thermal degradation of long-chain polymer molecules is done in a short time into smaller and less complex molecules in the absence of oxygen [24, 151] by breaking down the lignocellulose components thermally [21] at higher pressure and temperature (300°C - 600°C) [152]. The resultant products are biochar, bio-oil and non-condensable gases like CO, CO<sub>2</sub>, CH<sub>4</sub>, and H<sub>2</sub> [3, 152–154]. Higher the temperature, the less the biochar yield [22, 155]. An increase in the heating rate causes rapid volatilization.

On the other hand, a stable matrix is formed at a low heating rate due to biomass decomposition and lowering the release of volatile compounds [22, 23]. A structural shrinkage is caused due to loss of volatiles and physical and chemical changes in the pyrolysis process in which the temperature plays an important role. Heating rate and pressure govern the product structure and behaviour of the volatiles produced during the process [1].

##### 2.1.4.1 Conventional Pyrolysis

The different conventional biochar production methods include slow, fast, flash, gasification, and hydrothermal carbonization. Slow, fast, and flash pyrolysis processes are considered dry pyrolysis liberating 30%-35% of gases and vapour at a medium heating rate and high residence time [43] and producing 20%-40% of char [43, 130]. The processes are described briefly as under.

##### i. Fast pyrolysis

In this pyrolysis type, the heating of biomass and cooling of vapours obtained during the process is done rapidly [43]. The temperature and the heating rate at which the feedstock is burnt are high. In this process, the quantity of solid part (biochar) lies between 15% - 25%,

liquid part (bio-oil) 60% - 70% and gases about 10% - 20%, the quantity depending upon the different factors like temperature, rate of heating, residence time and feedstock type [21, 156]. It has also been observed that high oxygen quantity is present in biochar produced at a higher heating rate [139, 157].

ii. Flash pyrolysis

This process is more advanced but produces more quantity of liquid products (bio-oil) than solid (biochar) and has a conversion efficiency of 70% [144, 156, 158]. In the process, a high temperature of 400°C - 1000°C and a rate of heating of a range of 900°C/min to 1300°C/min for a residence time of about 2 seconds is applied. The feedstock particle size is kept small to achieve a high heating and heat transfer rate [144, 159].

iii. Slow pyrolysis

This type of pyrolysis is considered the primary biochar production process on a large scale [152], even though the end products are relatively roughly produced in a similar ratio. Biochar production is done at a relatively low temperature of 300°C - 500°C, with low heating rates and longer vapour residence time; criterion to generate charcoal earlier [139, 160]. Out of various factors which determine the slow pyrolysis and the production of the end products, the highest (peak) temperature, pressure, vapour residence, and moisture quantity are the important parameters [130, 139]. The biochar production is more if the temperature is less and vice-versa. The surface area and pore size distribution are dependent on temperature [139].

If the temperature is maintained at around 300°C, the process is known as torrefaction. However, if the temperature ranges between 300°C and 900°C, it is known as carbonization [161].

#### 2.1.4.2 Gasification

In this process, oxygen supply is allowed into the reactor, which causes partial combustion of the feedstock [43]. The thermochemical degradation of the feedstock creates a huge quantity of non-condensable gas at high temperatures (>800°C) [139, 160, 162]. A combustible gas (syngas) is produced by partial burning due to the presence of air (oxygen) [139], mainly consisting of H<sub>2</sub>, CO, CO<sub>2</sub>, and CH<sub>4</sub>. The solid char (charcoal or biochar) is produced in very small quantities [139].

#### 2.1.4.3 Hydrothermal carbonization

As the name indicates, this process usually uses water as a solvent. The raw material (usually sludge) surrounded by a liquid, usually water, is made to rise in high-pressure reactors by steam pressure. The temperature in the range of 180°C - 220°C, the pressure of 20 bars – 25 bars

and residence time of 1 to 72 hours are generally adopted [61]. The quantum of gases generated is low. The quantity of biochar obtained is more, but the process uses low temperature, heating rate, and longer residence time [21]. The long residence time increases the production cost due to the use of more energy. However, if the temperature increases to around 400°C and a catalyst is used, the quantity of gases and liquid hydrocarbons increases. The use of organic solvents instead of water is becoming more popular nowadays [43, 163]. The type of pyrolysis is also classified as liquefaction and vaporization (supercritical water gasification), depending upon the process and parameters adopted.

#### 2.1.4.4 Microwave-Assisted Pyrolysis (MAP)

This pyrolysis type uses a microwave-assisted reactor for thermochemical conversion of feedstock into end products; biochar, bio-oil, and syngas, even though the process is popularly used for bio-oil production. Modern pyrolysis uses comparatively less cost, provides more targeted heat radiation and uniform temperature, and a better quality output [145, 164–166]. The process is energy efficient, less time-consuming, and the product is of high quality compared to conventional and vacuum pyrolysis [145, 167–169]. Even though there are limitations in the process compared to solar-type, which include the need for electric energy and few feedstocks need the use of some absorbents to make them sensitive to microwaves of the reactor. But it outweighs the solar pyrolysis because it can be used in any weather, while solar pyrolysis depends on sunlight. One of its other advantages over other pyrolysis types is that due to its compact movable unit size, small movable units can be carried to far-off locations where feedstock is readily available to eliminate the cost of carrying raw materials to long distances. The agroforestry residues can be best treated at the source locations to produce useful products and reduce harmful emissions like greenhouse gases. Also, MAP can be best considered for producing biochar for engineering applications [170] where huge quantities are required, like in landfill covers, green rooftops and erosion control [145, 164, 171].

#### 2.1.4.5 Vacuum Pyrolysis

In vacuum pyrolysis, a properly designed reactor is used. A vacuum pump removes the air from the reactor to create a vacuum (an inert atmosphere). Nitrogen or argon is pumped into a conventional reactor to create an inert atmosphere. An inert atmosphere in the pressure range of 0.5 kPa to 50 kPa and 400°C - 600°C temperature is maintained in the reactor [145, 172–174]. Due to low pressure, the requirement of energy and temperature is very low, making this process more efficient [145, 175] in cost and the quality of biochar produced. As brought forward in the literature, one of the drawbacks is that the polycyclic macromolecular compounds concentrate on bio-oils [117, 145], for which treatment is required. Also, the reactor needs a proper design to prevent the burning of raw materials in the reactor [145].

#### 2.1.4.6 Solar Pyrolysis

The process of solar pyrolysis uses neither electricity nor fossil fuels; however, the capital cost for reactor construction is high. Also, reactor fabrication is complicated. The solar pyrolysis reactor works in the temperature range of 150°C - 2000°C [145, 147, 176] and has a rate of heating from 5°C/s - 450°C/s [145, 177]. The biochar yield in this process ranges from 8% - 29%, bio-fuel 25% - 78% and syngas 1.4% - 63%, but actually governed by temperature [145]. However, drawbacks include high capital cost, difficulty in continuous operation, and difficulty controlling operating conditions like temperature, heating rate, and other parameters.

**Table 2** Different types of thermochemical processes

	<b>Slow</b>	<b>Fast</b>	<b>Flash</b>	<b>Hydrothermal</b>	<b>Torrefaction</b>	<b>Solar</b>	<b>Gasification</b>
<b>Temperature</b>	400°C - 900°C	450°C - 800°C	600°C - 1200°C	180°C - 220°C	200°C - 300°C	150°C - 2000°C	600°C - 1800°C
<b>Heating rate</b>	0.1°C/sec - 10°C/sec	10°C/sec - 200°C/sec	>1000°C/sec	<10°C/min	<50°C/min	5°C/sec - 450°C/sec	-
<b>Residence time</b>	>5min	10 – 25 min	<1min	1 hour – 72 hours	30 minutes to hours	-	Seconds to minutes
<b>Biochar yield</b>	25% - 50%	15% - 25%	5% - 15%	10% - 25%	80%	8% - 29%	10%
<b>Bio-oil yield</b>	20% - 40%	60% - 25%	25% - 40%	68% - 75%	0%	25% - 78%	5%
<b>Syngas yield</b>	10% - 25%	10% - 20%	50% - 60%	3% - 9%	20%	1.4% – 63%	85%

### 2.1.5 Properties

Biochar is a novel material because of its inherent physicochemical properties. Particle size, surface area and porosity are the characteristics that help determine the physical properties of biochar. The chemical properties depend on its chemical stabilization, surface functional groups, CEC, pH, aromaticity, elemental composition, etc. Biochar has been observed to enhance soil organic content and aggregate stability, and as such, the soil properties are affected [100, 178–183]. Similarly, it has also been noticed that the CEC of the soil is increased, and the leaching of nutrients is decreased [100, 184]. Biochar being alkaline reduces the acidity of the soil. The porosity of biochar modifies the porosity of BAS, increasing the soil conductivity [100, 185]. Biochar has a large surface area causing the aggregate stability of soil to increase by increasing the charge density of biochar [98, 186, 187]. Also, biochar's high porosity increases soil porosity, increasing the WHC of soil in succession and increasing the root growth of plants, resulting in increased vegetation [100, 188]. Due to its high carbon content and the oxygen-carbon ratio [189] and microbial biomass, the biochar amendment increases the carbon content in the soil [98, 190–192].

The physicochemical and biological properties of soil are modified when amended with the biochar due to the novelty biochar characteristics [41, 63]. The hydraulic conductivity, WHC, porosity, aggregate stability, and bulk density of soil are affected by the related properties of biochar [64]. The porous structure and low bulk density of biochar reduce the bulk density of SBC [63, 65]. However, minute and no reduction was observed by some researchers in the bulk density of BAS [65]. Literature shows an increase in the formation and stability of soil aggregates and a decrease in soil strength due to the addition of biochar to soil [66–68]. It was observed by Chan et al. (2007) [44] that tensile strength was reduced by 52% and 72% at 50 t/ha and 100 t/ha treatment of biochar to the soil, respectively. Reddy et al. [70], while using biochar amendment of 5%, 10%, and 20% to the soil, observed an increase in shear strength. Similarly, Zong et al. [193] used three different types of biochars (obtained from three different feedstocks, woodchips, straw and wastewater sludge) and observed that the cohesion reduced and internal friction improved. The available literature shows an increase in the liquid limit, plastic limit, pH and moisture content and a decrease in the maximum dry density of biochar-treated soil compared to ordinary soil [69–71].

#### 2.1.5.1 Physical Properties of biochar

The biochar's physical properties help soil and environmental management in many ways. The physical properties of different soils are dependent on the quantity and character of their mineral and organic matter and their association with each other. The addition of biochar to soil may cause noticeable effects on the physical character of BAS, affecting the texture, depth, porosity, structure, and consistency by causing changes in the surface area, particle, and pore size distribution, packing, and density. Biochar may affect plant growth as the function of the penetration depth and accessibility of air and water in the root zone, determined mainly by the physical construction of soil horizons. It also influences the physical attributes, directly affecting soil's response to aggregation, water, workability during the soil sample formation,

swelling–shrinking dynamics and permeability, cation retention capacity, and reciprocation to temperature changes in the surrounding. Also, there are indirect effects such as the creation and flourishing of microbial sites and the development of flourishing sites for chemical reactions. Some of the major biochar characteristics which come under physical properties are specific surface area and porosity, density, hydrophilicity and hydrophobicity, water holding capacity, and mechanical strength. As discussed above, these properties are related to the production conditions, temperature, heating rate, residence time and feedstock. It has been observed from the literature that increasing the maximum reaction temperature and residence time significantly causes an increase in porosity and specific surface area of biochar [194–196]. As maximum temperature, microwave power and heating rate are interdependent, and they can be tuned to get the maximum specific surface area. At higher temperatures and for longer residence time, the volatiles is converted to condensable gases. These molecules leave their space to form voids, increasing the surface area [197]. Generally, the biochar derived from biomass possesses a larger specific surface area between 10 m<sup>2</sup>/g to 500 m<sup>2</sup>/g [194, 195]. Biochar with high porosity and specific surface area can be used in soil amendments to increase crop production [197, 198] or for adsorption of pollutants [199].

i. Particle size

The particle size influences the properties of soil biochar composite and the soil biochar interaction. The pyrolysis conditions can be adjusted to check the size of biochar particles. As reported by many researchers that using small-sized raw material in pyrolysis under conditions of high temperature and heating rate, the biochar produced is of high surface area and fine-grained otherwise, vice-versa and high ash content, pH [200–203] and sorption capacity. Sangani et al. [204] noticed that proper attention had not been given to the need to modify the particle size of biochar post pyrolysis. Liu et al. [205] reported that biochar used in the field has different sizes and shapes compared to soil. The grains of biochar, when applied to soil, change the inter pore structure of soil biochar composite, including shape, size, volume, and connectivity, which in turn affects not only the WHC and hydraulic conductivity but also the other properties like mechanical strength etc. The engineered biochar is a step further in use, and its particle size distribution may help the more efficient use of biochar in various applications [204–206].

ii. Soil bulk density

The operation, handling, application, and usage activities of biochar are related to biochar density. As such, it is an important property for consideration of the future of biochar. The researchers have defined the density of biochar in many ways like bulk density, envelop density, particle density, true density, etc. The density of the whole structure, including the pores and voids between feedstock particles and the solid mass, is called its bulk density. On the other hand, envelop density consists of particles,

internal voids and surface irregularities of the feedstock. The density of feedstock particles which considers pores within feedstock and solid biochar, is called particle density. The density of the solid mass of biochar only is called true density [152, 155

The bulk density of biochar is less than soil because of its porosity. Sandy soil has a bulk density of  $1.5 \text{ g/cm}^3$ , whereas clayey soil is  $1.1 \text{ g/cm}^3$ . However, the density of feedstock of biochar is less than that of biochar. As the degree of carbonization increases due to increased pyrolysis temperature, the solid material shrinks [207]. The density of the parent material is less than that of the product. The higher degree of porosity and low biochar density makes the SBC less dense than the soil [29, 208, 209]. However, the density of the mixture depends upon the ratio in which the soil and biochar are mixed. However, Pratiwi and Shinogi [210] observed no reduction in density of mix at 2% biochar addition in a loam soil mixture of sand (42%), silt (36%), and clay (19%), but 4% biochar addition to soil (bulk density =  $1.13 \text{ g/cm}^3$ ) noticed a significant reduction. In their study, Laird et al. (2010) [99], using silt soil, observed that the biochar addition at an amendment ratio of 25 g/kg reduced the bulk density of silt soil to  $1.33 \text{ g/cm}^3$  from  $1.52 \text{ g/cm}^3$  of controlled soil. Gluba et al. [211] reported that biochar amendment increases the bulk density of biochar-soil blends; therein, the most significant increase was observed for  $<100 \mu\text{m}$  of biochar fractions, and subsequently, bulk density decreases with increased biochar content in BAS.

iii. Porosity

The compaction achieved in the case of SBC has been observed less as compared to bare soil [212]. In other words, it can be said that the addition of biochar increases the porosity of the soil. Because of the porosity of biochar, it can hold more quantity of water and has high hydraulic conductivity [213–215]. In their study, Zhang et al. [215], while working on loamy clay soil in field conditions, noticed an increase of 23.8% water content in soils amended with biochar than bare soil, as such, showing that the biochar can be very effective in areas under drought or water scare areas. Also, the hydraulic conductivity increases with the addition of biochar to soil [216]. Many researchers made similar observations and have shown the direct interdependence of porosity and surface area on pyrolysis temperature and the direct connection between the two; as the temperature in the pyrolysis increases, the porosity and surface area increase accordingly [24, 217–219]. Sun and Lu [68] presented the implications of biochar particles enhancing macroporosity and mesoporosity in clay soils and biochar-soil agglomerates stability, including the rearrangement of soil pores distribution.

iv. Hydrophobicity/Hydrophilicity

The definition for hydrophilicity, hydrophobicity, and WHC is the attraction, repulsion and holding of water molecules, respectively [152]. As discussed earlier, the

use of biochar as a soil amendment or as a soil stabilization agent these properties plays a very important role. It is necessary to know that hydrophilicity and hydrophobicity are related to and dependent on surface characteristics and surface functional groups [213]. Water holding capacity is adsorption related to the porosity and specific surface area. It has also been discussed earlier that the surface functional groups are high at low pyrolysis temperature, and as such, as the temperature decreases, the surface functional groups increase. Thus, biochar produced at lower pyrolysis temperature has high surface functional groups, is hydrophilic, and biochar produced at high temperature has low surface functional groups and is hydrophobic. The high temperature converts the biochar into a hydrophobic character by breaking down the functional groups into simpler compounds [155]. But the water holding capacity of biochar is working in the opposite direction to the hydrophilicity/hydrophobicity. The increase in pyrolysis temperature creates more porosity in biochar, as such, the WHC of biochar increases [157]. Since hydrophobicity is the repulsive action, so hydrophobic biochar lowers the attraction for water uptake by the plant, WHC, and microbial interactions. It has also been observed that even though the hydrophilic biochar is produced at low temperatures, hydrophilicity may be reduced by increasing the pyrolysis residence time [25]. Besides, Patwa et al. [212], during a study on saturated biochar-soil mixes, reported that hydrophilic and hydrophobic networks of biochar induce the separation distance between soil particles, resulting in a decrease in the electrostatic force of attraction and drops in cohesion forces.

v. Aggregate stability

The stability of the aggregates in soil affects the retention and movement of air, water, and nutrients in the soil. The soil profile is composed of a heterogeneous matrix of sand, silt, clay, and traces of other organic and inorganic materials. The soil aggregates usually break down into macro-aggregates and then into microparticles of sand, silt, and clay when in water due to pressure of entrapped air and other reasons like low cohesion between soil particles. The literature shows that the stability of the soil aggregates increased due to biochar addition [220, 221], even though some researchers noticed stability of coarse soil more than fine after the addition of biochar [6, 220]. The physical properties of soil like infiltration and erosion are affected by soil aggregation [220, 222]; stable soil aggregates show good infiltration and less erosion and vice-versa. But contradictory results showing no effect on soil aggregation were also noticed by researchers [223].

vi. Hydraulic properties

There are contradictions in the literature about the water retention capacity of biochar; few researchers noticed that the hydraulic conductivity decreased when the

soil was amended with biochar [224–228], and some observed no effect [6, 48, 99, 229].

#### 2.1.5.2 Chemical Properties of Biochar

##### i. Surface Functional Groups

During pyrolysis, the chemical bonds in the feedstock break at a temperature of 350°C – 650°C and giving rise to new chemical bonds to form new functional groups (e.g. carboxyl, lactone, chromene, lactol, phenol, anhydride, ether, pyrone, pyridone, pyridine, and pyrrole) [230]. **Figure 11** and **Figure 12** show an example structure over the outer surface of the sheets of graphene [53, 231] and pores [47, 53, 232]. The oxygenated hydrocarbon functional groups dominate the surface of biochar in FTIR, considering the carbohydrate structure of cellulose and hemicellulose [53, 233]. The adsorption bands of feedstock are broken down in the pyrolysis process, and during the process of biochar formation, new bands are formed. In their study, Ghani et al. [233] conducted using sawdust biochar, pointed to a large band between 3000 and 3600  $\text{cm}^{-1}$ , peak maximum at 3339  $\text{cm}^{-1}$ , with a smaller band from 2700 to 3000  $\text{cm}^{-1}$  (maximum at 2907  $\text{cm}^{-1}$ ) [53, 233]. The band centred at 3339  $\text{cm}^{-1}$  was attributed to the presence of OH functional groups (alcoholic and phenolic) [234], while the band at ~ 2907  $\text{cm}^{-1}$  was attributed to alkyl C–H stretching [53, 235]. The band at 1600  $\text{cm}^{-1}$  was attributed to aromatic C–C and C–O stretching of conjugated ketones and quinones [53, 236]. The band at 1735  $\text{cm}^{-1}$  was attributed to the C=O stretching of ketones, aldehydes and esters [53, 237]. The band centred at 1238  $\text{cm}^{-1}$  was attributed to C–O–C groups and aryl ethers, phenolic associated with lignin [53, 238]. The intense band occurring at 1130  $\text{cm}^{-1}$  was characteristic of C–O–C stretching of ester groups in cellulose and hemicelluloses [53, 239]. These bands are typical for the FTIR of biochars [53, 54, 233, 235, 238, 240]. Observations have also been made that biochar produced at high temperatures possesses a high aromatic structure and surface area, which sequester increased carbon and help in environment remediation [57]. Nevertheless, it has also been noticed that an increase in pyrolysis temperature breaks down the structural and textural properties and decreases the surface area, as observed by [39, 41]. Ramola et al. [39] noticed a maximum surface area at a temperature of 500°C, which they observed decreased beyond 700°C. Ahmad et al. [58] and Ghanim et al. [59], in their experimentation, took notice that the carbon content increased due to an increase in pyrolytic temperature while the quantities of nitrogen, oxygen and hydrogen got decreased, perhaps due to decarboxylation and dehydration. The condensation of aromatic carbon structure at higher pyrolytic temperatures resulted in decreasing O/C and H/C ratios [60]. The increase in carbonization and loss of polar functional groups results in a decrease in the O/C ratio decrease. Removal of hydroxyl groups is caused by dehydration, and decarboxylation causes carboxyl and carbonyl group removal [61, 62].

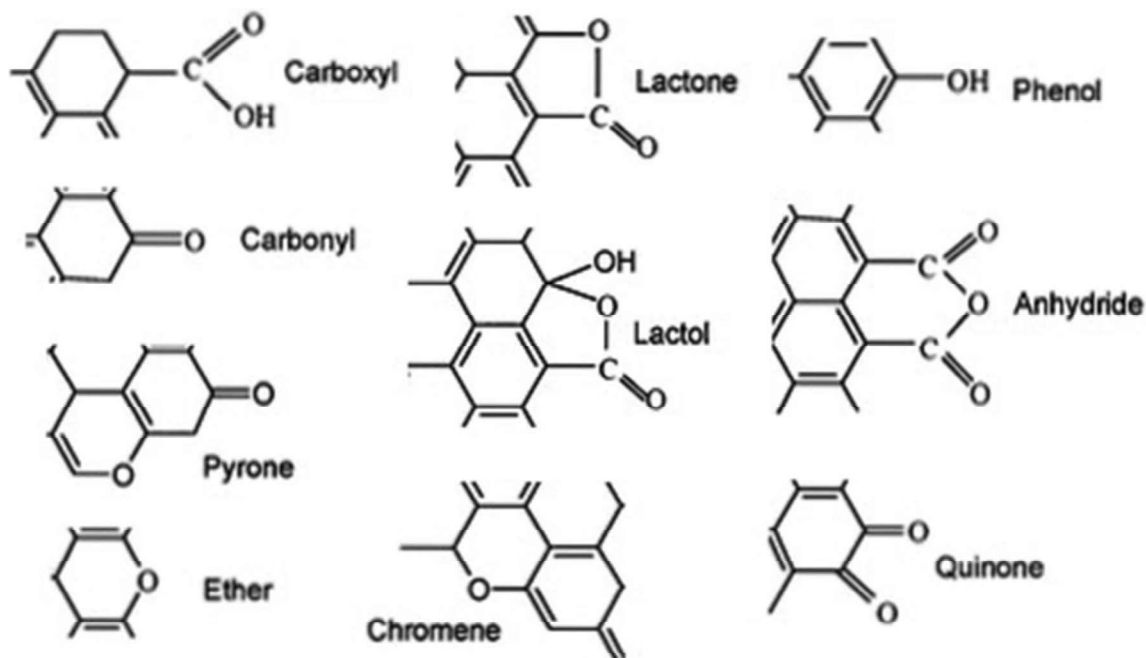


**Figure 11** Biochar surface acidic functional groups [53]

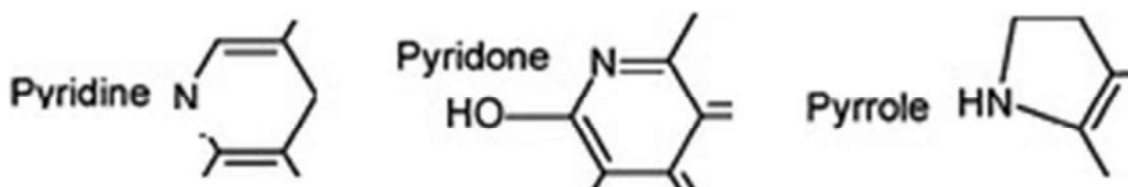


**Figure 12** Biochar surface basic functional groups [53]

**Figure 13** shows how the temperature affects the structure of biochar and different functional groups. Biochar obtained at a temperature of 600°C – 700°C It has been observed to possess high hydrophobic nature and organized C layers [53, 241]. Due to dehydration and deoxygenation of the feedstock, it has less content of H- and O- containing functional groups [53, 241, 242]. The electrons are donated and accepted by the surface functional groups and result in acidic or alkaline and hydrophilic or hydrophobic properties due to coexisting areas [53, 243]. The ion exchange capacity is less [50, 53]. However, biochar's aliphatic and cellulose-type structures produced at comparatively low temperatures (300°C – 400°C) possess a diversified organic character [4, 50, 53]. Probably it appears that the biochar produced at low temperature possesses more compact C layers (like graphene), and the quantum of functional groups is less [26, 53].

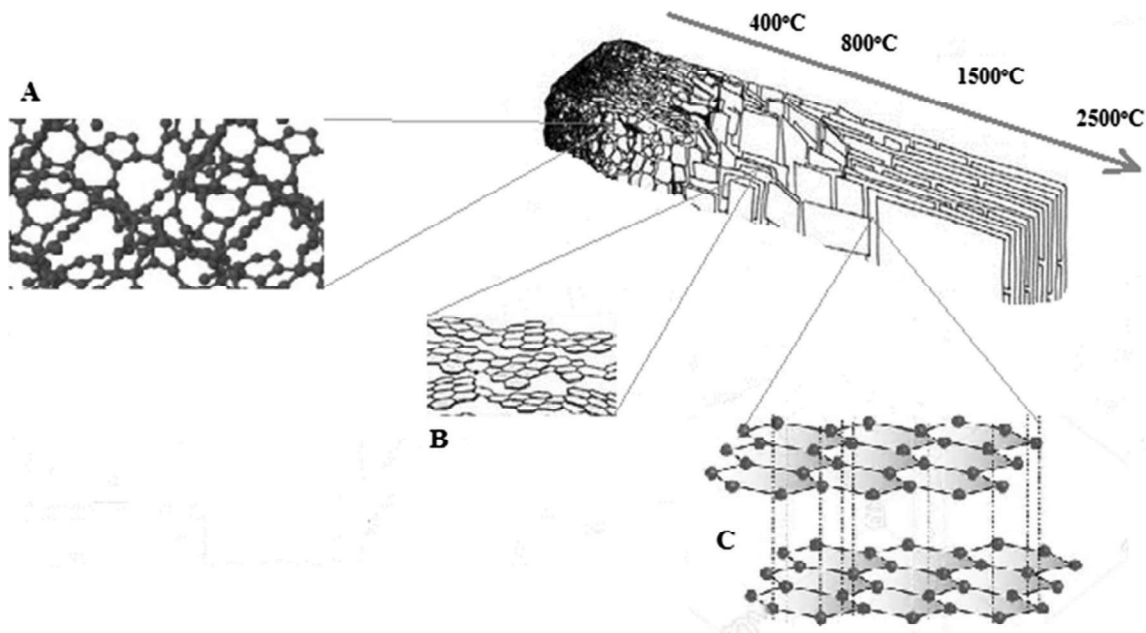


**Figure 13** Pyrolysis temperature effect on biochar: (a) amorphous carbon; (b) turbostratic carbon; (c) graphite carbon [53]

Cation exchange capacity (CEC) represents the cations available on the material's surface for the exchange. The nutrients, particularly in forms N, P, K, Cu, Zn etc., are present in the fertilizers as cations replace negative ions on the biochar surface. CEC is dependent on the pyrolysis temperature. Less the slow pyrolysis temperature, more is the CEC. In such conditions, the biochar has more porosity, less volatile content and negatively charged surface functional groups are not lost at lower temperatures [244]. CEC, pH and hydrophilicity/hydrophobicity determines the surface functionality of biochar; however, adsorption property is dependent on the properties like surface area, porosity and surface functional groups of biochar. Biochar has been observed as a good adsorbent of nitrates and phosphates[245], removal of carcinogenic Congo-red dye [246] and CO<sub>2</sub> adsorption [199].

ii. Elemental composition and functional groups

Elemental composition of biochar is the basis of aromatic biochar structure. C, H, N, and O are the main constituents of biochar (Zhang et al., 2015b). Besides this, main elements, Ca, Mg, Fe, S, Si, P, K, Zn, Cu, etc., are also present in biochar depending on feedstocks [247]. Depending on pyrolysis temperature, H and O elements decrease with increased temperature [248, 249]. Various functional groups, like -OH, -COOH, -C=O, and -COOR present on biochar surface, mainly determine cation exchange capacity, electro-kinetic potential, and alkaline biological carbon. In addition, functional groups associated with biochar also determine hydrophobic or hydrophilic surface and acidic or alkaline conditions. Zhang et al. [208] summarized

that pyrolyzing temperature governs the functional groups associated with biochar surface. For example, at 250°C–350°C, functional groups are significantly reduced due to decarboxylation and esterification, which reduces the carboxyl content and increases the hydroxyl content [208, 250, 251]. At high temperatures (500°C–700°C), aromaticity increases on biochar surfaces, and alcohol groups are converted to phenolic hydroxyl groups, increasing the content of functional groups on biochar surfaces [252, 253].

iii. Volatile matter

The biochar structure, release of volatiles, and formation and volatilization of intermediate melts depend upon the pyrolysis temperature [254]. If the temperature increases for the pyrolysis process, the quantity of volatiles produced is less in biochar [255, 256]. Zhao et al., in their study, when increased the pyrolysis temperature for the production of apple tree biochar, the quantity of volatiles decreased from 60.8% to 14.9% [54]. The same may be because the high temperature causes the breakdown of volatile fractions into low molecular liquids and gases [51]. Also, the hydroxyl groups may dehydrate, and more and more thermal degradation may occur due to increased temperature [56]. The hydroxyl, carbonyl, carboxyl and hemiacetal compounds have been found in biochar produced at low temperatures, and pyranones, ethers and quinines in biochars produced at high temperatures [257]. Antal and Grønli [130] reported that oligosaccharides dominated biochar as the temperature elevated to 290°C through the initial pyrolysis phase at temperatures up to 250°C. Phenols and furans appeared in biochar. Above a temperature of 290°C, alkyl furans, benzenoid aromatics, and condensed aromatics mainly formed a composition of biochar produced. The stability of the biochar is affected by the volatile content present in it [258], its N availability [259], plant growth [259, 260] and its sorption capacity [187]. The micropores on the surface of biochar get filled by the volatile components, dominating the surface of biochars. At higher production temperatures, the pores release the volatile matter, making them accessible to ions [187]. The amount of volatile matter can alter the growth of plants in two ways: toxic compounds such as phenol can cause inhibitions in the root growth, whilst oligosaccharides, produced in the first two steps, can act as labile carbon for microbial deterioration [261].

iv. Carbon and ash content

As the temperature of production increases, the carbon and ash contents of biochar also increase [262, 263]. If the biochar contains a high carbon content, it is understood that probably some amount of original organic plant remains as cellulose may still be present in the biochar [264]. Rafiq et al. reported that ash content increased by 5.7–18.7% by increasing the temperature of the production process [265]. The researchers attributed the progressive concentration of inorganic constituents and OM

combustion residues as causes for increased ash content [54, 110, 266]. Zama et al. attributed an increase in the concentrations of Mg, Ca, K, and P on biochar types pyrolyzed at higher temperatures due to the increase in ash content (ranging from 4.0% to 33.1%). Mineral matter forming ash remains in biochar following carbonization [21, 53, 267]. Due to high pyrolysis temperature, a higher polymerisation degree causes increased carbon content (ranging from 62.2 to 92.4%) [267], making the carbon structure more condensed in the biochar [1]. The same was observed in orange pomace biochar, where the carbon content increased when pyrolysis temperature was increased (ranging from 56.8% to 68.1%) [256]. Cantrell et al., however, noticed a decrease in the carbon content of poultry litter biochar when the pyrolysis temperature was increased (ranging from 27.0% to 35.5%) [268]. It has been noticed that biochar which has a greater degree of formation of aromatic structures, provides more resistance to degradation by microbes [218]. Higher amounts of PAHs and trace metals have been found in high ash content biochars [269]. Preliminary works have recommended that rigorous control of the feedstock and pyrolysis conditions caused a substantial decline in the emission levels of atmospheric pollutants (e.g., PAHs, dioxins) and particulate matter associated with the production of biochar [270].

v. pH

The pH (hydrogen potential) is the common scale for determining the acidity or alkalinity of biochar. It is the concentration of hydrogen ions in a liquid. It has been observed that the feedstock, which is generally acidic, changes to the alkaline character by the pyrolysis process in which the acidity is reduced by the release of the acidic functional groups such as carboxyl from their sites [244]. Generally, the pH of biochar is between 5.9 to 12.3 [197]. The temperature in the pyrolysis process has been observed as one of the basic parameters to determine the pH. As such, the addition of biochar neutralizes the acidity and raises the basic nature of soil [271]. Studies observed that at higher pyrolysis temperature, biochar produced has higher pH [51–54]. Researchers have observed contradictory results also. Studies like those conducted by Nguyen et al. and Zhang et al. [55, 56] noticed that biochar produced at 350°C to 600°C was acidic.

The acidity or the alkalinity (pH) of particular biochar is dependent on the functions of the carbonate formation and the inorganic alkali content [272]. The alkali character of biochar is due to the presence of these groups [273]. As stated above, the high pyrolysis temperature causes an increase in the pH of biochar due to an increase in the total base cations and carbonates (ranging from 6.5 to 10.8) [53, 273]. Also, the ash content and the oxygen functional groups produced due to high pyrolysis temperature increase the pH [51, 52, 54]. The alkaline character is further enhanced due to drying out of acidic (–COOH) and the presence of basic functional groups [248]. But the primary factor responsible for the increase in the pH is the high pyrolysis

temperature which separates the alkali salts and organic salts [272, 273], whereas the decomposition of cellulose and hemicelluloses takes place around 200°C – 300°C, yielding organic acids and phenolic substances that decreasing the product's pH [274]. At around 600°C, pH becomes almost constant due to the release of the alkali salts from the pyrolytic structure [275].

vi. Surface area and porosity

Increasing the temperature in the pyrolysis process leads to an increase in the surface area of biochar and porosity, which may be due to the organic matter decomposition and formation of micropores [53, 208, 276, 277]. Zhang et al. [208] summarized that carbonization retains micro-porosity in biochars, thus, resulting in increased surface area and porosity. It was observed that when the temperature reaches greater than 650°C, biochar becomes hydrophobic and thermally stable [53, 233]. Rafiq et al. [265] observed that increasing the temperature in the pyrolysis process drives off the pore blocking substances or cracks them thermally, thus increasing the surface area accessible externally. Similarly, Ahmad et al. [278] reported that soybean stover biochar and pine needles biochar synthesized at 700°C have a surface area of 420.33 m<sup>2</sup>/g and 390.52 m<sup>2</sup>/g, which are significantly higher than those synthesized at 300°C, surface area of 5.61 m<sup>2</sup>/g and 4.09 m<sup>2</sup>/g, respectively. In contrast, It was observed that biochars were obtained from poultry litter (17.7 m<sup>2</sup>/g) [50], cottonseed hull (4.7 m<sup>2</sup>/g) [237], and dairy manure (13.0 m<sup>2</sup>/g) [266] had low specific surface area and ash contents [53]. Besides, biochar obtained at high temperatures has a high surface area, high adsorption power and function as environment contaminant remediators and carbon sequesters [279]. In contrast, excessive heating of feedstock during pyrolysis may result in volatilization of organic compounds, with blockage of pore spaces and reduction of the surface area [39, 41]. The temperature to acquire the optimum surface area is also not discussed in literature except Chia et al. [280] and Ramola et al. [14], who suggested the optimum temperature is about 800°C and 900°C, and 500°C, respectively.

2.1.5.3 Biological properties of biochar

Various biological activities occur in and on the surface of the BAS. A safe habitat is provided by the biochar's porous structure that helps in its growth on and on its surface. The protozoa, mites, nematodes, and other soil biota use these micro-organisms as food and simultaneously help reduce greenhouse gas emissions. More the toxicity, less is the density of the microbes making the toxicity analysis of biochar necessary. Toxicity is caused by heavy metals, which are usually present in the parent feedstock of biochar, e.g., sewage sludge, textile dyeing sludge, etc. Observations have been made that a nitrogen atmosphere during pyrolysis causes more toxicity than a CO<sub>2</sub> atmosphere [281]. As such, to reduce the toxicity in the biochar, the pyrolysis process has to be more refined [281, 282].

## 2.2 Influence of biochar on the Water Holding Capacity (WHC) of various soils

The soil-water characteristic curve (SWCC) is a graphical plot between soil water content and water stress or suction in the soil's pores. It is a reflection of water in the soil and is dependent upon many factors. Some important ones are particle size distribution, pore size distribution, soil structure, and soil texture.

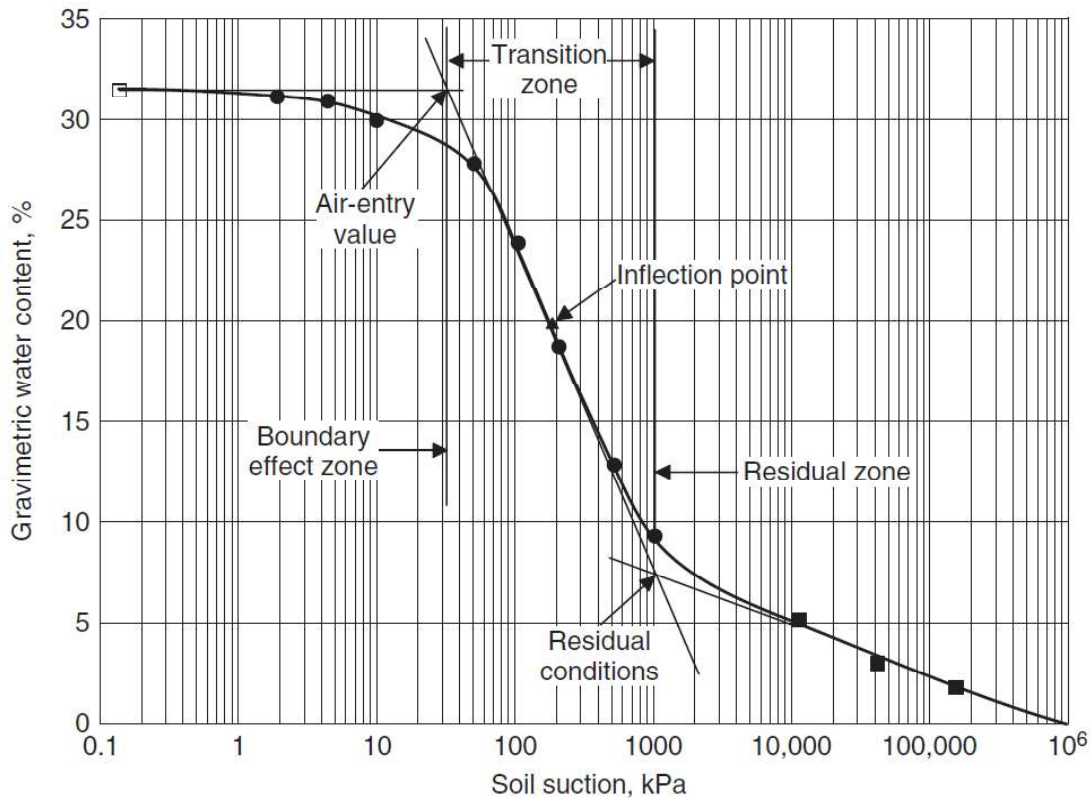


**Figure 14** Typical SWCC showing distinct zones of desaturation [283]

SWCC is defined as the relationship between the water content and soil suction. Water content is defined as the amount of water in the soil pores. The suction may be the matric suction (capillary pressure) or total suction (matric suction + osmotic suction). The forces including capillarity (surface tension), evaporation, transpiration, and osmotic pressure difference (movement of water from high concentration salt solution to low concentration) make water move in soil pores in the vadose zone (above the water table). This force (pressure) can be above or below the atmospheric pressure but is termed negative pore water pressure. The water table is taken as a reference, or zero. The pressure in these pores is due to the gravitational head (relative position) and its potential head (location). Water below the water table is in hydrostatic equilibrium, but above the water table, it flows from higher potential (higher pressure) to lower potential. It is worthwhile to mention that if there were no other forces except gravity, the soil in the vadose zone would have been dry. The gravitational forces cause infiltration, but the physical and chemical changes cause capillary action, evaporation, and transpiration, making the soil

layer suck water towards the top surface. This sucking force is called soil suction [177]; in other words, the attraction of dry soil towards the water in the vadose zone is called soil suction. The measurement of soil suction is the measurement of the attraction of soil towards the water. Mathematically suction is pressure differences between air pressure ( $u_a$ ) in the field and vapour pressure in the vadose zone ( $u_w$ ). The soil suction is measured either by piezometers or indirectly by measuring humidity and converting the measurement to soil suction. Soil suction or negative pore water pressure is important to developing strength and volume changes in the soil above the natural water table. It plays an important role in the engineering behaviour of unsaturated soils. Soil suction presence is particularly important in studying slopes [284]. If pore water pressure increases, stability brought about by suction-induced strength can be compromised [284, 285]. Soil suction consists of two major components: matric and osmotic suction.

Matric suction is associated with the capillary effects, evaporation and transpiration [284]. It has also been suggested that adsorption on solid surfaces may contribute to matric suction. Matric suction varies with time, mainly due to environmental changes [286]. It is represented as  $u_a - u_w$ . Matric suction (usually referred to as suction) is negative. Osmotic suction is closely related to the pore water's salt content or ionic concentration. It is represented as  $\Pi$ . Osmotic suction is due to the high salt concentration solution movement toward the low salt concentration solution. Osmotic suction is present in both saturated and unsaturated soils. As such total suction,  $\psi = (u_a - u_w) + \pi$ . Any change in suction affects the overall equilibrium of the soil mass.

The pressure above the water table is considered negative (although it may not be negative). When there is infiltration (due to rainfall or runoff), the soil gets wet. The pressure difference is reduced, and as such, matric suction is also gets reduced. As such, matric suction increases due to drying and decreases due to wetting [287]. The increase in matric suction causes pore water to come out, and air enters the pores. The value of matric suction at which air enters the largest pore is called air entry value. A stage is reached when further dryness does not change the value of matric suction, and any further water (vapour) does not come out of pores. The value of this water content is called residual water content. The graphical representation and relation of this available water content or its increase and decrease of soil suction is called the Soil Water Characteristic Curve. The water content is plotted along (Y-axis) and soil suction (X-axis) in the graph. Soil Water Characteristic Curve (SWCC) describes the amount of water retained in a soil (expressed as mass or volume water content) under equilibrium at a given matric potential [288–290]. The slope of the line at any point gives the water content at that point. It has been observed that the tensile strength of unsaturated soils is not constant but a function of soil suction. It increases with the increase in matric suction. Capillary forces (matric suction and capillary bonding) also contribute to tensile strength in cohesionless soils [291].

The flow of groundwater and slope stability of unsaturated soils can be investigated with SWCC [287, 292]. A typical SWCC is plotted and shows SWCC can be categorized into saturated, transition and residual zones. Pore water is not flowing out in the saturated zone until the matric suction exceeds the AEV [293]. Air entry value (AEV) is defined in Fredlund and Rahardjo [294] as the matric suction value exceeded before air recedes [295] into soil pores. In the transition zone, the air flows into the pore as the matric suction increases [287], and thus, pore water flows out. The characteristic of the transition

zone determines the slope of the SWCC. For the residual zone, while the matric suction increases, no water is flowing out. The constant VWC, which is called residual water content, is maintained.

Gravimetric water content (GWC) is used to define water content in geotechnical engineering, but for SWCC, volumetric water content (VWC) is usually adopted. Gravimetric water content (GWC) is the mass of water per unit of dry soil.

$$w = \frac{M_w}{M_s}$$

*Equation 1*

$w$  = gravimetric water content;  $M_w$  = mass of water;  $M_s$  = mass of soil solids

Volumetric water content is the volume of water per unit volume of soil and is expressed in the percentage of volume.

$$\theta = \frac{V_w}{V_v + V_s}$$

*Equation 2*

The transition points sub-divide the SWCC into the boundary effect zone, transition zone and residual zone. These zones determine the drying and wetting of the SWCC.

Saffari et al. [296] investigated the effects of corn residue biochar produced at different temperatures on the SWCC, soil penetration resistance, plant available water (PAW) and the available water content (AWC). It was observed that biochar produced at a temperature of 350°C at 2% biochar amendment indicated more enhancement in the SOC than control. A biochar amendment of 4% presented considerable changes in the WHC of the BAS irrespective of the temperature at which the biochar was produced. The improvement in the WHC of the soil using biochar is mainly attributed to the alteration of the pore size distribution of the BAS increase in the pore spaces and soil surface area [296–298]. Xing et al. [299] investigated the effect on the water retention capacity of sandy loam soils with biochar addition. Biochar was added to soil in percentages of 5%, 10% and 15% and then compacted. Biochar addition into the sandy soils decreases water infiltration in the soil. This reduces the percolation of water and decreases water loss from soil. It was observed that biochar addition decreased water infiltration, enhancing the WHC of the BAS. Biochar addition caused a decrease in the formation of inter-particle pore size, which caused an enhancement in the capillary action, thus increasing the WRC. The presence of the hydrophilic groups contributes to improving the WHC of the BAS. However, biochar causes different behaviour in different soils. If added to clayey textured soils, it may have adverse effects. It may not allow water to enter the soil and reduce infiltration. Zhang et al. [219] investigated the effect on the particle sizes of biochar produced on soils having varying textures. It was that at 2% biochar amendment and increase in the PAW was observed for sand (2.8% to 6.1%), silt loam (20.3% to 27.9%) and clay (22.5% to 26.5%). Lei and Zhang [29] investigated the effect for biochar addition on the properties of soil, physical and hydraulic. Two types of biochar were used, dairy manure and wood chip.

It was observed that treatment of soil with biochar increased both saturated hydraulic conductivity and WHC of the BAS.

**Table 3** Preparation of biochar using various biomass and its testing on different soil properties

Feedstock (Biomass)	Soil type	Application	Pyrolysis conditions		Objectives	Studied parameters	Results	References
			Temperature	Pyrolysis time Heating rate				
Olive stone (OSB), almond shell (ASB), wheat straw (WSB), pinewood chips (PWB), olive wood pruning (OPB)	Haplic levisol (Spain)			368°C – 507°C, 1.6 hours to 2.9 hours,	Investigate different biochar types on soil variables, pH, field capacity, bulk density, nutrient content, plant growth, etc.	Ash content by muffle furnace, pH by Supernatant with pH meter, organic C and organic N by elemental analyzer	The addition of Biochar enhances field capacity and decreases the bulk density	[300]
Water hyacinth	Silty sand mixture	engineering		300°C – 350°C 45 minutes	Investigation of water retention and permeability of gas of BAS and relation with SWC in an unsaturated state	Compaction, TGA, gas permeability	Decrease of $k_g$ for soil and BAS	[301]
Two scoria – green roof substrates		Agriculture		550°C, 45 min, 5 – 10°C / min	Investigation of chemical and physical properties of testing of BAS, Effects of substrates and additives on wheat biomass and allocation	Drought Experiment for one season	The addition of biochar increases WHC and plant available water	[302]
Water hyacinth	Sand clay mixture	engineering		350°C – 400°C	Investigation of water retention and gas permeability of BAS and its relationship with water content in an unsaturated state	FTIR, permeability experiments, Compaction, Measurement of CIF with a digital camera, VWC by Decagon devices, MPS – 6 and EC – 5 sensors to	The addition of 5 – 10 % of biochar could decrease gas permeability up to 50 – 65 %, the presence of biochar content increased SWC, and gas permeability increased linearly with soil suction	[93]

					measure suction and VWC, respectively,			
Water hyacinth	Sand clay mixture	Engineering	300°C – 600°C 40°C./min	Investigation of CIF, suction and VWC on infiltration rate for compacted SBC	Measurement of CIF with a digital camera, VWC by Decagon devices, MPS – 6 and EC – 5 sensors to measure suction and VWC, respectively, FE – SEM, 63 days	The addition of biochar decreased CIF and rate of infiltration and enhanced WRC	[92]	
A by-product of birch charcoal	Silt Loam	Agriculture	400°C, 2–2.5 h	Investigation of CH <sub>4</sub> uptake by adding biochar to agricultural soils	WHC, CH <sub>4</sub> absorption	increased soil WHC and CH <sub>4</sub> absorption because of soil aeration	[303]	
Magnolia tree leaves, Corn, Applewood chips	Clay rich Hapludert, well-drained sandy Alfisol, heavy clay Vertisol	Agriculture	300°C – 700°C 4 hours 5°C/min	Effects of properties of feedstock variation and temperature of pyrolysis on hydrologic behaviour of biochar and BAS	Determination of field capacity, WDPT, MED, FTIR, NMR, BET measurement	Field capacity and hydrophobicity of biochar depend upon feedstock and pyrolysis conditions. Biochar produced at 400 °C to 600 °C has the most desirable hydrological properties	[304]	
Wood chips and dairy manure	Forest soil		300°C, 500°C, 700°C, 10°C /min, 1 hour	Measurement of soil physical and hydraulic properties	Hydraulic conductivity by falling head method, FTIR, SEM, 180 days incubation period,	Biochar addition promoted soil aggregation, decreased soil bulk density, simulated microbial activity, increased saturated hydraulic conductivity and WRC	[305]	

straw biochar, woodchips biochar, Sludge biochar	Vertisol	Soil remediation, engineering	500°C, 2 hours	Study the possible positive effects of biochar, wastewater sludge and fly ash on physio mechanical parameters, including Atterberg limits, expansion and shrinkage and strengths on typical vertical soil	X-ray diffraction, standard methods for measuring physical and chemical properties, consistency limits, DST, crushing method	Plastic limit decreased for all amendments; liquid limit showed correlation with an angle of friction and tensile strength, a significant reduction and coefficient of linear extensibility reduced for all amendments	[306]
Dairy manure	Silty clay and sandy loam	Engineering	500°C, 1 hour	biochar amendment effect on the aggregate formation, stability and hydraulic properties of soil	Vario EL, (Elementar, Germany), SEM 90 days	The addition of biochar enhances the formation of macroaggregates and increases the hydraulic conductivity of the soil. Biochar amendment increases the saturated water content and decreases residual water content	[6]
Wood chips	Sandy loam	Agriculture	450°C, 4 hours	Comparing effects of vermicompost and biochar on SOC fractions and carbon mineralizations when applied with inorganic fertilizers	C mineralization study, soil analysis, plant analysis, two years	Upholding productivity, sequestering high SOC compared to vermicompost	[307]
deciduous mixed wood feedstock of sycamore, oak and bird cherry	Sandy loam	Agriculture	Up to 600°C, 16 hours	Effect of addition of biochar on SWR and nitrification process in organic and conventional management soils	Physical characteristics of biochar analyzed using mercury porosimetry and BET, organic C, N, and H analyzed by combustion	Reduction in bulk density and increase in soil moisture retention in sandy loam soils	[308]
Peanut shell biochar	clay	Soil remediation, engineering	500°C, 30 – 40 minutes, 5- 10°C/min	Study of the behaviour of retention of soil water in the clay, landfill cover material	VET, moisture content determination, microstructure analysis SEM with EDX	Biochar applications increase soil WRC of BAC, BAC potential landfill cover soil	[309]

Peanut shell	Kaolin clay	engineering	500°C, 30 minutes	Biochar effects on hydraulic conductivity of compacted clay	Hydraulic conductivity, microstructure analysis	Increase in $k_{sat}$ and compact use of BAC as a landfill cover material	[310]
--------------	-------------	-------------	----------------------	---	---	---	-------

### 2.3 Influence of biochar on erosion control

Around 44% – 93.7% of C content is present in the biomass, which can be ascertained by the feedstock, conditions, and methods used for production [97, 98]. Biochar quantity and quality rely on the type of pyrolysis process utilized [14, 34, 107, 141, 311] and the process conditions. The quality and quantity of biochar can be constrained in different pyrolysis processes, and a considerable quantity can be produced with cost-effectiveness. Some pyrolysis processes can be considered helpful for engineering purposes like soil erosion control [145, 164, 171].

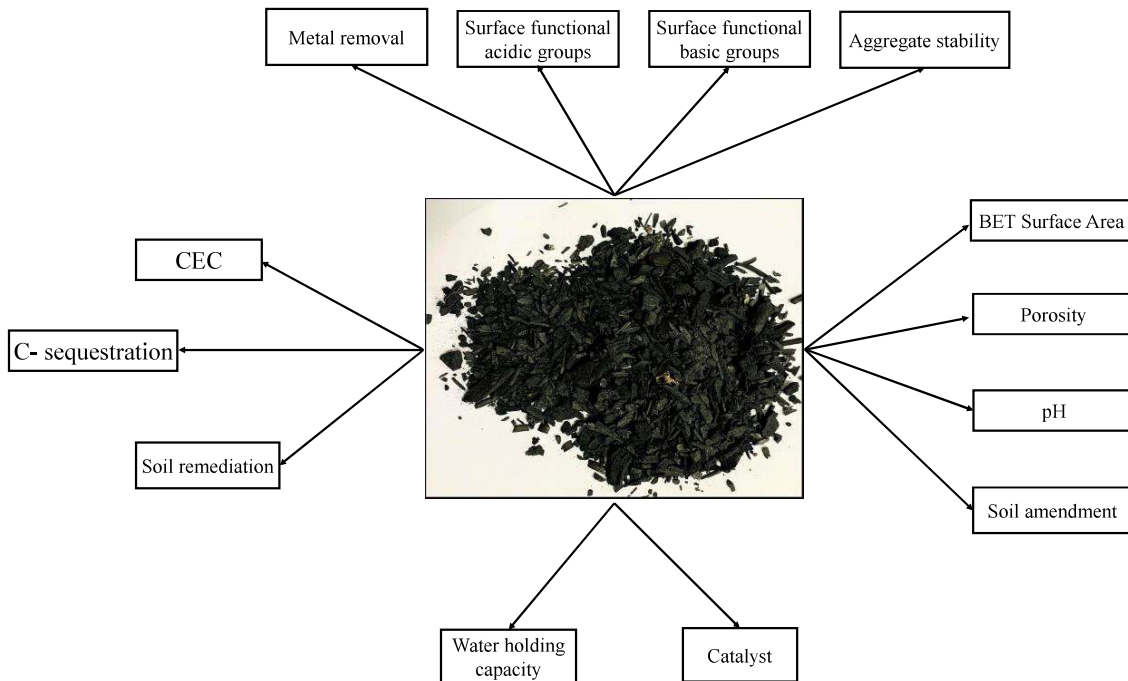


**Figure 15** Physicochemical properties of soil

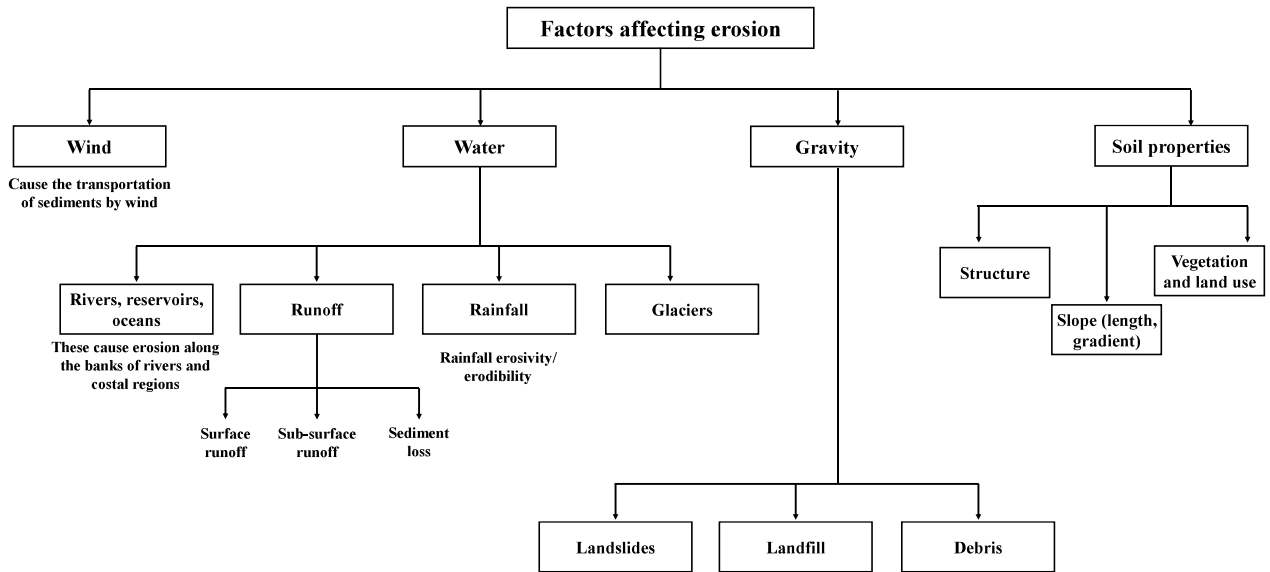


Figure 16 Factors affecting erosion [312]

As mentioned above, there are contradictory results for the influence of biochar on soil erosion. A detailed review is needed to analyze the mechanism of soil-biochar-water interaction in an erosion process. In addition, there is a lack of clarity as to what production process of biochar is adopted in studies related to erosion control. There is a need to explore a suitable production process of biochar that involves quality control and can be scaled for usage as construction material. To date, pyrolysis seems to be a popular production process for biofuels. However, biochar production using some pyrolysis processes is not very common on large-scale commercial projects. Also, the analysis of these pyrolysis processes and their economic aspects regarding capital and running costs for the large-scale production of biochar using pyrolysis needs technology implementation and research. A review is needed to analyze the feasibility of pyrolysis for biochar production for controlling soil erosion.

### 2.3.1 Physical Properties of Biochar and Erosion control

#### 2.3.1.1 Particle size distribution

The researchers are of the opinion that the WHC of fine biochar particles is higher than that of coarse particles [313]. In their experimentation, de Jesus Duarte et al. [314] noticed that particles of biochar of size less than 0.15  $\mu\text{m}$  held water much better than those of larger size. Similarly, when clay-rich soils were amended with biochar, Lim and Spokas [315] noticed an increase of 328% in saturated hydraulic conductivity. However, the influence of particle size of biochar on soil erosion does not seem to have been investigated as far as the author is aware of the literature. Taking full advantage of the available data in a few papers in the literature on the subject, a table has been framed (Table 4) showing the influence of fines (clay, silt, sand and biochar); however, a final trend has been framed of results could not be found. An attempt was made to develop a relationship between the fines and the biochar, their influence, effect of change in quantities and effect of raw materials, as shown in Table 4. The parameters selected

were rainfall rate, soil type, grain size distribution, ratio (fine/sand), biochar type, and content. An observation, however, came out from the table that by keeping the fine materials constant, there was a reduction in total flow and corresponding soil loss. But the WHC of the fine materials also reduces at a specific limit, resulting in the decrease of infiltration and increase in run-off and corresponding loss of soil due to erosion. In **Table 5**, a few other parameters like test duration, annual average rainfall, soil type, grain size distribution, ratio(fine/sand), biochar type, and content were taken from the studies (in the literature) to find a relation of these parameters with total run-off and the total loss of soil. It was observed from the results of these selected studies tabulated in **Table 5** that a 5% biochar amendment was an optimum biochar amendment percentage for controlling soil loss (erosion), beyond which the soil loss again increased. The loss of soil quantity was found to increase with an increase in runoff; less runoff produced less loss of soil. It was observed that the particle size distribution was directly related to hydraulic properties, nutrient mobility, and heat and air retention properties. Xu et al. [316] observed that the loss of fine soil particles causes soil degradation.

#### 2.3.1.2 Bulk Density

Biochar is a porous material obtained by pyrolysis of organic materials. Its porosity is much more than that of soil materials, making it lighter than soil. Also, the feedstock from which the biochar is obtained plays a role in determining the density of the product. When compared, it is observed that the density of sandy soil is about  $1.5\text{g/cm}^3$ , that of clayey soil about  $1.1\text{g/cm}^3$ , while that of biochar is generally less than  $1.00\text{ g/cm}^3$  depending upon the nature of the feedstock. Therefore, when biochar is mixed with soil, whose density is higher than that of biochar, the composite density is reduced accordingly. The change in the bulk density is directly proportional to the ratio in which the two are mixed. If the quantity of biochar mixed is less, the net change in the overall density of the composite shall be negligible, as was observed by Pratiwi and Shinogi [210] that 2% biochar addition was observed to produce no effects on the bulk density of composite. Some researchers observed a reduction in bulk density due to long-term soil interaction and observed the soil aggregation improvement [190]. Since the researchers have accepted that soil aggregation checks soil erosion, the biochar addition here also adds to the erosion control by adding to soil aggregation.

#### 2.3.1.3 Mechanical Properties

The basic two mechanical strength properties include tensile and shear strength and are the functions of cohesion between the material particles under consideration. More cohesion means more mechanical strength of the material, and less cohesive forces indicate less tensile and shear strength. The soil is considered weak in both tension as well as shear strength. The effect of biochar under such conditions is a topic of investigation. The researchers have put forward contradictory results for these properties in any soil biochar composite. While several researchers have given observations from their studies that these mechanical properties of a soil biochar composite increase, at the same time, many have reported opposite results. In their

study, Zong et al. [87] reported a reduction of 100%–184% in tensile strength when 6% biochar was added to the soil. Another study done by Lu et al. [317] observed a reduction of 164% in tensile strength. Similarly, Zong et al. [193], during their experimentation on wood biochar, noticed a reduction of 42–100%.

The less cohesion between particles of soil or SBC results in an easy breakdown of particles from the parent material by the weathering agencies like wind, water, snow or /and rain; as such, and there is more erosion due to less cohesive forces. If these cohesive forces were strong enough to withstand the effect of these forces, there would have been no erosion. But since the ideal conditions of such strong forces are not possible, increasing the mechanical strength in the soil can reduce the erosion effects. However, the departed particles are carried away by these forces, resulting in soil erosion. On the other hand, it is observed that vegetative growth increases with the decrease in these mechanical forces [48, 87, 262]. However, they are very detrimental to soil engineering and erosion.

As shown in **Table 6**, a study conducted by Kumar et al. [318] to determine soil's erodibility coefficient and critical shear stress. The authors used four different biochar, three from plants (sawdust, water hyacinth, peanut shell) and one from animals (poultry litter) in pinhole tests with soil samples with and without biochar. The results put forth by the authors show that the biochar amended soils could resist erosion more on the dry side than on the wet side of the optimum. The cause for the same as given was the flocculated and the dispersed orientation of the particles along the compaction curve, which is more vulnerable to erosion.

#### 2.3.1.4 Cracking and Atterberg limits

The plastic limit, liquid limit and shrinkage limit are called Atterberg limits. These limits give information about the critical water content at stages of transformation from solid to semi-solid and from semi-solid to a liquid state. The Atterberg limits are, as such, the parameters which provide information about the consistent behaviour of soil. The researchers believe that biochar as a soil amendment modifies the consistency due to organic composition, especially C-concentration [190]. The use of biochar in the soil increases the WRC of the soil, which in turn increases the plastic, liquid, and shrinkage limit. The increase in these limits, in other words, can be said to decrease the runoff (due to increased hydraulic conductivity); therefore, the erosion of soil is reduced accordingly. In their study, Zong et al. [87] reported that the liquid limit increased by 8%–22% and the plasticity index increased by 48%–99%. In a lab experiment, Similar results were reported by Lu et al. [319] for plastic and liquid limits in an experiment conducted in a laboratory. They noticed an increase of 15%–18% in these limit values.

Pan et al. [320], while working on two types of biochar, wooden and manure-based, reported wood biochar is more effective in controlling the expansion of soils. They noticed that higher biochar amendment ratios (5%) were more effective. The authors attributed this

phenomenon of biochar to the various properties of biochar like adsorption capacity, shape and the CEC between the soil and biochar particles. The authors observed that these properties control the movement of water in the soil. In this way, the soil's swelling, shrinking, and cracking (as such weathering) is reduced, thus controlling erosion.

Using rice husk biochar in the percentages amendment, while developing a model, Wani et al. [35] developed an ANN model on the available experimental data of biochar additions of 0%, 2%, 4%, and 6% in soil. They reported that biochar content and plastic limit are important parameters determining crack intensity factors. Higher the value of this factor is the erosion of soil.

#### 2.3.1.5 Aggregate stability

The physical behaviour of the soil, such as hydraulic conductivity and erosion, gets affected by the soil's aggregate stability, especially in water. The combination of organic (biochar) and inorganic (soil) particles under polyvalent cation bonding form micro aggregates. These micro aggregates further add to each other and form macroaggregate [190]. Similar observations were made by Hua et al. [321], who described the formation of the aggregates as a result of physicochemical and biological processes. Many researchers have reported the increase in aggregate stability by biochar addition. Ouyang et al. [6] and Burell et al. [322] reported that the aggregation was more stable in sandy soil than in silty clay and clayey soils [190]. Similar results were reported by Herath et al. [220] and Curaquo et al. [221], who observed enhanced soil aggregate stability with 10% and 4.5% c-concentration, respectively, when compared to bare soil. The literature shows that the coarse soils form more stable wet aggregates with biochar than fine soils and, as such, provide better results of erosion control in coarse-textured soils. However, the contradictory results were reported by a few researchers in this case also. Dong et al. [223] reported that they could not find any increase in the stability of wet aggregates when they added a C-concentration of 0.43 after biochar application.

#### 2.3.1.6 Hydraulic Properties

The ease of movement of water in the soil, which includes WRC and infiltration, defines the hydraulic conductivity of that soil. If water movement through the soil is not easy, the hydraulic conductivity decreases, resulting in more run-off. More run-offs indicate more erosion. Similarly, if the soil allows water to be retained in the soil and allows water to pass through it with ease, the runoff is accordingly reduced, and soil erosion is less. While working on the hydraulic conductivity of biochar amended soils, many researchers have reported an increase in hydraulic conductivity compared to bare soil. [216] observed an increase in unsaturated hydraulic conductivity of clay soil when biochar was added at the rate of 5% and 10%. However, a contradiction in observations was also reported in this field. Zhang et al. [323] reported a reduction in saturated hydraulic conductivity of biochar amended soils in which he used biochar particles of size 5 mm to 8 mm diameter. The literature shows that infiltration and

hydraulic conductivity decrease with biochar amendment in coarse-grained soils. At the same time, it increased in fine-grained (clayey) and compacted soils, but medium-textured soils showed no effect.

**Table 4** Literature indication effect of biochar on erosion taking into consideration soil fines

Study	Test	Rainfall flow rate (mm/h)	Soil type	Sand (%)	Silt (%)	Clay (%)	Ratio (sand/ (silt+clay))	Biochar type	Biochar content	Soil loss rate ( $\text{g}\cdot\text{m}^{-2}\cdot\text{min}^{-1}$ )	Biochar loss (%)	Flow rate ( $\text{ml}\cdot\text{m}^{-2}\cdot\text{min}^{-1}$ )	Remarks
[324]	Flume tests	60	Poorly graded sand	82% (medium) 16% (fine)	2%	0%	41	Water hyacinth	0%	1.254 (infiltration) 1.015 (runoff) 2.270 (Total flow)		370.763 (infiltration) 448.196 (runoff) 818.960 (Total flow)	
									5%	0.574 (infiltration) 0.476 (runoff) 1.050 (Total flow)	15.521	250.428 (infiltration) 304.841 (runoff) 568.532 (Total flow)	The soil loss rate becomes half nearly.
									10%	0.697 (infiltration) 0.770 (runoff) 1.467 (Total flow)	16.063	394.830 (infiltration) 322.629 (runoff) 725.491 (Total flow)	The soil loss rate values are similar to the 0% biochar case.

[325]	100	Loam	Poorly graded sand	82% (medium) 16% (fine)	2%	0%	41	Water hyacinth	0 Mg/ha	10%	0.966 (infiltration) 1.132 (runoff) 2.098 (Total flow)	15.883	467.032 (infiltration) 448.196 (runoff) 915.228 (Total flow)	478.542 (infiltration) 743.279 (runoff) 1221.821 (Total flow)	Similar observations as before. Runoff/Infiltration ratio reduces with the addition of biochar.
	90								0 Mg/ha	0%	1.524 (infiltration) 1.377 (runoff) 2.901 (Total flow)		346.696 (infiltration) 454.475 (runoff) 801.171 (Total flow)		

























[333]	Rainfall simulation	80	Typical Paleodults	16.2	40.2	43.6	0.193	White lead trees	0%	24.300				
									2.5%	12.167				
									5%	8.867				
									10%	4.439 (140 Days) 6.197 (100 Days) 10.101 (60 Days)				
										5.172 (140 Days) 9.846 (100 Days)				

**Table 5** Literature indicating the effect of biochar and soil fines on soil loss and total runoff volumes

Study	Test	Test duration	Annual average rainfall	Soil type	Sand (%)	Silt (%)	Clay (%)	Ratio (sand/ (silt+clay))	Biochar type	Biochar content	Soil loss yields (g/m <sup>2</sup> )	Total runoff volumes
[334]	Field experiment	October 2013-October 2014	1795 mm	Clay	29.1	33.9	3	0.41	Rice straw	0 t/ha	2603	249 mm
										2 t/ha	2115	233 mm
[335]	Field experiment	July 2014-June 2015	2847	Clay	34	27.6	38.4	0.515	wood	0 %	1550	382 mm
										2 %	1750	362 mm
[336]	Field experiment	1 year	1300-1500	Sandy loam					No mention	4%	(Addition of biochar increases yield)	345 mm
										0 t/ha	444 (2016) 456 (2017)	5603.76 mm (2016) 6346.92 mm (2017)



**Table 6** Previous studies indicating soil fines, biochar content, water content, critical shear stress and erodibility coefficient

Study	Test	Soil type	Sand (%)	Silt (%)	Clay (%)	Ratio (sand/ (silt+clay))	Biochar type	Biochar content	Water content (%)	Critical shear stress, $\tau_c$ (Pa)	Erodibility coefficient, $K_d$ (cm <sup>3</sup> /N-m)
[318]	Pinhole erosion test	Silty sand	47	28	21	0.959		0%	11.7	0.259	0.133
									16.7	0.119	0.065
									21.7	0.089	0.022
								5%	14.8	0.154	0.074
									19.8	0.112	0.064
									24.8	0.101	0.042
							10%	Sawdust	20	0.093	0.045
									25	0.101	0.026
									30	0.103	0.034
							5%	Water hyacinth	15.1	0.164	0.080
									20.1	0.306	0.126
									25.1	0.094	0.011
10%		19.1	0.130	0.060							
		24.1	0.109	0.038							



Study	Test	Test duration	Annual average rainfall	Soil type	Sand (%)	Silt (%)	Clay (%)	Ratio (sand/ (silt+clay))	Biochar type	Biochar content	Soil loss yields (g/m <sup>2</sup> )	Total runoff volumes
[334]	Field experiment	October 2013- October 2014	1795 mm	Clay	29.1	33.9	3	0.41	Rice straw	0 t/ha	2603	249 mm
										2 t/ha	2115	233 mm
[335]	Field experiment	July 2014- June 2015	2847	Clay	34	27.6	38.4	0.515	wood	0 %	1550	382 mm
										2 %	1750	362 mm
[336]	Field experiment	1 year	1300-1500	Sandy loam					No mention	4%	(Addition of biochar increases yield)	345 mm
										0 t/ha	444 (2016) 456 (2017)	5603.76 mm (2016) 6346.92 mm (2017)



**Table 6** shows a summary of a pinhole test/experiment on the soil with specific particle size distribution was carried out [291]. The water content and the biochar amendment were varied to obtain the critical shear stress and erodibility coefficient constants. The test results reveal that the increase in the biochar amendment and water content causes a decrease in the critical shear stress and the erodibility coefficient. It can be assumed that the biochar amendment can reduce soil erosion. But very little such knowledge was available in the literature as far as the authors are aware. The results could not be compared to present a more descriptive result. A more comprehensive investigation is also needed in this field to fill the knowledge gap.

### 2.3.2 *The influence of chemical properties of biochar on erosion*

Pyrolysis is the simplest process for biochar production, whether the biochar to be produced is in small or in large quantities. The process removes the moisture content from the feedstock (dehydration) up to a temperature of 200°C, beyond which and up to about 350°C, the decomposition of cellulose occurs. The other constituents, hemicellulose and lignin, decompose at 200°C to 280°C and 280°C to 500°C, respectively. The three main end products, solid, liquid and gases in biochar, bio-oils and syngas, respectively, are formed in the different ratios depending upon the pyrolysis conditions; temperature, heating rate and residence time [141]. The organic material helps make the aggregates of soil stable, but the main component of the organic matter is cellulose [337–341]. Many researchers have stressed the relationship between soil aggregation, stability, and erosion. It has been observed that erosion decreases in soils having suitable soil aggregates.

Water stable micro-aggregates have shown promising results of reduced run-off and soil loss [342, 343]. Researchers have put forth many experimental pieces of evidence that the addition of biochar to soil increases the stability of the aggregates of the soil [220, 343–345]. However, Six et al. [346] observed that soil aggregation is related to and affected by factors like soil – biota, roots growth, mineralogy and texture, soil availability, inorganic binding agents, and environmental conditions. Some other parameters increase the growth of the microbial colonies like high pH, soluble C, and high C/N ratio [339, 347], and indirectly help the soil aggregation [339, 348]. Similar to it, interparticle cohesive forces increase with the addition of organic matter as it causes a reduction in the slaking and dispersion of aggregates [349]. Another research by Bissonnais et al. [350] noticed that a film is formed by the organic matter around the soil aggregates, which is hydrophobic and reduces the wetting of the soil aggregates and prevents them from dispersion. Ferro et al. [351] said that the internal pressure built by air in a soil aggregate is reduced by the soil organic matter, due to which the soil aggregates dispersion is reduced. Exceptions have been observed in the form of contradictions have been noticed [339, 343, 352]. Either very negligible or no effect or even negative effect on the formation of soil aggregates by the addition of biochar.

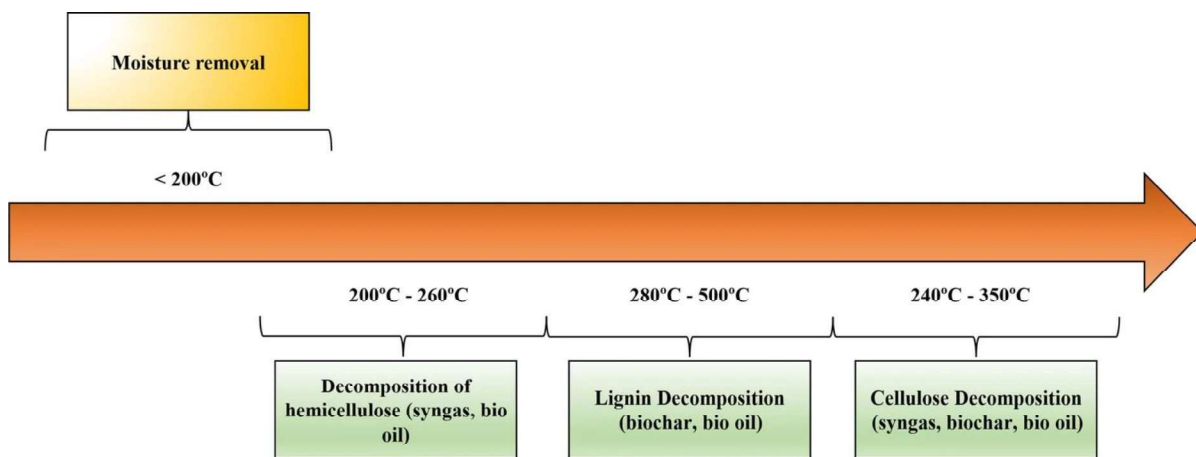


**Figure 17** Decomposition of biomass constituents

The literature shows that one researcher, Zhang et al. [353] in his, experimented with four types of feedstock [wheat straw, corn straw, rape straw, and rice straw] at different pyrolysis temperatures [300°C, 400°C, 500°C, 600°C]. An observation was made that the C-content, stability and structure of biochar prepared at the highest temperature were better than those produced at lower temperatures; however, a decrease was observed in the H, N and O content with increasing temperature. Chatterjee et al. [354], during his work on miscanthus, switchgrass, corn stover, and sugarcane bagasse biochars, gave similar observations [of increase in C-content, ash content, and pH and decrease in O, H, N at 500°C to 700°C. The increase in C-content, pH, surface area, pore-volume and reduction in the values of yield, H, O, and CEC was also reported by Zhao et al. [54]. Sun et al. [355] produced eight types of biochar from different types of biomass like agriculture waste, forest litter, and natural plants at a temperature of 300°C – 600°C. The authors observed that C – content, pH, and basic functional groups increased with temperature and yield, adsorption capacity, and acidic functional groups decreased. Even though there was no noticeable effect of residence time at higher pyrolysis temperatures, the increased residence time decreased yield and raised pH when the pyrolysis temperature was low. Feng et al.[356] in their experimentation put forth opposite results of C-content as presented by other researchers. They noticed a high C- content at low temperatures and low at high temperatures as 56.80% at 300°C and 48.40% at 500°C. He et al. [357] obtained ten pinewood biochar samples and classified their particle size distribution in groups of particle sizes as less than 5 µm, 25 µm – 75 µm, 150 µm – 2000 µm and 5000 µm. The authors observed that the fine-sized particles possess high values of C-content, H/C and O/C and low H, O and N content values. Opposite values were noticed for coarse size particles. Hale et al. [358] could not find a specific relation between physicochemical properties and PAHs while working on 50 types of biochar.

An increase was noticed in the surface area and porosity with increased pyrolysis temperature [24, 217, 218]. As per available literature, the slow pyrolysis biochar has low ash content, pH, CEC, basic functional groups, carbon stability, and total C, N, P, K, Ca, and Mg. The values of these parameters are high in biochar prepared at high temperatures. The values of O/C, H/C, (O+N)/C,

and (O+N+S)/C are also found to increase with increasing the temperature [248]. Hale et al. [359] reported that biochar produced at high pyrolysis temperature is more stable and sorptive than one produced at low pyrolysis temperature.

As far as the authors are aware, the available literature about the effectiveness of biochar as a soil amendment in erosion control concerning the increase or decrease in aggregate stability has many contradictions. Many researchers observe feedstock and production conditions and the corresponding factors that directly or indirectly influence erosion like C – content, pH, functional groups, nutrients, etc. Many support the increase in aggregate stability by biochar addition, but few do not support this fact. Therefore, a knowledge gap is observed which needs to be investigated.

### 2.3.3 Contradiction in the literature on the influence of biochar on erosion

The study of literature on the effect of biochar addition on soil concerning erosion shows contradictions in results; even though many researchers have furnished results that show that the biochar addition reduces soil erosion, some have reported negligible or even negative effects. A brief discussion about a few experiments and research is given below, showing the difference of opinion in this regard:

#### 2.3.3.1 Reduction in erosion using biochar

The researchers mostly seem in favour of the fact that the addition of biochar decreases soil erosion. Abrol et al. [326] reported an increase in infiltration rate by 1.7 times and a reduction of soil loss by 3.6 times in non-calcareous loamy sand with 2% biochar addition. With the same biochar amendment in calcareous loam soil, the authors found less soil loss by 1.3 times. However, there was no effect on the run-off. In their experiment with biochar amendment of 3 kg, 2 kg and 1 kg/square meter in soil plots of size 1.4 m \* 1.4 m \* 0.1 m under controlled rainfall intensity of 28 mm/h, Ahmadi et al. [328] reported that runoff and soil loss for 2 kg/m<sup>2</sup> application were observed to be lower as compared to 1 kg/m<sup>2</sup> and control. In a flume setup experiment with different slope, length, rainfall degree of compaction and biochar amendment ratios, Cai et al. [324] reported a reduction in erosion by 10% – 69% and an increase in WRC by 20% - 59% by the application of biochar. Ghavanloughajar et al. [360] worked on biochar amended roadside filters, stormwater infiltration, and removal of pollutants in such biofilters and reported that compaction reduced the hydraulic conductivity in biochar amended sand and that the wet biochar amended sand columns showed hydraulic conductivity more than dry columns. The authors also observed a reduced hydraulic conductivity in biochar amended columns than compost amended ones. Also, an observation was made that some biochar particles get disintegrated due to compaction, which gets released/eroded by different erosive forces. Still, their quantum is very insignificant concerning the quantity of biochar in the soil.

Bashagaluke et al. [336] used different comparison efforts to find out the effect of biochar on soil loss, among other things. The experimental setup consisted of four plots, soil and inorganic fertilizer, soil + biochar, soil + biochar + inorganic fertilizer and a control plot.

They used four crops viz, maize, soybean, cowpea and maize + soybean. All of them were compared with the control plot. It was noticed that the plot of land with soil + biochar + NPK fertilizer showed minimum loss of soil probably due to more growth of crops, more moisture in the soil, and very less run-off than the other plots, including control. Many other researchers reported similar results. Gholami et al. [330], during their experimentation, reported biochar application of 1.6t/ha as the optimum biochar application for erosion control. Sadeghi et al. [329] applied biochar, biochar + PAM and PAM in Iranian soil, with plot sizes of (0.5m\*0.5m) using biochar and PAM at the rate of 0.8 kg/m<sup>2</sup> and 2 g/m<sup>2</sup>, respectively with designed slope and rainfall conditions and similar control plots were made for comparison purpose. The authors reported that the soil plots amended with biochar and biochar + PAM produced less erosion than bare soil, and only PAM was amended. Peng et al. [98] reported a reduction of 21.34% in wheat straw biochar amended soil compared to control after an incubation period of three years. Still, the authors did not observe a significant change in the runoff. The reduced erosion was considered an effect of more aggregate stability and organic carbon due to the addition of biochar. The literature shows that the increase in run-off and the soil loss is due to the formation of a thin film/seal by fine soil mass, which is denser than the underlying material and allows very less infiltration due to very small and less pores. The film is strong than the underlying medium, and due to less permeability, there is less infiltration which increases runoff and, as such, soil loss [326]. The authors believed soil aggregate stability is increased by the biochar electrolytes, which dissolve in the soil reducing the clay particles from dispersion, thereby reducing soil scaling. Due to this process, the infiltration increases, and the runoff decreases, causing reduced soil erosion. Four different biochar amendments (2.5%, 5%, 7.5%, and 10%) were applied on acidic Hutton soil compared to bare soil by Nyambo et al. [100]. The incubation was done for 140 days on all the experimental plots by simulated rainfall at pre-designed time intervals. Authors reported an increase of 1.51 points in pH, an increase of SOM from 2.2% to 2.34%, and a decrease in soil loss from 27% to 70% compared to control. But the authors believed that for more specific and accurate results, long-term research should be done, and other options of alternatives should be explored.

#### 2.3.3.2 Increase in erosion using biochar

Negative effects on soil erosion due to the application of biochar to soil have been reported by many researchers. The results reported by Peng et al. [334] for biochar application compared to inorganic fertilizers and inorganic fertilizers + biochar showed more water erosion in biochar amended soils than other treatments.

In their experimentation, Zhang et al. [331] used three biochar ratios, 2%, 5%, and 8%, with loess-derived Miami soil and a control one for comparison purposes. All the samples were incubated for 140 days under simulated rainfall. The authors reported a decrease in the runoff, but increased erosion in the soils amended with biochar compared to bare soils. The conclusion put forth by the authors was that erosion could increase due to the addition of biochar in croplands on sloping ground.

## 2.4 Influence of biochar on cracking intensity of soils

Cracking has been termed with different meanings in various studies, such as pores, gaps, voids, and fractures. Crack formation results from interaction caused between the internal and external conditions of the soil. Cracks may be caused in the soils due to the tensile stress caused by suction exceeding the tensile strength of the soil. The formation of cracks affects the soil's strength, bearing capacity, permeability, and compressibility. Cracks increase the chances of damage caused by weathering, and these problems have been reported since early times.

Cracks have been observed in different types of soils. Researchers have observed desiccation cracks more in clayey soils than in sandy soils. Many factors influence the crack formation, such as the environmental conditions, soil type and properties, water content, soil structure and boundary conditions [361–363]. Shrinkage causes the setting up of tensile forces, and when the same exceeds the soil's tensile strength results in the crack formation in soils. Cracking increases the soil's hydraulic conductivity, increasing the washing away of soil layers and the mobility of harmful contaminants [361, 364].

However, the changes in strength properties and deformation characteristics are a point of further investigation. The soil is strong enough in compression and shear as compared to tension. The factors that determine the tensile strength include arrangement and the particle size distribution of the soil mass, porosity, and minerals. Cracks' development usually starts simultaneously, forming a network at intersections and cross-sections [365, 366]. However, intersections and cross-sections of the vicinity cracks prevent any perpendicular connect usually [365–368]. Out of the various techniques available for judging and measuring desiccation cracks, the digital image correlation is the most useful in determining the initiation, propagation, bifurcation and merging of cracks [365, 366, 369]. Many researchers have used FEM to analyze the desiccation cracks [365, 370–372], even though not a single method or technique has been recommended in the literature for the simulation of cracking and is still a matter of investigation.

As per the literature, Griffith et al. [373] gave an elementary concept of the evolution of cracking in the soil. The researchers opined that the cracks occur because the soil system does not provide the energy demanded by a developing crack [365, 373].

The development of cracks causes serious degradation and disintegration of soil by reducing mechanical strength, formation of infiltration channels [361, 374–376], and movement of pollutants into the soil due to increased infiltration [361, 364]. The researchers have observed that adding biochar to soil can effectively reduce the cracking mechanism by creating changes in the porosity and physical and chemical properties of BAS [190, 361]. Biochar addition to soil has been observed to reduce cracking by reducing the tensile strength on the soil surface, occupying the voids between the particles and the repulsive forces between the soil particles.

In coarse-grained soils, the biochar amendment has been observed to reduce saturated hydraulic conductivity and increase WHC and aggregate stability, the properties that reduce the evaporation of

moisture from soil [361, 377–379]. Saturated hydraulic conductivity increased by adding biochar at 5% and 20% by Reddy et al. [70] and Wang et al. [377]. However, Lim et al. [380] observed an increase in saturated hydraulic conductivity by 1% and 2% biochar addition but no change with 5% biochar addition. Zhang et al. [361] observed an effective reduction in soil cracking by biochar addition of 4% and 6%. Liu et al. [381], with 5% and 10% biochar amendment in soil, observed a decrease in the surface crack ratio by 11.59% and 34.32%, and crack by 14.83% and 34.51%, respectively.

## 2.5 Limitations

The literature review shows that the research done so far at various levels depicts many limitations. It was observed from the literature that the production and application of biochar are mainly limited to a laboratory level making it difficult to understand the biochar influence on the modified soil hydraulic and strength properties on a large scale and, thus, asking for further research. Further, contradictory results have been observed in the effect of biochar on soil water retention capacity and erosion of various types of unsaturated soils. The effect of biochar (and its physicochemical properties) produced from different types of feedstock on the water retention capacity of a particular soil with varying grain size distributions is not brought out. The influence of various biochar types and drying-wetting cycles of soils on cracking mechanisms needs further research. The use of biochar for soil remediation and geotechnical infrastructure needs to be investigated.

Further studies are needed to analyze the effect of different feedstock types and pyrolysis conditions (temperature, moisture, type of pyrolysis, atmosphere) on physicochemical properties of biochar and, ultimately, on erosion potential of the soil-biochar mix. Such studies can be useful in narrowing down the selection of suitable pyrolysis conditions and biochar types suitable for soil erosion control under given climate conditions. It may also help develop commercial industries specifically for producing biochar at a large scale for erosion and other construction purposes. Studies are needed to consider the effects of biochar on soil erosion in the long term, considering vegetation growth and seasonal variation. Further, quantification of loss of nutrients in soil erosion needs to be conducted. Since biochar may negatively impact strength, its combination with other amendments (such as fibres or vegetation) can be considered for soil erosion control.

The contradictions in the literature regarding the basic properties of biochar and the resultant properties of the soil-biochar composite are a significant knowledge gap. The basic requirements of any material from the geotechnical technology perspective are hydraulic conductivity, strength (shear, tension and compression), density and cost-effectiveness. However, in the case of biochar and biochar amended soils, all these requirements are not clearly brought out and demand a thorough understanding.

## 2.6 Motivation

The hydraulic properties determine the hydraulic conductivity of the soil. The hydraulic properties of soil (infiltration, water retention and available water content) are influenced by various soil properties like soil texture and structure, bulk density, porosity, mineral composition and the interactions of these properties. These properties help the water retention capacity, water flow rate, nutrient retention, chemicals and pollutants, and determine the soil's quality and behaviour.

The hydraulic conductivity of any material is the property under which a material allows water to pass through it. It includes water holding capacity, infiltration, sub-soil seepage flux and its subsidiary properties, which determine the behaviour of the material (soil) towards erosion and cracking. The water holding capacity plays a significant role in the determination of plantation and cohesive forces in soils and helps in controlling erosion, cracking, landslides, and infiltration and adds to soil strength. The soil's water retention is a very important parameter in soil engineering. Due to this reason, this property of soil biochar composite was selected for investigation in this thesis.

## Chapter 3: Methodology

---

### 3.1 Background

In this section, a detailed discussion has been given about the methodology adopted for the research in this thesis. The different AI models have been discussed in detail

#### 3.1.1 Artificial Neural Network (ANN)

Artificial Neural Networks (ANN) are architectures built using programming languages and software and are modelled after brain structure. ANN is derived from the biological neural networks that develop human brain structure. Artificial neural networks also have neurons connected in various network layers, as the human brain has neurons connected. These neurons are called nodes and are organized in layers [33]. The neurons exhibit global behaviour and are determined by establishing connections between the various processing elements and the related parameters within the neural network architecture. Architectures are the different topologies in which ANN can be organized. Elements and neurons can be connected in different ways for processing.

When a neural network is trained on the training set, it is initialized with weights. These weights are then optimized during the training period, producing the optimum weights. The structure of a neural network consists of an input layer, one or more hidden layers, and an output layer. The hidden layers and the number of neurons used in each layer depend on the system's complexity. Figure 23 shows a typical ANN architecture with two hidden layers.

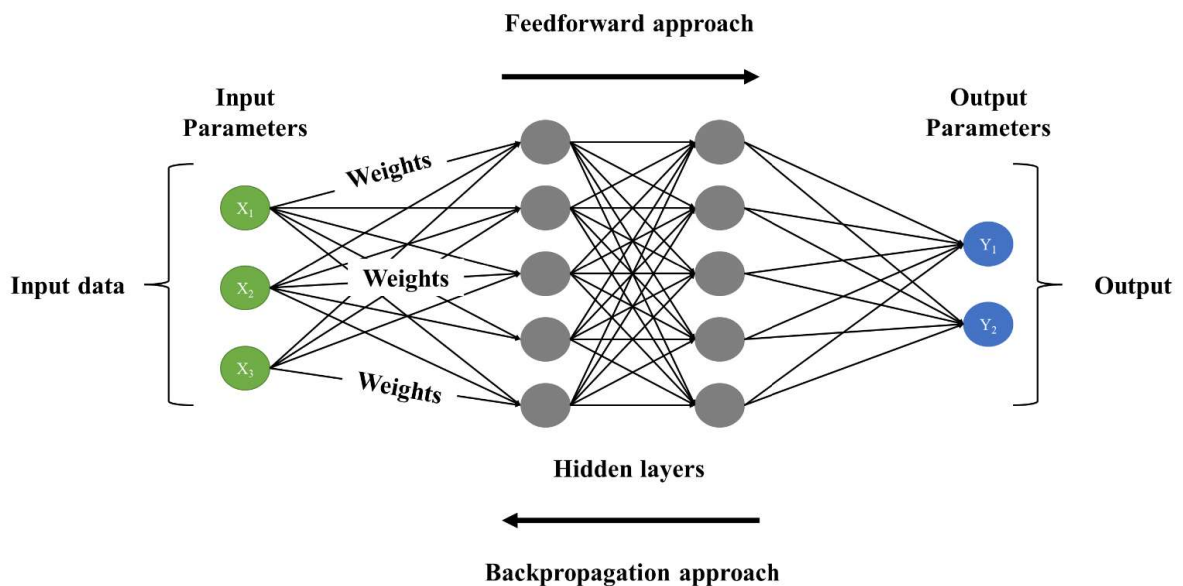


Figure 18 ANN Architecture

In an ANN, data is received through the input layer neurons and then transformed into the neurons in the first hidden layer through the weighted connections established between the input layer and the first hidden layer. Here, the data in each layer are mathematically processed, and then the result is transformed to the next layer.

The input layer receives the input information in texts, numbers, audio files, image pixels, etc., in the network format. After that, the hidden layer's data is passed into the hidden layers. There can be a single hidden layer, as in the case of a perceptron or multiple hidden layers. Hidden layers perform various mathematical computations on the input data to recognize the patterns that are part of it. In the output layer, results are obtained through rigorous computations performed in the hidden layer. Multiple parameters and hyper parameters affect the model's performance in a neural network. The output of these ANN models mostly depends on these parameters (weights, biases, learning rate, batch size etc.). Every node in the network has some weights assigned to it. Each connection that connects the neurons to the other layers is weighted. Weight in a neural network represents the relative importance of each input parameter to a processing element. Weights are the coefficients of the equation which you are trying to resolve. Negative weights reduce the value of an output. A neuron first computes the weighted sum of the inputs:

$$Y = \sum_{i=1}^n (\text{weight} \times \text{input}) + \text{bias}$$

Equation 3

The weights are essentially reflecting how important input is. A transfer function calculates the weighted sum of the inputs and bias (**Figure 19**).

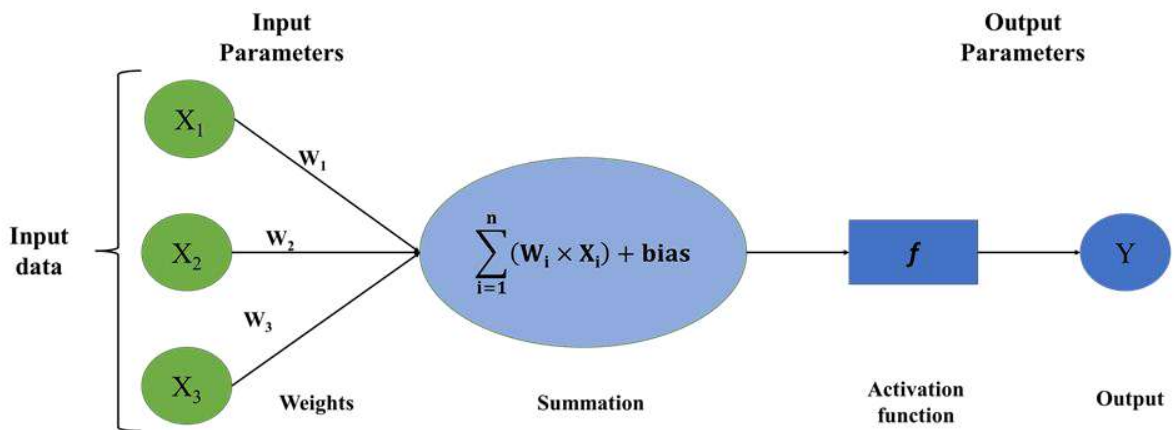


Figure 19 Weight and bias

After the sum has been calculated using the transfer function, the activation function obtains the result. The activation functions fire the appropriate result from the node based on the output received. Based on the value fired by the node, the final output is obtained. Then, by using

the error functions, discrepancies between the predicted output and resulting output are calculated and weights adjusted through a process known as backpropagation.

### 3.1.2 Multiple Regression Analysis

Regression analysis involves identifying a relationship between a dependent variable and one or more independent variables. A model of the relationship is hypothesized, and estimates of the parameter values are used to develop an estimated regression equation. Various tests are then used to determine the model to check if it is satisfactory. If the model is considered satisfactory, then the estimated regression equation can predict the value of the dependent variable given values for the independent variables.

#### 3.1.2.1 Regression model

For simple linear regression, the model is used to describe the relationship existing between a single dependent variable 'y' and a single independent variable 'x' is

$$y = \beta_0 + \beta_1 x + \varepsilon$$

*Equation 4*

Here, ' $\beta_0$ ' and ' $\beta_1$ ' are referred to as the model's parameters, and ' $\varepsilon$ ' is a probabilistic error term that accounts for the variability in 'y' that cannot be explained by the linear relationship with 'x'. If the error term is not present, the model would be deterministic. In that case, knowledge of the value of 'x' would be sufficient to determine the value of 'y'.

In multiple regression analysis, the model for simple linear regression is extended to determine the relationship that exists between the dependent variable 'y' and  $n$  independent variables  $x_1, x_2, \dots, x_n$ . The general form of the multiple regression model is

$$y = \beta_0 + \beta_1 x_1 + \beta_2 x_2 + \dots + \beta_n x_n + \varepsilon$$

*Equation 5*

The parameters of the model are the ' $\beta_0, \beta_1, \dots, \beta_n$ ', and ' $\varepsilon$ ' is the error term.

#### 3.1.2.2 Coefficient of determination ( $R^2$ )

Coefficient of determination, R-squared or  $R^2$ , is used to assess the model's ability to predict an outcome in linear regression.  $R^2$  indicates the proportion of variance in the dependent variable (y) predicted by the variance in the independent variable (x).

A high  $R^2$  value indicates a model that is a good fit for the data provided. For example, an  $R^2$  of 0.45 indicates that 45% of the variation in the outcome can be explained by the prediction of the outcome using the covariates in the model. These percentages vary

in different studies. In the case of social sciences, there might be a high proportion of variation in the prediction. In the case of physical sciences, it may be closer to 100%. The theoretical minimum for  $R^2$  is 0, and the maximum is 1. However, as linear regression is based on the best fit, the value of  $R^2$  will be greater than 0, even if no relationships exist between the dependent and the independent variables. If the  $R^2$  value is close to 1, the values of the independent parameters are close to the regression line, and if it is close to 0, the values are away from the regression line.

The value of  $R^2$  increases if new predictor variables are added and may or may not be associated with the outcome or the results. The  $R^2$  value is adjusted so that the same information can be incorporated, but the predictor variables of the model are also penalized. In multiple regression analysis, when new parameters are added,  $R^2$  is increased. An increase in the  $R^2$  greater than expected, will also increase the adjusted  $R^2$ .  $R^2$  helps find the explained and the total variation and determines the strength of the relationship between the independent and dependent variables.

### 3.1.2.3 $p$ -value and Significance testing

The  $p$ -value is the probability of obtaining the results at least as extreme as the observed results of a statistical hypothesis test, assuming that the null hypothesis is correct. The  $p$ -value acts as an alternative to reject the smallest significance level so that the null hypothesis can be rejected. If the  $p$ -value is small, there is strong evidence that the null hypothesis can be rejected. A  $p$ -value of 0.05 or less is considered statistically significant. If the  $p$ -value is less than the significance level, which is usually less than 0.05, the null hypothesis can be rejected, but it does not mean that there is a 95% probability that the alternative hypothesis can be accepted. The  $p$ -value is conditional to the null hypothesis being true.

In regression analysis, model building is the process in which a model is developed that describes a relationship between dependent and independent variables in the best possible way. The major issue in the process is finding a proper form of the relation to be developed and selecting the independent variables that are best fit to be used for the model. For the model building, it is best to use variables that are quantitative as well as qualitative. Quantitative variables measure the quantity and number and represent the type and category. Dummy variables are used to represent the qualitative variables in the regression analysis.

## **Chapter 4: Exploring the efficiency of biochar in enhancing water retention in soils with varying grain size distributions using the ANN technique**

---

### 4.1 Background

The discussion in the previous chapters was on the general background, introduction and methodology adopted for the thesis. It was clarified that the WHC of soil increases with the addition of biochar due to the increased porosity of the biochar. The porosity of biochar gives rise to more hydraulic pathways, enhancing hydraulic conductivity like infiltration and WHC, increasing available plant water and vegetation and reducing erosion problems [211, 297, 382]. The fine size of biochar adds more capillarity to the soil, which creates more suction; as such, the soil is capable of increased water retention. The increase in water retention also decreases the crack formation in the soil. Gluba et al. [211] observed that sandy soils amended with biochar possessed more available water content than unamended soil. Literature shows that available water content increased with the addition of biochar up to a certain ratio but decreased with higher percentages of biochar content [211, 382, 383]. Many researchers observed a 5% and 10% increase in unsaturated hydraulic conductivity in clay soils [209, 216, 220, 228, 384]. During their study, Zhang et al. [323], while working on the coarse and fine particle size of biochar, noticed that coarse sized biochar particles effectively increased the hydraulic conductivity of biochar amended soils. In contrast, fine-sized biochar particles decreased hydraulic conductivity in biochar amended soils.

The hydraulic conductivity of soil (seepage, soil water supply) determines the infiltration rate [92, 386]. The infiltration rate results from soil suction and volumetric water content [92]. The infiltration in soil depends upon the void ratio; the more the void ratio, the more will be the infiltration, i.e., the soil with a greater void ratio will have greater water holding capacity, and any change in the void ratio of an unsaturated soil changes its SWCC [291]. Mollindo et al. [387] observed that the fine-sized biochar particles change the soil pore arrangement, increase surface area and void ratio, and increase the WHC of soil biochar composite. Sufficient literature is available, which shows that the WHC of the biochar soil composite is increased compared to bare soil [388]. The WHC of soil increased by 11% [303] and 32% in sandy loam soil [389] when biochar was added to the soil. Gopal et al. [92], in their study on water hyacinth biochar of 0%, 5% and 10% amendment with soil, observed that the infiltration reduced and WHC increased with an increase in biochar amendment. It was observed that infiltration decreased with a decrease in suction. Similarly, Garg et al. [390] observed that biochar's addition increased the water retention capacity of unsaturated soils (loam and sandy loam).

Due to its ability to absorb large amounts of water, biochar has a large surface area and increased porosity. It has been observed to enhance the infiltration rate and reduce the runoff, which leads to an increase in soil moisture. The feedstock used is considered an important factor that affects the porosity in the soils amended with biochar. Applying biochar in the soil helps increase WRC and decrease gas permeability, which varies with feedstock, temperature, duration of pyrolysis, and soil type. Some authors have also pointed out

a negligible effect on the WRC. However, contradictions have been observed in the literature about the effect of biochar on the WHC of the soil. Some studies have observed an increase [391, 392], some a decrease, and some have observed no effect [280, 281]. WRC's contradictions and parameters with its effect in the engineering field need to be quantified by conducting experiments and studies. The increased porosity by adding biochar to the soil will make the soil more porous. Water will infiltrate the soil, increasing the permeability of gases and water, resulting in more desiccation cracks leading to a failure in slopes.

The soil type, initial void ratio, plasticity, and grain size distribution affect SWCC, and as such, shear strength, tensile strength, and slope stability can be predicted by using SWCC [287]. Zeng et al. [395], in their study, observed that the loading history, type and structure of the soil, its composition, permeability, water content and void ratio are the factors on which SWCC depends and determine the soil properties, strength, permeability, volume change, solute and thermal diffusion. In their study, Chen et al. [396] observed that soil shear strength increases with the increase in matric suction. When there is infiltration, the soil gets wet, and matric suction is reduced, the chances of slope failures increase. It was pointed out that stress, deformation, and flow are the three general geotechnical engineering problems in unsaturated soils. It was observed that soil water retention curves could predict hydraulic conductivity, shear strength, and volume changes.

## 4.2 Introduction

It is necessary to understand the water retention mechanism of biochar amended soils (BASs) to promote biochar as a soil amendment [397]. Sufficient literature shows that the biochar soil composite's water retention capacity (WRC) is increased compared to bare soil [388, 393]. Mollinedo et al. [398] observed that the fine-sized biochar particles change the soil pore arrangement and increase surface area, void ratio and WRC of soil-biochar composite. On applying biochar to soil, the WRC of soil (medium-textured boreal agriculture soil) increased by 11% [303] and 32% [399] in sandy loam soil. Gopal et al. [92] observed a reduction in infiltration rate and WRC enhancement with an increase in biochar amendment. Similarly, Garg et al. [390] observed that the addition of biochar increased the water retention capacity of unsaturated soils (loam and sandy loam). The study also demonstrated that the addition of biochar modified the soil-water characteristic curve.

Porosity, void ratio and soil structure get altered by biochar addition, specifically depending upon the particle shape, size and internal structure of biochar [400]. The internal structure of biochar particles determines their WRC and shape (elongated/oval/spherical), and size determines the complexity and density of soil-biochar composite and capillary system [205]. Liu et al. [205] observed the effect of 2% biochar amendment of three different particle size samples with sand. It was noticed that the saturation water content, field capacity, permanent wilting point (PWP) and PAW in the soil-water characteristic curve (SWCC) increased when compared with the other two samples: sand - fine sand and sand + coarse sand (replacing biochar with fine sand and coarse sand). The authors concluded that more porous and irregular shaped biochar particles are more effective in increasing water retention of sandy soils [205, 296, 400, 401]. Duarte et al. [314] modified eight samples with agricultural residue biochar of size [2 mm, 2–0.15 mm and <0.15 mm with

200 g soils (loamy and sandy) at 0.92 g of biochar (~ 25 Mg/hect). After allowing an incubation period of 1 year, it was noticed that a biochar particle size of <0.15 mm is most suitable for increasing water retention in the soils (particularly loamy soil). It was observed that soil's physical properties depended on the particle size of biochar. Similarly, in another study conducted by Alghamdi et al. [313], fine biochar particles < 0.1 mm increased the water content at field capacity and available water content more than that of particle size greater than 0.1 mm, probably due to increased surface area, microporosity and biochar's porous structure in light-textured soils after an incubation period of 120 days.

Though many studies reported an increase in WRC, some reported the effect of biochar has been either negligible or negative. Some authors observed both increase and decrease [6, 29, 402, 403], some reported increase only [391], whereas some reported no effect [394]. Bordoloi et al. [301] observed an increase in WRC of silty sandy soil, while Hardie et al. [393] observed no noticeable effect of biochar on drainable porosity, field capacity, PWP, PAW content or soil moisture content of a sandy, loamy soil. Further, the effect of biochar on WRC may vary with the type of feedstock from which biochar was produced [35, 404]. Biochars produced from plant feedstock types tend to have a higher porosity than animal feedstock [404–406]. As far as authors are aware, there is a lack of systematic study investigating the extent of biochar effect on WRC of soils with varying grain size distributions. It is difficult to interpret the extent or efficiency of biochar on WRC of soils from literature due to high variability in testing conditions such as instrumentation, climate, and type of biochar.

There are several numerical techniques to model material behaviour effectively in different disciplines [91, 407–412]. One of such techniques, artificial neural network (ANN), has proven to be an effective approach for analysing material behaviour from limited experimental results [24, 35, 91, 409, 413]. Many studies have reported using the ANN to study soil properties [414, 415]. ANNs are based on a learning technique that imitates the biological learning process occurring in the brain and presents a robust way to predict responses from a dataset [412, 416]. Using the Fredlund and Xing equation, Vasu et al. [417] used ANN to estimate the soil-water characteristic curve (SWCC) for Korea's weathered soil. Zainal and Fadhil [418] determined SWCC by ANN using properties like air entry point and residual degree of saturation. Similarly, Johari and Hooshmand [419] used gene expression programming to predict SWCC. Johari and Javadi [420] used clay and silt contents, void ratio, gravitational water content, and suction and estimated SWCC using the ANN technique. Hence, the ANN technique can be an important tool for developing models and analysing soil behaviour.

This study aims to investigate the efficiency of biochar in affecting the WRC of soils with varying grain size distributions. A database of SWCCs of soils with and without biochar amendment was systematically established. ANN models were developed based on an established data set. Models were developed as a function of parameters such as percentages of biochar amendment, clay, sand and a new factor (the ratio of fine (silt + clay) and coarse (sand) content).

## 4.3 Materials and Methodology

### 4.3.1 Experimental

The experimental procedure details and results obtained have been taken from [6, 90, 93, 421–423] studies. The soil and biochar type, soil biochar mix, pyrolysis conditions, parameters adopted, and the experimental procedural setup are discussed below.

The experimental objective of Garg et al. [93] involved the investigation of water retention and gas permeability in BAS. The soil used was a clay-sand mixture, and the biochar used was obtained from Water hyacinth. The water hyacinth was dried, cut into 5 cm pieces and then subjected to pyrolysis. The biochar was mixed in the amendment ratio of 0%, 5% and 10%. The suction, water content, and gas permeability parameters were measured for test samples of bare, 5% and 10% BAS. The experimental setup consisted of cylindrical columns with 20 cm diameter and 25 cm height. Each column had two chambers, 5 cm high, used to measure gas discharge and pressure. SBC compacted specimen was filled in the upper chamber to the desired degree of compaction. A mesh of size of pores 75  $\mu\text{m}$  covered with a linen cloth was provided in the base of the upper chamber. The rate flow of gas and the pressure were measured by a flow meter and digital pressure sensor, which were attached to the experimental setup. The Meter/Decagon group ( $\psi$  by MPS-6) and ( $\theta$  by EC-5) [424] sensors were used. The suction from the near-field capacity of 10 kPa to past wilting point of 3000 kPa) was measured using MPS-6.

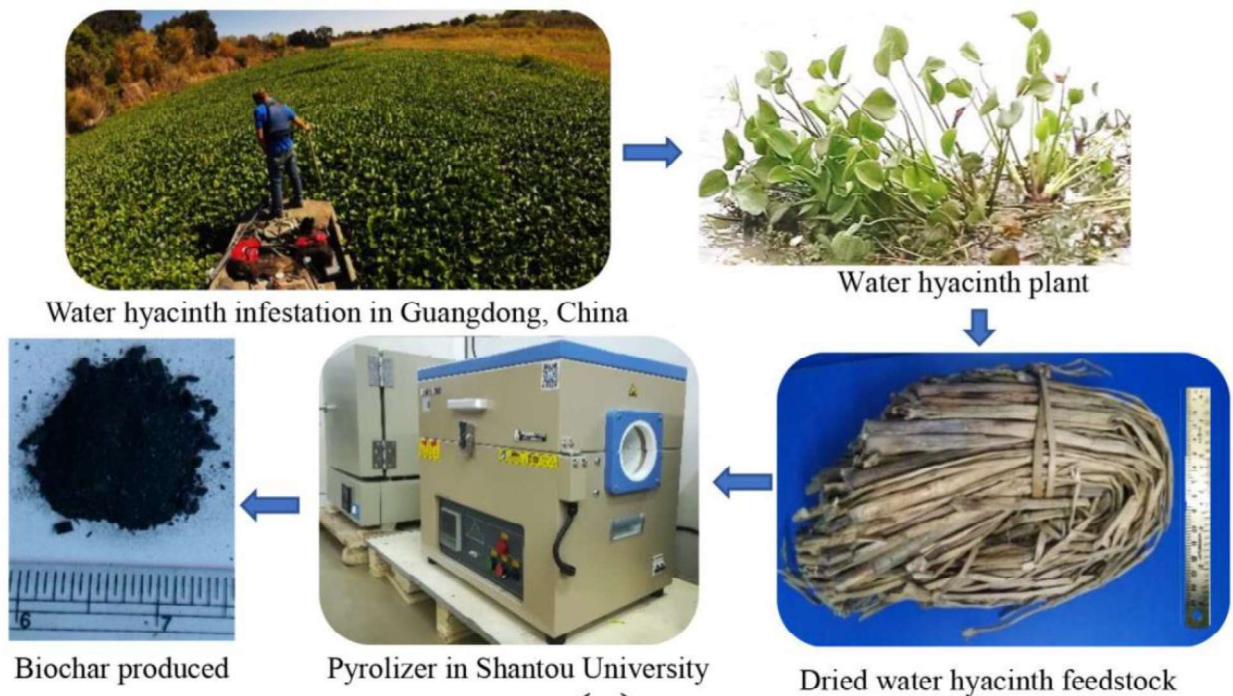


**Figure 20** Conversion of water hyacinth feedstock to biochar [93]

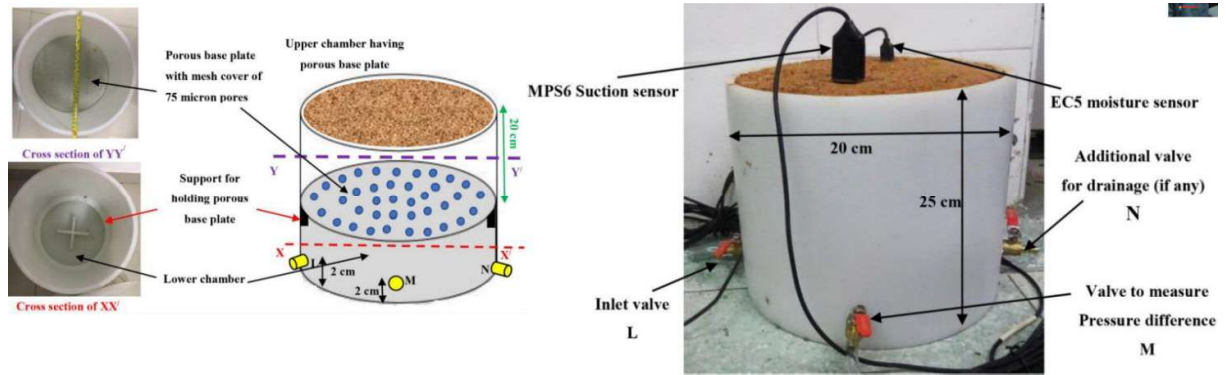


**Figure 21** Experimental setup for measurement of gas permeability [93]

The objective of the study conducted by Bordoloi et al. [90] was to observe the WHC and factor of cracking intensity of biochar amended soils. The experimental setup used biochar from water hyacinth feedstock obtained from Assam, India; with cellulose content (45.58%) and hemicellulose (21%) and medium plastic soil containing medium sand, fine sand, silt, and clay in the ratio of 37%, 21%, 37% and 5% respectively. The feedstock was dried, broken into pieces of 30 to 50 mm and then subjected to pyrolysis in a stainless cylindrical steel box of 500 ml of dimensions 11 cm (height)  $\times$  7 cm (diameter) at 300°C - 350°C temperature maintained for 45 minutes as the optimum condition required [12]. The maximum size of biochar particles was maintained below 2 mm. The biochar was mixed with soil in 0%, 2%, 5%, 10% and 15%, all samples compacted to the same compaction degree. The experiment apparatus consisted of fifteen identical PVC columns 300 mm and 250 mm in diameter and height, respectively, bottom fitted with a perforated plate to allow drainage. The soil loss was prevented by providing filter paper. The fifteen prepared columns were subjected to 9 cycles of drying and wetting conditions for seven days each by placing in a transparent enclosure fitted with a 1000 ml-controlled sprinkler irrigation apparatus. The record images with lapse of time was done with a digital camera. The suction was measured with 2 sensors measuring as low of 10 kPa to high of 100000 kPa [424]. Similarly for measurement of VWC, sensors were installed at a depth of 30 mm in the soil, fixed to the columns at opposite ends diametrically, which were further connected to EM-50 data logger systems [424].

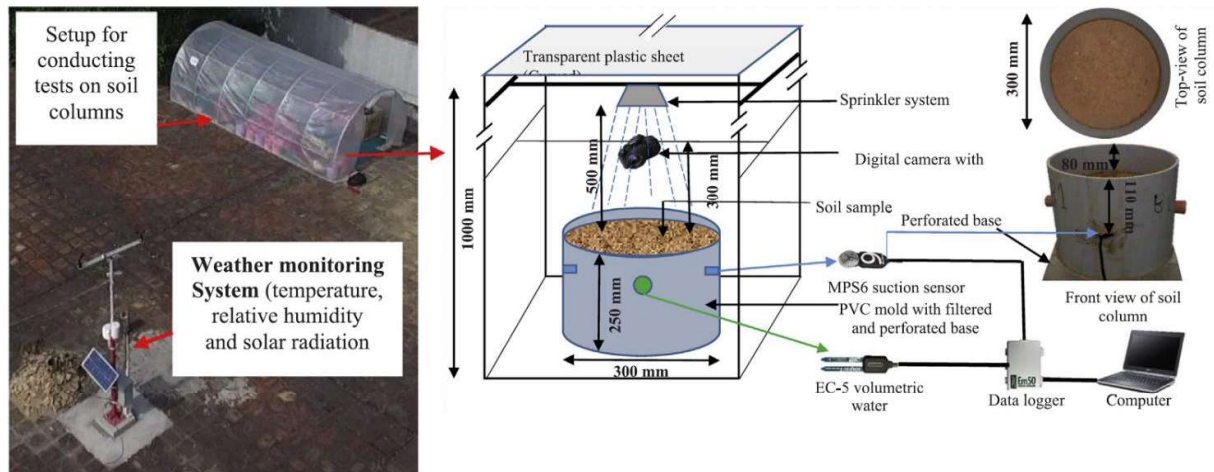


**Figure 22** Setup for conducting tests on soil columns [90]

The other study selected was by Ni et al. [423]. Their study was carried out in two years with one of the objectives to determine the hydraulic properties of biochar. The soil which was put in use was from tropical and sub-tropical zones consisting of granite (completely decomposed) with a clay content of 12%, gravel of 19%, the silt content of 27% and sand of 42%. Peanut shell biochar was obtained by pyrolysis at 400°C temperature for 30 – 40 minutes and was crushed and sieved in a 425µm sieve. The experimental setup consisted of 16 cylindrical columns of 400mm and 200 mm in height and diameter, respectively, filled at 90° compaction, with 5 mm holes at the bottom for drainage. Out of 16 columns, eight columns were for the determination of hydraulic conductivity, 6 for the determination of biochar effect on plant growth and the remaining were for bare soil. All the columns had similar environmental conditions by placing them in a single plant room. Tensiometer and two HDS were installed for measurement of suction of soil up to 90 kPa and 2500 kPa, respectively, as installing tensiometer and HDS is being adopted commonly to measure a suction over a wide range (0 - 1500 kPa) [425]. VWC of soil was measured by installing four moisture probes of SM 300, Delta -T Device Ltd., calibrated in the laboratory.

Another study from which the test data was taken was by Ouyang et al. [6]. The objective of this study was to determine the biochar addition effect on soil hydraulic properties and stability of aggregate formation. The feedstock used to prepare biochar in the experimentation was dairy manure. The same was first dried in air and, after sieving in a sieve of 2 mm, packed air-tight in crucibles. A muffle furnace was used for pyrolysis in which the temperature was slowly raised and then maintained at 500°C for one hour. The produced biochar was allowed to cool and sieved through a 250-µm sieve and then refrigerated at 4°C. The characterization like elemental composition (C, H, and N), structure and texture and pH were determined by instruments elemental analyzer (Vario EL, Elementar, Germany). Scanning electron microscopy (SEM) at magnifications of 1000 and 5000 times pH probe with biochar: water ratio of 1:5. The biochar was burnt in a ceramic crucible at 900°C for 6 min to calculate the weight of volatile matter. The soils used in this study were two; silty clay soil and sandy loam soil, taken from South China. The soil was dried in air and sieved in a 250-µm

sieve. The composition of Silty clay was sand (6.6%), silt (41.8%), and clay (51.6%), and that of sandy loam was sand (60%), silt (20%), and clay (20%). After the incubation of 90 days at a temperature of 25°C, 4 test samples were made consisting of each of the two soils with 2% biochar amendment and without biochar. The changes in hydraulic conductivity SWRC during the incubation period were measured by filling the sample in glass cylinders of 3 cm height and 4.5 cm diameter with a 300-mesh copper wire gauze placed at the bottom. The prepared samples were put wrapped in 1-L plastic bottles provided with small holes pricked on the plastic sheet to maintain atmospheric pressure inside the bottle. Three replicates were set up for each treatment on every sampling date.

The study by Wong et al. [402] used biochar (of size less than 425-µm) obtained by pyrolyzing peanut shells at 500°C (slow pyrolysis) at application rates of 0%, 5%, and 20 % with the soil of kaolin clay. The samples were compacted to 80%, 90%, and 100 % in test molds consisting of cylinders of a diameter of 70 mm and a height of 10 mm. The WRC was measured at high suction of 48.49–124.56 MPa). In total, using different amendment ratios, compaction and CWC 3, such replicates were formed.

For preparing the dataset for the training of models, the volumetric water content of the soils was normalized with their maximum water content (i.e., to establish normalized water content (NWC). NWC is defined as per the following equation:

$$\text{Normalized Water Content} = \frac{\text{Volumetric Water Content}}{\text{Maximum Water Content}}$$

*Equation 6*

This is done to minimize any fluctuations in the data caused due to variation in soil types, soil density, instrumentation type, etc. Future studies need to establish full-scale SWCCs for various soil types using the same instrumentation and testing conditions (i.e., soil density and soil type).

#### 4.3.2 ANN procedure

An artificial neural network (ANN) is a learning algorithm that implicitly describes the nonlinear and complex relationship between input data and output results [409, 426]. The commercially available Statistica, version 12 software, was used in the present study. Seven input parameters were used to develop the model, viz. soil suction, biochar content, sand content, silt content, clay content, fine content (silt and clay), and the ratio of fine content to sand content. The ANN architecture predicted normalised water content using two hidden layers corresponding to these seven parameters. **Figure 23** presents a flowchart that shows a methodology used for the implementation, and **Figure 24** illustrates the three-layer ANN architecture. In addition, sensitivity analysis was conducted using the newly developed ANN model. The sensitivity analysis is usually performed to identify the relative significance of any parameter, which is simply the importance values of each input parameter divided by the largest importance value of the highest contributing parameter. The relative significance of any parameter is expressed as a percentage and can be visualized in the form of a bar chart. Relative significance values are obtained through the software

corresponding to the selected architecture of the neural network, sorted in descending order of importance. This bar chart results from comparing the weights assigned to each input parameter.

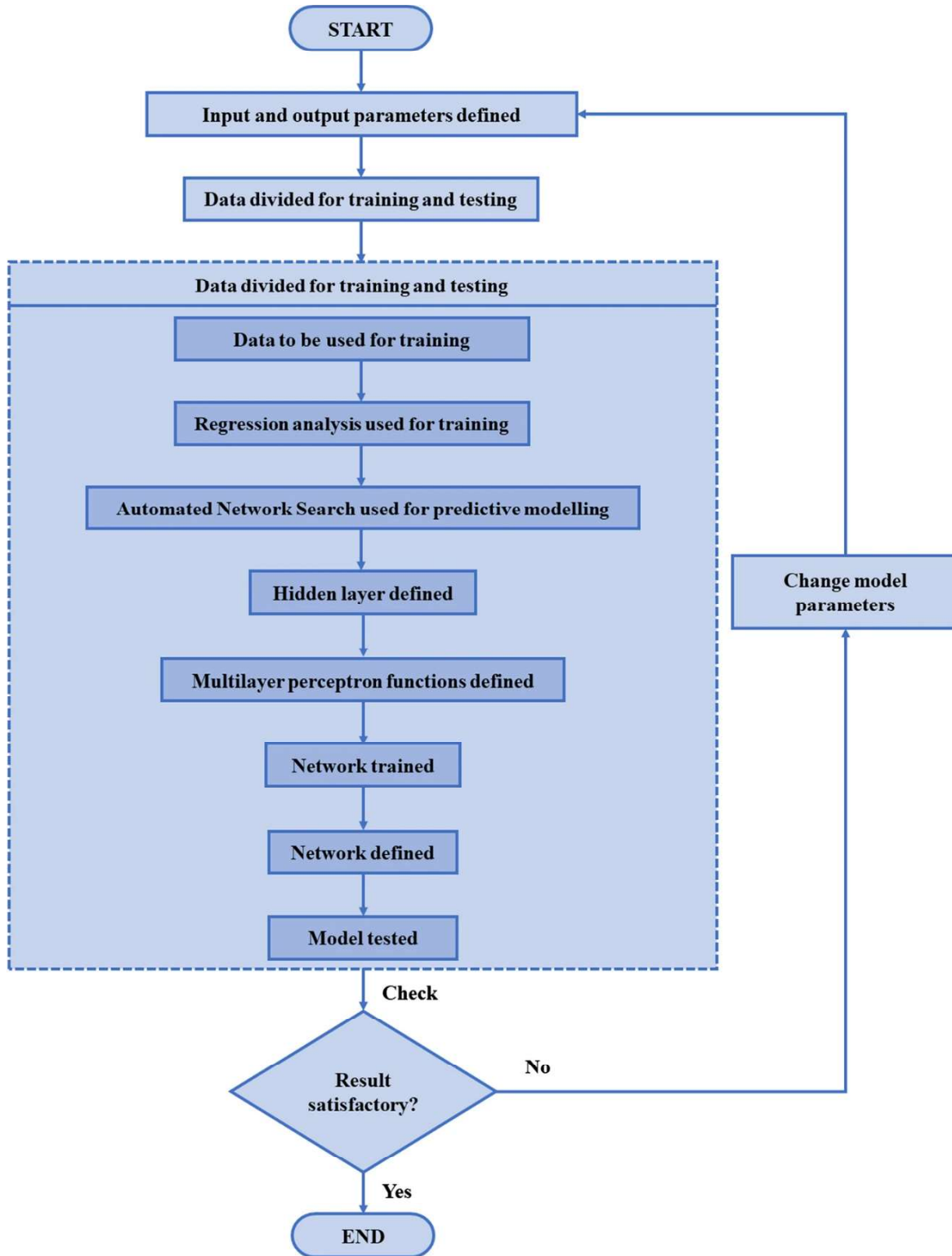
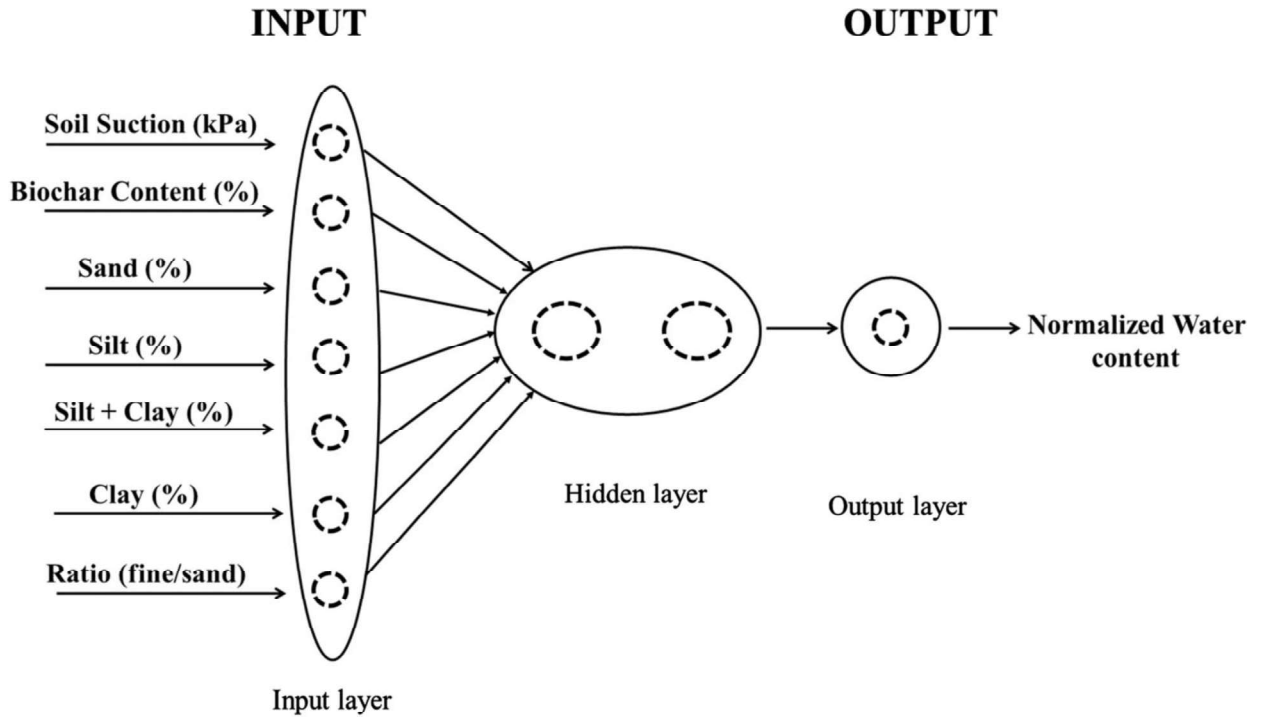


Figure 23 Flowchart for ANN modelling



**Figure 24** ANN architecture used for the prediction of normalized water content

### 4.3 Results and Discussions

#### 4.3.1 Comparison between measured and predicted results

The number of soil samples used in the study was 23. Seven hundred ninety-four data points were obtained from the literature corresponding to these samples. These data points were divided in the ratio of 80:20 for training and testing, respectively. **Figure 25** shows a comparison drawn between the measured and the predicted outputs. The SWCC is plotted between normalized water content and soil suction. The proposed model's coefficient of determination ( $R^2$ ) and mean absolute percentage deviation (MAPD) calculations were done using the formula given below:

$$MAPD = \frac{100}{n} \sum_{i=1}^n \frac{(M_i - P_i)}{M_i}$$

*Equation 7*

Where  $M_i$  = measured value,  $P_i$  is the predicted value, and  $n$  is the number of observations.

The  $R^2$  value was found to be 0.7109. It is observed that measured and predicted NWC follow a trend, indicating accuracy (in terms of  $R^2$ ) of the prediction of NWC. The error percentage as calculated by MAPD was reported to be 13.76%.

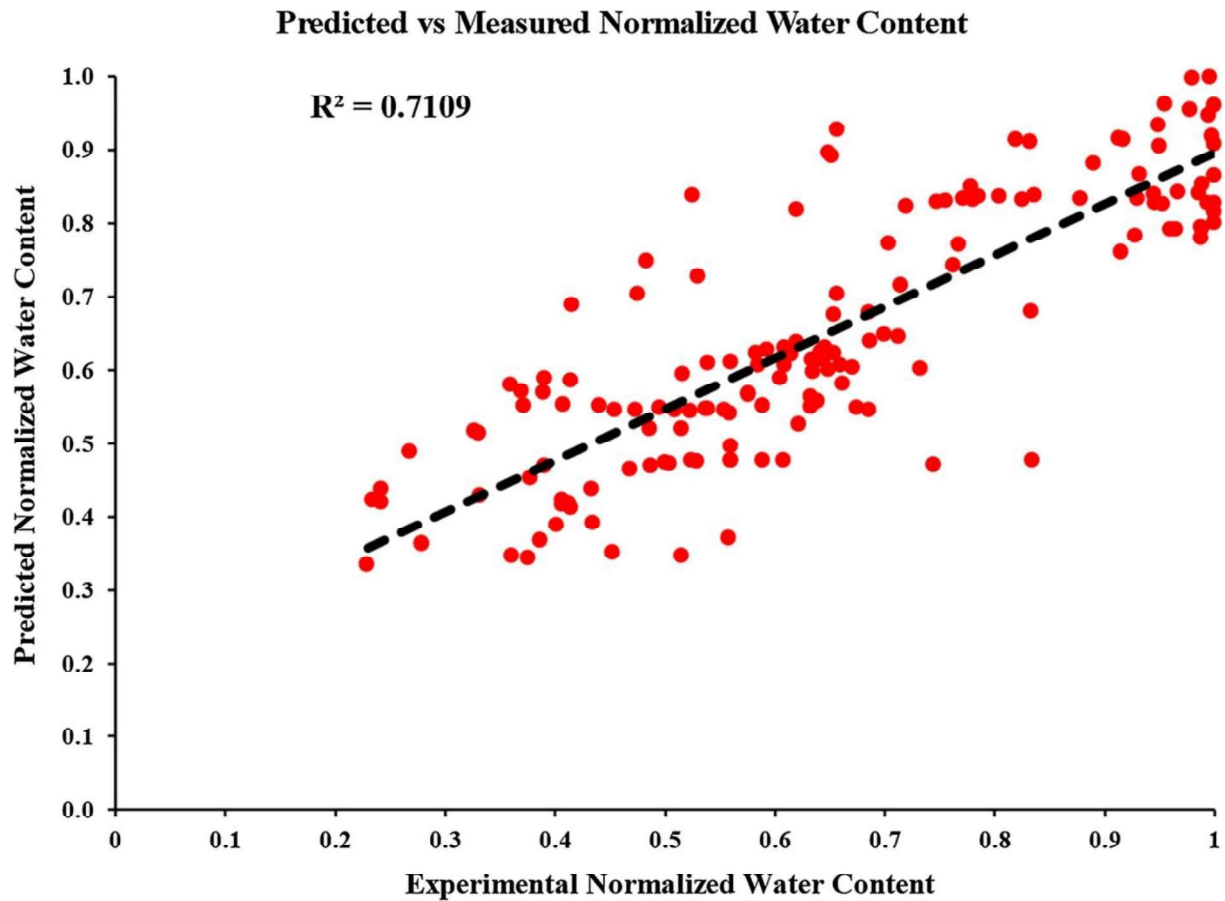


**Figure 25** Variation between predicted normalized water content and measured normalized water content ( $R^2$ )

To further visualize the predictive ability of the model, estimated SWCCs for three particular soils at different biochar contents of 0%, 5% and 10% were compared with the measured ones in **Figure 26**, respectively. It should be noted that only a few selected plots have been used for comparison. This has been done based on the availability of complete data [90, 93] of grain size distribution and reported SWCCs at different biochar contents (0%, 5% and 10%). The proportion of sand, silt and clay reported in Bordoloi et al. [90] is 58%, 37% and 5%, respectively. As per Garg et al. [93], the proportion of sand, silt and clay is 81.23%, 17% and 1.77%, respectively. Soils were compacted at 0.9 times maximum dry density and the optimum moisture content (OMC) (16.5%) in Bordoloi et al. [90], whereas in Garg et al. [93], soils were compacted at 0.8 times maximum dry density and an OMC of 18%. In addition to predictions made at similar grain size distributions, additional estimations were made using the developed model for clay contents. It is evident from the figures that the results of water content obtained from measured and predicted SWCCs are comparable.

It should be noted that there is a discrepancy between measured and predicted SWCC values at a higher suction range. Since the ANN model is based on the measured SWRC data, it is reasonable that the prediction may not be able to capture suctions at a higher range. This is because of the lack of measured SWRC data at higher suctions in most studies. As far as authors are aware, only a few studies

[90, 93, 421] have directly measured SWRC for a higher suction range. Additionally, the variation in soil suction at a higher range could also be caused due to different instrumentation being adopted in studies [427–429]. Wong et al. [402] adopted a humidity-based approach to establish suctions at a higher range, whereas Bordoloi et al. [301] utilized an MPS-6 sensor for measuring suction at a higher range. Further systematic studies are needed to measure SWRC for a higher suction range for soils amended with different biochar types and at varying compaction states.

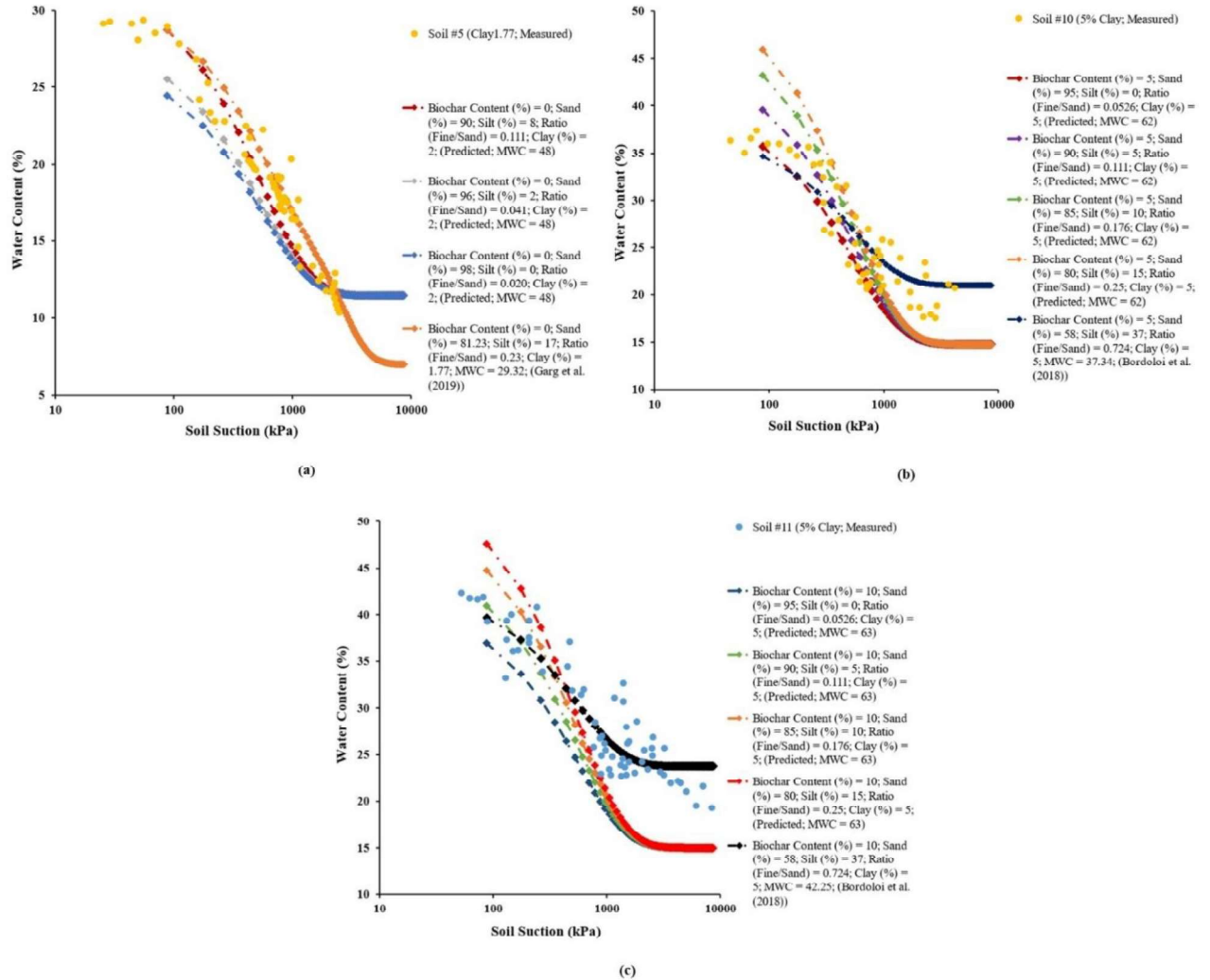


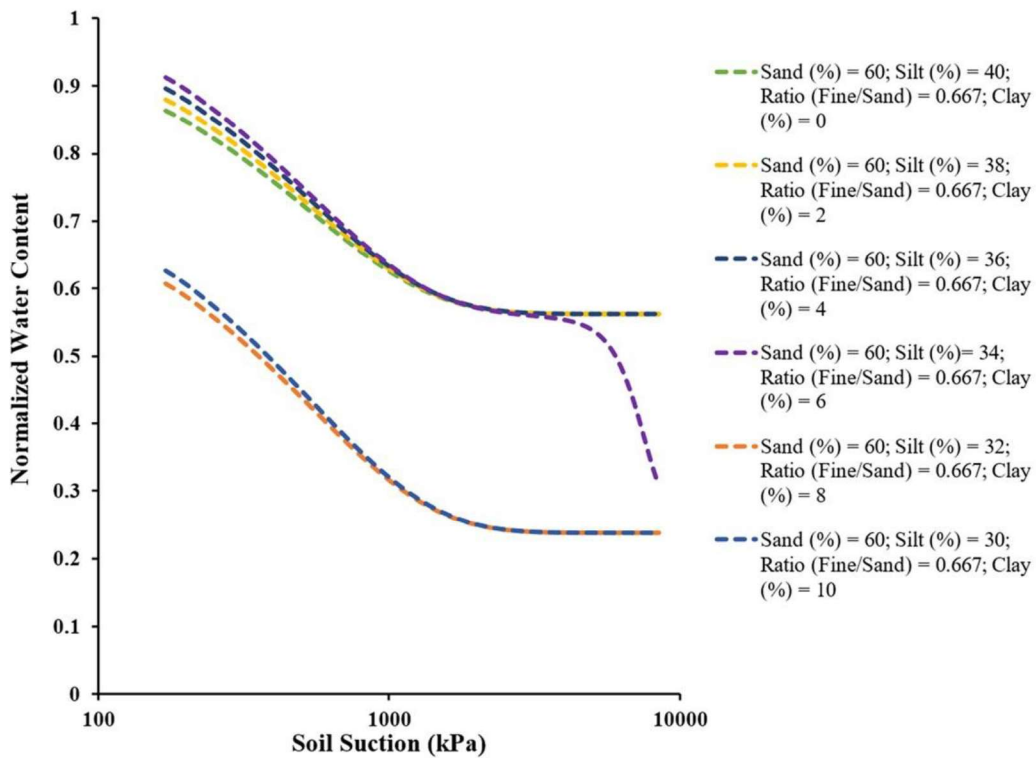
**Figure 26** Comparison of measured and predicted SWCCs corresponding to biochar content of (a) 0%, (b) 5% and (c) 10%

#### 4.3.2 Influence of clay and silt content on SWCC of soils amended with biochar at different contents

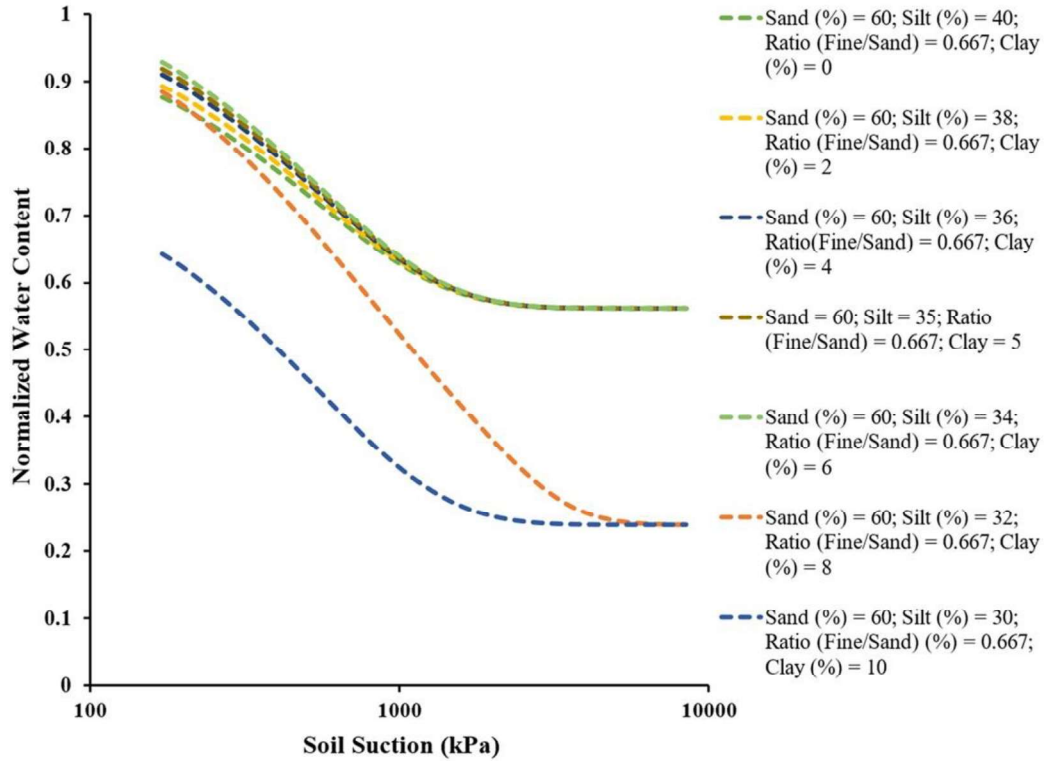
To interpret the influence of clay and silt content, prediction of SWCCs was made by systematically varying clay and silt contents. In one case, the silt content varied from 40% to 30%, while the corresponding clay content varied from 0% to 10%. Sand content is fixed at 60%, while fine to coarse content was kept at 0.667. **Figure 27 (a,b)** shows the biochar effectiveness on SWCCs

of soil with different silt and clay contents. Analyses were conducted by keeping the ratio of fine to coarse content (0.667), fine (silt and clay of 40%) and sand content (60%) constant. Clay was varied from 0% to 10%. Correspondingly, silt varied from 40 to 30%. The influence of silt and clay content on SWCCs was analysed for two different biochar percentages (i.e., 3% and 10%), as shown in **Figure 27**, respectively.

As observed in **Figure 27(a)**, NWC reduced from 0.9 to 0.65, with an increase in suction for clay contents up to 6%. NWC of 0.65 represents normalized water content corresponding to the drier part of the soil. However, for clay content of 6%, the minimum NWC reduced further up to 0.35. At 6% clay content, the change in normalized water content at the wetter side of SWCC is still insignificant. This suggests that with a constant biochar content of 3%, biochar's efficiency (change) to affect SWCC seems to reduce with an increase in clay content at 6%. The possible reason could be that the amount of smaller size of pores is enhanced with an increase in clay content at this optimal amount. Any further addition of finer biochar may not be significant since the existing smaller pores of clay will instead engulf biochar particles. Such pore-filling mechanism effects have also been discussed in the literature [314]. For clay content above 8%, a significant reduction in NWC is also observed in the wetter side of SWCC. It suggests that for higher clay contents, any effect of biochar may not be significant on the drier or wetter side of SWCC.



(a)



(b)

**Figure 27** The soil suction and NWC with varying silt and clay for biochar amendment of 3% and 10%

The trend of SWCCs for soils at a biochar content of 10% appears to be similar to that of 3%. However, some changes are observed in SWCCs when biochar content is increased to 10%. The threshold clay content beyond which reduction in NWC takes place increased from 6% (biochar content of 3%) to 8% (biochar content of 10%). It also suggests that the threshold clay content is higher for soils with a larger amount of biochar. These results suggest that any addition of biochars may not be useful for soils with clay content higher than 6%. This conclusion is dependent on the data used for training of model and prediction. However, this result suggests an important precaution for avoiding the excessive use of biochar in soils with higher fine content.

Similarly, the effect of biochar is likely to be lower in soils compacted at higher densities—compaction results in a reduction in average pore size. Garg et al. [422] also conducted a series of experiments to determine the influence of biochar on water retention in soils compacted at different densities. It was found in their study that biochar was found to be more efficient in soil compacted at 65%, followed by 80% compaction as compared to 95%. The pore-filling mechanism of biochar influences WRC and hence plant available water. The optimum biochar percentage addition makes a biochar soil composite with a higher hydraulic conductivity due to a large and continuous porous system [430]. Biochar addition of 5% showed more plant available water than 2.5% [378]. The review

conducted by Edeh et al. [431] observed that the biochar amendment  $> 30$  t/ha and  $< 30$  t/ha was feasible for coarse- and fine-grained soils, respectively.

It is interesting to note from **Figure 27** (a) that there is a tendency of bimodal behaviour for SWCC corresponding to clay content of 6% and biochar content of 5.4%. This might be possible due to the dual porous structure depicted by the simultaneous presence of a significant amount of clay and biochar content. Also, as understood from the literature, some biochars [432, 433] may depict dual porous structure itself, whose effect on water retention behaviour of soils needs to be investigated. Further studies are needed to explore the potential of different types of biochars, namely plant-based and animal-based, to understand their effect on the water retention behaviour of soils.

#### 4.3.3 Influence of biochar types on soil with higher sand content

**Figure 28** shows the influence of biochar content on SWCCs of soil with higher sand content (90%). It can be observed that with an increase in biochar content, there is a slight increase in NWC of soil at the wetter side of SWCC. On the other hand, the change in NWC on the drier side of SWCC is insignificant with an increase in biochar content (except for 10%). The observation is different from that of soils with a relatively higher ratio of fine to coarse content (refer to Figure 26). It was found in **Figure 26** that the influence of biochar is relatively more on the drier side of SWCC than on the wetter side. There was a threshold clay content beyond which the effect of biochar was significant on the wet and dry sides of SWCC. It was found in **Figure 28** that the presence of excessive biochar (10%) can cause a reduction in NWC. This implies a relatively high requirement of biochar content requirement for soil with very high sand content (at least 10%) to cause a significant change in NWC. Previous studies revealed the effects of biochar on hydraulic characteristics [402]. Biochar amendment increases the water retention capacity, which is also influenced by biochar feedstock, pyrolysis temperature, pyrolysis duration and soil types [29]. Arthur et al. [434] observed increased WRC due to biochar at a high suction range in non-compacted sandy loam soil.

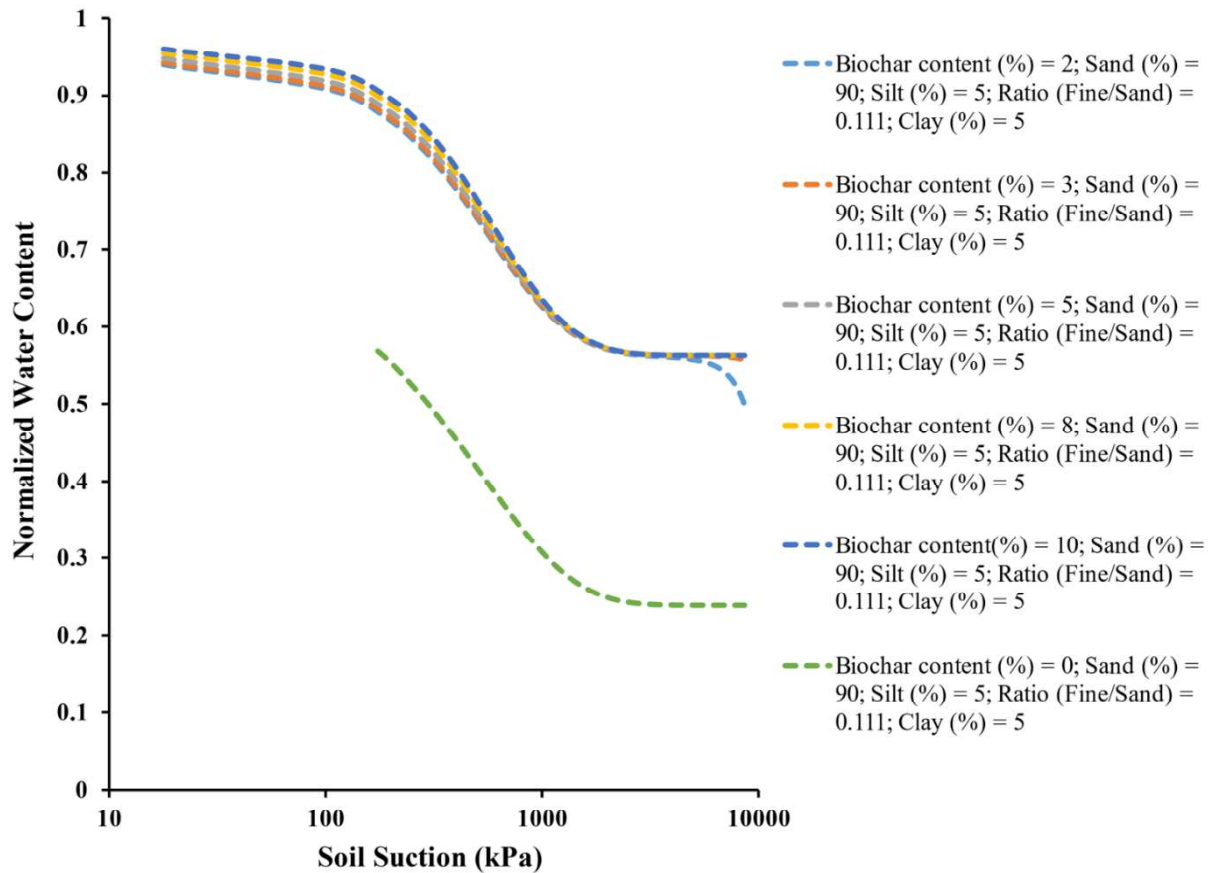


**Figure 28** Variation of NWC and soil suction at different biochar contents for soil with higher sand content

It should also be noted from **Figure 27** and **Figure 28** that the influence of the void ratio on SWRCs is not explicitly considered. The developed ANN model is based on data from heterogeneous sources, including studies from agriculture, hydrology and geotechnical engineering, where soil densities have contrasting differences. Further, very few studies have reported void ratio or soil density (in terms of DoC) in their studies. Studies from a geotechnical engineering perspective [90, 402, 422, 423] reported a DoC of 70%–95%, while agricultural studies reported a soil density of 1.3 g/cm<sup>3</sup> [6]. It is well known that the initial void ratio affects the SWCC behaviour [435, 436]. Zhai et al. [435] established a framework based on a pore-size distribution framework for estimating SWCCs. A considerable change in water retention behaviour is observed, especially in the lower range of suctions before the residual zone. Before considering it for model development, further studies are needed to quantify the effect of different initial void ratios on SWCCs of biochar amended soils.

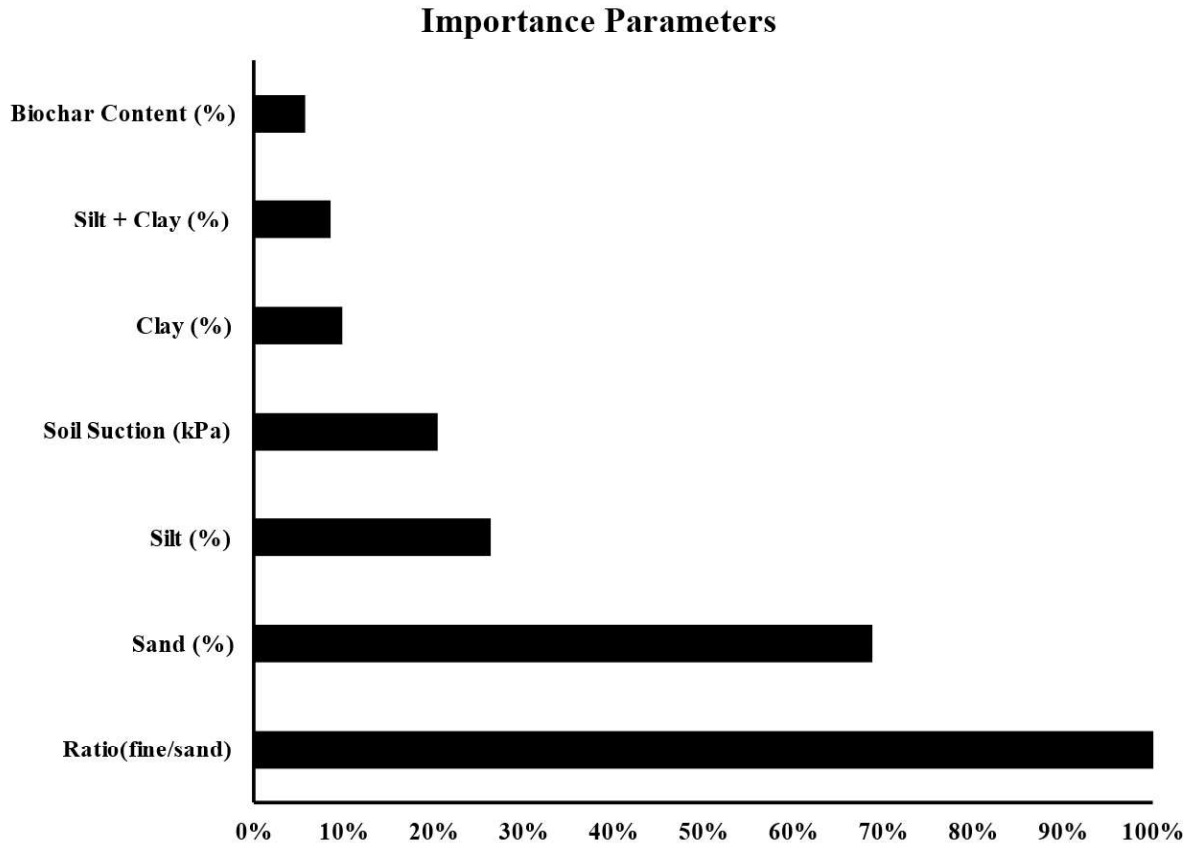


**Figure 29** Relative significance of parameters affecting SWCC

It can be found from **Figure 29** that the ratio of fine to sand content is the most influential parameter affecting NWC. The fine to sand content ratio indirectly influences the microstructural arrangement and, hence, water retention capacity. This is followed by sand content, silt content and soil suction. Interestingly, biochar content seems to be the least important parameter of all. The results suggest that the ratio of fine to sand content is an important parameter while determining the efficiency of biochar. It should be noted that the conclusions are based on a limited set of data, and any influence of soil compaction and feedstock type of biochar is not considered.

#### 4.4 Observation

This study aims to analyse the efficiency of biochar on SWCC of soil with varying grain size distributions. A new factor (ratio of fine to sand content) was defined to understand biochar's influence on SWCC. The ANN-based model was found to predict SWCC reasonably well. Based on predictions, it was found that there is a threshold clay content (6%–8%) beyond which any effect of biochar becomes less significant. However, for soils with higher sand content, there is a slight increase in NWC on the wetter side of SWCC with the presence of biochar. A relatively higher amount of biochar (i.e., 10%) is required to cause

changes in the drier side of SWCC for sandy soils. Based on sensitivity analyses, the ratio of fine to sand content was also the most important factor causing changes in NWC. The ratio indirectly influences the microstructural arrangement and soil water retention capacity.

In contrast, biochar content was found to be comparatively least influential. It should be noted that the above conclusions are based on the given set of measured data that was available in the literature. Further, there is also a lack of reliable data on SWCC at the higher range of soil suction and various types of biochar produced from different feedstock types. More systematic studies need to be conducted to establish full-scale SWCC for soils amended with various types of biochar (i.e., animal-based and plant-based). In addition, probabilistic approaches and Bayesian optimization techniques [437–439] can be adopted for considering uncertainties in measured SWCCs.

## Chapter 5: Application of Artificial Intelligence for Predicting Erosion of Biochar Amended Soils

---

### 5.1 Background

In the previous chapter, the water holding capacity of the BAS was discussed. In this chapter, the next important property coming under the scope of hydraulic properties and an objective in this thesis is the influence of biochar in controlling erosion.

Biochar's physical and chemical properties include its physical and chemical characteristics. The physical properties include particle size, surface area, and porosity. The chemical ones include chemical stabilization and their related effects on the soil, increase in soil organic content, and aggregate stability, as brought out by various studies [100, 179–183, 440]. The increase in CEC and reduction in nutrient leaching are also caused due to addition of biochar in the soils [100, 184]. As discussed in previous chapters, the alkaline nature of biochar decreases the acidity of soils. The porosity of biochar adds porosity to soil and makes the composite more hydraulic conductive [100, 185]. It is also observed that the biochar addition to soil increases the charge density and hence the aggregate stability of the soil [98, 186, 187].

Researchers have investigated biochar effectiveness in modifying the hydraulic conductivity, WRC [96, 220, 441–443], chemical properties (pH, CEC, etc.), and nutrients [4, 333, 335, 442, 444, 445]. These properties of biochar help make BAS erosion-resistant [333, 442] with a life period of thousands of years [359, 442, 446]. Materials have been recognized that, when used with biochar, increase the effectiveness of biochar in controlling soil erosion. One of such solutions was using polyacrylamide (PAM). Observations were made the PAM in combination with biochar was added to the soil to neutralize the damaging effects of biochar that cause an increase in soil erosion. When added to soil, PAM increased aggregation and improved the erosion resistance of the soil. However, some studies [183, 447–449] had observed different results on the erosion for two soils, loess and marl, when biochar and PAM were added together. In their study, Tang et al. [450] used PAM with biochar, and it was observed that the adverse biochar effects were obviated and retained the positive effect of soil conservation. Lee et al. [325] used a biochar and PAM mixture and observed that it was a better selection among the three for decreasing soil loss. Researchers have also pointed out that the fine particles of biochar can be flushed away under heavy rain (because of less specific gravity) and cause more erosion [98, 334, 451]. Cai et al. [324] noticed that at a biochar amendment of 5%, soil erosion was found to be minimum. The proportion of soil aggregates size and its redistribution by biochar addition is essential for the maintenance of porosity so that there is a decrease in the erosion of BAS [333]. It has also been observed that under the climate of humid subtropics, prolonged use of soils leads to their degradation in nutrient capacity, pH, and aggregation, causing weathering and soil dryness. These soils then become inclined to wind erosion [333, 338, 452–455]. When amended with biochar percentages of 2.3% and 5%, soil significantly showed erosion control by 50% and 64%, respectively, due to improved macroaggregate

formation [333, 455]. Biochar addition to the soil in a dry state causes a reduction in erosion, but in the wet state, the erosion increases [318].

## 5.2 Introduction

Soil erosion is the natural process of detachment, transportation, and soil deposition by water, wind, or gravitational forces [456]. Crop cultivation over a long time also decreases soil's organic content and causes acidification, making the soil prone to more erosion [333]. This leads to soil degradation and a decrease in the productivity of the land. Soil erosion also causes siltation of natural and artificial water bodies and flooding of lower plains. It may also lead to pollution of water/land downstream. Researchers believe that the loss of organic matter in the soil due to erosion might be a probable reason for global warming [457]. Effective measures such as maintaining the soil's organic and moisture content, improving aggregate stability, and optimizing soil's hydraulic conductivity need to be administered [17, 333, 458, 459] to limit soil erosion. Holz et al. [456] listed moisture content, porosity, surface roughness, texture, and soil aggregation as key soil properties that determine the possible extent of soil erosion. Soil erosion is influenced by various factors, amongst which slope condition, soil properties, and rainfall intensity are considered the most influential [324]. Rainfall (amount, duration, sequence, and intensity) is the most important factor determining the soil erosion quantity [456, 460, 461]. Long and steeper slopes are favourable for erosion [456, 461, 462]. It has been observed that compaction collapses micropores, decreases subsurface seepage flux, and increases runoff, thereby providing favourable conditions for increased erosion [456, 463, 464]. The effect of erosion has been experienced by 90% of the world's agricultural land. Given the above factors which influence erosion, it is observed that the topographical and climatic factors are beyond human control; however, the inherent soil properties and vegetation can be modified.

Soil conservation is important because the soil formation rate is generally far slower than its erosion rate [183, 465]. The topmost fertile soil layer is lost due to erosion [469, 470], making it less productive and creating siltation problems in water bodies and catchment areas. Vegetation cover and litter (grass, trees, herbs, shrubs, and residue) help reduce soil erosion [456, 460, 468–473]. Therefore, government bodies should encourage farmers to adopt soil conservation methods such as the growth of hedges, reduced tillage, and straw mulch [457, 474]. It is observed that the use of residues obtained from agriculture and forests as a soil amendment reduces soil erosion and nutrient loss [332, 457, 475]. Researchers use different measures and soil amendments to reduce soil erosion [13]. From the literature, it has also been observed that the use of biochar as a soil amendment is a novel and promising approach. It enhances soil quality for better water holding capacity (WHC), higher agricultural productivity, improves geoengineering works, and reduces environmental pollution and erosion [3, 24, 35, 60, 91, 96, 186, 312, 457, 476, 477].

United States Environmental Protection Agency (USEPA) guidelines advocate vegetation growth on the soil's surface to reduce erosion [318]. The vegetation growth depends on soil properties and, as such, can be increased by simply modifying them. The nutrient value of biochar and its function as a carbon sink increases vegetation growth, macroaggregate stability [324, 325, 333, 442], modifies soil properties, like

subsurface seepage flux, WHC, surface functionality and compaction [6, 90–92, 318, 333, 391], and directly or indirectly helps control erosion [31, 318, 333]. Pinhole tests demonstrated increased water content in biochar amended soils (BAS) decreases erosion rate [318]. Abrol et al. [326] hypothesised that the biochar amendment of sealing-prone soils causes electrolytes present in biochar to dissolve in soil solution and reduce erosion by increasing subsurface seepage flux. While using 2% biochar amendment in non-calcareous loamy sand, the subsurface seepage flux was high, and soil loss was less [326]. Various studies have reported the use of vermicompost in Northern Vietnam to increase vegetation in soils degraded by erosion. The influence of biochar on WHC, porosity and hydraulic conductivity of soil reduces erosion due to increased subsurface seepage flux and less runoff [31].

Computational techniques such as dimensional analysis [408], k-nearest neighbour (KNN) [412], multiple regression analysis [35], and Artificial Neural Network (ANN) are seen as multidimensional, less tedious, flexible, and advanced numerical approaches used by researchers for solving various types of engineering problems [189, 409, 411–413, 426]. Researchers have used ANN for explaining and predicting complex material behaviours in various studies. For example, Bordoloi et al. [300] adopted ANN modelling to study the distribution of the Crack Intensity Factor (CIF). Arif et al. [478] adopted ANN to develop an erosion model based on erosivity, erodibility, length, and slope. More recently, Wani et al. [24] used machine learning for model development to predict biochar properties like O/C and H/C from the pyrolysis conditions, volatile matter content, and pH value for different types of biochar.

This study aims to develop an ANN model for predicting erosion as a function of biochar content, degree of Compaction (DoC), slope gradient, slope length, and rainfall intensity. Further, the study also attempts to analyze the optimum percentage of biochar amendment for erosion control. Data for the development of the model was obtained from Cai et al. [324]. The study conducted by Cai et al. [324] investigated erosion control by using biochar at 5% and 10% amendment ratios on a small scale and in controlled laboratory conditions. However, some shortcomings have been noticed, including specific biochar and soil, slope, and rainfall conditions that limit the use of results for further research. The methodology for the experimental setup includes the use of simple bare soil. The vegetation in the soil has not been considered. The use of ANN has addressed the above shortcomings. The model developed is flexible and can predict erosion control with biochar amendment of any ratio, slope conditions, and rainfall intensity. The developed model can be useful in the preliminary design and analysis of green cover amended with biochar. Such a model can also provide the efficiency of biochar amendment and the required optimal content under various slope and soil conditions.

## 5.3 Materials and Methodology

### 5.3.1 Experimental Program for Measurement of Erosion in the Soil-Biochar Mix Using Flume Setup

Experimental data were obtained from a study where erosion tests using flume were conducted. In the study by Cai et al. [324], an in-house flume setup was developed containing a 1.50-m-high rainfall simulator designed to simulate 60 mm/hour and 90 mm/hour rainfall. The

actual rainfall intensity was measured using a pluviograph. In addition, a tank filled with distilled water was installed. The calibration was conducted using hydraulic pressure and pluviograph recordings at 0.1 MPa for 60 mm/hour and 0.15 MPa for 90 mm/hour. An alloy steel frame was added to the flume setup to measure rainfall-induced runoff and subsurface seepage flux. The flume's width was 0.6 m, and length was 1 m and 2 m, respectively, as shown in **Figure 30**. A drainage layer containing geotextile fiber (for minimizing soil particle flow) and a 6 cm thick gravel layer were placed below the soil layer.

Colluvial soil consisting of medium sand (82%), fine sand (16%), and silt and clay (2%) was adopted for flume tests. The sample was taken from the top (0–0.5-m depth) ground layer at the Shantou University campus (located not far from the South China sea) and classified by SP (ASTM-CS) as poorly graded sand. Biochar was produced from the invasive weed “Water hyacinth” collected from the coastal region of Shantou, China. Biochar is well known to have higher stability in terms of life (>100 years) [24] as compared to water hyacinth biomass, which is prone to degradation upon microbial activity. Therefore, biochar is a relatively stable carbon that can be utilized for geotechnical engineering structures (landfill cover, slope cover), which have more extended design periods (30–50 years) [24]. Shredded and air-dried water hyacinth stems were pyrolyzed [324] to prepare biochar. The slow pyrolysis process was done at a temperature starting from room temperature to 600°C at a 10°C/min heating rate. The maximum temperature maintained was 600°C. Biochar produced in-house possesses a porous structure, large surface area, and high surface functional groups. Biochar was powdered by crushing to below 2 mm size. The chemical properties were analyzed by Zeta ( $\xi$ ) potential and Fourier Transform Infrared (FTIR) [479]. Zeta ( $\xi$ ) potential and surface charge values were 16.9 mV and  $1.54 \times 10^{-6}$  C/cm<sup>2</sup>, respectively. Physical characteristics of biochar particle surface were analyzed using particle shape analysis (Occhio, Angleur, Belgium). Properties of biochar indicate a high degree of irregularity, convexity, and roughness. A higher surface area of biochar ( $15 \mu\text{m}^{-1}$ ) is also likely to enhance the interaction between biochar, soil and water [480].

After preparation, biochar was added to the soil with an amendment ratio of 5% and 10%. Measured optimum water content and dry density for bare soil were 12% and 19 kN/m<sup>3</sup>, respectively. Compaction rates of 65% and 95% corresponding to agricultural and engineering applications were considered. An increase in water content and a decrease in dry density were observed upon mixing biochars. The optimum water content values for 5% and 10% BAS were 12% and 13%, whereas dry density was 18.8 kN/m<sup>3</sup> and 18.6 kN/m<sup>3</sup>, respectively. The specific gravity of bare soil and soil amended with 5% and 10% biochar was 2.59, 2.59, and 2.55, respectively. The void ratios of bare soil, 5% and 10% biochar amended soil at 65% compaction degree were found as 1.31, 1.34, and 1.33, respectively. In contrast, the sample's void ratios at 95%

compaction were found as 0.58, 0.60, and 0.59, respectively. Thus, the results showed an increase in void ratio and a decrease in specific gravity with the addition of percentages of biochar to soil.

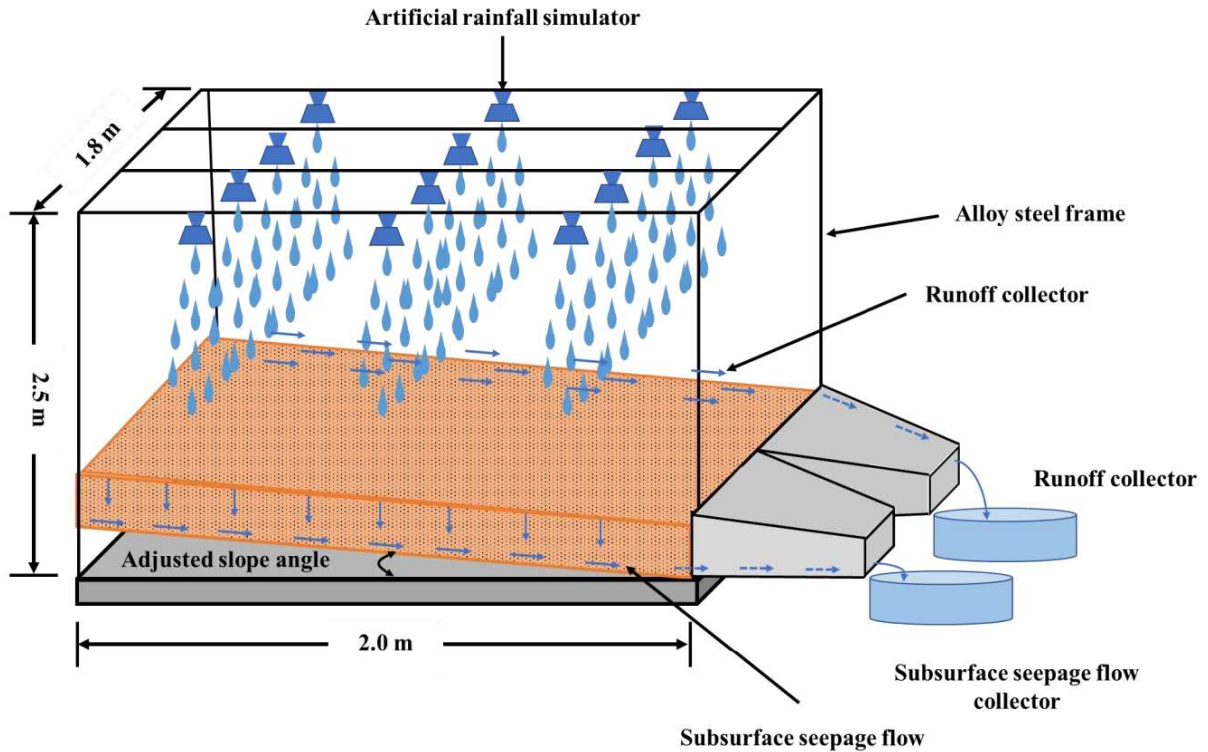


**Figure 30** Illustrative sketch of flume experiment [481]

### 5.3.2 Test Plan and Procedure

A full factorial experimental plan was designed considering possible coupled effects of combinations of low and high levels of all parameters [482]. To meet the practical engineering slope design, as suggested by [483], [484], and [485], the authors considered mild ( $7^\circ$ ) and moderate slopes ( $20^\circ$ ) in combination with four other factors (slope gradient, compaction, rainfall, and slope length). The soil-biochar mix was subjected to 60 mm/hour and 90 mm/hour rainfall intensity. The slope lengths of 1 m and 2 m were selected [483, 484]. Sixteen (16) experimental runs on three different soils, viz. bare soil, 5% biochar amended soil, and 10% biochar amended soil, were made as per the formula  $2^n = 16$ , where  $n$  is the number of factors. A total of 96 experiments, including duplicates, were conducted considering combinations of high and low levels of each factor.

The biochar and soil composite samples were prepared by mixing designed quantities and placed over the flume. The samples were compacted to the desired degree of 65% and 95% compaction in three layers. Samples were then subjected to three hours of rainfall with minimum soil loss, left overnight for moisture equilibrium and maintained under similar initial conditions. Rainwater could penetrate the soil medium and retain in the soil pores, leading to excess water subsurface seepage flux. Infiltrated and runoff water was collected separately and measured.

Afterwards, the samples were subjected to two hours of rainfall, and the measurements of subsurface seepage flux and runoff were taken every 5 min for 30 s [486]. The runoff and subsurface seepage flux quantities were deduced from these measurements. The sum of two quantities (runoff and subsurface seepage) constituted the total water flow rate. The total soil erosion rate was calculated by oven drying the collected water from runoff and subsurface seepage flux (infiltration) quantities at 105°C.

### 5.3.3 Artificial Neural Network

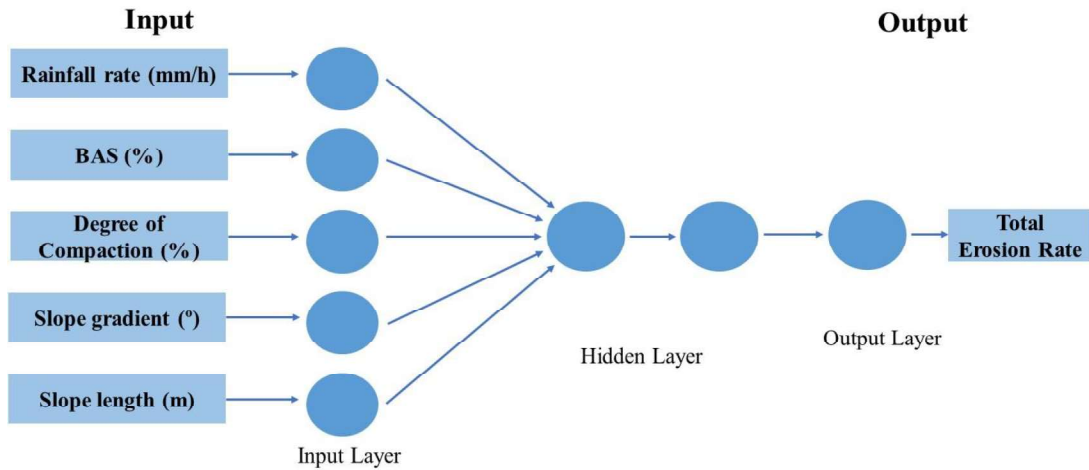
The commercially available STATISTICA version 12 [61] was used in the present study. During the development stage of the model, gradient descent was adopted. To develop the model rainfall rate, BAS, DoC, slope gradient, and slope length were taken as input parameters to predict the total erosion rate and total water flow rate using two hidden layers. The ANN model architecture used to predict the total erosion rate, and total water flow rate is shown in Figure 31(a, b). The ANN algorithm ranks the influence of each input parameter on the output. Figure 32 shows a flowchart indicating the methodology implemented to model the network [409, 426].

ANN model development needs a clear definition and performance criterion [414, 487]. The performance determination is checked by the Coefficient of Determination ( $R^2$ ) and the mean absolute percentage error. The error is calculated from the predicted and experimental values by determining MAPD by the equation:

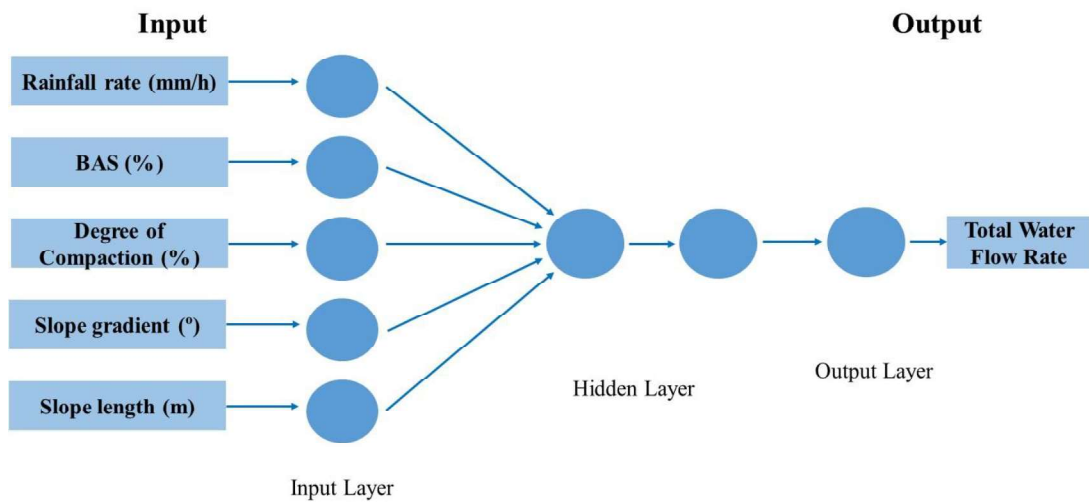
$$MAPD = \frac{100}{n} \sum_{i=1}^n \frac{(M_i - P_i)}{M_i}$$

Equation 8

where  $M_i$ : Measured Value  
 $P_i$ : Predicted Values  
 $n$ : number of data points



(a)



(b)

**Figure 31** ANN design model used for prediction of (a) Total Flow (b) Flow Rate [481]

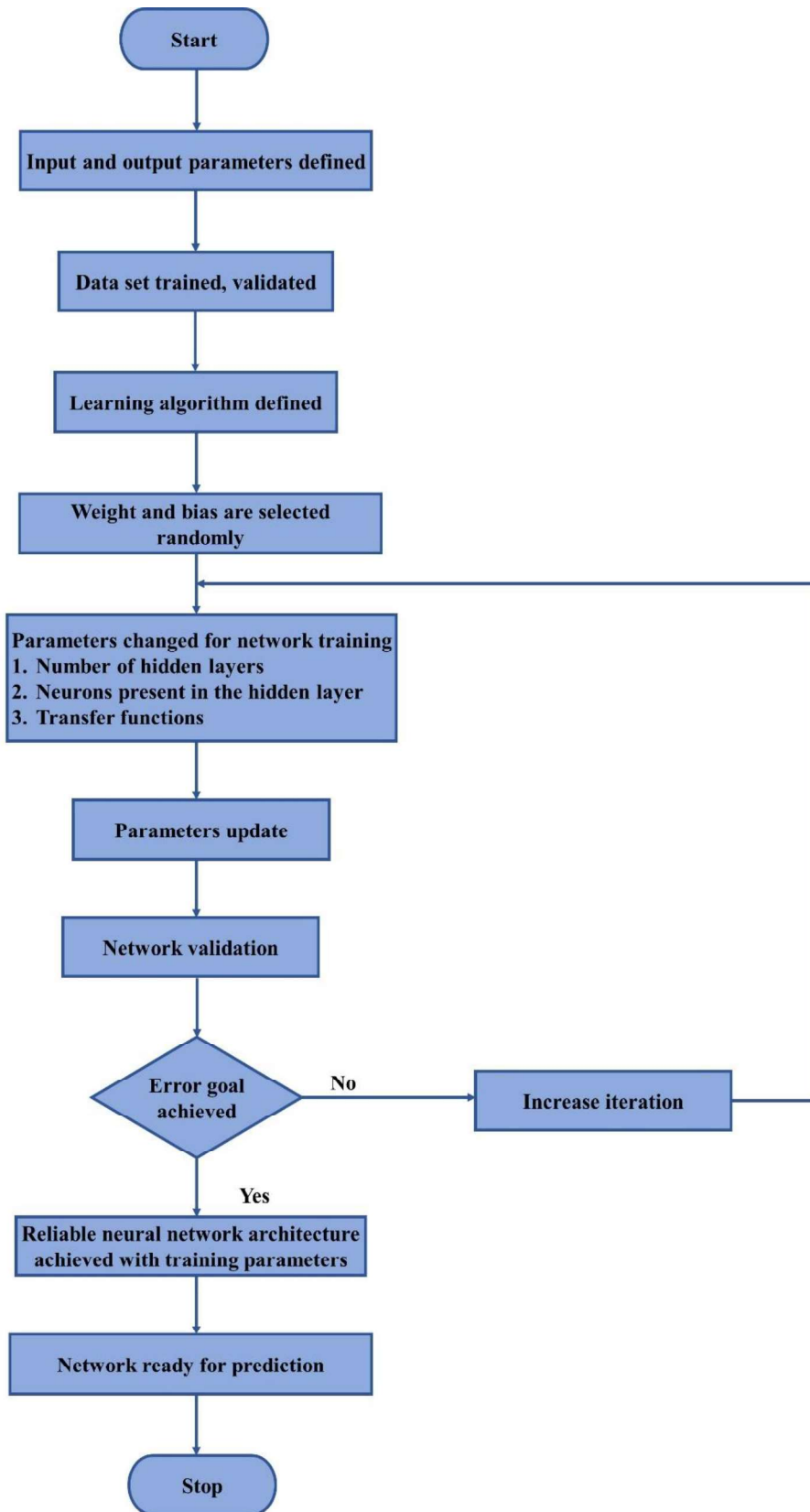
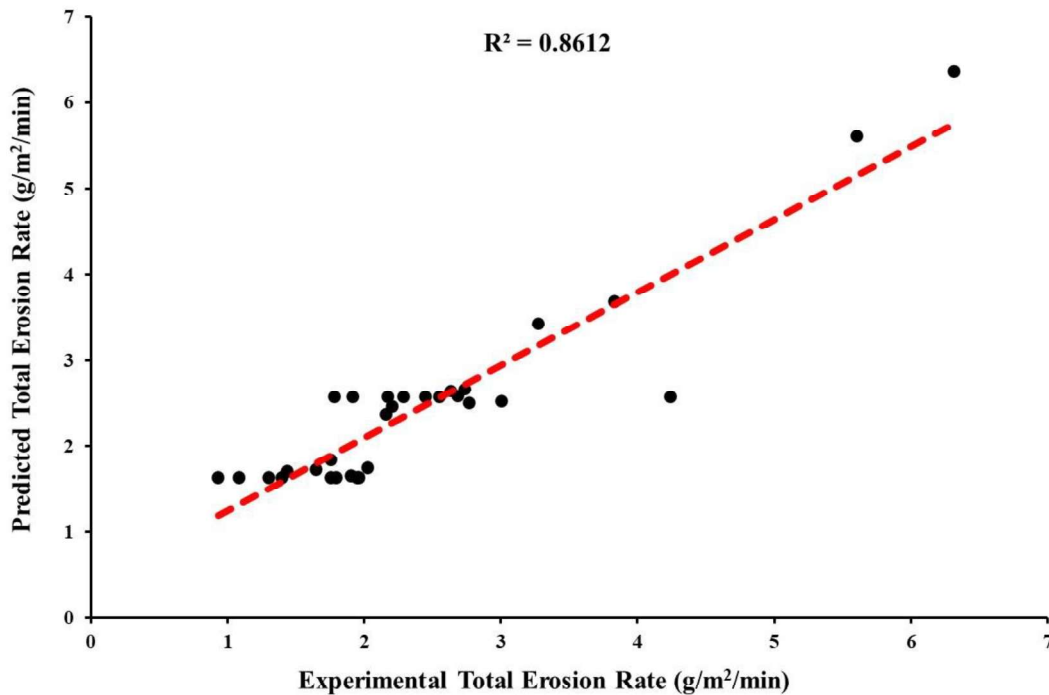


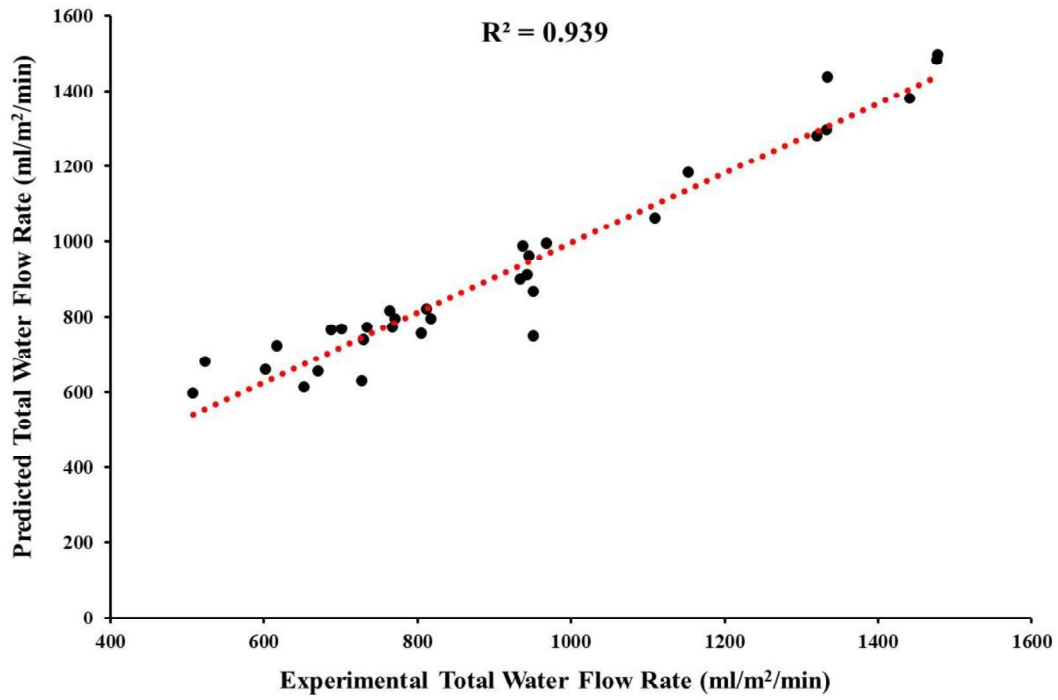
Figure 32 Flowchart for ANN modelling [481]

Graphs were plotted using ANN prediction in STATISTICA; a relationship was developed between the output and input parameters. The degree by which each parameter varies, corresponding to the input parameter's value difference, directly measures each variable's importance. Each time one input parameter effect was taken on the output parameter by keeping the rest of the parameters constant while plotting the graph.

**Figure 33(a,b)** compares the predicted and measured values for total erosion and water flow rates. The  $R^2$  value is 0.788 and 0.939 for total erosion and water flow rates, respectively. The error was calculated between the experimental and predicted values. The average error (MAPD) is around 15% for the total erosion rate and 7% for total water flow rates. Based on these errors, the ANN model's accuracy for erosion and flow rate is 85% and 93%, respectively. A bar chart has been plotted for quantitative comparison between the experimental and predicted values of the erosion rate and total water flow rate, respectively, as shown in **Figure 34 (a,b)**.

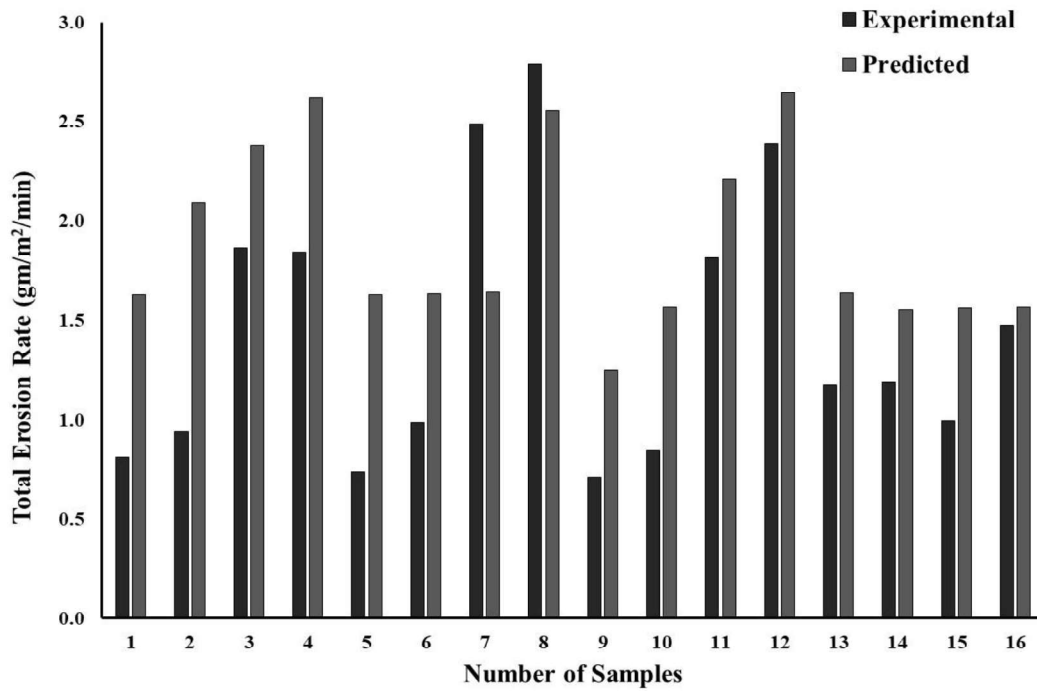


(a)

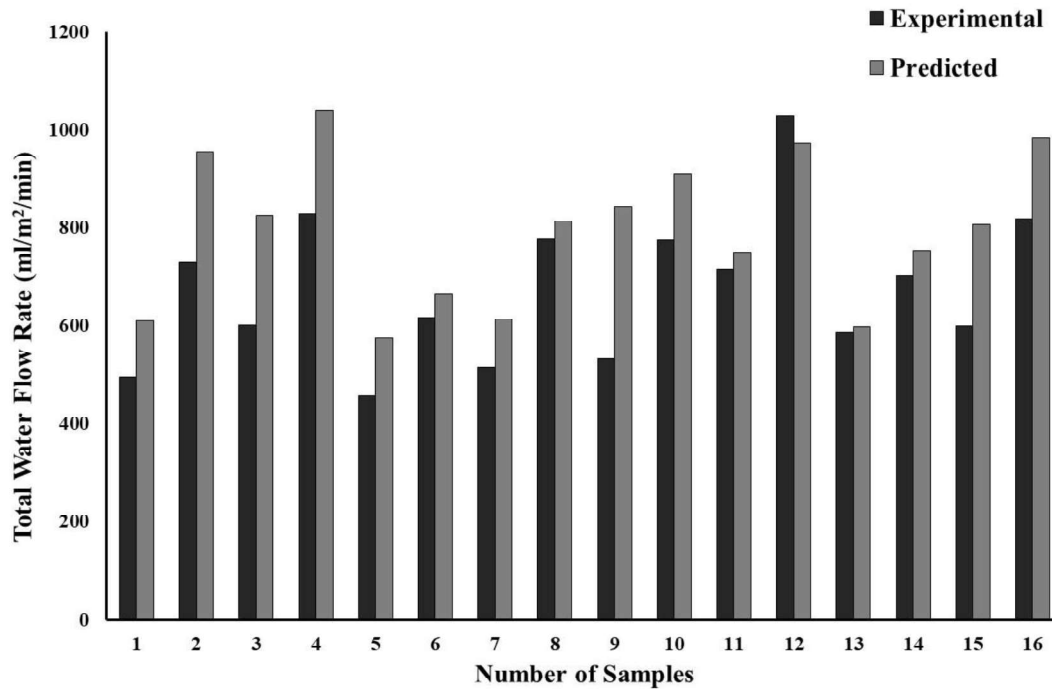


(b)

Figure 33 Comparison between Experimental and Predicted (a) Total Erosion Rate and (b) Total Water Flow [481]



(a)



(b)

**Figure 34** Variation of experimental with ANN predicted values for (a) Total Erosion Rate and (b) Total Water Flow Rate [481]

## 5.4 Results and Discussions

### 5.4.1 Influence of Degree of Compaction on Total Erosion Rate and Total Water Flow Rate

**Figure 35** shows that soil compaction has an important effect on infiltration and runoff. As shown in **Figure 35**, both total erosion and water flow rate increased as the compaction rate increased total erosion rate and total water flow rate increased with the compaction of soil (i.e., DoC). The predicted values of the ANN (STATISTICA) model for the degree of compaction was applied to draw the graph for DoC with total erosion rate, and the total water flow rate was plotted using ANN prediction in STATISTICA. The DoC is an input given to the model to notice the effect on total erosion and water flow rate (output). The effect was observed on the output parameters by keeping the rest of the parameters (biochar content, slope length, slope gradient, and rainfall rate) constant while plotting the graph.

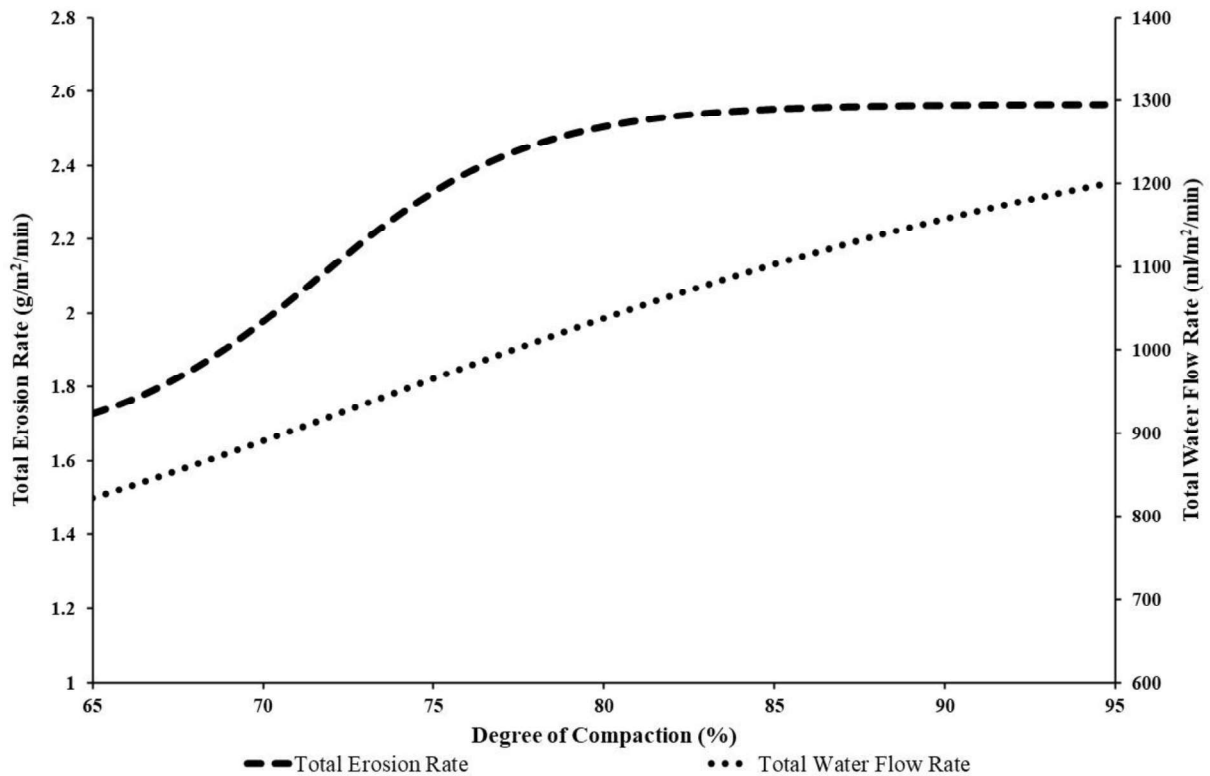


**Figure 35** Graph showing the effect of change in DoC on total erosion and total water flow rate [481]

It is observed that with an increase in compaction, the total erosion rate increases from 1.75 g/m<sup>2</sup>/min to 2.55 g/m<sup>2</sup>/min. Similarly, the total water flow rate increases by almost 48.75% (i.e., 810 mL/m<sup>2</sup>/min to 1200 mL/m<sup>2</sup>/min). However, the increase in flow rate is almost linear. In contrast, the enhancement is more substantial for erosion rate during an increase of compaction from 65% to 80%. It is expected that an increase in compaction should reduce soil erosion; however, under prolonged rainfall, there is likely an enhancement in water logging due to lower permeability. This may cause erosion of fine soil and biochar particles present in the upper layers of compacted soil. Similar results have been observed in the previous studies for bare soil [456, 463, 464]. Correlation can also be made because the soil structure and its hydrology are changed when the bulk density of soil is enhanced, leading to a decrease in the porosity of soil and subsurface seepage flux capacity. This eventually leads to an increase in runoff [488]. Compared to bare soil, BAS has a higher porosity, void ratio, and WHC. The same applies when soil is compacted, even though the void ratio is reduced in both cases (bare soil and BAS).

Irrespective of the DoC, the runoff in BAS is lower, while the subsurface seepage flux is higher than bare soil. This is opposite to the observation of Gopal et al. [92], where a decrease in infiltration was observed in biochar amended soil compared to bare soil. The difference might be due to the applied boundary condition. In the study of Gopal et al. [92], a suction head was applied using a mini-disk infiltrometer, while in the current study, rainfall was simulated on the upper surface of the soil. Studies are needed in future to characterize the influence of boundary conditions

on the effectiveness of biochar in controlling soil erosion. Higher runoff tends to cause more erosion in bare soil. For an implication in landfill liners and slopes, there is a need to identify the optimal compaction rate considering the effect of erosion under natural rainfall. Further, variation in soil water retention and strength characteristics also need to be considered while considering the DoC of a landfill liner [422].

The runoff in bare soil was lowest in soil amended with 5% biochar than bare soil and 10% BAS. The model predictability seems reasonable as the results are similar to the experimental data and the available literature [324, 456, 463, 464].

#### 5.4.2 *Influence of Rainfall Rate on Total Erosion Rate and Total Water Flow Rate*

Figure 36 shows that the total erosion rate and total water flow rate are enhanced with increased rainfall intensity. ANN prediction was used for plotting the graph for rainfall rate with the total erosion rate and total water flow rate. Rainfall rate was an input parameter. Its effect was observed on the output parameter (total erosion rate and total flow rate) by keeping the rest of the parameters (biochar content, slope length, slope gradient, DoC and biochar percentage) constant while plotting the graph. The erosion rate increases from 1.78 g/m<sup>2</sup>/min to 2.4 g/m<sup>2</sup>/min, increasing rainfall intensity by 50%. The corresponding increase in total water flow is around 59% (i.e., 820 mL/m<sup>2</sup>/min to 1290 mL/m<sup>2</sup>/min). Studies [456, 460, 461] have demonstrated that rainfall is important for determining soil erosion. Lower intensity rainfall will produce more subsurface seepage flux and, therefore, less runoff and erosion. It should be noted that the above graph is based on two measured rainfall data points (60 mm/hour and 90 mm/hour), and any interpretation of variation in total erosion rate and total flow rate between them is subjected to it. Nevertheless, the result related to the increase in total erosion rate is consistent with that of laboratory studies on bare soil by Fu et al. [489].

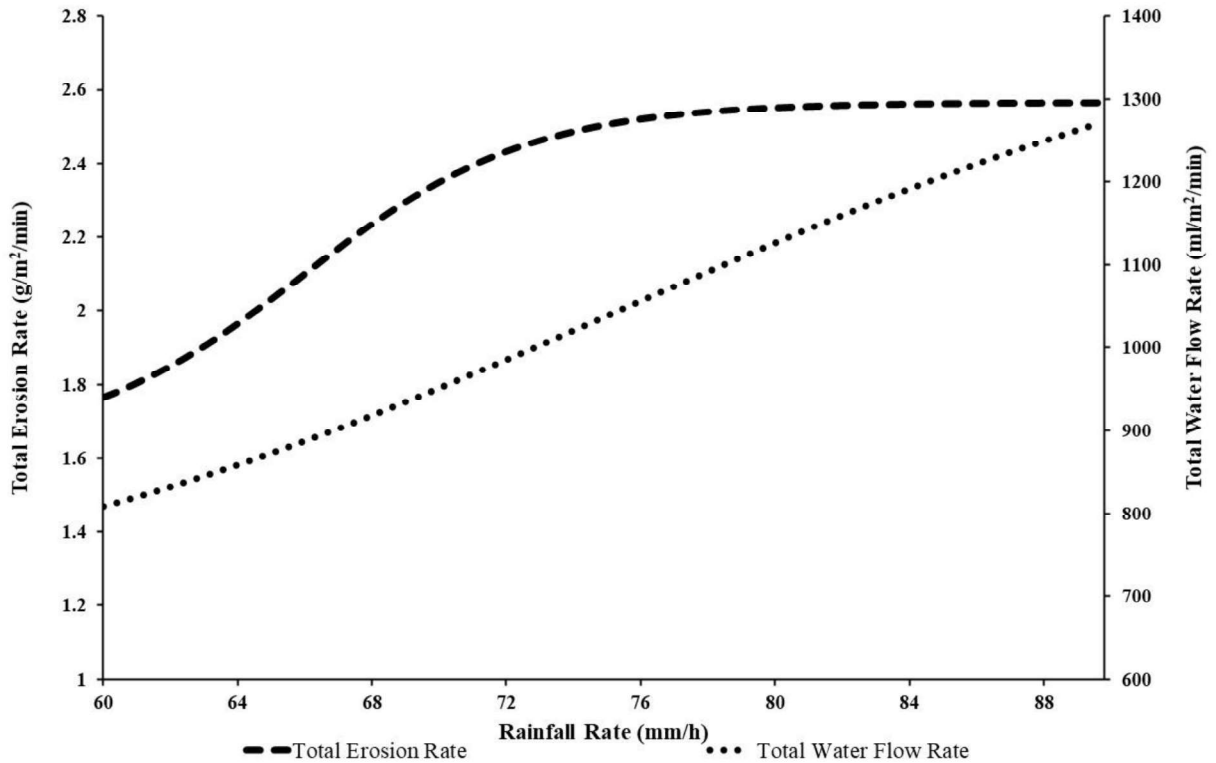


**Figure 36** Variation of Total Erosion Rate and Total Water Flow Rate with the Rainfall Rate [481]

#### 5.4.3 Influence of Slope Length on Total Erosion Rate and Total Water Flow Rate

**Figure 37** shows the variation of total erosion rate and water flow with the slope length. The graph was plotted using ANN prediction for slope length with total erosion rate and water flow. The input parameter was the slope length. The observations were taken for the output parameter (total erosion rate and total flow rate) by keeping the other parameters (biochar content, rainfall rate, slope gradient, DoC, and biochar percentage) constant while plotting the graph. It was observed that there is a decrease in both the parameters with the slope length. This is expected since eroded particles are likely to travel shorter distances or are transported to local depressions [490]. In addition, the presence of biochar may add to discontinuity and surface roughness, which can resist further movement of particles. Fu et al. [489] also observed a lower correlation of runoff with the slope surface area than the rainfall intensity. The mechanism is relatively more complex, as the slope length (or surface area) is enhanced than the rainfall intensity, directly associated with the runoff.

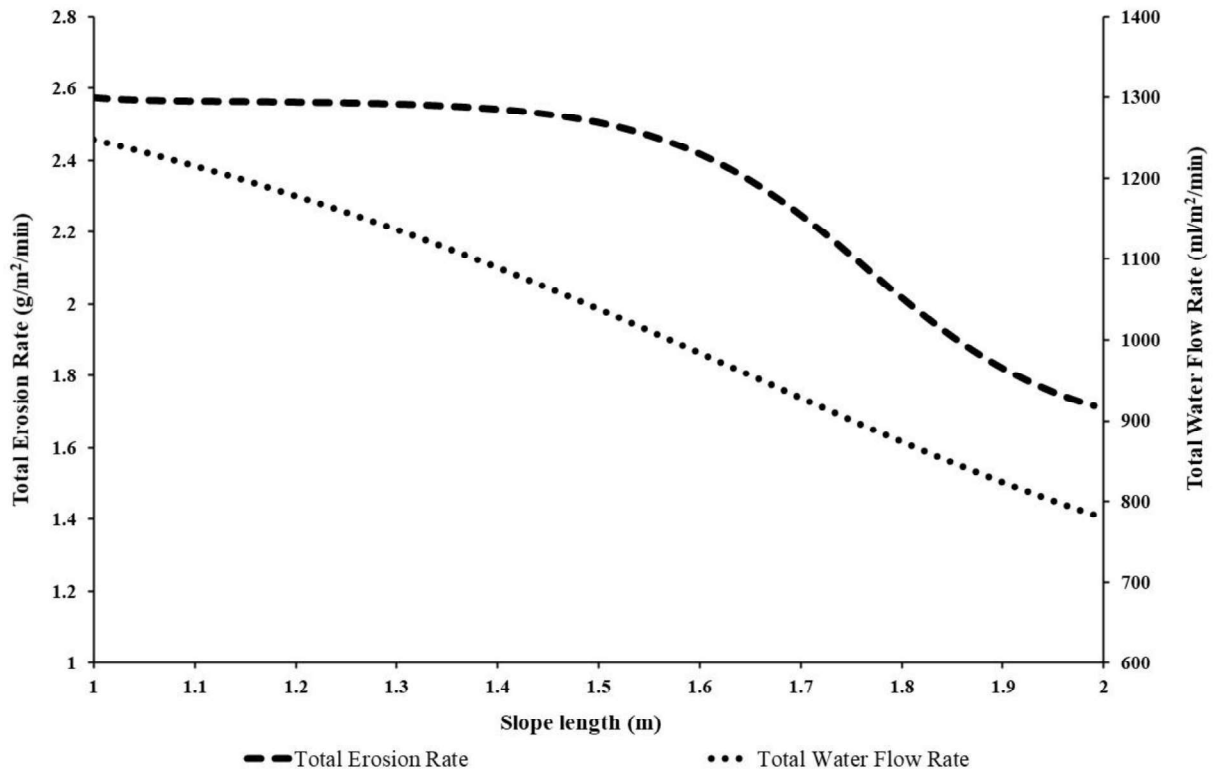


**Figure 37** Variation of Total Erosion Rate and Total Water Flow Rate with the Slope Length [481]

It can also be observed that the reduction in erosion is relatively minimal during an increase in slope length to 1.55 m, whereas it reduces sharply beyond that. It implies that at this threshold slope length (1.55 m), under a given rainfall intensity, eroded particles can no longer settle down or be translocated to other parts of the slope. At a slope length of 2 m, erosion is reduced by 33% (i.e., 2.6 to 1.75), whereas the total flow rate decreases linearly from 1250 mL/m<sup>2</sup>/min to 790 mL/m<sup>2</sup>/min. The above findings suggest that the influence of slope length on erosion is critical for given rainfall intensity. However, it should be noted that the study does not consider extreme rainfall (up to 115 mm/hour [491]). To better understand the mechanism of influence of slope length, a longer flume in a range of 10 m [489] needs to be built and investigated under natural rainfall in the field.

#### 5.4.4 Influence of Slope Gradient on Total Erosion Rate and Total Water Flow Rate

**Figure 38** shows the variation of the total erosion rate and water flow rate with the slope gradient. The graph was plotted using ANN prediction for slope gradient with total erosion rate and total water flow rate. The slope gradient was taken as an input parameter. The effect slope length had on the output parameter (total erosion rate and total flow rate) was observed by keeping the rest of the parameters (biochar content, rainfall rate, slope length, DoC, and biochar percentage) constant when the graph was plotted. It can be observed from the figure that the erosion rate

increases gradually from 2.1 g/m<sup>2</sup>/min to 2.55 g/m<sup>2</sup>/min with an increase in the slope gradient from 7° to 20°. The increase is more significant from 7° to 12° and after that is more gradual.

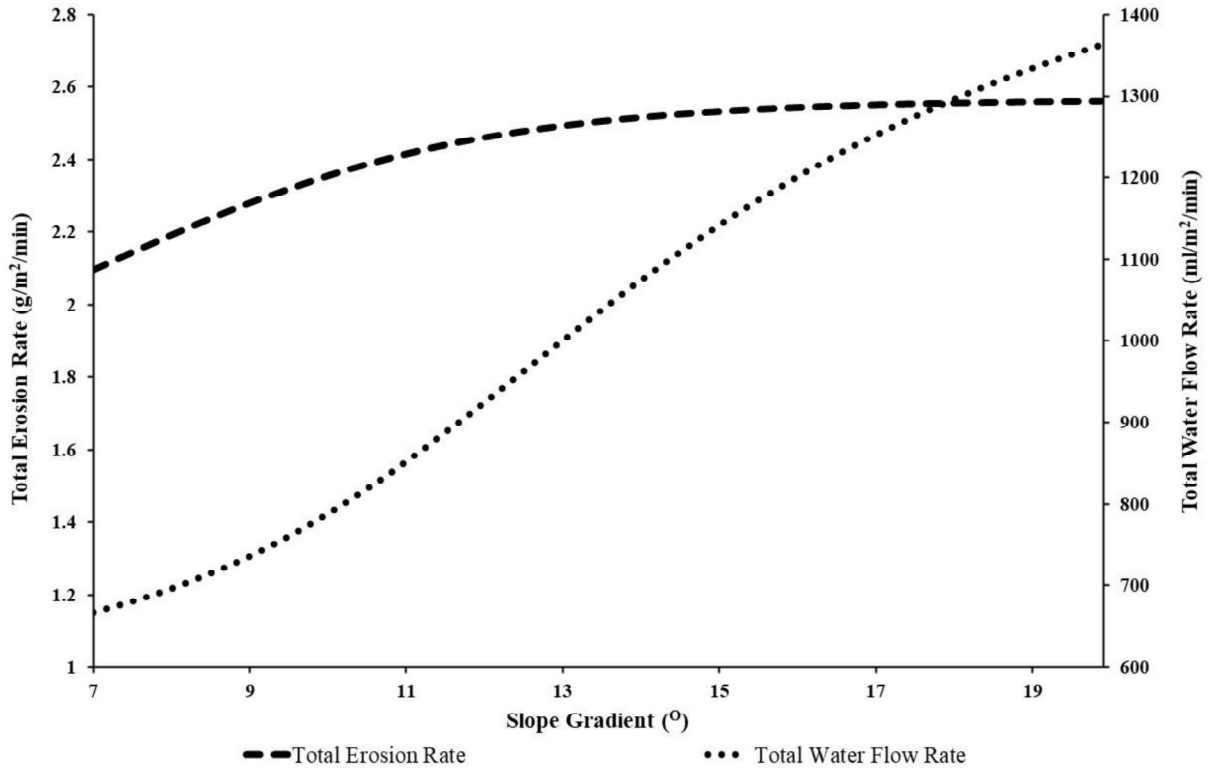


**Figure 38** Variation of Erosion Total Rate and Total Water Flow Rate with the Slope Gradient [481]

On the other hand, the total water flow rate tends to increase more substantially (i.e., by 110%) from 660 mL/m<sup>2</sup>/min to 1370 mL/m<sup>2</sup>/min. This is interesting as with an increase in gradient, and the effect is more visible on flow than on erosion rate. The mechanism can be visualized from the point of view that the erodibility of soil-biochar particle mix is not significantly affected. Instead, the water flow rate (i.e., runoff) is enhanced mainly due to gravity. This implies that more attention needs to be paid to water flow management for steeper slopes than the erosion itself. The result is consistent with that of observed literature [324, 484, 492, 493], thus implying the model's reliability.

#### 5.4.5 Influence of BAS on Total Erosion Rate and Total Water Flow Rate

**Figure 39** shows the variation of total erosion rate and water flow rate with the biochar amendment ratio. The graph was plotted using ANN prediction for biochar amendment with total erosion rate and total water flow rate by taking biochar amendment percentage as an input parameter. Its effect was observed on the output parameter (total erosion rate and total flow rate) by keeping the rest of the parameters (slope length, rainfall rate, slope gradient, and DoC) constant when the graph was plotted. It can be observed that the erosion rate reduces from 2.57 g/m<sup>2</sup>/min to 1.63 g/m<sup>2</sup>/min (i.e., by 36.5%) with an increase in amendment ratio from 0 to 10%. The reduction

in erosion rate is minimal between biochar amendment ratio of 0 to 5%. This implies that the effect of biochar on erosion is not significant during the initial addition of 5% of biochar. This is inconsistent with Bordoloi et al. [301] and Huang et al. [494], who found a substantial influence of biochar on water retention capacity at an amendment ratio of 5%. The findings also suggest that biochar content of 5% may not be the optimal content for reducing erosion rate.

On the contrary, the total water flow rate does not trend with the biochar amendment ratio. The total water flow rate is found first to be enhanced (950 mL/m<sup>2</sup>/min to 1085 mL/m<sup>2</sup>/min) with an increase in biochar content from 0% to 5%, and then decreases (to 720 mL/m<sup>2</sup>/min at 10% biochar content) beyond it. This suggests that the erosion rate is not directly proportional to the total water flow rate. Interestingly, despite the highest water flow at 5% biochar content, the erosion rate remains unchanged (regarding bare soil). This phenomenon might be due to biochar's optimum pore filling effect, which maximizes the water holding capacity [301] and tends to keep soil and biochar particles intact. With an increase in biochar to 10%, the subsurface flow is enhanced, reducing runoff rate and, hence, the total water flow rate and erosion. The effect of biochar on erosion rate seems to be more dominant at 10% content. However, such a percentage may induce higher alkalinity. It is observed from the literature that a biochar content of 5% is most suitable [333]. Higher alkalinity may reduce the vegetation growth [300], causing an increase in runoff, reducing subsurface seepage flux, and leading to more erosion. Additionally, the tensile strength of the soil is reduced by the addition of biochar [495], which in other words means that the soil cannot be compacted to its maximum density, making the soil less suitable for engineering purposes. Further studies are needed to identify the optimal content of biochar for maximizing its overall benefits, including reducing erosion.

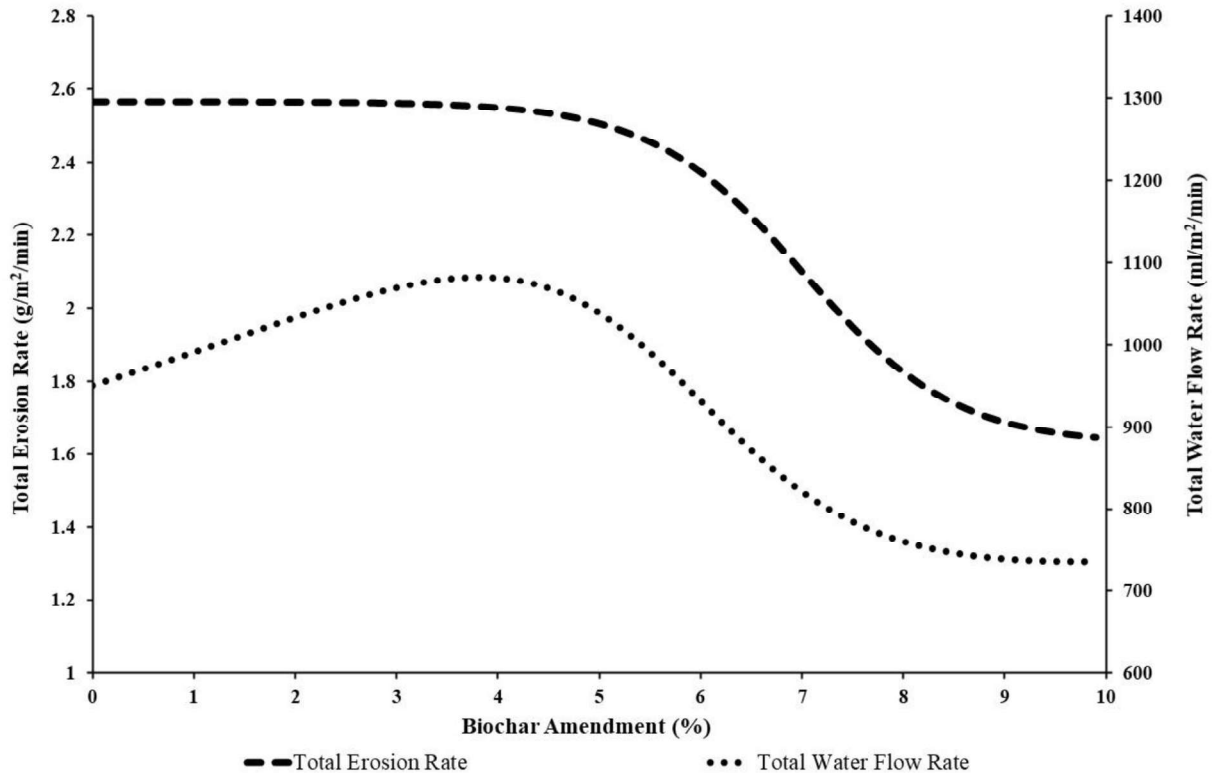
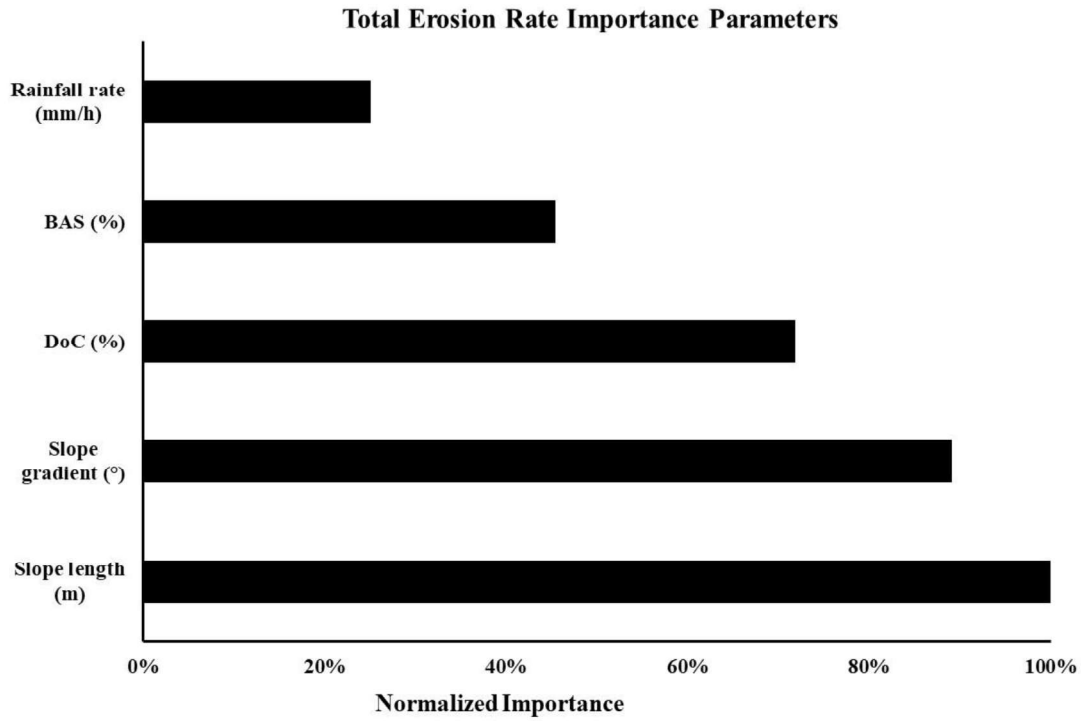


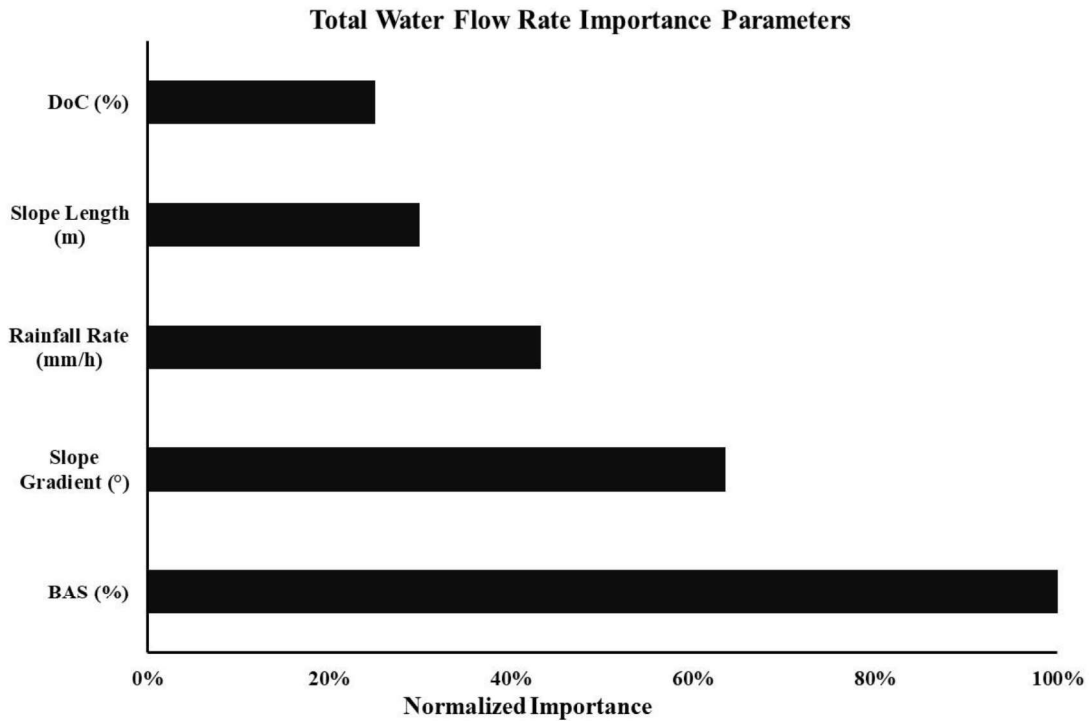
**Figure 39** Variation of Erosion Rate and Total Water Flow Rate with the Biochar Amendment Ratio [481]

5.4.6 *Relative Importance of Factors Influencing Erosion*

**Figure 40** (a) shows the relative importance of various input parameters, slope length, slope gradient, DoC, BAS, and rainfall rate. Slope length was the most important parameter in determining erosion rate, followed by slope gradient, DoC, the percentage of biochar amendments, and rainfall rate. The previous study shows that the effect of slope length on runoff and erosion is not adequately understood [496]. The slope gradient is the second most closely related factor to erosion rate. During water movement on the surface, the slope gradient will affect the subsurface water flow velocity, enhancing the impact force on the surface of the soil-biochar mix. Soils that are heavily compacted have a small number of large pores, leading to reduced subsurface seepage flux and drainage rates. The percentage of biochar amendment and rainfall rate seems to have a lower significant effect on erosion rate.



(a)



(b)

**Figure 40** Relative Significance of Various Parameters on (a) Total Erosion Rate, (b) Total Water Flow Rate

[481]

**Figure 40** (b) shows the relative importance of the input parameters on the total water flow rate. The biochar amendment percentage seemed to play an important role in determining total water flow rate, followed by slope gradient, rainfall rate, slope length, and DoC. Biochar has high porosity and a large specific surface area. Biochar addition to soil can alter the soil's physical properties (soil structure, pore size distribution, and bulk density) and hydraulic properties (soil water retention capacity and hydraulic conductivity). Studies show that biochar addition increases water subsurface seepage flux, reduces surface runoff, and decreases soil erosion [29]. The following influential parameter is slope length, which directly influences seepage velocity. As expected, rainfall rate (3rd significant parameter) also influences total runoff and water flow rate, as observed in other studies [489]. Unlike in the case of erosion rate, slope length and DoC are the least influential in affecting water flow rate. The relative importance of parameters suggests that the criteria for choosing an appropriate biochar amendment ratio and other slope geometry (i.e., for artificial slopes) depends on rainfall characteristics, which need to be considered carefully. The results on the relative significance of parameters differ from those of Cai et al. [324].

In the study conducted by [324] the relative significance for the runoff was slope gradient > slope length > biochar content > rainfall rate > compaction. For total flow, the relative significance of parameters was biochar content > rainfall rate > slope gradient > slope length > compaction. This is because Cai et al. [324] determined the relative influence of different parameters by using 5% and 10% biochar separately. However, in the current study, the whole data was taken into account to determine the relative influence of parameters. The model developed using ANN is more flexible in application and has better accuracy. Further studies are needed to study the relative significance of parameters by enhancing the slope scale and including other conditions.

## 5.5 Observation

The ANN model developed for erosion is consistent with the experimental and literature data. The  $R^2$  value from the newly developed ANN models was 0.788 and 0.939 for erosion rate and total water flow rate, respectively. The error percentage for erosion and total water flow rates was 15% and 7%, respectively. Such models can assist in the preliminary design of green cover by choosing the required optimal biochar content under various slope and rainfall conditions. Biochar content of 5% seems to have a negligible effect on erosion rate, while the 10% amendment ratio has the lowest erosion rate and total water flow rate. This is different from water retention studies of the soil-biochar mix, where a 5% amendment ratio considerably impacts water-holding ability.

The most significant parameter for total erosion rate is the slope condition (length and gradient), followed by compaction, percentage of biochar amendment and rainfall rate. The slope gradient and length are the other two factors that play a decisive role in erosion control. Longer slopes provide enough surface area for subsurface seepage flux and localized transportation of sediments, due to which runoff reduces, ultimately reducing erosion in both cases. ANN modelling indicates a threshold slope length of 1.55 m, beyond which a sharp reduction in erosion rate is observed.

Under a higher slope gradient, runoff due to gravity increases, and subsurface seepage flux decreases, resulting in more erosion, even though comparatively less in BAS. Similarly, if the intensity or duration of rainfall is more, runoff and erosion increase, and it is observed that biochar amendment is more influential in affecting water flow rate. Slope length is the least influential in affecting water flow rate. It is observed that biochar content, slope gradient, and rainfall intensities govern the water flow rate.

The study provides the relative importance of various factors concerned with determining erosion in the soil-biochar mix. In the current study, taking all the data into account, slope length was the most significant parameter, followed by slope gradient, DoC, biochar content, and rainfall rate for total erosion rate. Biochar content was the most significant parameter for total water flow rate, followed by slope gradient, rainfall rate, slope length, and compaction. In future, studies need to be carried out to understand the combined effect of vegetation and biochar with different slope and soil conditions. The application of biochar in geotechnical engineering is still being investigated. Many agencies such as International Biochar Initiative (IBI) and European Biochar Certificate (EBC) are currently investigating the determination of biochar characteristics, which should be used in various aspects of soil conservation. Recently, financial support has been provided to develop commercial biochar production capacity to maximize its usage for soil remediation and other construction purposes to achieve the overall aim of reducing the carbon emission goal of 2030 and also to develop a circular economy. Our current study is one of the first steps in promoting biochar use for soil remediation and the construction of geotechnical infrastructure.

## Chapter 6: Multiple Regression Model for Predicting Cracks in Soil Amended with Pig Manure Biochar and Wood Biochar

---

### 6.1 Background

The addition of biochar has been observed to greatly impact the hydraulic properties of sandy and sandy loam soils by enhancing the pore size distribution and allowing greater water holding capacity, which is beneficial for the long dry periods and in areas having scanty rainfall. The addition of fine biochar particles to the soil reduces saturated hydraulic conductivity by forming small pores [269, 378]. Researchers have observed that adding biochar to coarse-grained soils reduces the saturated hydraulic conductivity [224, 378, 380, 497]. The wetting and drying cycles greatly influence the soil structure and texture. [378, 498] Observations have also been made that the wet and dry cycles cause a reduction in the saturated hydraulic conductivity in coarse-textured soils but increase the same in sandy loam and silty soils [378, 497]. The addition of biochar to sandy soils inhibits the cracking by improving the WHC of soil. Shrinkage and swelling of soils influence the cracking of soils, causing a rearrangement of the particles, making soils less sensitive to deformation.

### 6.2 Introduction

The engineering properties of soil, such as specific gravity (SG), plastic limit (PL), particle-size distribution (PSD), and degree of compaction (DoC), can influence the behaviour of soil. In agricultural applications, the crop yield depends on the geophysical properties of soil, such as carbon content, nutrient availability, water-retention capacity (WRC), cation-exchange capacity (CEC), and so on. [1, 318]. Several types of biochar have been used as soil remediation amendments to control some soil properties. Previous studies show that agricultural soils are loosely compacted at approximately 65% of maximum dry density (MDD), and soils for geoenvironmental applications are densely compacted at approximately 80%–90% of MDD [91, 96, 333]. The formation of cracks is a natural process that involves weathering, chemical changes, and biological changes in soils. The intensity of crack formation depends on the soil's physicochemical and engineering properties. Unavailability of adequate water in arid regions leads to crack formation in compacted soils. The desiccation cracks (cracks developed due to seasonal temperature variation) affect the performance of surface soils by reducing their strength and WRC [499].

The desiccation cracks occur due to variation in environmental temperature that causes wetting–drying and freeze–thaw cycles. Seasonal temperature variation causes the non-uniform distribution of soil moisture, temperature, and stress. It also severely affects soil water retention and ultimate strength [500, 501]. Water evaporation in soils due to environmental temperature can cause the development of soil suction that

leads to shrinkage and cracking. The shrinkage and cracking of soil can be minimized by adding a suitable amendment, such as biochar, in specific proportions [406, 502]. Interaction of biochar with loosely and densely compacted soil has distinguished mechanisms due to different particle packing, pore size, and pore volume. Surface functional groups present in biochar can help to enhance the bond among the particles by chemical and van der Waals forces [107]. Quantitatively, the crack intensity is measured in terms of a crack intensity factor (CIF). The CIF is defined as the ratio of the total planar area of cracks to the total surface area. To achieve the minimum CIF and maximum WC, different experimental studies have been reported using the various types of feedstocks [90, 318]. The addition of biochar shows promising results in reducing the crack formation and intensity. Currently, limited studies consider the effect of engineering properties such as plastic limit (PL), liquid limit (LL), specific gravity, and DoC of soil on desiccation cracks. The fundamental understanding of each influencing parameter can be used to interpret the behaviour of crack formation. This study utilizes the multiple regression analysis (MRA) technique to develop a base model and perform a sensitivity analysis to understand the relative influence of soil DoC, PL, LL, specific gravity, and biochar content (%) on crack intensity.

Multiple linear regression analysis (MLRA) has been successfully used in multiple geotechnical applications, such as embankments and slopes, and to estimate the factor of safety. The results obtained from the prediction model were compared with finite element analysis of some case studies [503]. The MLA model has been used to relate the Californian bearing ratio (CBR) test to other soil parameters. The study confirmed that this model shows a reliable coefficient of correlation ( $R^2$ ), 0.9454, and it was observed that the model could be used to predict CBR with a  $\pm 3.4\%$  error. MLRA offers a technical guide and solution for predicting soil properties in foundation designs [504]. Different methods, such as machine learning, k-nearest neighbour regression, MRA, and linear regression, are available for the model development and prediction of output variables [17, 24, 91, 408, 409, 426, 501]. In this study, MRA has been used for developing a model for CIF prediction due to its simplicity and simple user interface. MRA is a statistical technique that can predict the output variable by using dependent and independent input variables [504]. The MRA model proposes a relationship between input and output variables that helps to predict the output at given input conditions. In this study, MRA has been used to develop a relationship between biochar type, DoC, biochar content (biochar content), specific gravity (SG) (influencing soil parameters) and CIF (influenced parameters). For CIF prediction, data was collected by performing laboratory experiments [406]. The developed relationships help to understand the effect of each influencing parameter on biochar soil mixture when soil is treated individually with two types of biochar. To study the biochar influence using MRA, two biochars, wood biochar (WB) and pig manure biochar (PMB), were selected. The biochars have been selected based on physiochemical properties and their abundant availability. Wood biochar has a high aromatic character, excessive amounts of carbon (C) concentration, and Fourier transform infrared spectroscopy (FTIR) spectra features, which help in improving the C storage when compared with other biochars having high nutrient content [267]. Biochar obtained from pig manure has higher amounts of ash content, brings an improvement in the pH of the soil and increases the CEC in soil [16, 505].

The major objective of the study was to perform MRA, which helps in understanding the effect of the various soil properties and biochar content on the crack intensity of biochar-amended soil (BAS). A

multiple regression model (MRM) was developed that predicts a relationship among the soil parameters to achieve the defined objective. In this study, data were collected using small-scale dish experiments in the laboratory. Experiments were conducted for 60 days, and images of each sample were captured every 24 h. The captured images have been used to calculate the CIF using an image processing technique. The obtained CIF data from laboratory experiments were used to perform MRA analysis and identify the effect of DoC on soils, PL, LL, biochar content (%), and SG.

## 6.3 Materials and Methodology

### 6.3.1 *Soil–Biochar Characteristic Properties and Experimental Program for Calculating CIF*

The effects of different biochar were investigated to quantify the cracks in clayey sandy soil while considering the various biochar content (5% and 10% by weight) and soil DoC (65% and 80% of MDD). LL and PL were found to be 28.85% and 21.56%, respectively, for bare soil. The maximum dry density (MDD) and optimum moisture content (OMC) of soil were found to be 1.84 g/cc and 13.6%, respectively, with a specific gravity of 2.61. WB and PMB were produced by pyrolyzing the cedarwood and pig manure using an in-house pyrolyser [406]. Both biochars were mixed with oven-dried clayey sandy soil in 5%, 10%, and 15% biochar by weight ratio. BAS was compacted in glass petri dishes of dimensions 10.3 cm in diameter and 1.7 cm in height (**Figure 41**). After preparing the samples, four drying and three wetting cycles (each with a period of 12–15 days) were alternately simulated. The compacted clayey sand was subjected to drying–wetting cycles for 60 days. The duration of each cycle was selected based on the criteria of negligible change in soil weight (when evaporation was less than 1 g/day, it was considered a negligible change in soil weight) [506]. Images were captured in the red, green, and blue (RGB) scale with 8-bit depth using high-resolution cameras every 24 h. Images were analyzed using an open code, Image J [507], for calculating CIF.

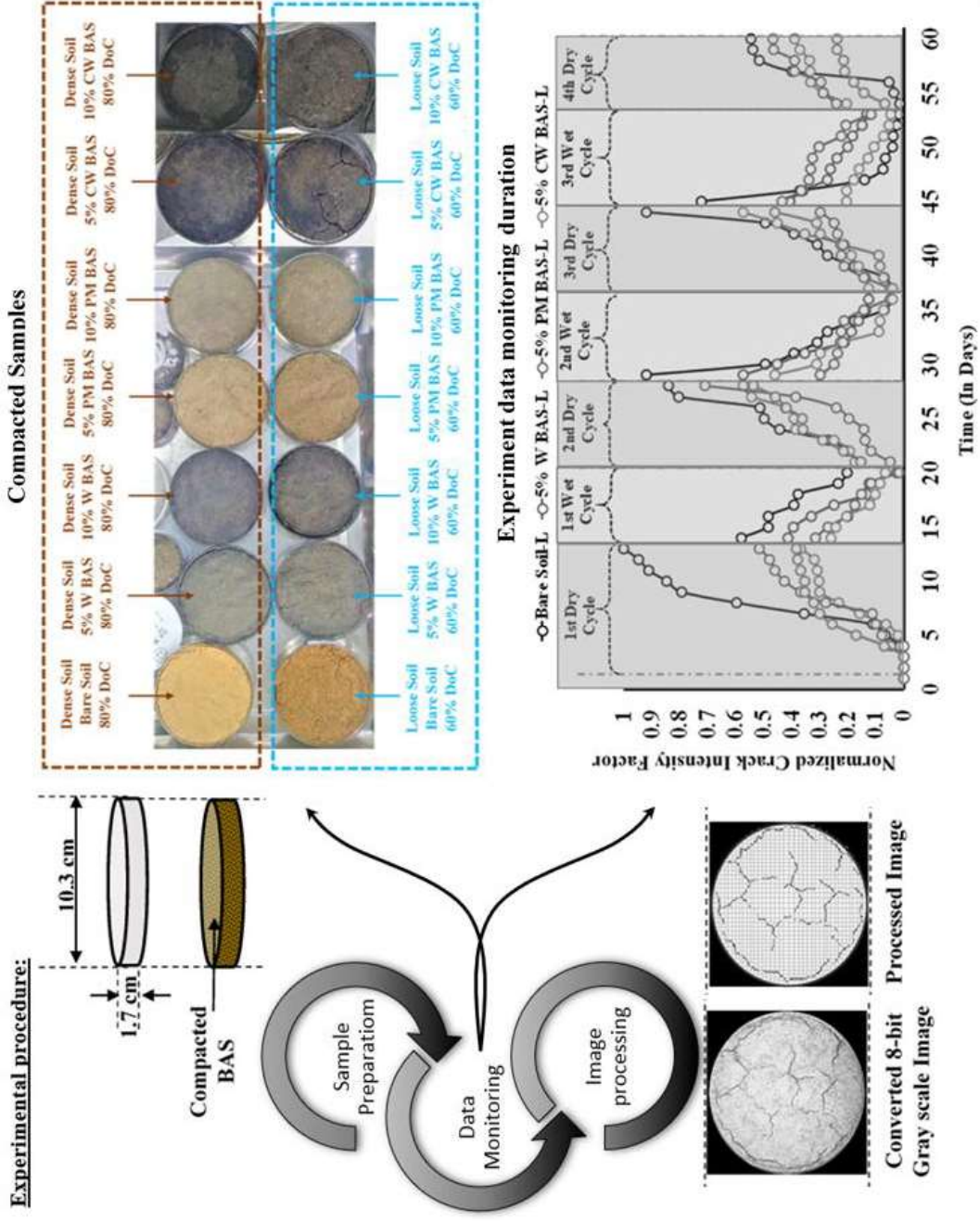


**Figure 41** Experimental procedure for determining crack intensity factor (CIF) for biochar amended samples (BAS) [35, 406]

### 6.3.2 *Multiple Regression Analysis*

Regression analysis is a statistical practice that helps to examine the relationship between two or more variables. The analysis helps to establish a functional relation connecting input variables to output variables, thereby providing a model for forecasting the output variable. In the current study, MRA has been used to understand the influence of soil DoC, PL, LL, SG, and the biochar content on the CIF. MRA is a dependable method for analyzing the effect of individual variables that may have an impact on an output parameter (i.e., CIF). MRA helps in formulating and determining functional relations among independent variables. It can be used for both linear and nonlinear independent variables. To validate the accuracy of the model, an error has been minimized. It is used to measure the variability or the spread of values of the dependent variables concerning the regression line. The *p*-value tests the null hypothesis in the regression analysis for each independent data, whether the variable relates to the dependent parameter. If the value of *p* is less than the significance level (significance level=0.05), then the null hypothesis can be rejected. If the *p*-value is higher than the significance level, then there is not enough evidence to conclude that a nonzero relation exists. Significance level ( $\alpha$ ) gives a probability of the null hypothesis rejection when it is true. For example, a significance level of 0.05 indicates a 5% risk of a difference existing when there is no difference. If the significance levels are low, they indicate that more substantial evidence is required for rejecting the null hypothesis.

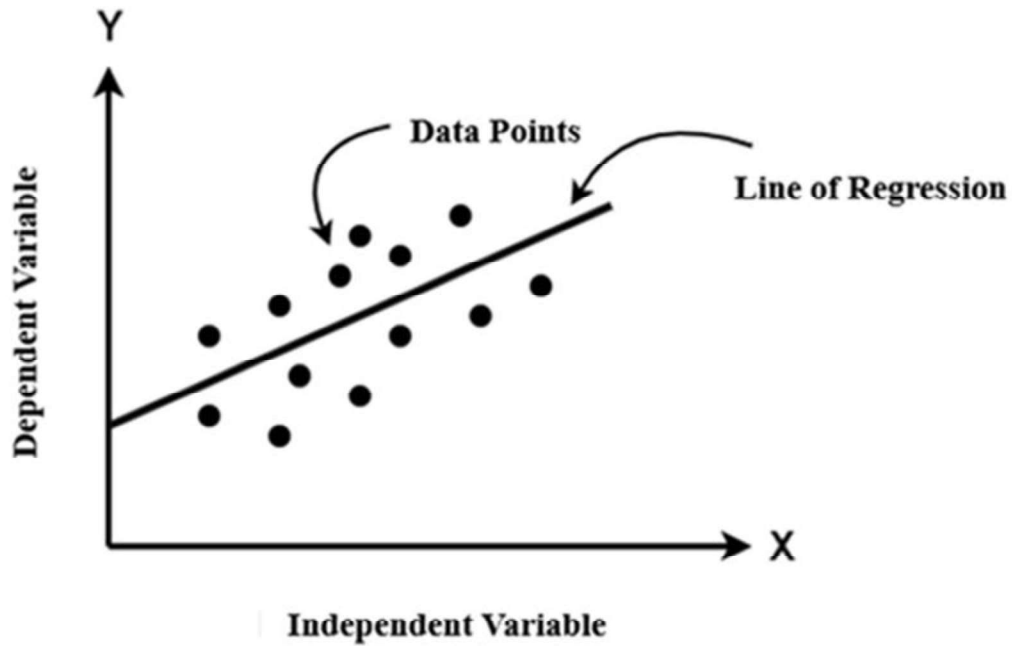


**Figure 42** Graphical representation of linear regression model

MRA helps in predicting the value of  $Y$ , which is a dependent variable, for given values of  $X_1, X_2 \dots X_n$ , which are independent variables. For example, the rice yield per acre (dependent variable) depends on the seed quality, fertilizer in use, temperature, and rainfall (the independent variables). MRA can be used to study the effect of all the parameters on the rice yield. Another advantage of MRA is that it helps to determine the effects of individual parameters on the rice yield. In MRMs, there is one dependent and two or more independent variables. The general equation of multiple regression of  $Y$  on  $X_1, X_2 \dots, X_n$  is derived from:

$$Y = b_0 + b_1X_1 + b_2X_2 + \dots + b_nX_n$$

*Equation 9*

where  $b_0$  = intercept on the dependent variable axis (**Figure 42**) and  $b_1, b_2, b_3 \dots b_n$  are related to the slope in the equation of linear regression, also known as regression coefficients. The sloped straight line represents a relationship that fits a given data to obtain the lowest mean square error (MSE) and is called a regression line. MRA, however, has a limitation in that it does not test to check whether the data used is linear. Instead, it proceeds by assuming that there is a linear relation between  $Y$  and each  $X_i$ . The multicollinearity has been checked using bivariate correlation among the influencing parameters, which was found to be less than 0.15 [508]. It implies that no relationship exists between the independent variables. This can be tested on a fundamental level by calculating the value of the coefficient of correlation between every pair of independent variables.

Figure 43 describes the network design that was used for the prediction of CIF using five parameters: biochar content, SG, soil DoC, LL, and PL.

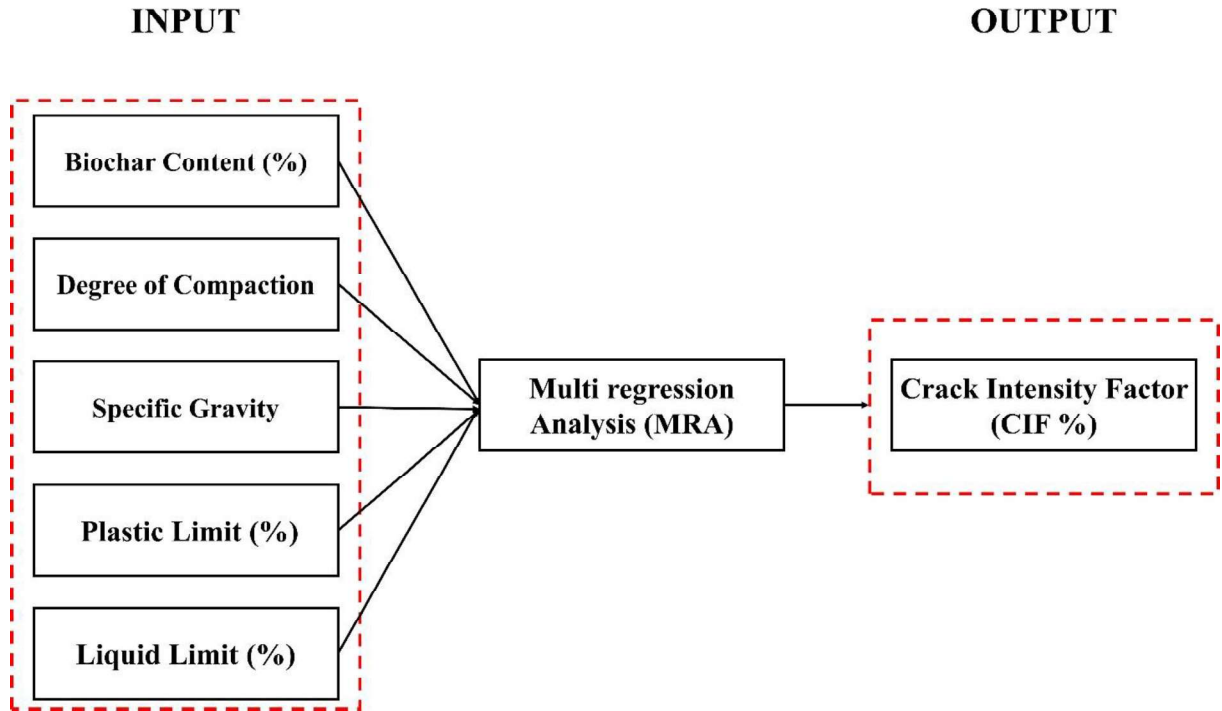


Figure 43 Framework of MRA approach showing input and predicted parameters [35]

#### 6.4 Results and Discussion

MRA analysis has been conducted to predict the percentage of CIF. Table 7 presents the influence of biochar content, soil DoC, PL, LL, and SG, the p-values obtained from MRA.

Table 7 calculated p-values for all influencing parameters

Parameter					
Statistical Parameter	Biochar content	Soil compaction	Plastic limit	Liquid limit	Specific gravity
<i>p</i> -values	0.0003	0.022	0.007	0.949	0.079
Significance levels	(<0.05)	(<0.05)	(<0.05)	(>0.05)	(>0.05)

Figure 44 shows the plot between predicted and measured CIF. The R<sup>2</sup> value for the predicted and measured CIF was found to be 0.925. The proposed regression coefficients for each parameter are

$$\begin{aligned}
 CIF = & -0.045 - (1.197 \times \text{biochar content (\%)}) - (0.013 \times \text{specific gravity}) \\
 & - (0.011 \times \text{liquid limit (\%)}) + (0.809 \times \text{plastic limit (\%)}) \\
 & - (0.062 \times \text{compaction (\%)})
 \end{aligned}$$

Equation 10

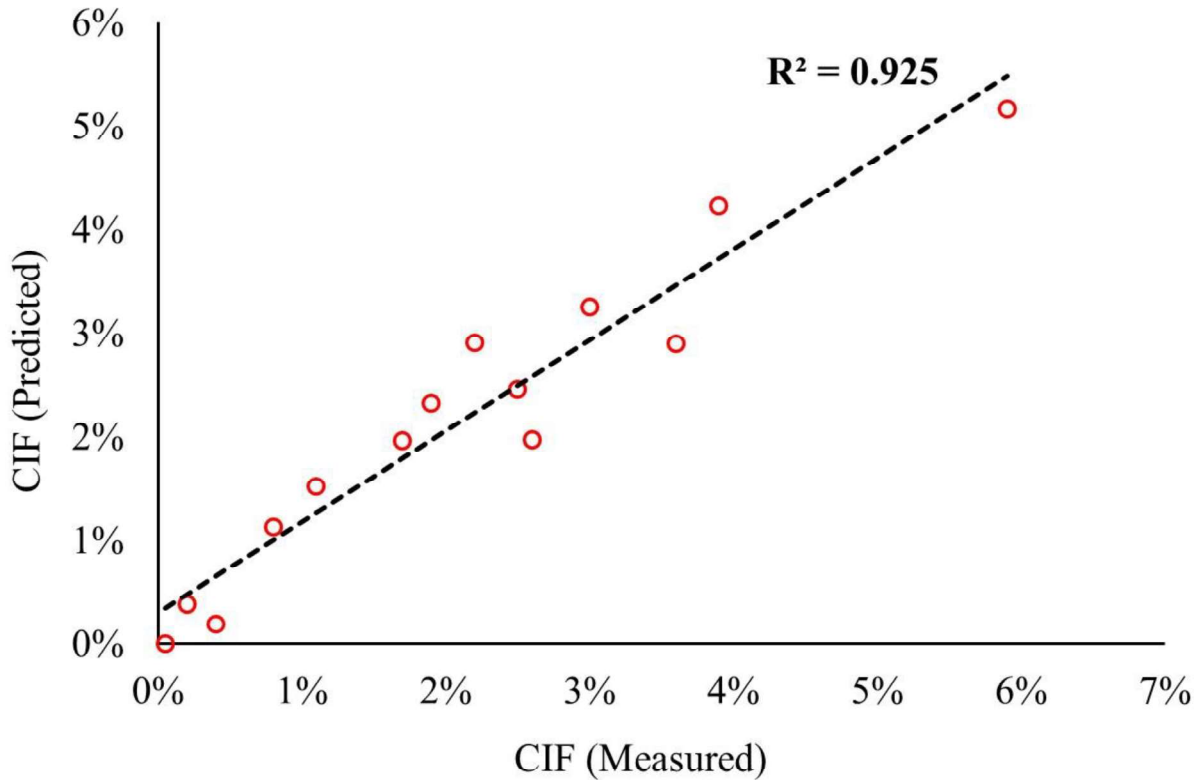


**Figure 44** Plot between measured CIF and predicted CIF to demonstrate the performance of the MRA model, including all influencing parameters [35]

Since the  $p$ -value of LL and SG are found to be 0.949 and 0.079, respectively, which are greater than 0.05, they are not statistically significant and can be rejected for MRA. By having a large  $p$ -value, they represent the convincing evidence to reject the null hypothesis. **Figure 44** shows the plot between predicted and measured CIF considering all the influencing parameters. The  $R^2$  value for the predicted and measured CIF was found to be 0.925. To verify the sensitivity of each significant parameter, the MRA analysis for biochar content, soil DoC, and PL was a rerun. By considering only statistically significant parameters, the  $p$ -values for each parameter were obtained and are given in Table 8. The obtained  $p$ -values were found to be less than 0.05; thereby, no convincing evidence has been found to reject the hypothesis. The new  $p$ -values obtained from MRA show that the higher regression coefficient of biochar content means it is the most significant parameter in CIF prediction, followed by PL and DoC. Taking into consideration the aforementioned most significant parameters, the final empirical relationship for CIF prediction is shown as

$$CIF = (-1.02 \times \text{biochar content (\%)}) + (0.756 \times \text{plastic limit (\%)}) + (-0.062 \times \text{compaction (\%)}) - 0.075$$

Equation 11

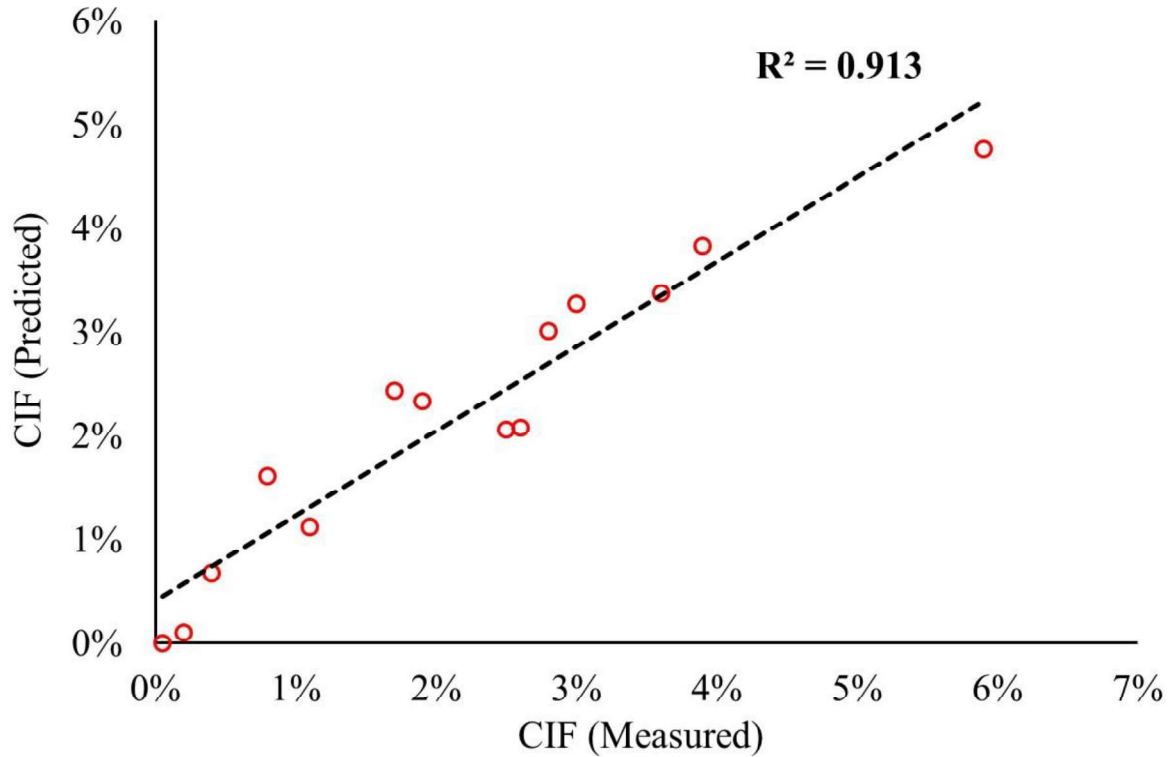


**Figure 45** Plot between measured CIF and predicted CIF to demonstrate the performance of the MRA model, including only statistically significant parameters [35]

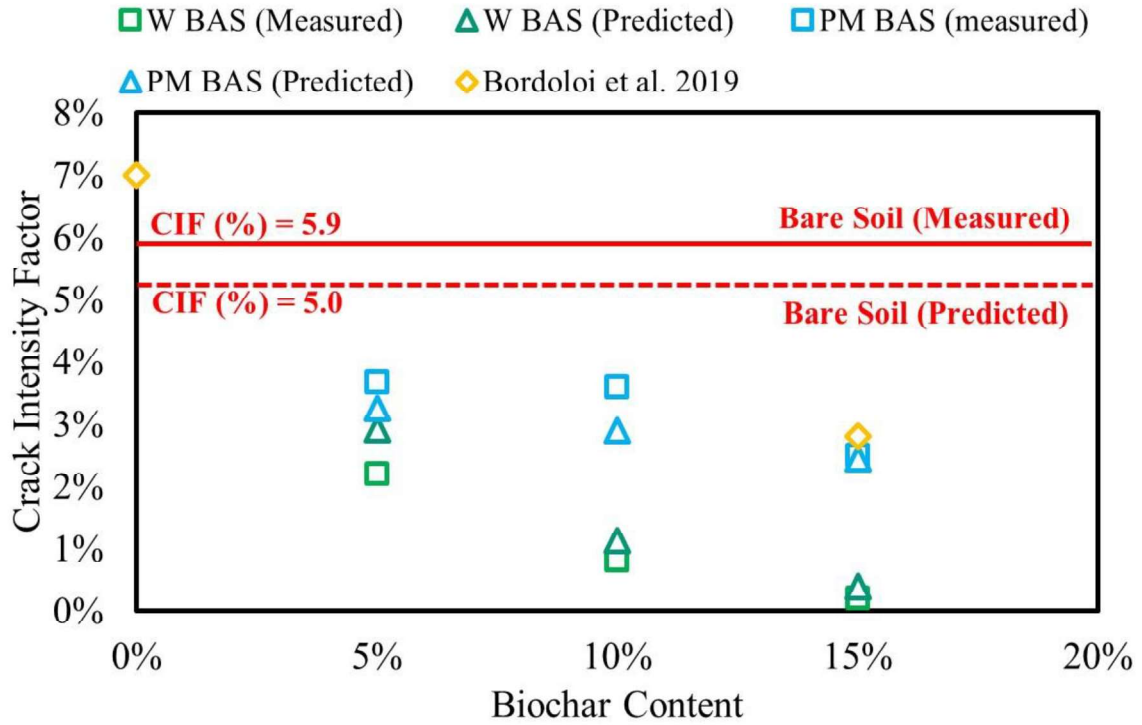
**Figure 45** shows the plot between predicted and measured CIF considering the most significant parameters. The  $R^2$  value for the predicted and measured CIF was found to be 0.913 (almost similar to the previous analysis, approximately 0.925). A better  $R^2$  value ensures better performance of the model. The MSE of the predicted CIF is found to be  $1.93 \times 10^{-5}$ .

**Table 8** Calculated p values for significant parameters

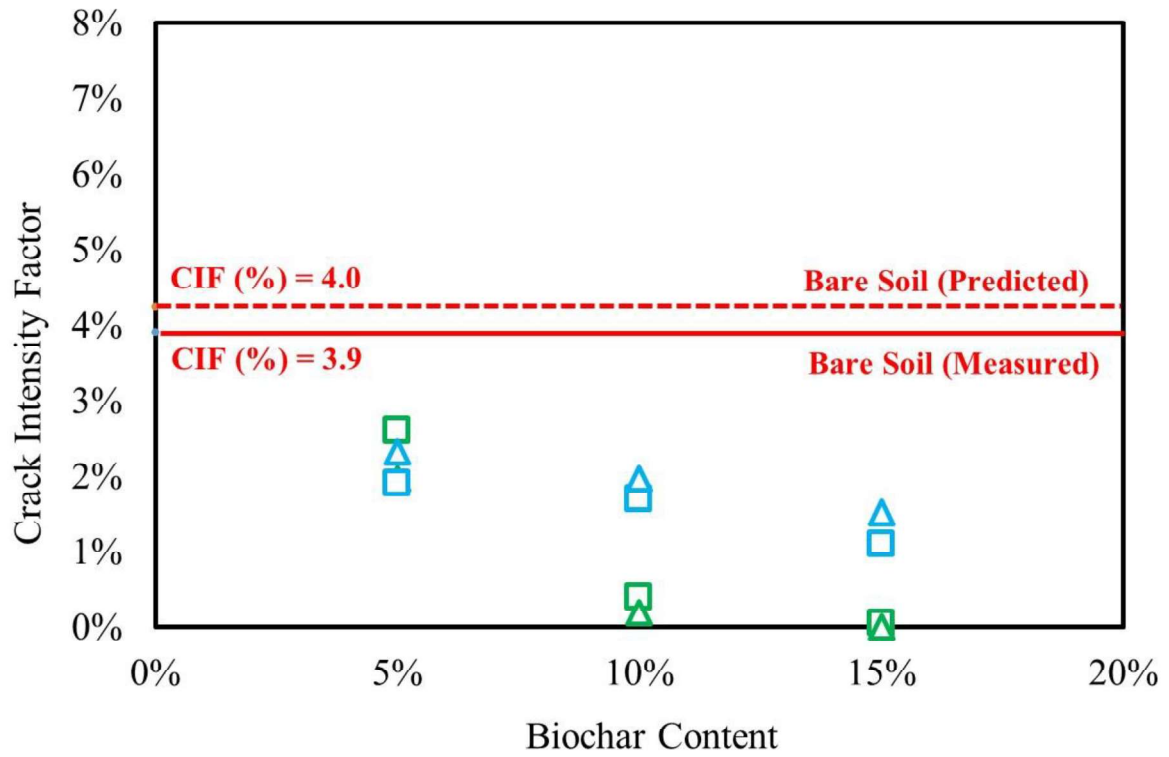
Parameter			
Statistical Parameter	Biochar content	Soil compaction	Plastic limit
p-values	0.0005	0.03	0.002
Significance level	<0.05	<0.05	<0.05

**Figure 46(a and b)** represent the comparison between predicted and measured CIF for 5%, 10%, and 15% biochar content by weight at 65% and 80% DoC. The CIF percentage decreases with increasing

biochar content for WB and PMB. As biochar content increases, the number of intrapores in the soil also increases, and thereby specific surface area increases, promoting the adsorption of water on the surface of the biochar. Increased water content reduced the stress in soil and reduced the formation of cracks. Furthermore, the CIF percentage has been predicted using the proposed MRA model. The maximum error for the prediction of bare soil was found to be approximately 20%. However, for the maximum error in the prediction of BAS percentage, CIF was found to be 15%. It can be observed that the error of the prediction model for dense BAS is relatively low compared with loose BAS.

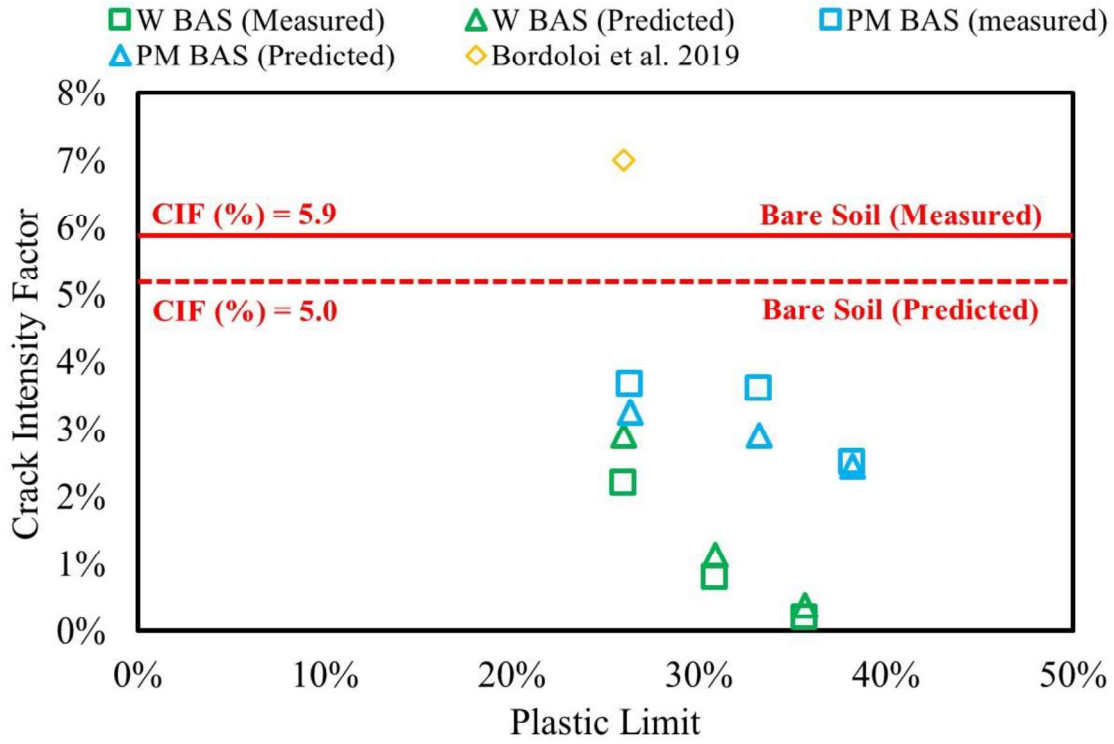


(a)

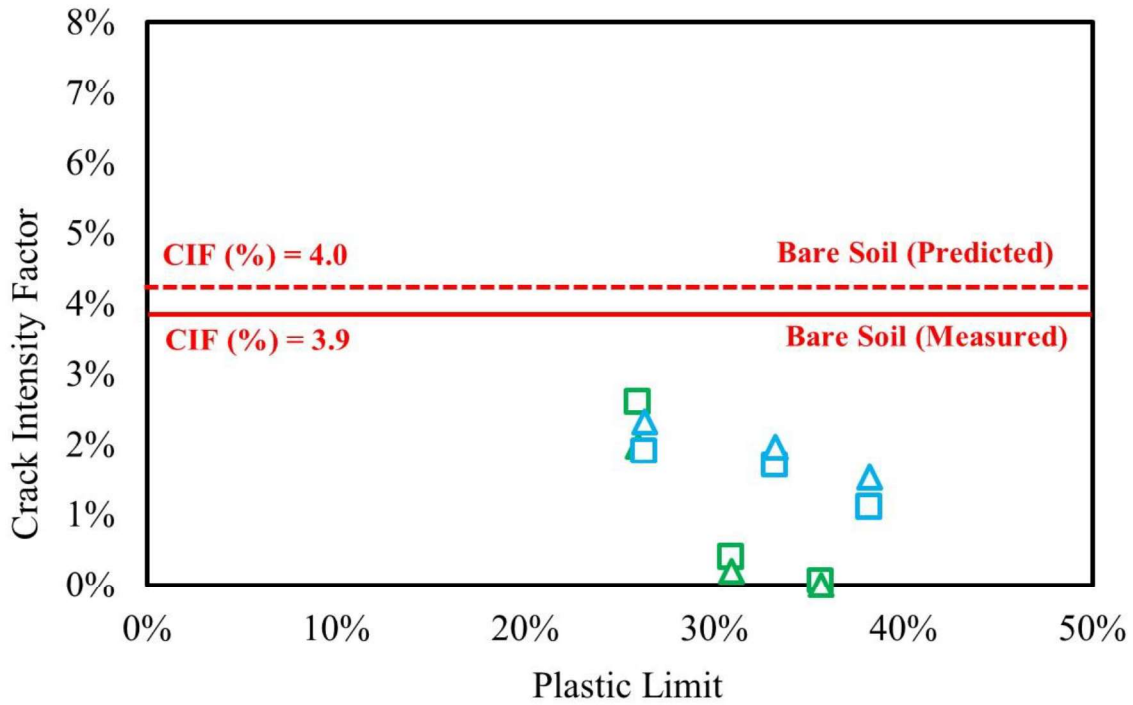


(b)

**Figure 46** Comparison between predicted and measured CIF with different biochar content [35]



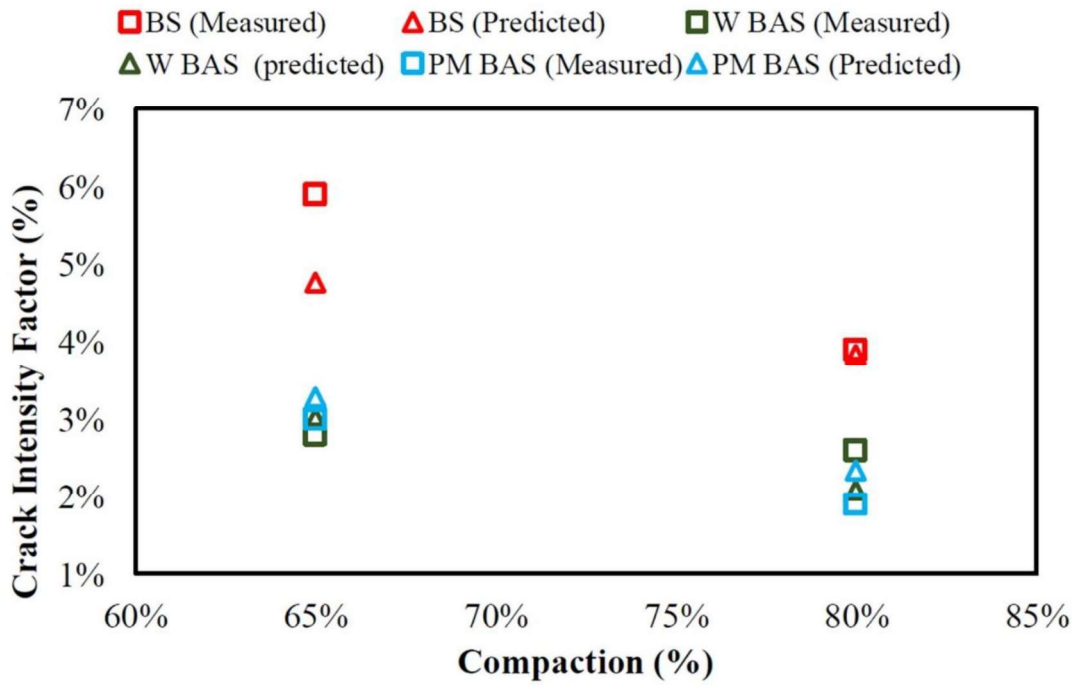
(a)



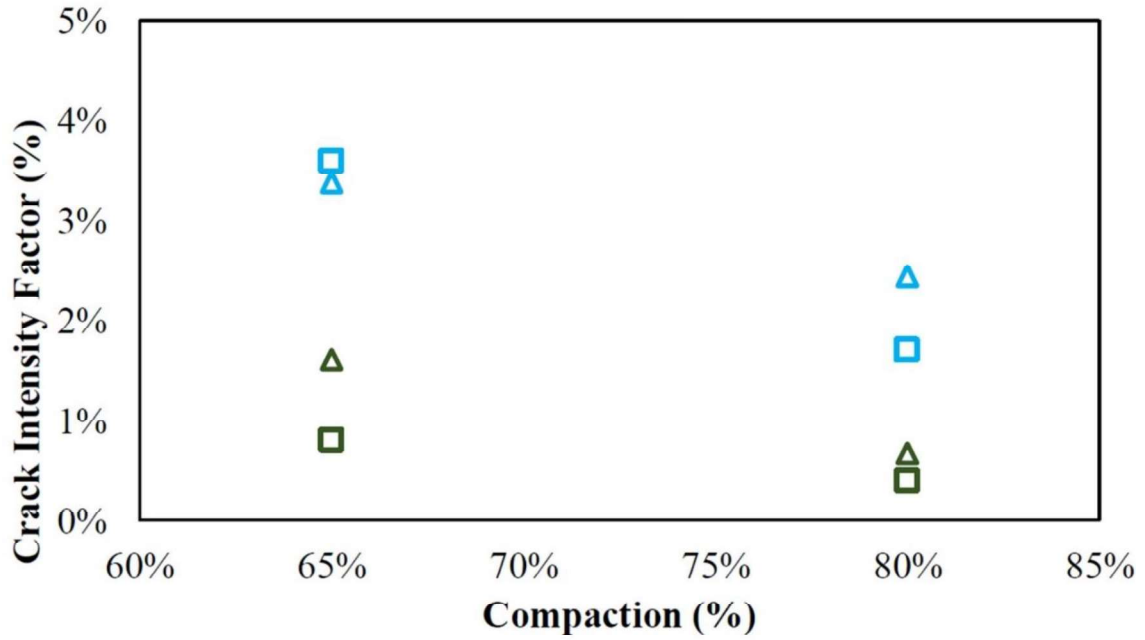
(b)

Figure 47 Comparison between measured and predicted CIF for different plastic limits [35]

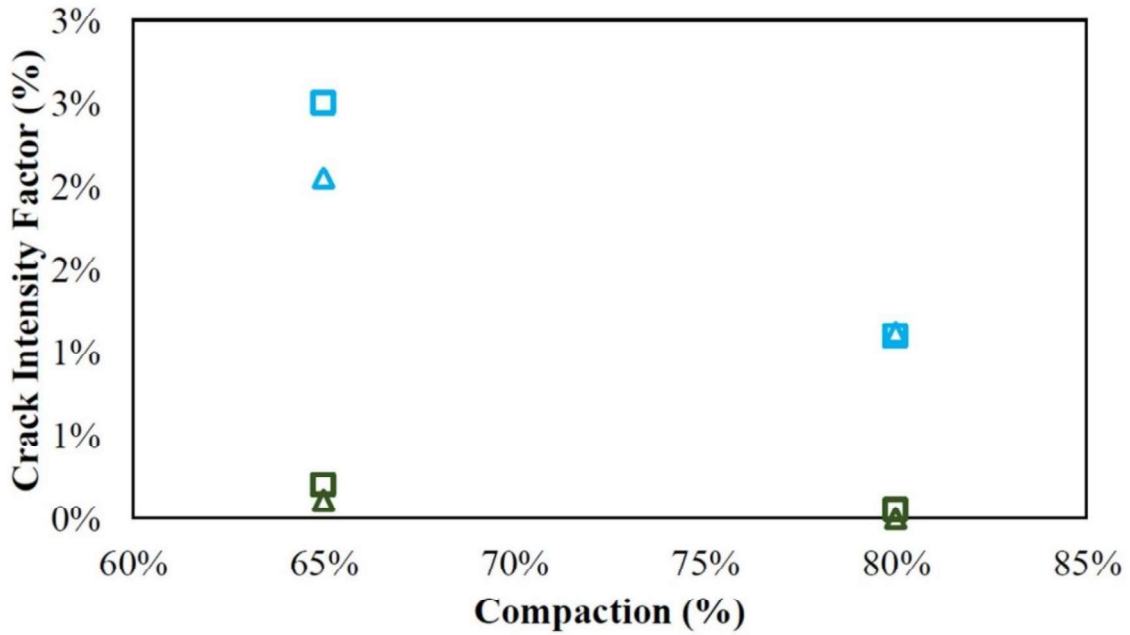
Plasticity limit is another significant parameter that influences crack propagation. **Figure 47** (a and b) represent the measured and predicted CIF for different PL at 65% and 80% DoC. It can be observed that as the PL of BAS increases, the CIF percentage decreases. The high plasticity of the material can help to reduce the stress at the tip of the crack. When cracks start to propagate in a medium, high stress is developed at the tip of the crack. If the material is not plastic enough, brittle failure can occur. However, in the case of high plasticity, stress concentration at the tip of the crack is reduced and crack formation decreases. Based on the MRA model, the maximum percentage error has been found to be 12% in CIF prediction. For the dense compacted BAS, the prediction error is significantly less.



(a)



(b)



(c)

**Figure 48** Measured and predicted CIF % using proposed MRA model at 65% and 80% DoC for (a) 5%; (b) 10% and (c) 15% biochar amendment [35]

**Figure 48** (a–c) represents the CIF for 5%, 10%, and 15% biochar content by weight at different compaction states. The compaction state of BAS plays an important role in controlling the behaviour of cracks. It can be seen that as compaction of BAS is increased, the intensity of cracks is reduced. Wood biochar

shows a better performance in suppressing the crack formation than PMB. Wood biochars have a high number of intrapores due to the presence of biopolymers (cellulose, hemicellulose, and lignin), which are evaporated during the pyrolysis process. Numerous intrapores can provide many functional groups (such as the hydroxyl group) to absorb water at the surface, which reduces the crack development. Water hyacinth biochar (WHB) has been used in the past, which also reduces cracks [90]. The maximum error in the prediction of BAS CIF percentage using MRA is found to be less than 6%.

**Figure 49** represents a systematic flowchart to conduct the MRA analysis to predict CIF. Initially, all influencing parameters, such as biochar content, DoC, PL, LL, and SG, have been considered to predict the CIF percentage. To validate the influence of each parameter on the prediction of CIF percentage, the  $p$ -value has been determined. The  $p$ -value can decide whether a parameter is statistically significant or not. If it is statistically significant, it must be considered in predicting the CIF percentage. Conducting MRA for all influencing parameters found that only biochar content, DoC, and PL are the most significant parameters that can affect crack intensity. The less-significant parameters, LL and SG, have been dropped from further analysis. After dropping the LL and SG parameters, the most significant parameters were tested for statistical influence. They were found to have a  $p$ -value less than 0.05, which provides no strong evidence to drop biochar content, DoC, or PL. It has also been verified that there is a notable change in the value of  $R^2$ .

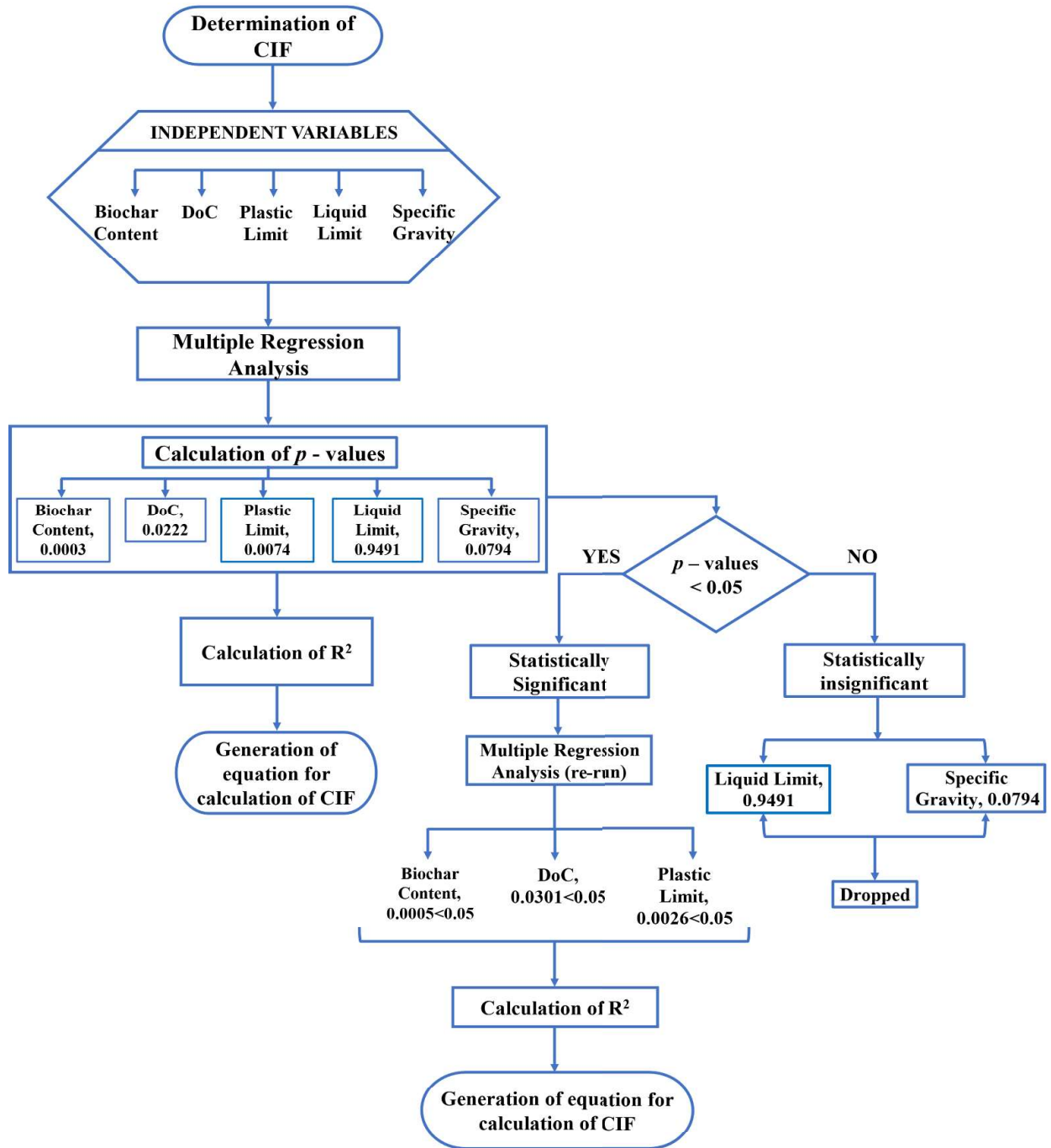


**Figure 49** Framework for MRA approach with input and predicted parameters [35]

## 6.5 Observations

This study demonstrates the development of an MRA model in the estimation of CIF (dependent variable) for WB- and PMB-amended soils, considering influencing independent variables biochar content, SG, LL, PL, and DoC. MRA was applied to the experimental data. The following observations were made:

1. A comparison was made between the measured and predicted CIF with varying biochar content in the BAS at 65% and 80% compaction states of the samples. When the soils were treated with two types of biochar, the intensity of cracks decreased. A drastic reduction was observed in the CIF with an increase in biochar content, which is because of the presence of high intrapores of biochar. Highly porous biochar can retain more water, which leads to low crack intensity.
2. Cracking in the soil is found to be reduced with an increase in PL and DoC. At both the compaction states, WB shows a higher reduction in the CIF than with PMB with increasing PL. For PMB, in both the compaction states, there is a slight decrease in the CIF with increasing PL as compared with a decrease of CIF while using WB.
3. The MRA shows that biochar content, PL, and DoC are the most statistically significant parameters for the determination of CIF. The parameters LL and SG have a low statistical impact on the prediction of CIF.

It is concluded that high biochar content, DoC, and PL helps to reduce the CIF significantly. Other geomaterials with high plasticity should also be able to reduce the CIF when mixed with soil. However, a more systematic investigation is needed to identify the correlation between basic parameters of soil (i.e., LL, PL, DoC, SG, and so on) for diverse types of BAS.

## Chapter 7: Conclusion

---

The principal objective of the research is to understand the efficiency of biochar on the hydraulic properties (SWCC, erosion and cracking) of BAS by developing and using AI-based models. There are apparent contradictions in research results about this property of biochar. This dissertation was a step forward to bringing down the level of contradictions by finding solutions through artificial intelligence modelling. Also, to overcome the time and cost factors involved in the experimentation, this new approach was introduced, even though it can be helpful mostly for preliminary design. The following conclusions can be drawn from the study:

- i. The biochar's influence on SWCC with varying grain size distribution was explored by developing and using an ANN-based model. The following conclusions were made:
  - The influence of biochar in increasing the WRC of soils was observed in clayey soils. At clay content of 6%, the increase in WRC by 3% biochar amendment was similar to 10% biochar amendment for clay content of 8%. The influence of biochar beyond these amendment ratios became insignificant (in increasing or decreasing the WRC). This result suggests an important precaution for avoiding the excessive use of biochar in soils with higher fine content. However, this conclusion depends on the available literature data for the training model and prediction. The SWCC obtained by model predictions reasonably matched the SWCC obtained from measured values
  - In soils with higher sand content, the influence of biochar in increasing NWC seems more pronounced on the dry side than on the wet side of SWCC, even though a relatively higher amount of biochar (10%) was required to cause changes in the SWCC.
  - Based on sensitivity analyses, the ratio of fine to sand content was observed as the most important factor causing changes in NWC. The ratio indirectly influences the microstructural arrangement and soil water retention capacity.
- ii. The biochar's influence in reducing erosion was observed by developing and using an ANN model. The  $R^2$  value from the newly developed ANN models was 0.788 and 0.939 for total erosion and water flow rates, respectively. The error percentage for erosion and total water flow rates was 15% and 7%, respectively. The following conclusions were made:
  - The 10% biochar amendment influenced erosion and the total water flow rate. In comparison, 5% seems to have a negligible effect rate.
  - The most significant parameter for total erosion rate is the slope condition (length and gradient), followed by compaction, percentage of biochar amendment and rainfall rate.
- iii. This study demonstrates the development of an MRA model in estimating CIF (dependent variable) for WB- and PMB amended soils, considering influencing independent variables: biochar content, SG, LL, PL, and DoC. MRA was applied to the experimental data. The following observations were made:
  - A comparison was made between the measured and predicted CIF with varying biochar content in the BAS at 65% and 80% compaction states of the samples. When the soils were treated with two types of biochar, the intensity of cracks decreased. A drastic reduction was observed in the

CIF with an increase in biochar content because of high intrapores of biochar. Highly porous biochar can retain more water, which leads to low crack intensity.

- Cracking in the soil is reduced with an increase in PL and DoC. WB shows a higher CIF reduction than PMB at both compaction states with increasing PL. For PMB, in both the compaction states, there is a slight decrease in the CIF with increasing PL compared with a decrease of CIF while using WB.
- The MRA shows that biochar content, PL, and DoC are the most statistically significant parameters for CIF determination. The parameters LL and SG have a low statistical impact on the prediction of CIF.
- Even though it has been observed from the predictions that a biochar amendment of 15% reduced cracking substantially, practically, it may not be possible. Higher percentages of biochar can cause soil to become excessively alkaline, thus causing adverse effects on soil properties and vegetation. For engineering purposes, biochar addition percentage must be investigated very carefully as it may adversely affect soil strength properties and application cost.
- It is concluded that high biochar content, DoC, and PL helps to reduce the CIF significantly. However, a more systematic investigation is needed to identify the correlation between basic soil parameters (i.e., LL, PL, DoC, SG, and so on) for diverse types of BAS.

## Chapter 8: Future Scope

---

In this research study, the influence of biochar was investigated on soil hydraulic properties and determining the net effect on water holding capacity, erosion and cracking of the biochar amended soils at various percentages of biochar amendment. The sensitivity analysis of various parameters was also done to check the most influential factors affecting the property investigated. However, some of the results obtained differed from the literature, while most observations agreed with the experimental results. The research shows a road map for the preliminary design of different biochar-soil compositions (for geoen지니어ing utilization) with the help of artificial intelligence. However, a few limitations exist in the current work. A summary of the limitations and the future scope is given as follows:

- It should be noted that the conclusions are based on the given sets of measured data available in the literature. There was also a lack of reliable data on SWCC at the higher range of soil suction. More systematic studies need to be conducted to establish full-scale SWCC for soils amended with various biochars (i.e., animal-based and plant-based). In addition, probabilistic approaches and Bayesian optimization techniques [60, 61, 76] can be adopted for considering uncertainties in measured SWCCs.
- The study has developed models based on the data from the literature, as experimentation could not be carried out due to COVID-19 restrictions. Future work can be supported with on-site experimentation.
- Further studies are needed to analyze the effect of different feedstock types and pyrolysis conditions (temperature, moisture, type of pyrolysis, atmosphere) on physicochemical properties of biochar and, ultimately, on erosion potential of the soil-biochar mix. Studies are needed to consider the effects of biochar on soil erosion in the long term, considering vegetation growth and seasonal variation. Further, quantification of loss of nutrients in soil erosion needs to be conducted. Since biochar may negatively impact strength, its combination with other amendments (such as fibres or vegetation) can be considered for soil erosion control.
- In future, studies need to be carried out to understand the combined effect of vegetation and biochar with different slope and soil conditions. Recently, financial support has been provided to develop commercial biochar production capacity to maximize its use for soil remediation and other construction purposes. This is done to achieve the overall aim of reducing the carbon emission goal of 2030 and also to develop a circular economy. Our current study is one of the first steps in promoting biochar use for soil remediation and construction in geotechnical infrastructure.

## Bibliography

---

1. Lehmann J, Joseph S (2015) *Biochar for Environmental Management: Science, Technology and Implementation*. Routledge
2. Xu R, Qafoku NP, Van Ranst E, et al (2016) Chapter One - Adsorption Properties of Subtropical and Tropical Variable Charge Soils: Implications from Climate Change and Biochar Amendment. In: Sparks DL (ed) *Advances in Agronomy*. Academic Press, pp 1–58
3. Wani I, Ramola S, Garg A, Kushvaha V (2021) Critical review of biochar applications in geoengineering infrastructure: moving beyond agricultural and environmental perspectives. *Biomass Conv Bioref*. <https://doi.org/10.1007/s13399-021-01346-8>
4. Glaser B, Lehmann J, Zech W (2002) Ameliorating physical and chemical properties of highly weathered soils in the tropics with charcoal – a review. *Biol Fertil Soils* 35:219–230. <https://doi.org/10.1007/s00374-002-0466-4>
5. Mokrzycki J, Michalak I, Rutkowski P (2021) Biochars obtained from freshwater biomass—green macroalga and hornwort as Cr(III) ions sorbents. *Biomass Conv Bioref* 11:301–313. <https://doi.org/10.1007/s13399-020-00649-6>
6. Ouyang L, Wang F, Tang J, et al (2013) Effects of biochar amendment on soil aggregates and hydraulic properties. *Journal of soil science and plant nutrition* 13:991–1002. <https://doi.org/10.4067/S0718-95162013005000078>
7. Yang W, Wang Y, Sharma P, et al (2017) Effect of naphthalene on transport and retention of biochar colloids through saturated porous media. *Colloids and Surfaces A: Physicochemical and Engineering Aspects* 530:146–154. <https://doi.org/10.1016/j.colsurfa.2017.07.010>
8. De Bhowmick G, Sarmah AK, Sen R (2018) Production and characterization of a value added biochar mix using seaweed, rice husk and pine sawdust: A parametric study. *Journal of Cleaner Production* 200:641–656. <https://doi.org/10.1016/j.jclepro.2018.08.002>
9. Yang CD, Lu SG (2021) Effects of five different biochars on aggregation, water retention and mechanical properties of paddy soil: A field experiment of three-season crops. *Soil and Tillage Research* 205:104798. <https://doi.org/10.1016/j.still.2020.104798>
10. Aj C, Na P, R de N, Da R (2017) Good for sewage treatment and good for agriculture: Algal based compost and biochar. *J Environ Manage* 200:105–113. <https://doi.org/10.1016/j.jenvman.2017.05.082>

11. Kumar S, Mastro RE, Ram LC, et al (2013) Biochar preparation from *Parthenium hysterophorus* and its potential use in soil application. *Ecological Engineering* 55:67–72. <https://doi.org/10.1016/j.ecoleng.2013.02.011>
12. Mastro RE, Kumar S, Rout TK, et al (2013) Biochar from water hyacinth (*Eichornia crassipes*) and its impact on soil biological activity. *CATENA* 111:64–71. <https://doi.org/10.1016/j.catena.2013.06.025>
13. Patwa D, Muigai HH, Ravi K, et al (2022) A Novel Application of Biochar Produced from Invasive Weeds and Industrial Waste in Thermal Backfill for Crude Oil Industries. *Waste Biomass Valor.* <https://doi.org/10.1007/s12649-022-01694-0>
14. Ramola S, Belwal T, Srivastava DrR (2020) Thermochemical Conversion of Biomass Waste-Based Biochar for Environment Remediation. pp 1–16
15. Ramanathan V, Carmichael G (2008) Global and regional climate changes due to black carbon. *Nature Geoscience* 1:221–227. <https://doi.org/10.1038/ngeo156>
16. Singh B, Singh BP, Cowie AL (2010) Characterisation and evaluation of biochars for their application as a soil amendment. *Soil Res* 48:516–525. <https://doi.org/10.1071/SR10058>
17. Garg A, Reddy NG, Huang H, et al (2020) Modelling contaminant transport in fly ash–bentonite composite landfill liner: mechanism of different types of ions. *Scientific Reports* 10:11330. <https://doi.org/10.1038/s41598-020-68198-6>
18. Kong S-H, Loh S-K, Bachmann RT, et al (2014) Biochar from oil palm biomass: A review of its potential and challenges. *Renewable and Sustainable Energy Reviews* 39:729–739. <https://doi.org/10.1016/j.rser.2014.07.107>
19. Ren S, Lei H, Wang L, et al (2014) Hydrocarbon and hydrogen-rich syngas production by biomass catalytic pyrolysis and bio-oil upgrading over biochar catalysts
20. Liu W-J, Jiang H, Yu H-Q (2015) Development of Biochar-Based Functional Materials: Toward a Sustainable Platform Carbon Material. *Chem Rev* 115:12251–12285. <https://doi.org/10.1021/acs.chemrev.5b00195>
21. Zaman CZ, Pal K, Yehye WA, et al (2017) Pyrolysis: A Sustainable Way to Generate Energy from Waste
22. Pandey D, Daverey A, Arunachalam K (2020) Biochar: Production, properties and emerging role as a support for enzyme immobilization. *Journal of Cleaner Production* 255:120267. <https://doi.org/10.1016/j.jclepro.2020.120267>
23. Varma AK, Thakur LS, Shankar R, Mondal P (2019) Pyrolysis of wood sawdust: Effects of process parameters on products yield and characterization of products. *Waste Management* 89:224–235. <https://doi.org/10.1016/j.wasman.2019.04.016>

24. Wani I, Sharma A, Kushvaha V, et al (2020) Effect of pH, Volatile Content, and Pyrolysis Conditions on Surface Area and O/C and H/C Ratios of Biochar: Towards Understanding Performance of Biochar Using Simplified Approach. *Journal of Hazardous, Toxic, and Radioactive Waste* 24:04020048. [https://doi.org/10.1061/\(ASCE\)HZ.2153-5515.0000545](https://doi.org/10.1061/(ASCE)HZ.2153-5515.0000545)
25. Weber K, Quicker P (2018) Properties of biochar. *Fuel* 217:240–261. <https://doi.org/10.1016/j.fuel.2017.12.054>
26. Ahmad M, Rajapaksha AU, Lim JE, et al (2014) Biochar as a sorbent for contaminant management in soil and water: A review. *Chemosphere* 99:19–33. <https://doi.org/10.1016/j.chemosphere.2013.10.071>
27. Ippolito JA, Cui L, Kammann C, et al (2020) Feedstock choice, pyrolysis temperature and type influence biochar characteristics: a comprehensive meta-data analysis review. *Biochar* 2:421–438. <https://doi.org/10.1007/s42773-020-00067-x>
28. Roberts DA, Paul NA, Dworjanyn SA, et al (2015) Biochar from commercially cultivated seaweed for soil amelioration. *Sci Rep* 5:9665. <https://doi.org/10.1038/srep09665>
29. Lei O, Zhang R (2013) Effects of biochars derived from different feedstocks and pyrolysis temperatures on soil physical and hydraulic properties. *J Soils Sediments* 13:1561–1572. <https://doi.org/10.1007/s11368-013-0738-7>
30. Ramola S, Mishra T, Rana G, Srivastava RK (2014) Characterization and pollutant removal efficiency of biochar derived from baggase, bamboo and tyre. *Environ Monit Assess* 186:9023–9039. <https://doi.org/10.1007/s10661-014-4062-5>
31. Doan TT, Henry-des-Tureaux T, Rumpel C, et al (2015) Impact of compost, vermicompost and biochar on soil fertility, maize yield and soil erosion in Northern Vietnam: A three year mesocosm experiment. *Science of The Total Environment* 514:147–154. <https://doi.org/10.1016/j.scitotenv.2015.02.005>
32. Jiang J, Xu R, Jiang T, Li Z (2012) Immobilization of Cu(II), Pb(II) and Cd(II) by the addition of rice straw derived biochar to a simulated polluted Ultisol. *Journal of Hazardous Materials* 229–230:145–150. <https://doi.org/10.1016/j.jhazmat.2012.05.086>
33. Ramola S, Kumar Srivastava R, Vasudevan P (2013) Effect of biochar application in combination with domestic wastewater on biomass yield of bioenergy plantations. *International Journal of Energy Sector Management* 7:355–363. <https://doi.org/10.1108/IJESM-03-2013-0005>
34. Wang S, Dai G, Yang H, Luo Z (2017) Lignocellulosic biomass pyrolysis mechanism: A state-of-the-art review. *Progress in Energy and Combustion Science* 62:33–86. <https://doi.org/10.1016/j.pecs.2017.05.004>

35. Wani I, Kumar H, Rangappa SM, et al (2021) Multiple Regression Model for Predicting Cracks in Soil Amended with Pig Manure Biochar and Wood Biochar. *Journal of Hazardous, Toxic, and Radioactive Waste* 25:04020061. [https://doi.org/10.1061/\(ASCE\)HZ.2153-5515.0000561](https://doi.org/10.1061/(ASCE)HZ.2153-5515.0000561)
36. Glaser B, Haumaier L, Guggenberger G, Zech W (2001) The “Terra Preta” phenomenon: a model for sustainable agriculture in the humid tropics. *Naturwissenschaften* 88:37–41. <https://doi.org/10.1007/s001140000193>
37. Ogawa M, Okimori Y (2010) Pioneering works in biochar research, Japan. *Soil Res* 48:489. <https://doi.org/10.1071/SR10006>
38. Ahmad T, Belwal T, Li L, et al (2020) Utilization of wastewater from edible oil industry, turning waste into valuable products: A review. *Trends in Food Science & Technology* 99:21–33. <https://doi.org/10.1016/j.tifs.2020.02.017>
39. Ramola S, Belwal T, Li CJ, et al (2020) Improved lead removal from aqueous solution using novel porous bentonite - and calcite-biochar composite. *Science of The Total Environment* 709:136171. <https://doi.org/10.1016/j.scitotenv.2019.136171>
40. Chen X-W, Wong JT-F, Ng CW-W, Wong M-H (2016) Feasibility of biochar application on a landfill final cover—a review on balancing ecology and shallow slope stability. *Environ Sci Pollut Res* 23:7111–7125. <https://doi.org/10.1007/s11356-015-5520-5>
41. Atkinson CJ, Fitzgerald JD, Hipps NA (2010) Potential mechanisms for achieving agricultural benefits from biochar application to temperate soils: a review. *Plant Soil* 337:1–18. <https://doi.org/10.1007/s11104-010-0464-5>
42. Dugan B, Liu Z, Masiello CA, et al (2015) Effect of Freeze-Thaw Cycles on Grain Size of Biochar. *AGU Fall Meeting Abstracts* 21:B21B-0427
43. Libra JA, Ro KS, Kammann C, et al (2011) Hydrothermal carbonization of biomass residuals: a comparative review of the chemistry, processes and applications of wet and dry pyrolysis
44. Chan KY, Van Zwieten L, Meszaros I, et al (2007) Agronomic values of greenwaste biochar as a soil amendment. *Soil Res* 45:629. <https://doi.org/10.1071/SR07109>
45. Major J, Rondon M, Riha S, Lehmann J (2010) Major J, Rondon M, Molina D, Riha SJ, Lehmann J.. Maize yield and nutrition during 4 years after biochar application to a Colombian savanna oxisol. *Plant Soil* 333: 117-128. *Plant and Soil* 333:117–128. <https://doi.org/10.1007/s11104-010-0327-0>
46. Steiner C, Glaser B, Teixeira W, et al (2008) Nitrogen retention and plant uptake on a highly weathered central Amazonian Ferralsol amended with compost and charcoal. *Journal of Plant Nutrition and Soil Science* 171:893–899. <https://doi.org/10.1002/jpln.200625199>

47. Van Zwieten L, Kimber S, Morris S, et al (2010) Effects of biochar from slow pyrolysis of papermill waste on agronomic performance and soil fertility. *Plant Soil* 327:235–246. <https://doi.org/10.1007/s11104-009-0050-x>
48. Busscher WJ, Novak JM, Evans DE, et al (2010) Influence of Pecan Biochar on Physical Properties of a Norfolk Loamy Sand. *Soil Science* 175:10–14. <https://doi.org/10.1097/SS.0b013e3181cb7f46>
49. Mukherjee A, Lal R (2013) Biochar Impacts on Soil Physical Properties and Greenhouse Gas Emissions. *Agronomy* 3:313–339. <https://doi.org/10.3390/agronomy3020313>
50. Novak JM, Lima I, Xing B, et al (2009) Characterization of Designer Biochar Produced at Different Temperatures and Their Effects on a Loamy Sand. *Annals of Environmental Science* 3:
51. Ronsse F, Hecke S van, Dickinson D, Prins W (2013) Production and characterization of slow pyrolysis biochar: influence of feedstock type and pyrolysis conditions. *GCB Bioenergy* 5:104–115. <https://doi.org/10.1111/gcbb.12018>
52. Spokas KA, Cantrell KB, Novak JM, et al (2012) Biochar: a synthesis of its agronomic impact beyond carbon sequestration. *J Environ Qual* 41:973–989. <https://doi.org/10.2134/jeq2011.0069>
53. Tomczyk A, Sokołowska Z, Boguta P (2020) Biochar physicochemical properties: pyrolysis temperature and feedstock kind effects. *Rev Environ Sci Biotechnol* 19:191–215. <https://doi.org/10.1007/s11157-020-09523-3>
54. Zhao S-X, Ta N, Wang X-D (2017) Effect of Temperature on the Structural and Physicochemical Properties of Biochar with Apple Tree Branches as Feedstock Material. *Energies* 10:1293. <https://doi.org/10.3390/en10091293>
55. Nguyen BT, Lehmann J, Hockaday WC, et al (2010) Temperature Sensitivity of Black Carbon Decomposition and Oxidation. *Environ Sci Technol* 44:3324–3331. <https://doi.org/10.1021/es903016y>
56. Zhang J, Liu J, Liu R (2015) Effects of pyrolysis temperature and heating time on biochar obtained from the pyrolysis of straw and lignosulfonate. *Bioresource Technology* 176:288–291. <https://doi.org/10.1016/j.biortech.2014.11.011>
57. Lehmann J (2007) Bio-energy in the black. *Frontiers in Ecology and the Environment* 5:381–387. [https://doi.org/10.1890/1540-9295\(2007\)5\[381:BITB\]2.0.CO;2](https://doi.org/10.1890/1540-9295(2007)5[381:BITB]2.0.CO;2)
58. Ahmad M, Lee SS, Dou X, et al (2012) Effects of pyrolysis temperature on soybean stover- and peanut shell-derived biochar properties and TCE adsorption in water. *Bioresource Technology* 118:536–544. <https://doi.org/10.1016/j.biortech.2012.05.042>

59. Ghanim BM, Pandey DS, Kwapinski W, Leahy JJ (2016) Hydrothermal carbonisation of poultry litter: Effects of treatment temperature and residence time on yields and chemical properties of hydrochars. *Bioresource Technology* 216:373–380. <https://doi.org/10.1016/j.biortech.2016.05.087>
60. Mohan D, Sarswat A, Ok YS, Pittman CU (2014) Organic and inorganic contaminants removal from water with biochar, a renewable, low cost and sustainable adsorbent – A critical review. *Bioresource Technology* 160:191–202. <https://doi.org/10.1016/j.biortech.2014.01.120>
61. Funke A, Ziegler F (2010) Hydrothermal carbonization of biomass: A summary and discussion of chemical mechanisms for process engineering. *Biofuels, Bioproducts and Biorefining* 4:160–177. <https://doi.org/10.1002/bbb.198>
62. Smith AM, Singh S, Ross AB (2016) Fate of inorganic material during hydrothermal carbonisation of biomass: Influence of feedstock on combustion behaviour of hydrochar. *Fuel* 169:135–145. <https://doi.org/10.1016/j.fuel.2015.12.006>
63. Castellini M, Giglio L, Niedda M, et al (2015) Impact of biochar addition on the physical and hydraulic properties of a clay soil. *Soil and Tillage Research* 154:1–13. <https://doi.org/10.1016/j.still.2015.06.016>
64. Lehmann J (2009) Terra Preta Nova – Where to from Here? In: Woods WI, Teixeira WG, Lehmann J, et al (eds) *Amazonian Dark Earths: Wim Sombroek’s Vision*. Springer Netherlands, Dordrecht, pp 473–486
65. Haefele SM, Konboon Y, Wongboon W, et al (2011) Effects and fate of biochar from rice residues in rice-based systems. *Field Crops Research* 121:430–440. <https://doi.org/10.1016/j.fcr.2011.01.014>
66. Ekwue EI (1990) Organic-matter effects on soil strength properties. *Soil and Tillage Research* 16:289–297. [https://doi.org/10.1016/0167-1987\(90\)90102-J](https://doi.org/10.1016/0167-1987(90)90102-J)
67. Piccolo A, Pietramellara G, Mbagwu JSC (1997) Use of humic substances as soil conditioners to increase aggregate stability. *Geoderma* 75:267–277. [https://doi.org/10.1016/S0016-7061\(96\)00092-4](https://doi.org/10.1016/S0016-7061(96)00092-4)
68. Sun F, Lu S (2014) Biochars improve aggregate stability, water retention, and pore-space properties of clayey soil. *Journal of Plant Nutrition and Soil Science* 177:26–33. <https://doi.org/10.1002/jpln.201200639>
69. Ni JJ, Chen XW, Ng CWW, Guo HW (2018) Effects of biochar on water retention and matric suction of vegetated soil. *Géotechnique Letters* 8:124–129. <https://doi.org/10.1680/jgele.17.00180>
70. Reddy KR, Yaghoubi P, Yukselen-Aksoy Y (2015) Effects of biochar amendment on geotechnical properties of landfill cover soil. *Waste Manag Res* 33:524–532. <https://doi.org/10.1177/0734242X15580192>
71. Williams JM, Latifi N, Vahedifard F (2018) Effects of Biochar Amendment on Mechanical Properties of Buckshot Clay. 125–134. <https://doi.org/10.1061/9780784481592.013>

72. Choi WC, Yun HD, Lee JY (2012) Mechanical Properties of Mortar Containing Bio-Char From Pyrolysis. *Journal of the Korea institute for structural maintenance and inspection* 16:67–74. <https://doi.org/10.11112/jksmi.2012.16.3.067>
73. Gupta S, Kua HW (2017) Factors Determining the Potential of Biochar As a Carbon Capturing and Sequestering Construction Material: Critical Review. *Journal of Materials in Civil Engineering* 29:04017086. [https://doi.org/10.1061/\(ASCE\)MT.1943-5533.0001924](https://doi.org/10.1061/(ASCE)MT.1943-5533.0001924)
74. Asada T, Ishihara S, Yamane T, et al (2002) Science of Bamboo Charcoal: Study on Carbonizing Temperature of Bamboo Charcoal and Removal Capability of Harmful Gases. *Journal of Health Science* 48:473–479. <https://doi.org/10.1248/jhs.48.473>
75. Khushnood RA, Ahmad S, Restuccia L, et al (2016) Carbonized nano/microparticles for enhanced mechanical properties and electromagnetic interference shielding of cementitious materials. *Front Struct Civ Eng* 10:209–213. <https://doi.org/10.1007/s11709-016-0330-5>
76. Zhao MY, Enders A, Lehmann J (2014) Short- and long-term flammability of biochars. *Biomass and Bioenergy* 69:183–191. <https://doi.org/10.1016/j.biombioe.2014.07.017>
77. Suarez-Riera D, Restuccia L, Ferro GA (2020) The use of Biochar to reduce the carbon footprint of cement-based materials. *Procedia Structural Integrity* 26:199–210. <https://doi.org/10.1016/j.prostr.2020.06.023>
78. Gupta S, Kua HW, Low CY (2018) Use of biochar as carbon sequestering additive in cement mortar. *Cement and Concrete Composites* 87:110–129. <https://doi.org/10.1016/j.cemconcomp.2017.12.009>
79. Chebil S, Chalaal A, Roy C (2000) Use of softwood bark charcoal as a modifier for road bitumen. *Fuel* 79:671–683. [https://doi.org/10.1016/S0016-2361\(99\)00196-9](https://doi.org/10.1016/S0016-2361(99)00196-9)
80. Walters RC, Fini EH, Abu-Lebdeh T (2014) ENHANCING ASPHALT RHEOLOGICAL BEHAVIOR AND AGING SUSCEPTIBILITY USING BIO-CHAR AND NANO-CLAY. *American Journal of Engineering and Applied Sciences* 7:66–76. <https://doi.org/10.3844/ajeassp.2014.66.76>
81. Zhao S, Huang B, Shu X, Ye P (2014) Laboratory Investigation of Biochar-Modified Asphalt Mixture. *Transportation Research Record* 2445:56–63. <https://doi.org/10.3141/2445-07>
82. Zhao S, Huang B, Ye XP, et al (2014) Utilizing bio-char as a bio-modifier for asphalt cement: A sustainable application of bio-fuel by-product. *Fuel* 133:52–62. <https://doi.org/10.1016/j.fuel.2014.05.002>
83. Liu S, Su Z, Li M, Shao L (2020) Slope stability analysis using elastic finite element stress fields. *Engineering Geology* 273:105673. <https://doi.org/10.1016/j.enggeo.2020.105673>
84. Wu Z, Chen C, Lu X, et al (2020) Discussion on the allowable safety factor of slope stability for high rockfill dams in China. *Engineering Geology* 272:105666. <https://doi.org/10.1016/j.enggeo.2020.105666>

85. Yaghoubi P (2012) Development of Biochar-Amended Landfill Cover for Landfill Gas Mitigation. Thesis, University of Illinois at Chicago
86. Pardo GS, Sarmah AK, Orense RP (2018) Mechanism of improvement of biochar on shear strength and liquefaction resistance of sand. *Géotechnique* 69:471–480. <https://doi.org/10.1680/jgeot.17.P.040>
87. Zong Y, Xiao Q, Lu S (2016) Acidity, water retention, and mechanical physical quality of a strongly acidic Ultisol amended with biochars derived from different feedstocks. *J Soils Sediments* 16:177–190. <https://doi.org/10.1007/s11368-015-1187-2>
88. Wallace CA, Afzal MT, Saha GC (2019) Effect of feedstock and microwave pyrolysis temperature on physio-chemical and nano-scale mechanical properties of biochar. *Bioresources and Bioprocessing* 6:33. <https://doi.org/10.1186/s40643-019-0268-2>
89. GuhaRay A, Guoxiong M, Sarkar A, et al (2019) Geotechnical and chemical characterization of expansive clayey soil amended by biochar derived from invasive weed species *Prosopis juliflora*. *Innov Infrastruct Solut* 4:44. <https://doi.org/10.1007/s41062-019-0231-2>
90. Bordoloi S, Garg A, Sreedeeep S, et al (2018) Investigation of cracking and water availability of soil-biochar composite synthesized from invasive weed water hyacinth. *Bioresource Technology* 263:665–677. <https://doi.org/10.1016/j.biortech.2018.05.011>
91. Garg A, Huang H, Kushvaha V, et al (2019) Mechanism of biochar soil pore–gas–water interaction: gas properties of biochar-amended sandy soil at different degrees of compaction using KNN modeling. *Acta Geophys*. <https://doi.org/10.1007/s11600-019-00387-y>
92. Gopal P, Bordoloi S, Ratnam R, et al (2019) Investigation of infiltration rate for soil-biochar composites of water hyacinth. *Acta Geophys* 67:231–246. <https://doi.org/10.1007/s11600-018-0237-8>
93. Garg A, Bordoloi S, Ni J, et al (2019) Influence of biochar addition on gas permeability in unsaturated soil. *Géotechnique Letters* 9:66–71. <https://doi.org/10.1680/jgele.18.00190>
94. Sadasivam BY, Reddy KR (2015) Engineering properties of waste wood-derived biochars and biochar-amended soils. *International Journal of Geotechnical Engineering* 9:521–535. <https://doi.org/10.1179/1939787915Y.0000000004>
95. Jyoti Bora M, Bordoloi S, Kumar H, et al (2020) Influence of biochar from animal and plant origin on the compressive strength characteristics of degraded landfill surface soils. *International Journal of Damage Mechanics* 1056789520925524. <https://doi.org/10.1177/1056789520925524>
96. Huang H, Cai W-L, Zheng Q, et al (2020) Gas permeability in soil amended with biochar at different compaction states. *IOP Conf Ser: Earth Environ Sci* 463:012073. <https://doi.org/10.1088/1755-1315/463/1/012073>

97. Gul S, Whalen JK, Thomas BW, et al (2015) Physico-chemical properties and microbial responses in biochar-amended soils: Mechanisms and future directions. *Agriculture, Ecosystems & Environment* 206:46–59. <https://doi.org/10.1016/j.agee.2015.03.015>
98. Peng X, Tong X, Hao L, Wu F (2019) Applicability of biochar for limiting interrill erosion and organic carbon export of sloping cropland in a semi-arid area of China. *Agriculture, Ecosystems & Environment* 280:68–76. <https://doi.org/10.1016/j.agee.2019.04.021>
99. Laird DA, Fleming P, Davis DD, et al (2010) Impact of biochar amendments on the quality of a typical Midwestern agricultural soil. *Geoderma* 158:443–449. <https://doi.org/10.1016/j.geoderma.2010.05.013>
100. Nyambo P, Taeni T, Chiduza C, Araya T (2018) Effects of Maize Residue Biochar Amendments on Soil Properties and Soil Loss on Acidic Hutton Soil. *Agronomy* 8:256. <https://doi.org/10.3390/agronomy8110256>
101. Vijayaraghavan K (2019) Recent advancements in biochar preparation, feedstocks, modification, characterization and future applications. *Environmental Technology Reviews* 8:47–64. <https://doi.org/10.1080/21622515.2019.1631393>
102. Anae J, Ahmad N, Kumar V, et al (2021) Recent advances in biochar engineering for soil contaminated with complex chemical mixtures: Remediation strategies and future perspectives. *Science of The Total Environment* 767:144351. <https://doi.org/10.1016/j.scitotenv.2020.144351>
103. da Costa ML, Kern DC (1999) Geochemical signatures of tropical soils with archaeological black earth in the Amazon, Brazil. *Journal of Geochemical Exploration* 66:369–385. [https://doi.org/10.1016/S0375-6742\(99\)00038-2](https://doi.org/10.1016/S0375-6742(99)00038-2)
104. Schmidt MWI, Noack AG (2000) Black carbon in soils and sediments: Analysis, distribution, implications, and current challenges. *Global Biogeochemical Cycles* 14:777–793. <https://doi.org/10.1029/1999GB001208>
105. Leinweber P, Schulten H-R (1999) Advances in analytical pyrolysis of soil organic matter. *Journal of Analytical and Applied Pyrolysis* 49:359–383. [https://doi.org/10.1016/S0165-2370\(98\)00082-5](https://doi.org/10.1016/S0165-2370(98)00082-5)
106. Bridgwater AV, Meier D, Radlein D (1999) An overview of fast pyrolysis of biomass. *Organic Geochemistry* 30:1479–1493. [https://doi.org/10.1016/S0146-6380\(99\)00120-5](https://doi.org/10.1016/S0146-6380(99)00120-5)
107. Liu W-J, Jiang H, Yu H-Q (2015) Development of Biochar-Based Functional Materials: Toward a Sustainable Platform Carbon Material. *Chem Rev* 115:12251–12285. <https://doi.org/10.1021/acs.chemrev.5b00195>
108. Heymann K, Lehmann J, Solomon D, et al (2011) C 1s K-edge near edge X-ray absorption fine structure (NEXAFS) spectroscopy for characterizing functional group chemistry of black carbon. *Organic Geochemistry* 42:1055–1064. <https://doi.org/10.1016/j.orggeochem.2011.06.021>

109. Kiersch K, Kruse J, Eckhardt K-U, et al (2012) Impact of grassland burning on soil organic matter as revealed by a synchrotron- and pyrolysis–mass spectrometry-based multi-methodological approach. *Organic geochemistry*
110. Chen C-P, Cheng C-H, Huang Y-H, et al (2014) Converting leguminous green manure into biochar: changes in chemical composition and C and N mineralization. *Geoderma* 232–234:581–588. <https://doi.org/10.1016/j.geoderma.2014.06.021>
111. Vidal BC, Dien BS, Ting KC, Singh V (2011) Influence of Feedstock Particle Size on Lignocellulose Conversion—A Review. *Appl Biochem Biotechnol* 164:1405–1421. <https://doi.org/10.1007/s12010-011-9221-3>
112. Finnveden G (Stockholm U (Sweden) Foer MS (1999) A critical review of operational valuation/weighting methods for life cycle assessment. Survey. AFR-report (Sweden)
113. Banyasz JL, Li S, Lyons-Hart J, Shafer KH (2001) Gas evolution and the mechanism of cellulose pyrolysis. *Fuel* 80:1757–1763. [https://doi.org/10.1016/S0016-2361\(01\)00060-6](https://doi.org/10.1016/S0016-2361(01)00060-6)
114. Li S, Lyons-Hart J, Banyasz J, Shafer K (2001) Real-time evolved gas analysis by FTIR method: an experimental study of cellulose pyrolysis. *Fuel* 80:1809–1817. [https://doi.org/10.1016/S0016-2361\(01\)00064-3](https://doi.org/10.1016/S0016-2361(01)00064-3)
115. Wooten JB, Seeman JI, Hajaligol MR (2004) Observation and Characterization of Cellulose Pyrolysis Intermediates by <sup>13</sup>C CPMAS NMR. A New Mechanistic Model. *Energy Fuels* 18:1–15. <https://doi.org/10.1021/ef0300601>
116. Luo, Wang, Liao, Cen (2004) Mechanism Study of Cellulose Rapid Pyrolysis. *Ind Eng Chem Res* 43:5605–5610. <https://doi.org/10.1021/ie030774z>
117. Lopez G, Aguado R, Olazar M, et al (2009) Kinetics of scrap tyre pyrolysis under vacuum conditions. *Waste Management* 29:2649–2655. <https://doi.org/10.1016/j.wasman.2009.06.005>
118. Patwardhan PR, Dalluge DL, Shanks BH, Brown RC (2011) Distinguishing primary and secondary reactions of cellulose pyrolysis. *Bioresource Technology* 102:5265–5269. <https://doi.org/10.1016/j.biortech.2011.02.018>
119. Mettler MS, Paulsen AD, Vlachos DG, Dauenhauer PJ (2012) Pyrolytic conversion of cellulose to fuels: levoglucosan deoxygenation via elimination and cyclization within molten biomass. *Energy Environ Sci* 5:7864–7868. <https://doi.org/10.1039/C2EE21305B>
120. Zhang X, Yang W, Blasiak W (2012) Thermal decomposition mechanism of levoglucosan during cellulose pyrolysis. *Journal of Analytical and Applied Pyrolysis* 96:110–119. <https://doi.org/10.1016/j.jaap.2012.03.012>

121. Vinu R, Broadbelt LJ (2012) A mechanistic model of fast pyrolysis of glucose-based carbohydrates to predict bio-oil composition. *Energy Environ Sci* 5:9808–9826. <https://doi.org/10.1039/C2EE22784C>
122. Di Blasi C, Signorelli G, Di Russo C, Rea G (1999) Product Distribution from Pyrolysis of Wood and Agricultural Residues. *Ind Eng Chem Res* 38:2216–2224. <https://doi.org/10.1021/ie980711u>
123. Huang J, Liu C, Tong H, et al (2012) Theoretical studies on pyrolysis mechanism of xylopyranose. *Computational and Theoretical Chemistry* 1001:44–50. <https://doi.org/10.1016/j.comptc.2012.10.015>
124. Peng Y, Wu S (2010) The structural and thermal characteristics of wheat straw hemicellulose. *Journal of Analytical and Applied Pyrolysis* 88:134–139. <https://doi.org/10.1016/j.jaap.2010.03.006>
125. Peters B (2011) Prediction of pyrolysis of pistachio shells based on its components hemicellulose, cellulose and lignin. *Fuel Processing Technology* 92:1993–1998. <https://doi.org/10.1016/j.fuproc.2011.05.023>
126. Sefain MZ, El-Kalyoubi SF, Shukry N (1985) Thermal behavior of holo- and hemicellulose obtained from rice straw and bagasse. *Journal of Polymer Science: Polymer Chemistry Edition* 23:1569–1577. <https://doi.org/10.1002/pol.1985.170230527>
127. Shen D, Xiao R, Gu S, Luo K (2011) The pyrolytic behavior of cellulose in lignocellulosic biomass: a review. *RSC Adv* 1:1641–1660. <https://doi.org/10.1039/C1RA00534K>
128. Shen DK, Gu S, Bridgwater AV (2010) The thermal performance of the polysaccharides extracted from hardwood: Cellulose and hemicellulose. *Carbohydrate Polymers* 82:39–45. <https://doi.org/10.1016/j.carbpol.2010.04.018>
129. Wiedner K, Rumpel C, Steiner C, et al (2013) Chemical evaluation of chars produced by thermochemical conversion (gasification, pyrolysis and hydrothermal carbonization) of agro-industrial biomass on a commercial scale. *Biomass and Bioenergy* 59:264–278. <https://doi.org/10.1016/j.biombioe.2013.08.026>
130. Antal MJ, Grønli M (2003) The Art, Science, and Technology of Charcoal Production. *Ind Eng Chem Res* 42:1619–1640. <https://doi.org/10.1021/ie0207919>
131. Lin Y-C, Cho J, Tompsett GA, et al (2009) Kinetics and Mechanism of Cellulose Pyrolysis. *J Phys Chem C* 113:20097–20107. <https://doi.org/10.1021/jp906702p>
132. Ben H, Ragauskas AJ (2011) NMR Characterization of Pyrolysis Oils from Kraft Lignin. *Energy Fuels* 25:2322–2332. <https://doi.org/10.1021/ef2001162>
133. Chu S, Subrahmanyam AV, Huber GW (2012) The pyrolysis chemistry of a  $\beta$ -O-4 type oligomeric lignin model compound. *Green Chem* 15:125–136. <https://doi.org/10.1039/C2GC36332A>

134. Kosa M, Ben H, Theliander H, Ragauskas AJ (2011) Pyrolysis oils from CO<sub>2</sub> precipitated Kraft lignin. *Green Chem* 13:3196–3202. <https://doi.org/10.1039/C1GC15818J>
135. Mu W, Ben H, Ragauskas A, Deng Y (2013) Lignin Pyrolysis Components and Upgrading—Technology Review. *Bioenerg Res* 6:1183–1204. <https://doi.org/10.1007/s12155-013-9314-7>
136. Cetin E, Moghtaderi B, Gupta R, Wall TF (2004) Influence of pyrolysis conditions on the structure and gasification reactivity of biomass chars. *Fuel* 83:2139–2150. <https://doi.org/10.1016/j.fuel.2004.05.008>
137. Melligan F, Auccaise R, Novotny EH, et al (2011) Pressurised pyrolysis of Miscanthus using a fixed bed reactor. *Bioresource Technology* 102:3466–3470. <https://doi.org/10.1016/j.biortech.2010.10.129>
138. Antal Michael Jerry, Croiset E, Dai X, et al (1996) High-Yield Biomass Charcoal. *Energy Fuels* 10:652–658. <https://doi.org/10.1021/ef9501859>
139. Manyà JJ (2012) Pyrolysis for Biochar Purposes: A Review to Establish Current Knowledge Gaps and Research Needs. *Environ Sci Technol* 46:7939–7954. <https://doi.org/10.1021/es301029g>
140. Michael Jerry Antal J, Mok WSL, Varhegyi G, Szekely T (2002) Review of methods for improving the yield of charcoal from biomass. <https://pubs.acs.org/doi/pdf/10.1021/ef00021a001>. Accessed 25 Apr 2020
141. Zaman CZ, Pal K, Yehye WA, et al (2017) Pyrolysis: A Sustainable Way to Generate Energy from Waste. *Pyrolysis*. <https://doi.org/10.5772/intechopen.69036>
142. Demirbaş A (2002) Partly chemical analysis of liquid fraction of flash pyrolysis products from biomass in the presence of sodium carbonate. *Energy Conversion and Management* 43:1801–1809. [https://doi.org/10.1016/S0196-8904\(01\)00137-6](https://doi.org/10.1016/S0196-8904(01)00137-6)
143. Brownsort PA (2009) Biomass pyrolysis processes: performance parameters and their influence on biochar system benefits
144. Li L, Rowbotham JS, Christopher Greenwell H, Dyer PW (2013) Chapter 8 - An Introduction to Pyrolysis and Catalytic Pyrolysis: Versatile Techniques for Biomass Conversion. In: Suib SL (ed) *New and Future Developments in Catalysis*. Elsevier, Amsterdam, pp 173–208
145. Foong SY, Liew RK, Yang Y, et al (2020) Valorization of biomass waste to engineered activated biochar by microwave pyrolysis: Progress, challenges, and future directions. *Chemical Engineering Journal* 389:124401. <https://doi.org/10.1016/j.cej.2020.124401>
146. Yek PNY, Peng W, Wong CC, et al (2020) Engineered biochar via microwave CO<sub>2</sub> and steam pyrolysis to treat carcinogenic Congo red dye. *Journal of Hazardous Materials* 395:122636. <https://doi.org/10.1016/j.jhazmat.2020.122636>

147. Zeng K, Gauthier D, Soria J, et al (2017) Solar pyrolysis of carbonaceous feedstocks: A review. *Solar Energy* 156:73–92. <https://doi.org/10.1016/j.solener.2017.05.033>
148. Julkapli NM, Bagheri S (2015) Graphene supported heterogeneous catalysts: An overview. *International Journal of Hydrogen Energy* 40:948–979. <https://doi.org/10.1016/j.ijhydene.2014.10.129>
149. Matos I, Bernardo M, Fonseca I (2017) Porous carbon: A versatile material for catalysis. *Catalysis Today* 285:194–203. <https://doi.org/10.1016/j.cattod.2017.01.039>
150. Chen Y, Zhang L, Xu Z (2017) Vacuum pyrolysis characteristics and kinetic analysis of liquid crystal from scrap liquid crystal display panels. *Journal of Hazardous Materials* 327:55–63. <https://doi.org/10.1016/j.jhazmat.2016.12.026>
151. Vijayakumar A, Sebastian J (2018) Pyrolysis process to produce fuel from different types of plastic – a review. *IOP Conf Ser: Mater Sci Eng* 396:012062. <https://doi.org/10.1088/1757-899X/396/1/012062>
152. Kambo HS, Dutta A (2015) A comparative review of biochar and hydrochar in terms of production, physico-chemical properties and applications. *Renewable and Sustainable Energy Reviews* 45:359–378. <https://doi.org/10.1016/j.rser.2015.01.050>
153. Brownsort PA (2009) Biomass pyrolysis processes: performance parameters and their influence on biochar system benefits
154. Mohan D, Pittman CU, Steele PH (2006) Pyrolysis of Wood/Biomass for Bio-oil: A Critical Review. *Energy Fuels* 20:848–889. <https://doi.org/10.1021/ef0502397>
155. Chandra S, Bhattacharya J (2019) Influence of temperature and duration of pyrolysis on the property heterogeneity of rice straw biochar and optimization of pyrolysis conditions for its application in soils. *Journal of Cleaner Production* 215:1123–1139. <https://doi.org/10.1016/j.jclepro.2019.01.079>
156. Demirbas A, Arin G (2002) An Overview of Biomass Pyrolysis. *Energy Sources* 24:471–482. <https://doi.org/10.1080/00908310252889979>
157. Yanik J, Kornmayer C, Saglam M, Yüksel M (2007) Fast pyrolysis of agricultural wastes: Characterization of pyrolysis products. *Fuel Processing Technology* 88:942–947. <https://doi.org/10.1016/j.fuproc.2007.05.002>
158. Demirbaş A (2001) Biomass resource facilities and biomass conversion processing for fuels and chemicals. *Energy Conversion and Management* 42:1357–1378. [https://doi.org/10.1016/S0196-8904\(00\)00137-0](https://doi.org/10.1016/S0196-8904(00)00137-0)
159. Gerçel HF (2002) Production and characterization of pyrolysis liquids from sunflower-pressed bagasse. *Bioresour Technol* 85:113–117. [https://doi.org/10.1016/s0960-8524\(02\)00101-3](https://doi.org/10.1016/s0960-8524(02)00101-3)

160. Zhang L, Xu C (Charles), Champagne P (2010) Overview of recent advances in thermo-chemical conversion of biomass. *Energy Conversion and Management* 51:969–982. <https://doi.org/10.1016/j.enconman.2009.11.038>
161. Hagemann N, Spokas K, Schmidt H-P, et al (2018) Activated Carbon, Biochar and Charcoal: Linkages and Synergies across Pyrogenic Carbon's ABCs. *Water* 10:182. <https://doi.org/10.3390/w10020182>
162. Pan YG, Velo E, Roca X, et al (2000) Fluidized-bed co-gasification of residual biomass/poor coal blends for fuel gas production. *Fuel* 79:1317–1326. [https://doi.org/10.1016/S0016-2361\(99\)00258-6](https://doi.org/10.1016/S0016-2361(99)00258-6)
163. Behrendt F, Neubauer Y, Oevermann M, et al (2008) Direct Liquefaction of Biomass. *Chemical Engineering & Technology* 31:667–677. <https://doi.org/10.1002/ceat.200800077>
164. Lam SS, Liew RK, Jusoh A, et al (2016) Progress in waste oil to sustainable energy, with emphasis on pyrolysis techniques. *Renewable and Sustainable Energy Reviews* 53:741–753. <https://doi.org/10.1016/j.rser.2015.09.005>
165. Akhtar A, Krepl V, Ivanova T (2018) A Combined Overview of Combustion, Pyrolysis, and Gasification of Biomass. *Energy Fuels* 32:7294–7318. <https://doi.org/10.1021/acs.energyfuels.8b01678>
166. Rajasekhar Reddy B, Vinu R (2018) Microwave-assisted co-pyrolysis of high ash Indian coal and rice husk: Product characterization and evidence of interactions. *Fuel Processing Technology* 178:41–52. <https://doi.org/10.1016/j.fuproc.2018.04.018>
167. Lam SS, Liew RK, Wong YM, et al (2017) Microwave-assisted pyrolysis with chemical activation, an innovative method to convert orange peel into activated carbon with improved properties as dye adsorbent. *Journal of Cleaner Production* 162:1376–1387. <https://doi.org/10.1016/j.jclepro.2017.06.131>
168. Lam SS, Liew RK, Cheng CK, Chase HA (2015) Catalytic microwave pyrolysis of waste engine oil using metallic pyrolysis char. *Applied Catalysis B: Environmental* 176–177:601–617. <https://doi.org/10.1016/j.apcatb.2015.04.014>
169. Liew RK, Azwar E, Yek PNY, et al (2018) Microwave pyrolysis with KOH/NaOH mixture activation: A new approach to produce micro-mesoporous activated carbon for textile dye adsorption. *Bioresource Technology* 266:1–10. <https://doi.org/10.1016/j.biortech.2018.06.051>
170. Liu Z, Wang J, Kushvaha V, et al (2011) Poptube approach for ultrafast carbon nanotube growth. *Chem Commun* 47:9912–9914. <https://doi.org/10.1039/C1CC13359D>
171. Liew RK, Azwar E, Yek PNY, et al (2018) Microwave pyrolysis with KOH/NaOH mixture activation: A new approach to produce micro-mesoporous activated carbon for textile dye adsorption. *Bioresource Technology* 266:1–10. <https://doi.org/10.1016/j.biortech.2018.06.051>

172. de Jongh WA, Carrier M, Knoetze JH (Hansie) (2011) Vacuum pyrolysis of intruder plant biomasses. *Journal of Analytical and Applied Pyrolysis* 92:184–193. <https://doi.org/10.1016/j.jaap.2011.05.015>
173. Nam WL, Phang XY, Su MH, et al (2018) Production of bio-fertilizer from microwave vacuum pyrolysis of palm kernel shell for cultivation of Oyster mushroom (*Pleurotus ostreatus*). *Science of The Total Environment* 624:9–16. <https://doi.org/10.1016/j.scitotenv.2017.12.108>
174. Roy C, Pakdel H, Brouillard D (1990) The role of extractives during vacuum pyrolysis of wood. *Journal of Applied Polymer Science* 41:337–348. <https://doi.org/10.1002/app.1990.070410126>
175. Chen Z, Niu B, Zhang L, Xu Z (2018) Vacuum pyrolysis characteristics and parameter optimization of recycling organic materials from waste tantalum capacitors. *Journal of Hazardous Materials* 342:192–200. <https://doi.org/10.1016/j.jhazmat.2017.08.021>
176. Yek PNY, Liew RK, Osman MS, et al (2017) Microwave pyrolysis using self-generated pyrolysis gas as activating agent: An innovative single-step approach to convert waste palm shell into activated carbon. *E3S Web Conf* 22:00195. <https://doi.org/10.1051/e3sconf/20172200195>
177. Salema AA, Ani FN (2012) Microwave-assisted pyrolysis of oil palm shell biomass using an overhead stirrer. *Journal of Analytical and Applied Pyrolysis* 96:162–172. <https://doi.org/10.1016/j.jaap.2012.03.018>
178. Dai Z, Zhang X, Tang C, et al (2017) Potential role of biochars in decreasing soil acidification - A critical review. *Science of The Total Environment* 581–582:601–611. <https://doi.org/10.1016/j.scitotenv.2016.12.169>
179. Liu X-H, Han F-P, Zhang XC (2012) Effect of Biochar on Soil Aggregates in the Loess Plateau: Results from Incubation Experiments. *International Journal of Agriculture and Biology* 14:975–979
180. Mukherjee A, Lal R, Zimmerman AR (2014) Effects of biochar and other amendments on the physical properties and greenhouse gas emissions of an artificially degraded soil. *Science of The Total Environment* 487:26–36. <https://doi.org/10.1016/j.scitotenv.2014.03.141>
181. Raboin L-M, Razafimahafaly AHD, Rabenjarisoa MB, et al (2016) Improving the fertility of tropical acid soils: Liming versus biochar application? A long term comparison in the highlands of Madagascar. *Field Crops Research* 199:99–108. <https://doi.org/10.1016/j.fcr.2016.09.005>
182. Tammeorg P, Bastos AC, Jeffery S, et al (2017) Biochars in soils: towards the required level of scientific understanding. *Journal of Environmental Engineering and Landscape Management* 25:192–207. <https://doi.org/10.3846/16486897.2016.1239582>
183. Verheijen FGA, Jones RJA, Rickson RJ, Smith CJ (2009) Tolerable versus actual soil erosion rates in Europe. *Earth-Science Reviews* 94:23–38. <https://doi.org/10.1016/j.earscirev.2009.02.003>

184. Rutigliano FA, Romano M, Marzaioli R, et al (2014) Effect of biochar addition on soil microbial community in a wheat crop. *European Journal of Soil Biology* 60:9–15. <https://doi.org/10.1016/j.ejsobi.2013.10.007>
185. Asai H, Samson BK, Stephan HM, et al (2009) Biochar amendment techniques for upland rice production in Northern Laos: 1. Soil physical properties, leaf SPAD and grain yield. *Field Crops Research* 111:81–84. <https://doi.org/10.1016/j.fcr.2008.10.008>
186. Lehmann J, Rillig MC, Thies J, et al (2011) Biochar effects on soil biota – A review. *Soil Biology and Biochemistry* 43:1812–1836. <https://doi.org/10.1016/j.soilbio.2011.04.022>
187. Mukherjee A, Zimmerman AR, Harris W (2011) Surface chemistry variations among a series of laboratory-produced biochars. *Geoderma* 163:247–255. <https://doi.org/10.1016/j.geoderma.2011.04.021>
188. Makoto K, Tamai Y, Kim YS, Koike T (2010) Buried charcoal layer and ectomycorrhizae cooperatively promote the growth of *Larix gmelinii* seedlings. *Plant Soil* 327:143–152. <https://doi.org/10.1007/s11104-009-0040-z>
189. Garg A, Wani I, Zhu H, Kushvaha V (2021) Exploring efficiency of biochar in enhancing water retention in soils with varying grain size distributions using ANN technique. *Acta Geotech.* <https://doi.org/10.1007/s11440-021-01411-6>
190. Blanco-Canqui H (2017) Biochar and Soil Physical Properties. *Soil Science Society of America Journal* 81:687–711. <https://doi.org/10.2136/sssaj2017.01.0017>
191. Wang J, Xiong Z, Kuzyakov Y (2016) Biochar stability in soil: meta-analysis of decomposition and priming effects. *GCB Bioenergy* 8:512–523. <https://doi.org/10.1111/gcbb.12266>
192. Yang X, Wang D, Lan Y, et al (2018) Labile organic carbon fractions and carbon pool management index in a 3-year field study with biochar amendment. *J Soils Sediments* 18:1569–1578. <https://doi.org/10.1007/s11368-017-1874-2>
193. Zong Y, Chen D, Lu S (2014) Impact of biochars on swell-shrinkage behavior, mechanical strength, and surface cracking of clayey soil. *J Plant Nutr Soil Sci* 177:920–926. <https://doi.org/10.1002/jpln.201300596>
194. Al-Wabel MI, Hussain Q, Usman ARA, et al (2018) Impact of biochar properties on soil conditions and agricultural sustainability: A review. *Land Degradation and Development* 29:2124–2161. <https://doi.org/10.1002/ldr.2829>
195. Qambrani NA, Rahman MM, Won S, et al (2017) Biochar properties and eco-friendly applications for climate change mitigation, waste management, and wastewater treatment: A review. *Renewable and Sustainable Energy Reviews* 79:255–273. <https://doi.org/10.1016/j.rser.2017.05.057>

196. Ahmed MB, Zhou JL, Ngo HH, Guo W (2016) Insight into biochar properties and its cost analysis. *Biomass and Bioenergy* 84:76–86. <https://doi.org/10.1016/j.biombioe.2015.11.002>
197. Yu H, Zou W, Chen J, et al (2019) Biochar amendment improves crop production in problem soils: A review. *Journal of Environmental Management* 232:8–21. <https://doi.org/10.1016/j.jenvman.2018.10.117>
198. Zhang Q, Song Y, Wu Z, et al (2020) Effects of six-year biochar amendment on soil aggregation, crop growth, and nitrogen and phosphorus use efficiencies in a rice-wheat rotation. *Journal of Cleaner Production* 242:118435. <https://doi.org/10.1016/j.jclepro.2019.118435>
199. Huang YF, Chiueh P Te, Shih CH, et al (2015) Microwave pyrolysis of rice straw to produce biochar as an adsorbent for CO<sub>2</sub> capture. *Energy* 84:75–82. <https://doi.org/10.1016/j.energy.2015.02.026>
200. Chen J, Li S, Liang C, et al (2017) Response of microbial community structure and function to short-term biochar amendment in an intensively managed bamboo (*Phyllostachys praecox*) plantation soil: Effect of particle size and addition rate. *Science of The Total Environment* 574:24–33. <https://doi.org/10.1016/j.scitotenv.2016.08.190>
201. Sun H, Hockaday WC, Masiello CA, Zygourakis K (2012) Multiple Controls on the Chemical and Physical Structure of Biochars. *Ind Eng Chem Res* 51:3587–3597. <https://doi.org/10.1021/ie201309r>
202. Valenzuela-Calahorra C, Bernalte-García A, Gómez-Serrano V, Bernalte-García MJ (1987) Influence of particle size and pyrolysis conditions on yield, density and some textural parameters of chars prepared from holm-oak wood. *Journal of Analytical and Applied Pyrolysis* 12:61–70. [https://doi.org/10.1016/0165-2370\(87\)80015-3](https://doi.org/10.1016/0165-2370(87)80015-3)
203. Xie T, Reddy KR, Wang C, et al (2015) Characteristics and Applications of Biochar for Environmental Remediation: A Review. *Critical Reviews in Environmental Science and Technology* 45:939–969. <https://doi.org/10.1080/10643389.2014.924180>
204. Fazeli Sangani M, Abrishamkesh S, Owens G (2020) Physicochemical characteristics of biochars can be beneficially manipulated using post-pyrolyzed particle size modification. *Bioresource Technology* 306:123157. <https://doi.org/10.1016/j.biortech.2020.123157>
205. Liu Z, Dugan B, Masiello CA, Gonnermann HM (2017) Biochar particle size, shape, and porosity act together to influence soil water properties. *PLOS ONE* 12:e0179079. <https://doi.org/10.1371/journal.pone.0179079>
206. Liang C, Gascó G, Fu S, et al (2016) Biochar from pruning residues as a soil amendment: Effects of pyrolysis temperature and particle size. *Soil and Tillage Research* 164:3–10. <https://doi.org/10.1016/j.still.2015.10.002>

207. Brown RA, Kercher AK, Nguyen TH, et al (2006) Production and characterization of synthetic wood chars for use as surrogates for natural sorbents. *Organic Geochemistry* 37:321–333. <https://doi.org/10.1016/j.orggeochem.2005.10.008>
208. Zhang Y, Wang J, Feng Y (2021) The effects of biochar addition on soil physicochemical properties: A review. *CATENA* 202:105284. <https://doi.org/10.1016/j.catena.2021.105284>
209. Oguntunde PG, Abiodun BJ, Ajayi AE, Giesen N van de (2008) Effects of charcoal production on soil physical properties in Ghana. *Journal of Plant Nutrition and Soil Science* 171:591–596. <https://doi.org/10.1002/jpln.200625185>
210. Pratiwi EPA, Shinogi Y (2016) Rice husk biochar application to paddy soil and its effects on soil physical properties, plant growth, and methane emission. *Paddy and Water Environment* 14:521–532. <https://doi.org/10.1007/s10333-015-0521-z>
211. Gluba Ł, Rafalska-Przysucha A, Szewczak K, et al (2021) Effect of Fine Size-Fractionated Sunflower Husk Biochar on Water Retention Properties of Arable Sandy Soil. *Materials* 14:1335. <https://doi.org/10.3390/ma14061335>
212. Patwa D, Chandra A, Ravi K, Sreedeeep S (2021) Influence of Biochar Particle Size Fractions on Thermal and Mechanical Properties of Biochar-Amended Soil. *Journal of Materials in Civil Engineering* 33:04021236. [https://doi.org/10.1061/\(ASCE\)MT.1943-5533.0003915](https://doi.org/10.1061/(ASCE)MT.1943-5533.0003915)
213. A.E Ajayi, R. Horn (2016) Modification of chemical and hydrophysical properties of two texturally differentiated soils due to varying magnitudes of added biochar. *Soil & tillage research* 164:34–44. <https://doi.org/10.1016/j.still.2016.01.011>
214. Liao W, Thomas S (2019) Biochar Particle Size and Post-Pyrolysis Mechanical Processing Affect Soil pH, Water Retention Capacity, and Plant Performance. *Soil Syst* 3:14. <https://doi.org/10.3390/soilsystems3010014>
215. Zhang X, Wang K, Sun C, et al (2022) Differences in soil physical properties caused by applying three organic amendments to loamy clay soil under field conditions. *Journal of Soils and Sediments* 22:. <https://doi.org/10.1007/s11368-021-03049-z>
216. Kameyama K, Miyamoto T, Shiono T, Shinogi Y (2012) Influence of sugarcane bagasse-derived biochar application on nitrate leaching in calcaric dark red soil. *J Environ Qual* 41:1131–1137. <https://doi.org/10.2134/jeq2010.0453>
217. Bird MI, Wurster CM, de Paula Silva PH, et al (2011) Algal biochar--production and properties. *Bioresour Technol* 102:1886–1891. <https://doi.org/10.1016/j.biortech.2010.07.106>
218. Keiluweit M, Nico PS, Johnson MG, Kleber M (2010) Dynamic Molecular Structure of Plant Biomass-Derived Black Carbon (Biochar). *Environ Sci Technol* 44:1247–1253. <https://doi.org/10.1021/es9031419>

219. Zhang J, Amonette JE, Flury M (2021) Effect of biochar and biochar particle size on plant-available water of sand, silt loam, and clay soil. *Soil and Tillage Research* 212:104992. <https://doi.org/10.1016/j.still.2021.104992>
220. Herath HMSK, Camps-Arbestain M, Hedley M (2013) Effect of biochar on soil physical properties in two contrasting soils: An Alfisol and an Andisol. *Geoderma* 209–210:188–197. <https://doi.org/10.1016/j.geoderma.2013.06.016>
221. Curaqueo G, Meier S, Khan N, et al (2014) Use of biochar on two volcanic soils: effects on soil properties and barley yield. *Journal of soil science and plant nutrition* 14:911–924. <https://doi.org/10.4067/S0718-95162014005000072>
222. Kelly CN, Benjamin J, Calderón FC, et al (2017) Incorporation of Biochar Carbon into Stable Soil Aggregates: The Role of Clay Mineralogy and Other Soil Characteristics. *Pedosphere* 27:694–704. [https://doi.org/10.1016/S1002-0160\(17\)60399-0](https://doi.org/10.1016/S1002-0160(17)60399-0)
223. Dong X, Guan T, Li G, et al (2016) Long-term effects of biochar amount on the content and composition of organic matter in soil aggregates under field conditions. *J Soils Sediments* 16:1481–1497. <https://doi.org/10.1007/s11368-015-1338-5>
224. Barnes RT, Gallagher ME, Masiello CA, et al (2014) Biochar-Induced Changes in Soil Hydraulic Conductivity and Dissolved Nutrient Fluxes Constrained by Laboratory Experiments. *PLOS ONE* 9:e108340. <https://doi.org/10.1371/journal.pone.0108340>
225. Brockhoff SR, Christians NE, Killorn RJ, et al (2010) Physical and Mineral-Nutrition Properties of Sand-Based Turfgrass Root Zones Amended with Biochar. *Agronomy Journal* 102:1627–1631. <https://doi.org/10.2134/agronj2010.0188>
226. Githinji L (2014) Effect of biochar application rate on soil physical and hydraulic properties of a sandy loam. *Archives of Agronomy and Soil Science* 60:457–470. <https://doi.org/10.1080/03650340.2013.821698>
227. Uzoma KC, Inoue M, Andry H, et al (2011) Effect of cow manure biochar on maize productivity under sandy soil condition. *Soil Use and Management* 27:205–212. <https://doi.org/10.1111/j.1475-2743.2011.00340.x>
228. Uzoma KC, Inoue M, Andry H, et al (2011) Influence of biochar application on sandy soil hydraulic properties and nutrient retention. *Journal of Food, Agriculture & Environment* 9:1137–1143
229. Rogovska N, Laird DA, Rathke SJ, Karlen DL (2014) Biochar impact on Midwestern Mollisols and maize nutrient availability. *Geoderma* 230–231:340–347. <https://doi.org/10.1016/j.geoderma.2014.04.009>
230. Mia S, Singh B, Dijkstra FA (2017) Aged biochar affects gross nitrogen mineralization and recovery: a 15N study in two contrasting soils. *GCB Bioenergy* 9:1196–1206. <https://doi.org/10.1111/gcbb.12430>

231. Harris PJF, Tsang SC (1997) High-resolution electron microscopy studies of non-graphitizing carbons. *Philosophical Magazine A* 76:667–677. <https://doi.org/10.1080/01418619708214028>
232. Zheng W, Sharma BK, Rajagopalan N (2010) Using Biochar as a Soil Amendment for Sustainable Agriculture
233. Ghani WAWAK, Mohd A, da Silva G, et al (2013) Biochar production from waste rubber-wood-sawdust and its potential use in C sequestration: Chemical and physical characterization. *Industrial Crops and Products* 44:18–24. <https://doi.org/10.1016/j.indcrop.2012.10.017>
234. Pretsch E, Bühlmann P, Badertscher M (2020) Introduction. In: Pretsch E, Bühlmann P, Badertscher M (eds) *Structure Determination of Organic Compounds: Tables of Spectral Data*. Springer, Berlin, Heidelberg, pp 1–3
235. Claoston N, Samsuri AW, Ahmad Husni MH, Mohd Amran MS (2014) Effects of pyrolysis temperature on the physicochemical properties of empty fruit bunch and rice husk biochars. *Waste Manag Res* 32:331–339. <https://doi.org/10.1177/0734242X14525822>
236. Manimaran R, Abdullah E, Kogiladas T, Mujawar M (2015) Synthesis of magnetic biochar from *Garcinia Mangostana* peel using muffle furnace for adsorption of Zn<sup>2+</sup> ions from aqueous solution. *International Journal of Chemical Engineering–IJCE* 2:18–21. <https://doi.org/10.15224/978-1-63248-068-2-03>
237. Uchimiya M, Wartelle LH, Klasson KT, et al (2011) Influence of Pyrolysis Temperature on Biochar Property and Function as a Heavy Metal Sorbent in Soil. *J Agric Food Chem* 59:2501–2510. <https://doi.org/10.1021/jf104206c>
238. Green Nanotechnology for Bioremediation of Toxic Metals from Waste Water. In: [springerprofessional.de. https://www.springerprofessional.de/en/green-nanotechnology-for-bioremediation-of-toxic-metals-from-was/3719398](https://www.springerprofessional.de/en/green-nanotechnology-for-bioremediation-of-toxic-metals-from-was/3719398). Accessed 6 Mar 2022
239. Preparation and Characterization of Micro Crystalline Cellulose Fiber Reinforced Chitosan based Polymer Composites - ProQuest. <https://www.proquest.com/openview/ac640958a14849850ca233ca6f2d6ee4/1?pq-origsite=gscholar&cbl=1096446>. Accessed 6 Mar 2022
240. Liu Y, He Z, Uchimiya M (2015) Comparison of Biochar Formation from Various Agricultural By-Products Using FTIR Spectroscopy. *Modern Applied Science* 9:p246. <https://doi.org/10.5539/mas.v9n4p246>
241. Uchimiya M, Chang S, Klasson KT (2011) Screening biochars for heavy metal retention in soil: Role of oxygen functional groups. *Journal of Hazardous Materials* 190:432–441. <https://doi.org/10.1016/j.jhazmat.2011.03.063>

242. Ahmad M, Lee SS, Lim JE, et al (2014) Speciation and phytoavailability of lead and antimony in a small arms range soil amended with mussel shell, cow bone and biochar: EXAFS spectroscopy and chemical extractions. *Chemosphere* 95:433–441. <https://doi.org/10.1016/j.chemosphere.2013.09.077>
243. Amonette JE, Joseph S (2009) Characteristics of Biochar: Microchemical Properties. In: *Biochar for Environmental Management*. Routledge
244. Weber K, Quicker P (2018) Properties of biochar. *Fuel* 217:240–261. <https://doi.org/10.1016/j.fuel.2017.12.054>
245. Shukla N, Sahoo D, Remya N (2019) Biochar from microwave pyrolysis of rice husk for tertiary wastewater treatment and soil nourishment. *Journal of Cleaner Production* 235:1073–1079. <https://doi.org/10.1016/j.jclepro.2019.07.042>
246. Yek PNY, Peng W, Wong CC, et al (2020) Engineered biochar via microwave CO<sub>2</sub> and steam pyrolysis to treat carcinogenic Congo red dye. *Journal of Hazardous Materials* 395:.. <https://doi.org/10.1016/j.jhazmat.2020.122636>
247. Behl K, Sinha S, Sharma M, et al (2019) One-time cultivation of *Chlorella pyrenoidosa* in aqueous dye solution supplemented with biochar for microalgal growth, dye decolorization and lipid production. *Chemical Engineering Journal* 364:552–561. <https://doi.org/10.1016/j.cej.2019.01.180>
248. Al-Wabel MI, Al-Omran A, El-Naggar AH, et al (2013) Pyrolysis temperature induced changes in characteristics and chemical composition of biochar produced from conocarpus wastes. *Bioresource Technology* 131:374–379. <https://doi.org/10.1016/j.biortech.2012.12.165>
249. El-Naggar A, Lee SS, Rinklebe J, et al (2019) Biochar application to low fertility soils: A review of current status, and future prospects. *Geoderma* 337:536–554. <https://doi.org/10.1016/j.geoderma.2018.09.034>
250. Hassan M, Liu Y, Naidu R, et al (2020) Influences of feedstock sources and pyrolysis temperature on the properties of biochar and functionality as adsorbents: A meta-analysis. *Science of The Total Environment* 744:140714. <https://doi.org/10.1016/j.scitotenv.2020.140714>
251. Harvey OR, Herbert BE, Kuo L-J, Louchouart P (2012) Generalized Two-Dimensional Perturbation Correlation Infrared Spectroscopy Reveals Mechanisms for the Development of Surface Charge and Recalcitrance in Plant-Derived Biochars. *Environ Sci Technol* 46:10641–10650. <https://doi.org/10.1021/es302971d>
252. Sun Y, Xiong X, He M, et al (2021) Roles of biochar-derived dissolved organic matter in soil amendment and environmental remediation: A critical review. *Chemical Engineering Journal* 424:130387. <https://doi.org/10.1016/j.cej.2021.130387>

253. Song Y, Tahmasebi A, Yu J (2014) Co-pyrolysis of pine sawdust and lignite in a thermogravimetric analyzer and a fixed-bed reactor. *Bioresour Technol* 174:204–211. <https://doi.org/10.1016/j.biortech.2014.10.027>
254. Shaaban A, Se S-M, Dimin MF, et al (2014) Influence of heating temperature and holding time on biochars derived from rubber wood sawdust via slow pyrolysis. *Journal of Analytical and Applied Pyrolysis* 107:31–39. <https://doi.org/10.1016/j.jaap.2014.01.021>
255. Crombie K, Mašek O, Sohi SP, et al (2013) The effect of pyrolysis conditions on biochar stability as determined by three methods. *GCB Bioenergy* 5:122–131. <https://doi.org/10.1111/gcbb.12030>
256. Tag AT, Duman G, Ucar S, Yanik J (2016) Effects of feedstock type and pyrolysis temperature on potential applications of biochar. *Journal of Analytical and Applied Pyrolysis* 120:200–206. <https://doi.org/10.1016/j.jaap.2016.05.006>
257. Bourke J, Manley-Harris M, Fushimi C, et al (2007) Do All Carbonized Charcoals Have the Same Chemical Structure? 2. A Model of the Chemical Structure of Carbonized Charcoal. *Ind Eng Chem Res* 46:5954–5967. <https://doi.org/10.1021/ie070415u>
258. Zimmerman AR (2010) Abiotic and Microbial Oxidation of Laboratory-Produced Black Carbon (Biochar). *Environ Sci Technol* 44:1295–1301. <https://doi.org/10.1021/es903140c>
259. Deenik JL, McClellan T, Uehara G, et al (2010) Charcoal Volatile Matter Content Influences Plant Growth and Soil Nitrogen Transformations. *Soil Science Society of America Journal* 74:1259–1270. <https://doi.org/10.2136/sssaj2009.0115>
260. Denyes MJ, Parisien MA, Rutter A, Zeeb BA (2014) Physical, Chemical and Biological Characterization of Six Biochars Produced for the Remediation of Contaminated Sites. *JoVE (Journal of Visualized Experiments)* e52183. <https://doi.org/10.3791/52183>
261. Fernandes MB, Brooks P (2003) Characterization of carbonaceous combustion residues: II. Nonpolar organic compounds. *Chemosphere* 53:447–458. [https://doi.org/10.1016/S0045-6535\(03\)00452-1](https://doi.org/10.1016/S0045-6535(03)00452-1)
262. Chen B, Zhou D, Zhu L (2008) Transitional Adsorption and Partition of Nonpolar and Polar Aromatic Contaminants by Biochars of Pine Needles with Different Pyrolytic Temperatures. *Environ Sci Technol* 42:5137–5143. <https://doi.org/10.1021/es8002684>
263. Fuertes AB, Arbestain MC, Sevilla M, et al (2010) Chemical and structural properties of carbonaceous products obtained by pyrolysis and hydrothermal carbonisation of corn stover. *Australian journal of soil research*
264. Chun Y, Sheng G, Chiou CT, Xing B (2004) Compositions and Sorptive Properties of Crop Residue-Derived Chars. *Environ Sci Technol* 38:4649–4655. <https://doi.org/10.1021/es035034w>

265. Rafiq MK, Bachmann RT, Rafiq MT, et al (2016) Influence of Pyrolysis Temperature on Physico-Chemical Properties of Corn Stover (*Zea mays* L.) Biochar and Feasibility for Carbon Capture and Energy Balance. PLOS ONE 11:e0156894. <https://doi.org/10.1371/journal.pone.0156894>
266. Cao X, Harris W (2010) Properties of dairy-manure-derived biochar pertinent to its potential use in remediation. Bioresour Technol 101:5222–5228. <https://doi.org/10.1016/j.biortech.2010.02.052>
267. Domingues RR, Trugilho PF, Silva CA, et al (2017) Properties of biochar derived from wood and high-nutrient biomasses with the aim of agronomic and environmental benefits. PLOS ONE 12:e0176884. <https://doi.org/10.1371/journal.pone.0176884>
268. Cantrell KB, Hunt PG, Uchimiya M, et al (2012) Impact of pyrolysis temperature and manure source on physicochemical characteristics of biochar. Bioresour Technol 107:419–428. <https://doi.org/10.1016/j.biortech.2011.11.084>
269. Yargicoglu EN, Sadasivam BY, Reddy KR, Spokas K (2015) Physical and chemical characterization of waste wood derived biochars. Waste Management 36:256–268. <https://doi.org/10.1016/j.wasman.2014.10.029>
270. European Commission. Joint Research Centre. Institute for Environment and Sustainability. (2010) Biochar application to soils: a critical scientific review of effects on soil properties, processes and functions. Publications Office, LU
271. Chintala R, Mollinedo J, Schumacher TE, et al (2014) Effect of biochar on chemical properties of acidic soil. Archives of Agronomy and Soil Science 60:393–404. <https://doi.org/10.1080/03650340.2013.789870>
272. Ding W, Dong X, Ime IM, et al (2014) Pyrolytic temperatures impact lead sorption mechanisms by bagasse biochars. Chemosphere 105:68–74. <https://doi.org/10.1016/j.chemosphere.2013.12.042>
273. Yuan J-H, Xu R-K, Zhang H (2011) The forms of alkalis in the biochar produced from crop residues at different temperatures. Bioresource Technology 102:3488–3497. <https://doi.org/10.1016/j.biortech.2010.11.018>
274. Yu H, Zhang Z, Li Z, Chen D (2014) Characteristics of tar formation during cellulose, hemicellulose and lignin gasification. Fuel 118:250–256. <https://doi.org/10.1016/j.fuel.2013.10.080>
275. Shinogi Y, Kanri Y (2003) Pyrolysis of plant, animal and human waste: physical and chemical characterization of the pyrolytic products. Bioresource Technology 90:241–247. [https://doi.org/10.1016/S0960-8524\(03\)00147-0](https://doi.org/10.1016/S0960-8524(03)00147-0)
276. Bonelli PR, Buonomo EL, Cukierman AL (2007) Pyrolysis of Sugarcane Bagasse and Co-pyrolysis with an Argentinean Subbituminous Coal. Energy Sources, Part A: Recovery, Utilization, and Environmental Effects 29:731–740. <https://doi.org/10.1080/00908310500281247>

277. Katyal S, Thambimuthu K, Valix M (2003) Carbonisation of bagasse in a fixed bed reactor: influence of process variables on char yield and characteristics. *Renewable Energy* 28:713–725. [https://doi.org/10.1016/S0960-1481\(02\)00112-X](https://doi.org/10.1016/S0960-1481(02)00112-X)
278. Ahmad M, Ok YS, Kim B-Y, et al (2016) Impact of soybean stover- and pine needle-derived biochars on Pb and As mobility, microbial community, and carbon stability in a contaminated agricultural soil. *J Environ Manage* 166:131–139. <https://doi.org/10.1016/j.jenvman.2015.10.006>
279. Lehmann J (2007) A handful of carbon. *Nature* 447:143–144. <https://doi.org/10.1038/447143a>
280. Chia CH, Downie A, Munroe P (2015) Characteristics of Biochar: Physical and Structural Properties. *Biochar for Environmental Management* 89–109
281. Kończak M, Pan B, Ok YS, Oleszczuk P (2020) Carbon dioxide as a carrier gas and mixed feedstock pyrolysis decreased toxicity of sewage sludge biochar. *Science of the Total Environment* 723:. <https://doi.org/10.1016/j.scitotenv.2020.137796>
282. Kończak M, Oleszczuk P (2020) Co-pyrolysis of sewage sludge and biomass in carbon dioxide as a carrier gas affects the total and leachable metals in biochars. *Journal of Hazardous Materials* 400:0–8. <https://doi.org/10.1016/j.jhazmat.2020.123144>
283. Fredlund DG (2006) Unsaturated Soil Mechanics in Engineering Practice. *Journal of Geotechnical and Geoenvironmental Engineering* 132:286–321. [https://doi.org/10.1061/\(ASCE\)1090-0241\(2006\)132:3\(286\)](https://doi.org/10.1061/(ASCE)1090-0241(2006)132:3(286))
284. Ridley AM (2015) Soil suction — what it is and how to successfully measure it. Australian Centre for Geomechanics
285. Teerachaikulpanich N, Kosaka T (2015) Chapter 10 - High Pressure for Vacuum Consolidation Method Using Air-Water Separation System. In: Indraratna B, Chu J, Rujikiatkamjorn C (eds) *Ground Improvement Case Histories*. Butterworth-Heinemann, pp 293–314
286. Fredlund DG, Rahardjo H, Fredlund MD (2012) *Unsaturated Soil Mechanics in Engineering Practice*. John Wiley & Sons
287. Hong W-T, Jung Y-S, Kang S, Lee J-S (2016) Estimation of Soil-Water Characteristic Curves in Multiple-Cycles Using Membrane and TDR System. *Materials* 9:1019. <https://doi.org/10.3390/ma9121019>
288. Fredlund DG, Xing A (2011) Equations for the soil-water characteristic curve. *Canadian Geotechnical Journal*. <https://doi.org/10.1139/t94-061>
289. Gao Y, Sun D, Zhu Z, Xu Y (2019) Hydromechanical behavior of unsaturated soil with different initial densities over a wide suction range. *Acta Geotech* 14:417–428. <https://doi.org/10.1007/s11440-018-0662-5>

290. Tuller M, Or D (2005) WATER RETENTION AND CHARACTERISTIC CURVE. In: Hillel D (ed) Encyclopedia of Soils in the Environment. Elsevier, Oxford, pp 278–289
291. Zhai Q, Rahardjo H, Satyanaga A, Dai G (2020) Estimation of tensile strength of sandy soil from soil–water characteristic curve. *Acta Geotech.* <https://doi.org/10.1007/s11440-020-01013-8>
292. Rahardjo H, Kim Y, Satyanaga A (2019) Role of unsaturated soil mechanics in geotechnical engineering. *Geo-Engineering* 10:8. <https://doi.org/10.1186/s40703-019-0104-8>
293. Fredlund DG, Houston S (2013) Interpretation of soil-water characteristic curves when volume change occurs as soil suction is changed. In: *Advances in Unsaturated Soils - Proceedings of the 1st Pan-American Conference on Unsaturated Soils, PanAmUNSAT 2013.* Taylor and Francis - Balkema, pp 15–31
294. Fredlund DG, Rahardjo H (1993) *Soil Mechanics for Unsaturated Soils.* John Wiley & Sons
295. Reinson JR, Fredlund DG, Wilson GW (2011) Unsaturated flow in coarse porous media. *Canadian Geotechnical Journal.* <https://doi.org/10.1139/t04-070>
296. Saffari N, Hajabbasi MA, Shirani H, et al (2021) Influence of corn residue biochar on water retention and penetration resistance in a calcareous sandy loam soil. *Geoderma* 383:114734. <https://doi.org/10.1016/j.geoderma.2020.114734>
297. Obia A, Cornelissen G, Mulder J, et al (2017) Effect of biochar on crust formation, penetration resistance and hydraulic properties of two coarse-textured tropical soils. *Soil & tillage research*
298. Wang D, Li C, Parikh SJ, Scow KM (2019) Impact of biochar on water retention of two agricultural soils – A multi-scale analysis. *Geoderma* 340:185–191. <https://doi.org/10.1016/j.geoderma.2019.01.012>
299. Xing X, Liu Y, Garg A, et al (2021) An improved genetic algorithm for determining modified water-retention model for biochar-amended soil. *CATENA* 200:105143. <https://doi.org/10.1016/j.catena.2021.105143>
300. Albuquerque JA, Calero JM, Barrón V, et al (2014) Effects of biochars produced from different feedstocks on soil properties and sunflower growth. *Journal of Plant Nutrition and Soil Science* 177:16–25. <https://doi.org/10.1002/jpln.201200652>
301. Bordoloi S, Gopal P, Boddu R, et al (2019) Soil-biochar-water interactions: Role of biochar from *Eichhornia crassipes* in influencing crack propagation and suction in unsaturated soils. *Journal of Cleaner Production* 210:847–859. <https://doi.org/10.1016/j.jclepro.2018.11.051>
302. Cao CTN, Farrell C, Kristiansen PE, Rayner JP (2014) Biochar makes green roof substrates lighter and improves water supply to plants. *Ecological Engineering* 71:368–374. <https://doi.org/10.1016/j.ecoleng.2014.06.017>

303. Karhu K, Mattila T, Bergström I, Regina K (2011) Biochar addition to agricultural soil increased CH<sub>4</sub> uptake and water holding capacity – Results from a short-term pilot field study. *Agriculture, Ecosystems & Environment* 140:309–313. <https://doi.org/10.1016/j.agee.2010.12.005>
304. Kinney TJ, Masiello CA, Dugan B, et al (2012) Hydrologic properties of biochars produced at different temperatures. *Biomass and Bioenergy* 41:34–43. <https://doi.org/10.1016/j.biombioe.2012.01.033>
305. Lei O, Zhang R (2013) Effects of biochars derived from different feedstocks and pyrolysis temperatures on soil physical and hydraulic properties. *J Soils Sediments* 13:1561–1572. <https://doi.org/10.1007/s11368-013-0738-7>
306. Malik Z, Yutong Z, ShengGao L, et al (2018) Effect of biochar and quicklime on growth of wheat and physicochemical properties of Ultisols. *Arab J Geosci* 11:496. <https://doi.org/10.1007/s12517-018-3863-1>
307. Sarma B, Farooq M, Gogoi N, et al (2018) Soil organic carbon dynamics in wheat - Green gram crop rotation amended with vermicompost and biochar in combination with inorganic fertilizers: A comparative study. *Journal of Cleaner Production* 201:471–480. <https://doi.org/10.1016/j.jclepro.2018.08.004>
308. Ulyett J, Sakrabani R, Kibblewhite MG, Hann M (2014) Impact of biochar addition on water retention, nitrification and carbon dioxide evolution from two sandy loam soils
309. Wong JTF, Chen Z, Chen X, et al (2017) Soil-water retention behavior of compacted biochar-amended clay: a novel landfill final cover material. *J Soils Sediments* 17:590–598. <https://doi.org/10.1007/s11368-016-1401-x>
310. Wong JTF, Chen Z, Wong AYY, et al (2018) Effects of biochar on hydraulic conductivity of compacted kaolin clay. *Environmental Pollution* 234:468–472. <https://doi.org/10.1016/j.envpol.2017.11.079>
311. Bharath KN, Madhu P, Gowda TGY, et al (2020) Alkaline Effect on Characterization of Discarded Waste of Moringa oleifera Fiber as a Potential Eco-friendly Reinforcement for Biocomposites. *J Polym Environ* 28:2823–2836. <https://doi.org/10.1007/s10924-020-01818-4>
312. Wani I, Narde SR, Huang X, et al (2021) Reviewing role of biochar in controlling soil erosion and considering future aspect of production using microwave pyrolysis process for the same. *Biomass Conv Bioref*. <https://doi.org/10.1007/s13399-021-02060-1>
313. Alghamdi AG, Alkhasha A, Ibrahim HM (2020) Effect of biochar particle size on water retention and availability in a sandy loam soil. *Journal of Saudi Chemical Society* 24:1042–1050. <https://doi.org/10.1016/j.jscs.2020.11.003>

314. de Jesus Duarte S, Glaser B, Pellegrino Cerri CE (2019) Effect of Biochar Particle Size on Physical, Hydrological and Chemical Properties of Loamy and Sandy Tropical Soils. *Agronomy* 9:165. <https://doi.org/10.3390/agronomy9040165>
315. Lim T-J, Spokas K (2018) Impact of Biochar Particle Shape and Size on Saturated Hydraulic Properties of Soil. *Korean J Environ Agric* 37:1–8. <https://doi.org/10.5338/KJEA.2018.37.1.09>
316. Xu G, Li Z, Li P (2013) Fractal features of soil particle-size distribution and total soil nitrogen distribution in a typical watershed in the source area of the middle Dan River, China. *CATENA* 101:17–23. <https://doi.org/10.1016/j.catena.2012.09.013>
317. Lu S-G, Sun F-F, Zong Y-T (2014) Effect of rice husk biochar and coal fly ash on some physical properties of expansive clayey soil (Vertisol). *CATENA* 114:37–44. <https://doi.org/10.1016/j.catena.2013.10.014>
318. Kumar H, Ganesan SP, Bordoloi S, et al (2019) Erodibility assessment of compacted biochar amended soil for geo-environmental applications. *Science of The Total Environment* 672:698–707. <https://doi.org/10.1016/j.scitotenv.2019.03.417>
319. Lu K, Yang X, Shen J, et al (2014) Effect of bamboo and rice straw biochars on the bioavailability of Cd, Cu, Pb and Zn to *Sedum plumbizincicola*. *Agriculture, Ecosystems & Environment* 191:124–132. <https://doi.org/10.1016/j.agee.2014.04.010>
320. Pan Z, Garg A, Huang S, Mei G (2021) Swelling Suppression Mechanism of Compacted Expansive Soil Amended with Animal and Plant Based Biochar. *Waste Biomass Valor* 12:2653–2664. <https://doi.org/10.1007/s12649-020-01172-5>
321. Hua L, Lu Z, Ma H, Jin S (2014) Effect of biochar on carbon dioxide release, organic carbon accumulation, and aggregation of soil. *Environmental Progress & Sustainable Energy* 33:941–946. <https://doi.org/10.1002/ep.11867>
322. Burrell LD, Zehetner F, Rampazzo N, et al (2016) Long-term effects of biochar on soil physical properties. *Geoderma* 282:96–102. <https://doi.org/10.1016/j.geoderma.2016.07.019>
323. Zhang J, Chen Q, You C (2016) Biochar Effect on Water Evaporation and Hydraulic Conductivity in Sandy Soil. *Pedosphere* 26:265–272. [https://doi.org/10.1016/S1002-0160\(15\)60041-8](https://doi.org/10.1016/S1002-0160(15)60041-8)
324. Cai W, Huang H, Chen P, et al (2020) Effects of biochar from invasive weed on soil erosion under varying compaction and slope conditions: comprehensive study using flume experiments. *Biomass Conv Bioref*. <https://doi.org/10.1007/s13399-020-00943-3>
325. Lee SS, Shah HS, Awad YM, et al (2015) Synergy effects of biochar and polyacrylamide on plants growth and soil erosion control. *Environ Earth Sci* 74:2463–2473. <https://doi.org/10.1007/s12665-015-4262-5>

326. Abrol V, Ben-Hur M, Verheijen FGA, et al (2016) Biochar effects on soil water infiltration and erosion under seal formation conditions: rainfall simulation experiment. *J Soils Sediments* 16:2709–2719. <https://doi.org/10.1007/s11368-016-1448-8>
327. Chen L, Yu Z, Xu H, et al (2019) Microwave-assisted co-pyrolysis of *Chlorella vulgaris* and wood sawdust using different additives. *Bioresource Technology* 273:34–39. <https://doi.org/10.1016/j.biortech.2018.10.086>
328. Ahmadi SH, Ghasemi H, Sepaskhah AR (2020) Rice husk biochar influences runoff features, soil loss, and hydrological behavior of a loamy soil in a series of successive simulated rainfall events. *CATENA* 192:104587. <https://doi.org/10.1016/j.catena.2020.104587>
329. Sadeghi SH, Kiani-Harchegani M, Hazbavi Z, et al (2020) Field measurement of effects of individual and combined application of biochar and polyacrylamide on erosion variables in loess and marl soils. *Science of The Total Environment* 728:138866. <https://doi.org/10.1016/j.scitotenv.2020.138866>
330. Gholami L, Karimi N, Kaviani A (2019) Soil and water conservation using biochar and various soil moisture in laboratory conditions. *CATENA* 182:104151. <https://doi.org/10.1016/j.catena.2019.104151>
331. Zhang F, Huang C, Yang M, et al (2019) Rainfall simulation experiments indicate that biochar addition enhances erosion of loess-derived soils. *Land Degradation & Development* 30:2272–2286. <https://doi.org/10.1002/ldr.3399>
332. Sadeghi SH, Hazbavi Z, Harchegani MK (2016) Controllability of runoff and soil loss from small plots treated by vinasse-produced biochar. *Science of The Total Environment* 541:483–490. <https://doi.org/10.1016/j.scitotenv.2015.09.068>
333. Jien S-H, Wang C-S (2013) Effects of biochar on soil properties and erosion potential in a highly weathered soil. *CATENA* 110:225–233. <https://doi.org/10.1016/j.catena.2013.06.021>
334. Peng X, Zhu QH, Xie ZB, et al (2016) The impact of manure, straw and biochar amendments on aggregation and erosion in a hillslope Ultisol. *CATENA* 138:30–37. <https://doi.org/10.1016/j.catena.2015.11.008>
335. Lee C-H, Wang C-C, Lin H-H, et al (2018) In-situ biochar application conserves nutrients while simultaneously mitigating runoff and erosion of an Fe-oxide-enriched tropical soil. *Sci Total Environ* 619–620:665–671. <https://doi.org/10.1016/j.scitotenv.2017.11.023>
336. Bashagaluke JB, Logah V, Opoku A, et al (2019) Soil loss and run-off characteristics under different soil amendments and cropping systems in the semi-deciduous forest zone of Ghana. *Soil Use and Management* 35:617–629. <https://doi.org/10.1111/sum.12531>

337. Abiven S, Menasseri S, Angers DA, Leterme P (2007) Dynamics of aggregate stability and biological binding agents during decomposition of organic materials. *European Journal of Soil Science* 58:239–247. <https://doi.org/10.1111/j.1365-2389.2006.00833.x>
338. Annabi M, Le Bissonnais Y, Le Villio-Poitrenaud M, Houot S (2011) Improvement of soil aggregate stability by repeated applications of organic amendments to a cultivated silty loam soil. *Agriculture, Ecosystems & Environment* 144:382–389. <https://doi.org/10.1016/j.agee.2011.07.005>
339. Sarker TC, Incerti G, Spaccini R, et al (2018) Linking organic matter chemistry with soil aggregate stability: Insight from <sup>13</sup>C NMR spectroscopy. *Soil Biology and Biochemistry* 117:175–184. <https://doi.org/10.1016/j.soilbio.2017.11.011>
340. Spaccini R, Piccolo A, Mbagwu JSC, et al (2002) Influence of the addition of organic residues on carbohydrate content and structural stability of some highland soils in Ethiopia. *Soil Use and Management* 18:404–411. <https://doi.org/10.1111/j.1475-2743.2002.tb00259.x>
341. Spaccini R, Mbagwu JSC, Igwe CA, et al (2004) Carbohydrates and aggregation in lowland soils of Nigeria as influenced by organic inputs. *Soil and Tillage Research* 75:161–172. [https://doi.org/10.1016/S0167-1987\(03\)00158-2](https://doi.org/10.1016/S0167-1987(03)00158-2)
342. Barthès B, Roose E (2002) Aggregate stability as an indicator of soil susceptibility to runoff and erosion; validation at several levels. *CATENA* 47:133–149. [https://doi.org/10.1016/S0341-8162\(01\)00180-1](https://doi.org/10.1016/S0341-8162(01)00180-1)
343. Heikkinen J, Keskinen R, Soinne H, et al (2019) Possibilities to improve soil aggregate stability using biochars derived from various biomasses through slow pyrolysis, hydrothermal carbonization, or torrefaction. *Geoderma* 344:40–49. <https://doi.org/10.1016/j.geoderma.2019.02.028>
344. Soinne H, Hovi J, Tammeorg P, Turtola E (2014) Effect of biochar on phosphorus sorption and clay soil aggregate stability. *Geoderma* 219–220:162–167. <https://doi.org/10.1016/j.geoderma.2013.12.022>
345. Wang D, Fonte SJ, Parikh SJ, et al (2017) Biochar additions can enhance soil structure and the physical stabilization of C in aggregates. *Geoderma* 303:110–117. <https://doi.org/10.1016/j.geoderma.2017.05.027>
346. Six J, Bossuyt H, Degryze S, Denef K (2004) A history of research on the link between (micro)aggregates, soil biota, and soil organic matter dynamics. *Soil and Tillage Research* 79:7–31. <https://doi.org/10.1016/j.still.2004.03.008>
347. Eiland F, Klamer M, Lind A-M, et al (2001) Influence of Initial C/N Ratio on Chemical and Microbial Composition during Long Term Composting of Straw. *Microb Ecol* 41:272–280. <https://doi.org/10.1007/s002480000071>
348. Alami Y, Achouak W, Marol C, Heulin T (2000) Rhizosphere Soil Aggregation and Plant Growth Promotion of Sunflowers by an Exopolysaccharide-Producing *Rhizobium* sp. Strain Isolated from Sunflower Roots. *Appl Environ Microbiol* 66:3393–3398

349. Bachmann J, Guggenberger G, Baumgartl T, et al (2008) Physical carbon-sequestration mechanisms under special consideration of soil wettability. *Journal of Plant Nutrition and Soil Science* 171:14–26. <https://doi.org/10.1002/jpln.200700054>
350. Bissonnais YL (1996) Aggregate stability and assessment of soil crustability and erodibility: I. Theory and methodology. *European Journal of Soil Science* 47:425–437. <https://doi.org/10.1111/j.1365-2389.1996.tb01843.x>
351. Ferro ND, Berti A, Francioso O, et al (2012) Investigating the effects of wettability and pore size distribution on aggregate stability: the role of soil organic matter and the humic fraction. *European Journal of Soil Science* 63:152–164. <https://doi.org/10.1111/j.1365-2389.2012.01427.x>
352. Zhang Q, Du Z, Lou Y, He X (2015) A one-year short-term biochar application improved carbon accumulation in large macroaggregate fractions. *CATENA* 127:26–31. <https://doi.org/10.1016/j.catena.2014.12.009>
353. Zhang X, Zhang P, Yuan X, et al (2020) Effect of pyrolysis temperature and correlation analysis on the yield and physicochemical properties of crop residue biochar. *Bioresource Technology* 296:122318. <https://doi.org/10.1016/j.biortech.2019.122318>
354. Chatterjee R, Sajjadi B, Chen W-Y, et al (2020) Effect of Pyrolysis Temperature on PhysicoChemical Properties and Acoustic-Based Amination of Biochar for Efficient CO<sub>2</sub> Adsorption. *Front Energy Res* 8:. <https://doi.org/10.3389/fenrg.2020.00085>
355. Sun J, He F, Pan Y, Zhang Z (2017) Effects of pyrolysis temperature and residence time on physicochemical properties of different biochar types. *Acta Agriculturae Scandinavica, Section B— Soil & Plant Science* 67:12–22. <https://doi.org/10.1080/09064710.2016.1214745>
356. Feng Y, Xu Y, Yu Y, et al (2012) Mechanisms of biochar decreasing methane emission from Chinese paddy soils. *Soil Biology and Biochemistry* 46:80–88. <https://doi.org/10.1016/j.soilbio.2011.11.016>
357. He P, Liu Y, Shao L, et al (2018) Particle size dependence of the physicochemical properties of biochar. *Chemosphere* 212:385–392. <https://doi.org/10.1016/j.chemosphere.2018.08.106>
358. Hale SE, Lehmann J, Rutherford D, et al (2012) Quantifying the Total and Bioavailable Polycyclic Aromatic Hydrocarbons and Dioxins in Biochars. *Environ Sci Technol* 46:2830–2838. <https://doi.org/10.1021/es203984k>
359. Hale SarahE, Hanley K, Lehmann J, et al (2011) Effects of Chemical, Biological, and Physical Aging As Well As Soil Addition on the Sorption of Pyrene to Activated Carbon and Biochar. *Environ Sci Technol* 45:10445–10453. <https://doi.org/10.1021/es202970x>
360. Ghavanloughajar M, Valenca R, Le H, et al (2020) Compaction conditions affect the capacity of biochar-amended sand filters to treat road runoff. *Science of the Total Environment* 735:

361. Zhang Y, Gu K, Li J, et al (2020) Effect of biochar on desiccation cracking characteristics of clayey soils. *Geoderma* 364:114182. <https://doi.org/10.1016/j.geoderma.2020.114182>
362. Hallett PD, Newson TA (2005) Describing soil crack formation using elastic–plastic fracture mechanics. *European Journal of Soil Science* 56:31–38. <https://doi.org/10.1111/j.1365-2389.2004.00652.x>
363. Vogel H-J, Hoffmann H, Roth K (2005) Studies of crack dynamics in clay soil: I. Experimental methods, results, and morphological quantification. *Geoderma* 125:203–211. <https://doi.org/10.1016/j.geoderma.2004.07.009>
364. Shen Z, Hou D, Xu W, et al (2018) Assessing long-term stability of cadmium and lead in a soil washing residue amended with MgO-based binders using quantitative accelerated ageing. *Science of The Total Environment* 643:1571–1578. <https://doi.org/10.1016/j.scitotenv.2018.06.321>
365. Wei X, Gao C, Liu K (2020) A Review of Cracking Behavior and Mechanism in Clayey Soils Related to Desiccation. *Advances in Civil Engineering* 2020:e8880873. <https://doi.org/10.1155/2020/8880873>
366. Bazant ZP, Wittmann FH, Wiley J, Young F Contents Preface PART I: FOUNDATIONS AND GENERAL ASPECTS 1 The Microstructure of Hardened Portland Cement Paste..
367. Wei X, Hattab M, Bompard P, Fleureau J-M (2016) Highlighting some mechanisms of crack formation and propagation in clays on drying path. *Géotechnique* 66:287–300. <https://doi.org/10.1680/jgeot.14.P.227>
368. Kodikara J, Barbour S, Fredlund D (1999) Changes in Clay Structure and Behaviour due to Wetting and Drying
369. Tang H, Dong Y, Wang T, Dong Y (2019) Simulation of strain localization with discrete element-Cosserat continuum finite element two scale method for granular materials. *Journal of the Mechanics and Physics of Solids* 122:450–471. <https://doi.org/10.1016/j.jmps.2018.09.029>
370. Péron H, Hu L, Laloui L, Hueckel T (2007) Numerical and experimental investigation of desiccation of soil
371. Rodríguez R, Sánchez M, Ledesma A, Lloret A (2007) Experimental and numerical analysis of desiccation of a mining waste. *Can Geotech J* 44:644–658. <https://doi.org/10.1139/t07-016>
372. Coussy O, Brisard S (2009) Prediction of drying shrinkage beyond the pore isodeformation assumption. *Journal of Mechanics of Materials and Structures* 4:263. <https://doi.org/10.2140/jomms.2009.4.263>
373. Griffith AA, Taylor GI (1921) VI. The phenomena of rupture and flow in solids. *Philosophical Transactions of the Royal Society of London Series A, Containing Papers of a Mathematical or Physical Character* 221:163–198. <https://doi.org/10.1098/rsta.1921.0006>

374. Rayhani MH, Yanful EK, Fagher A (2007) Desiccation-induced cracking and its effect on the hydraulic conductivity of clayey soils from Iran. *Can Geotech J* 44:276–283. <https://doi.org/10.1139/t06-125>
375. Li JH, Li L, Chen R, Li DQ (2016) Cracking and vertical preferential flow through landfill clay liners. *Engineering Geology* 206:33–41. <https://doi.org/10.1016/j.enggeo.2016.03.006>
376. Hewitt PJ, Philip LK (1999) Problems of clay desiccation in composite lining systems. *Engineering Geology* 53:107–113. [https://doi.org/10.1016/S0013-7952\(99\)00023-X](https://doi.org/10.1016/S0013-7952(99)00023-X)
377. Wang T, Stewart CE, Sun C, et al (2018) Effects of biochar addition on evaporation in the five typical Loess Plateau soils. *CATENA* 162:29–39. <https://doi.org/10.1016/j.catena.2017.11.013>
378. Villagra-Mendoza K, Horn R (2018) Effect of biochar addition on hydraulic functions of two textural soils. *Geoderma* 326:88–95. <https://doi.org/10.1016/j.geoderma.2018.03.021>
379. Günel E, Erdem H, ÇelİK I (2018) Effects of three different biochars amendment on water retention of silty loam and loamy soils. *Agricultural Water Management* 208:232–244
380. Lim TJ, Spokas KA, Feyereisen G, Novak JM (2016) Predicting the impact of biochar additions on soil hydraulic properties. *Chemosphere* 142:136–144. <https://doi.org/10.1016/j.chemosphere.2015.06.069>
381. Lu Y, Gu K, Zhang Y, et al (2021) Impact of biochar on the desiccation cracking behavior of silty clay and its mechanisms. *Science of The Total Environment* 794:148608. <https://doi.org/10.1016/j.scitotenv.2021.148608>
382. Moragues-Saitua L, Arias-González A, Gartzia-Bengoetxea N (2017) Effects of biochar and wood ash on soil hydraulic properties: A field experiment involving contrasting temperate soils. *Geoderma* 305:144–152. <https://doi.org/10.1016/j.geoderma.2017.05.041>
383. Głab T, Palmowska J, Zaleski T, Gondek K (2016) Effect of biochar application on soil hydrological properties and physical quality of sandy soil. *Geoderma* 281:11–20. <https://doi.org/10.1016/j.geoderma.2016.06.028>
384. Major J, Lehmann J, Rondon M, Goodale C (2010) Fate of soil-applied black carbon: downward migration, leaching and soil respiration. *Global Change Biology* 16:1366–1379. <https://doi.org/10.1111/j.1365-2486.2009.02044.x>
385. Zhang J, Chen Q, You C (2016) Biochar Effect on Water Evaporation and Hydraulic Conductivity in Sandy Soil. *Pedosphere* 26:265–272. [https://doi.org/10.1016/S1002-0160\(15\)60041-8](https://doi.org/10.1016/S1002-0160(15)60041-8)
386. Alaoui A, Goetz B (2008) Dye tracer and infiltration experiments to investigate macropore flow. *Geoderma* 144:279–286. <https://doi.org/10.1016/j.geoderma.2007.11.020>

387. Mollinedo J, Schumacher TE, Chintala R (2015) Influence of feedstocks and pyrolysis on biochar's capacity to modify soil water retention characteristics. *Journal of Analytical and Applied Pyrolysis* 114:100–108. <https://doi.org/10.1016/j.jaap.2015.05.006>
388. Novak JM, Busscher WJ, Laird DL, et al (2009) IMPACT OF BIOCHAR AMENDMENT ON FERTILITY OF A SOUTHEASTERN COASTAL PLAIN SOIL
389. Bruun EW (2011) Application of fast pyrolysis biochar to a loamy soil - Effects on carbon and nitrogen dynamics and potential for carbon sequestration
390. Garg A, Xing X, Bordoloi S (2020) Water retention models for soils mixed with waste residues: application of the modified van-Genuchten and Brooks-Corey models. *Biomass Conv Bioref.* <https://doi.org/10.1007/s13399-020-00957-x>
391. Abel S, Peters A, Trinks S, et al (2013) Impact of biochar and hydrochar addition on water retention and water repellency of sandy soil. *Geoderma* 202–203:183–191. <https://doi.org/10.1016/j.geoderma.2013.03.003>
392. Gray M, Johnson MG, Dragila MI, Kleber M (2014) Water uptake in biochars: The roles of porosity and hydrophobicity. *Biomass and Bioenergy* 61:196–205. <https://doi.org/10.1016/j.biombioe.2013.12.010>
393. Hardie M, Clothier B, Bound S, et al (2014) Does biochar influence soil physical properties and soil water availability? *Plant Soil* 376:347–361. <https://doi.org/10.1007/s11104-013-1980-x>
394. Jeffery S, Meinders MBJ, Stoof CR, et al (2015) Biochar application does not improve the soil hydrological function of a sandy soil. *Geoderma* 251–252:47–54. <https://doi.org/10.1016/j.geoderma.2015.03.022>
395. Zeng L, Li F, Liu J, et al (2019) Effect of initial gravimetric water content and cyclic wetting-drying on soil-water characteristic curves of disintegrated carbonaceous mudstone. *transp saf environ* 1:230–240. <https://doi.org/10.1093/tse/tdz018>
396. Chen Y (2020) Soil–Water Retention Curves Derived as a Function of Soil Dry Density. *GeoHazards* 1:3–19. <https://doi.org/10.3390/geohazards1010002>
397. Yi S, Chang NY, Imhoff PT (2020) Predicting water retention of biochar-amended soil from independent measurements of biochar and soil properties. *Advances in Water Resources* 142:103638. <https://doi.org/10.1016/j.advwatres.2020.103638>
398. Mollinedo J, Schumacher TE, Chintala R (2015) Influence of feedstocks and pyrolysis on biochar's capacity to modify soil water retention characteristics. *Journal of Analytical and Applied Pyrolysis* 114:100–108. <https://doi.org/10.1016/j.jaap.2015.05.006>

399. Bruun E (2011) Application of Fast Pyrolysis Biochar to a Loamy soil - Effects on carbon and nitrogen dynamics and potential for carbon sequestration. Technical University of Denmark. Risø National Laboratory for Sustainable Energy, Roskilde
400. Yang CD, Lu SG (2021) Effects of five different biochars on aggregation, water retention and mechanical properties of paddy soil: A field experiment of three-season crops. *Soil and Tillage Research* 205:104798. <https://doi.org/10.1016/j.still.2020.104798>
401. Razzaghi F, Obour PB, Arthur E (2020) Does biochar improve soil water retention? A systematic review and meta-analysis. *Geoderma* 361:114055. <https://doi.org/10.1016/j.geoderma.2019.114055>
402. Wong JTF, Chen Z, Chen X, et al (2017) Soil-water retention behavior of compacted biochar-amended clay: a novel landfill final cover material. *J Soils Sediments* 17:590–598. <https://doi.org/10.1007/s11368-016-1401-x>
403. Hussain R, Garg A, Ravi K (2020) Soil-biochar-plant interaction: differences from the perspective of engineered and agricultural soils. *Bull Eng Geol Environ*. <https://doi.org/10.1007/s10064-020-01846-3>
404. Kumar H, Huang S, Mei G, Garg A (2021) Influence of feedstock type and particle size on efficiency of biochar in improving tensile crack resistance and shear strength in lean clayey soil. *International Journal of Damage Mechanics* 30:646–661. <https://doi.org/10.1177/1056789521991194>
405. Ganesan SP, Bordoloi S, Ni J, et al (2020) Exploring implication of variation in biochar production on geotechnical properties of soil. *Biomass Conv Bioref*. <https://doi.org/10.1007/s13399-020-00847-2>
406. Kumar H, Cai W, Lai J, et al (2020) Influence of in-house produced biochars on cracks and retained water during drying-wetting cycles: comparison between conventional plant, animal, and nano-biochars. *J Soils Sediments* 20:1983–1996. <https://doi.org/10.1007/s11368-020-02573-8>
407. Isanaka BR, Akbar MA, Mishra BP, Kushvaha V (2020) Free vibration analysis of thin plates: Bare versus Stiffened. *Eng Res Express* 2:015014. <https://doi.org/10.1088/2631-8695/ab6264>
408. Kushvaha V, Kumar SA, Madhushri P (2019) Dynamic fracture toughness index: a new integrated methodology for mode-I fracture behaviour of polymer composite under impact loading. *Mater Res Express* 6:115342. <https://doi.org/10.1088/2053-1591/ab4e35>
409. Kushvaha V, Kumar SA, Madhushri P, Sharma A (2020) Artificial neural network technique to predict dynamic fracture of particulate composite. *Journal of Composite Materials* 54:3099–3108. <https://doi.org/10.1177/0021998320911418>
410. Kushvaha V, Sharma A (2021) Dimensional Analysis for Predicting the Fracture Behavior of Particulate Polymer Composite Under the Effect of Impact Loading. In: Mavinkere Rangappa S, Satishkumar TP, Cuadrado MMM, et al (eds) *Fracture Failure Analysis of Fiber Reinforced Polymer Matrix Composites*. Springer, Singapore, pp 149–160

411. Sharma A, Mukhopadhyay T, Rangappa SM, et al (2021) Advances in Computational Intelligence of Polymer Composite Materials: Machine Learning Assisted Modeling, Analysis and Design
412. Sharma A, Madhushri P, Kushvaha V, Kumar A (2020) Prediction of the Fracture Toughness of Silicafilled Epoxy Composites using K-Nearest Neighbor (KNN) Method. In: 2020 International Conference on Computational Performance Evaluation (ComPE). pp 194–198
413. Sharma A, Kushvaha V (2020) Predictive modelling of fracture behaviour in silica-filled polymer composite subjected to impact with varying loading rates using artificial neural network. *Engineering Fracture Mechanics* 239:107328. <https://doi.org/10.1016/j.engfracmech.2020.107328>
414. Albaradeya I, Hani A, Shahrour I (2011) WEPP and ANN models for simulating soil loss and runoff in a semi-arid Mediterranean region. *Environ Monit Assess* 180:537–556. <https://doi.org/10.1007/s10661-010-1804-x>
415. Cai W, Kumar H, Huang S, et al (2020) ANN Model Development for Air Permeability in Biochar Amended Unsaturated Soil. *Geotech Geol Eng* 38:1295–1309. <https://doi.org/10.1007/s10706-019-01091-w>
416. Filippis LACD, Serio LM, Mummolo FF and G (2017) ANN Modelling to Optimize Manufacturing Process. *Advanced Applications for Artificial Neural Networks*. <https://doi.org/10.5772/intechopen.71237>
417. Vasu NN, Lee SR, Lee D, Park JY (2016) ANN based estimation of SWCC fitting parameters for Korean weathered soil considering in-situ characteristics. *The 2016 World Congress on Advances in Civil, Environmental, and Materials Research (ACEM16)*
418. Zainal AK, Fadhil S (2018) Prediction of soil water characteristic curve using artificial neural network: a new approach. *MATEC Web of Conferences* 162:01014. <https://doi.org/10.1051/mateconf/201816201014>
419. Johari A, Hooshmand A (2015) Prediction of soil-water characteristic curve using gene expression programming. *Iranian Journal of Science and Technology Transaction B: Engineering* 39:
420. Johari A, Javadi AA (2010) Prediction of soil-water characteristic curve using neural network. In: *Unsaturated Soils, Two Volume Set*. CRC Press
421. Wong JTF, Chen Z, Ng CWW, Wong MH (2016) Gas permeability of biochar-amended clay: potential alternative landfill final cover material. *Environ Sci Pollut Res* 23:7126–7131. <https://doi.org/10.1007/s11356-015-4871-2>
422. Garg A, Huang H, Cai W, et al (2021) Influence of soil density on gas permeability and water retention in soils amended with in-house produced biochar. *Journal of Rock Mechanics and Geotechnical Engineering* 13:593–602. <https://doi.org/10.1016/j.jrmge.2020.10.007>

423. Ni JJ, Bordoloi S, Shao W, et al (2020) Two-year evaluation of hydraulic properties of biochar-amended vegetated soil for application in landfill cover system. *Science of The Total Environment* 712:136486. <https://doi.org/10.1016/j.scitotenv.2019.136486>
424. Devices D (2016) MPS-2 & MPS-6 dielectric water potential sensors operator's manual. Decagon Devices, Pullman, WA
425. Ni N, Song Y, Shi R, et al (2017) Biochar reduces the bioaccumulation of PAHs from soil to carrot (*Daucus carota* L.) in the rhizosphere: A mechanism study. *Science of The Total Environment* 601–602:1015–1023. <https://doi.org/10.1016/j.scitotenv.2017.05.256>
426. Sharma A, Anand Kumar S, Kushvaha V (2020) Effect of aspect ratio on dynamic fracture toughness of particulate polymer composite using artificial neural network. *Engineering Fracture Mechanics* 228:106907. <https://doi.org/10.1016/j.engfracmech.2020.106907>
427. Rahardjo H, Leong EC (2012) Suction Measurements. 81–104. [https://doi.org/10.1061/40802\(189\)3](https://doi.org/10.1061/40802(189)3)
428. Malaya C, Sreedeeep S (2011) A Laboratory Procedure for Measuring High Soil Suction. *GTJ* 34:396–405. <https://doi.org/10.1520/GTJ103613>
429. Zhai Q, Rahardjo H (2012) Determination of soil–water characteristic curve variables. *Computers and Geotechnics* 42:37–43. <https://doi.org/10.1016/j.compgeo.2011.11.010>
430. Schoonover JE, Crim JF (2015) An Introduction to Soil Concepts and the Role of Soils in Watershed Management. *Journal of Contemporary Water Research & Education* 154:21–47. <https://doi.org/10.1111/j.1936-704X.2015.03186.x>
431. Edeh IG, Mašek O, Buss W (2020) A meta-analysis on biochar's effects on soil water properties – New insights and future research challenges. *Science of The Total Environment* 714:136857. <https://doi.org/10.1016/j.scitotenv.2020.136857>
432. Behazin E, Ogunsona E, Rodriguez-Urbe A, et al (2016) Mechanical, Chemical, and Physical Properties of Wood and Perennial Grass Biochars for Possible Composite Application. *BioResources* 11:1334–1348
433. Sokołowska Z, Szewczuk-Karpisz K, Turski M, et al (2020) Effect of Wood Waste and Sunflower Husk Biochar on Tensile Strength and Porosity of Dystric Cambisol Artificial Aggregates. *Agronomy* 10:244. <https://doi.org/10.3390/agronomy10020244>
434. Arthur E, Tuller M, Moldrup P, de Jonge LW (2015) Effects of biochar and manure amendments on water vapor sorption in a sandy loam soil. *Geoderma* 243–244:175–182. <https://doi.org/10.1016/j.geoderma.2015.01.001>

435. Zhai Q, Rahardjo H, Satyanaga A, et al (2020) Framework to estimate the soil-water characteristic curve for soils with different void ratios. *Bull Eng Geol Environ* 79:4399–4409. <https://doi.org/10.1007/s10064-020-01825-8>
436. Zhai Q, Rahardjo H, Satyanaga A, Dai G (2020) Estimation of the soil-water characteristic curve from the grain size distribution of coarse-grained soils. *Engineering Geology* 267:105502. <https://doi.org/10.1016/j.enggeo.2020.105502>
437. Zhang W, Wu C, Zhong H, et al (2021) Prediction of undrained shear strength using extreme gradient boosting and random forest based on Bayesian optimization. *Geoscience Frontiers* 12:469–477. <https://doi.org/10.1016/j.gsf.2020.03.007>
438. Wang L, Wu C, Tang L, et al (2020) Efficient reliability analysis of earth dam slope stability using extreme gradient boosting method. *Acta Geotech* 15:3135–3150. <https://doi.org/10.1007/s11440-020-00962-4>
439. Wang L, Wu C, Gu X, et al (2020) Probabilistic stability analysis of earth dam slope under transient seepage using multivariate adaptive regression splines. *Bull Eng Geol Environ* 79:2763–2775. <https://doi.org/10.1007/s10064-020-01730-0>
440. Dai Z, Zhang X, Tang C, et al (2017) Potential role of biochars in decreasing soil acidification - A critical review. *Science of The Total Environment* 581–582:601–611. <https://doi.org/10.1016/j.scitotenv.2016.12.169>
441. Abel S, Peters A, Trinks S, et al (2013) Impact of biochar and hydrochar addition on water retention and water repellency of sandy soil. *Geoderma* 202–203:183–191. <https://doi.org/10.1016/j.geoderma.2013.03.003>
442. Li Y, Zhang F, Yang M, et al (2019) Impacts of biochar application rates and particle sizes on runoff and soil loss in small cultivated loess plots under simulated rainfall. *Science of The Total Environment* 649:1403–1413. <https://doi.org/10.1016/j.scitotenv.2018.08.415>
443. Uzoma KC, Inoue M, Andry H, et al (2011) Influence of biochar application on sandy soil hydraulic properties and nutrient retention. *Journal of Food, Agriculture & Environment* 9:1137–1143
444. Deal C, Brewer CE, Brown RC, et al (2012) Comparison of kiln-derived and gasifier-derived biochars as soil amendments in the humid tropics. *Biomass and Bioenergy* 37:161–168. <https://doi.org/10.1016/j.biombioe.2011.12.017>
445. Han F, Ren L, Zhang X-C (2016) Effect of biochar on the soil nutrients about different grasslands in the Loess Plateau. *CATENA* 137:554–562. <https://doi.org/10.1016/j.catena.2015.11.002>
446. Ameloot N, Graber ER, Verheijen FGA, Neve SD (2013) Interactions between biochar stability and soil organisms: review and research needs. *European Journal of Soil Science* 64:379–390. <https://doi.org/10.1111/ejss.12064>

447. Gu B, Schmitt J, Chen Z, et al (1995) Adsorption and desorption of different organic matter fractions on iron oxide. *Geochimica et Cosmochimica Acta* 59:219–229. [https://doi.org/10.1016/0016-7037\(94\)00282-Q](https://doi.org/10.1016/0016-7037(94)00282-Q)
448. Brodowski S, Amelung W, Haumaier L, et al (2005) Morphological and chemical properties of black carbon in physical soil fractions as revealed by scanning electron microscopy and energy-dispersive X-ray spectroscopy. *Geoderma* 128:116–129. <https://doi.org/10.1016/j.geoderma.2004.12.019>
449. Sadeghi SH, Hazbavi Z, Kiani-Harchegani M, et al (2021) The hydrologic behavior of Loess and Marl soils in response to biochar and polyacrylamide mulching under laboratorial rainfall simulation conditions. *Journal of Hydrology* 592:125620. <https://doi.org/10.1016/j.jhydrol.2020.125620>
450. Tang S, She D, Wang H (2021) Combining polyacrylamide amendment to mitigate negative effect of biochar on the soil conservation of saline-sodic soil. *Arab J Geosci* 14:1627. <https://doi.org/10.1007/s12517-021-07993-5>
451. Rumpel C, Chaplot V, Planchon O, et al (2006) Preferential erosion of black carbon on steep slopes with slash and burn agriculture. *CATENA* 65:30–40. <https://doi.org/10.1016/j.catena.2005.09.005>
452. De Meyer A, Poesen J, Isabirye M, et al (2011) Soil erosion rates in tropical villages: A case study from Lake Victoria Basin, Uganda. *CATENA* 84:89–98. <https://doi.org/10.1016/j.catena.2010.10.001>
453. Hoyos N (2005) Spatial modeling of soil erosion potential in a tropical watershed of the Colombian Andes. *CATENA* 63:85–108. <https://doi.org/10.1016/j.catena.2005.05.012>
454. Tejada M, Gonzalez JL (2007) Influence of organic amendments on soil structure and soil loss under simulated rain. *Soil and Tillage Research* 93:197–205. <https://doi.org/10.1016/j.still.2006.04.002>
455. Wani I, Ramola S, Garg A, Kushvaha V (2021) Critical review of biochar applications in geoengineering infrastructure: moving beyond agricultural and environmental perspectives. *Biomass Conv Bioref*. <https://doi.org/10.1007/s13399-021-01346-8>
456. Holz DJ, Williard KWJ, Edwards PJ, Schoonover JE (2015) Soil Erosion in Humid Regions: A Review. *Journal of Contemporary Water Research & Education* 154:48–59. <https://doi.org/10.1111/j.1936-704X.2015.03187.x>
457. Li Z, Gu C, Zhang R, et al (2017) The benefic effect induced by biochar on soil erosion and nutrient loss of slopping land under natural rainfall conditions in central China. *Agricultural Water Management* 185:145–150. <https://doi.org/10.1016/j.agwat.2017.02.018>
458. Materechera SA (2009) Aggregation in a surface layer of a hardsetting and crusting soil as influenced by the application of amendments and grass mulch in a South African semi-arid environment. *Soil and Tillage Research* 105:251–259. <https://doi.org/10.1016/j.still.2009.07.008>

459. Wuddivira MN, Stone RJ, Ekwue EI (2009) Structural Stability of Humid Tropical Soils as Influenced by Manure Incorporation and Incubation Duration. *Soil Science Society of America Journal* 73:1353–1360. <https://doi.org/10.2136/sssaj2008.0080>
460. Smith DD, Wischmeier WH (1962) Rainfall Erosion. In: Norman AG (ed) *Advances in Agronomy*. Academic Press, pp 109–148
461. Fox DM, Bryan RB (2000) The relationship of soil loss by interrill erosion to slope gradient. *CATENA* 38:211–222. [https://doi.org/10.1016/S0341-8162\(99\)00072-7](https://doi.org/10.1016/S0341-8162(99)00072-7)
462. Neal JH (1938) The Effect of the Degree of Slope and Rainfall Characteristics on Runoff and Soil Erosion. *Soil Science Society of America Journal* 2:525–532. <https://doi.org/10.2136/sssaj1938.036159950002000C0083x>
463. Fullen MA (1985) Compaction, hydrological processes and soil erosion on loamy sands in east Shropshire, England. *Soil and Tillage Research* 6:17–29. [https://doi.org/10.1016/0167-1987\(85\)90003-0](https://doi.org/10.1016/0167-1987(85)90003-0)
464. Batey T (2009) Soil compaction and soil management – a review. *Soil Use and Management* 25:335–345. <https://doi.org/10.1111/j.1475-2743.2009.00236.x>
465. Li Y, Zhang F, Yang M, Zhang J (2019) Effects of adding biochar of different particle sizes on hydro-erosional processes in small scale laboratory rainfall experiments on cultivated loessial soil. *CATENA* 173:226–233. <https://doi.org/10.1016/j.catena.2018.10.021>
466. Ledermann T, Herweg K, Liniger HP, et al (2010) Applying erosion damage mapping to assess and quantify off-site effects of soil erosion in Switzerland. *Land Degradation & Development* 21:353–366. <https://doi.org/10.1002/ldr.1008>
467. Yang X, Zhang X, Lv D, et al (2020) Remote sensing estimation of the soil erosion cover-management factor for China's Loess Plateau. *Land Degradation & Development* 31:1942–1955. <https://doi.org/10.1002/ldr.3577>
468. Swift LW (1984) Gravel and Grass Surfacing Reduces Soil Loss From Mountain Roads. *for sci* 30:657–670. <https://doi.org/10.1093/forestscience/30.3.657>
469. Quinton JN, Edwards GM, Morgan RPC (1997) The influence of vegetation species and plant properties on runoff and soil erosion: results from a rainfall simulation study in south east Spain. *Soil Use and Management* 13:143–148. <https://doi.org/10.1111/j.1475-2743.1997.tb00575.x>
470. Loch RJ (2000) Effects of vegetation cover on runoff and erosion under simulated rain and overland flow on a rehabilitated site on the Meandu Mine, Tarong, Queensland. *Soil Res* 38:299–312. <https://doi.org/10.1071/sr99030>

471. Bissonnais YL, Lecomte V, Cerdan O (2004) Grass strip effects on runoff and soil loss. *Agronomie* 24:129–136. <https://doi.org/10.1051/agro:2004010>
472. Raya AM, Zuazo VHD, Martínez JRF (2006) Soil erosion and runoff response to plant-cover strips on semiarid slopes (SE Spain). *Land Degradation & Development* 17:1–11. <https://doi.org/10.1002/ldr.674>
473. Winteraeken HJ, Spaan WP (2010) A new approach to soil erosion and runoff in south Limburg—The Netherlands. *Land Degradation & Development* 21:346–352. <https://doi.org/10.1002/ldr.1009>
474. Zhuang Y, Zhang L, Du Y, et al (2016) Identification of critical source areas for nonpoint source pollution in the Danjiangkou Reservoir Basin, China. *Lake and Reservoir Management* 32:341–352. <https://doi.org/10.1080/10402381.2016.1204396>
475. Kuoppamäki K, Hagner M, Lehvävirta S, Setälä H (2016) Biochar amendment in the green roof substrate affects runoff quality and quantity. *Ecological Engineering* 88:1–9. <https://doi.org/10.1016/j.ecoleng.2015.12.010>
476. Tripathi M, Sahu J, Ganesan P (2016) Effect of process parameters on production of biochar from biomass waste through pyrolysis: A review. *Renewable and Sustainable Energy Reviews* 55:467–481. <https://doi.org/10.1016/j.rser.2015.10.122>
477. Xia L, Wang Y, Meng J, et al (2016) The Influencing Factors of Biochar's Characteristics and the Development of Carbonization Equipments: A Review. In: Bian F, Xie Y (eds) *Geo-Informatics in Resource Management and Sustainable Ecosystem*. Springer, Berlin, Heidelberg, pp 760–769
478. Arif N, Danoedoro P, Hartono (2017) Analysis of Artificial Neural Network in Erosion Modeling: A Case Study of Serang Watershed. 98:012027. <https://doi.org/10.1088/1755-1315/98/1/012027>
479. Suliman W, Harsh JB, Abu-Lail NI, et al (2016) Influence of feedstock source and pyrolysis temperature on biochar bulk and surface properties. *Biomass and Bioenergy* 84:37–48. <https://doi.org/10.1016/j.biombioe.2015.11.010>
480. Li Y, Ruan G, Jalilov AS, et al (2016) Biochar as a renewable source for high-performance CO<sub>2</sub> sorbent. *Carbon* 107:344–351. <https://doi.org/10.1016/j.carbon.2016.06.010>
481. Garg A, Wani I, Kushvaha V (2022) Application of Artificial Intelligence for Predicting Erosion of Biochar Amended Soils. *Sustainability* 14:684. <https://doi.org/10.3390/su14020684>
482. Poulsen TG, Cai W, Garg A (2020) Water evaporation from cracked soil under moist conditions as related to crack properties and near-surface wind speed. *European Journal of Soil Science* 71:627–640. <https://doi.org/10.1111/ejss.12926>
483. Cuomo S, Della Sala M, Pierri M (2016) Experimental evidences and numerical modelling of runoff and soil erosion in flume tests. *CATENA* 147:61–70. <https://doi.org/10.1016/j.catena.2016.06.044>

484. Zhao Q, Li D, Zhuo M, et al (2015) Effects of rainfall intensity and slope gradient on erosion characteristics of the red soil slope. *Stochastic environmental research and risk assessment*
485. Aksoy H, Gedikli A, Yilmaz M, et al (2020) Soil erosion model tested on experimental data of a laboratory flume with a pre-existing rill. *Journal of Hydrology* 581:124391. <https://doi.org/10.1016/j.jhydrol.2019.124391>
486. Ran Q, Su D, Li P, He Z (2012) Experimental study of the impact of rainfall characteristics on runoff generation and soil erosion. *Journal of Hydrology* 424–425:99–111. <https://doi.org/10.1016/j.jhydrol.2011.12.035>
487. Maier HR, Dandy GC (2000) Neural networks for the prediction and forecasting of water resources variables: a review of modelling issues and applications. *Environmental Modelling & Software* 15:101–124. [https://doi.org/10.1016/S1364-8152\(99\)00007-9](https://doi.org/10.1016/S1364-8152(99)00007-9)
488. Chukwuka KS, Alimba CG, Ataguba GA, Jimoh WA (2018) Chapter 9 - The Impacts of Petroleum Production on Terrestrial Fauna and Flora in the Oil-Producing Region of Nigeria. In: Ndimele PE (ed) *The Political Ecology of Oil and Gas Activities in the Nigerian Aquatic Ecosystem*. Academic Press, pp 125–142
489. Fu XT, Zhang LP, Wang Y (2019) Effect of Slope Length and Rainfall Intensity on Runoff and Erosion Conversion from Laboratory to Field. *Water Resour* 46:530–541. <https://doi.org/10.1134/S0097807819040080>
490. Heras MM las, Nicolau JM, Merino-Martín L, Wilcox BP (2010) Plot-scale effects on runoff and erosion along a slope degradation gradient. *Water Resources Research* 46:. <https://doi.org/10.1029/2009WR007875>
491. Stibinger jakub LAND USE, SOIL CONSERVATION AND RAIN HARVESTING STRUCTURES ON A SLOPE LAND ORCHARD AT SUFEN (TAIWAN) DURING OF ACTION OF TYPHOON HERB – ELEMENTARY NUMERICAL EXPERIMENT. *AGRICULTURA TROPICA ET SUBTROPICA* 44:22–29
492. Parker DB, Michel TG, Smith JL (1995) Compaction and Water Velocity Effects on Soil Erosion in Shallow Flow. *Journal of Irrigation and Drainage Engineering* 121:170–178. [https://doi.org/10.1061/\(ASCE\)0733-9437\(1995\)121:2\(170\)](https://doi.org/10.1061/(ASCE)0733-9437(1995)121:2(170))
493. Zhao X, Huang J, Gao X, et al (2014) Runoff features of pasture and crop slopes at different rainfall intensities, antecedent moisture contents and gradients on the Chinese Loess Plateau: A solution of rainfall simulation experiments. *CATENA* 119:90–96. <https://doi.org/10.1016/j.catena.2014.03.007>
494. Huang X, Niu R, Huang X, et al (2021) Influence of Sustainable Biochars Produced from Kitchen Waste, Pig Manure, and Wood on Soil Erosion. *Water* 13:2296. <https://doi.org/10.3390/w13162296>

495. Chan KY, Zwieten LV, Meszaros I, et al (2008) Using poultry litter biochars as soil amendments. *Soil Res* 46:437–444. <https://doi.org/10.1071/SR08036>
496. Lal R (1988) Effect of slope length, slope, gradient, Tillage methods and cropping systems and run-off and soil erosion on a Tropical Alfisol: Preliminary results. 174:
497. Ajayi AE, Horn R (2016) Modification of chemical and hydrophysical properties of two texturally differentiated soils due to varying magnitudes of added biochar. *Soil and Tillage Research* 164:34–44. <https://doi.org/10.1016/j.still.2016.01.011>
498. Horn PL (1994) Review of Les chagrins et la beauté du monde. *World Literature Today* 68:335–335. <https://doi.org/10.2307/40150162>
499. Zhao B, Santamarina JC (2019) Desiccation crack formation beneath the surface. *Géotechnique* 70:181–186. <https://doi.org/10.1680/jgeot.18.T.019>
500. Yang Lu SL, Yang Lu SL (2018) Cracking in an expansive soil under freeze–thaw cycles. *Sciences in Cold and Arid Regions* 9:392–397. <https://doi.org/10.3724/SP.J.1226.2017.00392>
501. Prakash A, Bordoloi S, Hazra B, et al (2020) Modeling Dependence Among Suction, Moisture, and Cracking of a Novel Biochar Synthesized from Weed Species. *ACEM* 9:90–104. <https://doi.org/10.1520/ACEM20180092>
502. Bordoloi S, Ni J, Ng CWW (2020) Soil desiccation cracking and its characterization in vegetated soil: A perspective review. *Science of The Total Environment* 729:138760. <https://doi.org/10.1016/j.scitotenv.2020.138760>
503. Chakraborty A, Goswami D (2017) Prediction of slope stability using multiple linear regression (MLR) and artificial neural network (ANN). *Arab J Geosci* 10:385. <https://doi.org/10.1007/s12517-017-3167-x>
504. Egbe JO, Ewa D, Ubi S, et al (2018) Application of multilinear regression analysis in modeling of soil properties for geotechnical civil engineering works in Calabar South
505. Wan Q, Yuan J-H, Xu R-K, Li X-H (2014) Pyrolysis temperature influences ameliorating effects of biochars on acidic soil. *Environ Sci Pollut Res* 21:2486–2495. <https://doi.org/10.1007/s11356-013-2183-y>
506. An N, Tang C-S, Xu S-K, et al (2018) Effects of soil characteristics on moisture evaporation. *Engineering Geology* 239:126–135. <https://doi.org/10.1016/j.enggeo.2018.03.028>
507. Schneider CA, Rasband WS, Eliceiri KW (2012) NIH Image to ImageJ: 25 years of Image Analysis. *Nat Methods* 9:671–675

508. Wheeler D, Tiefelsdorf M (2005) Multicollinearity and correlation among local regression coefficients in geographically weighted regression. *J Geograph Syst* 7:161–187. <https://doi.org/10.1007/s10109-005-0155-6>
-

## List of Publications

---

### Journal Papers

1. **Wani I**, Sharma A, Kushvaha V, et al. (2020) Effect of pH, Volatile Content, and Pyrolysis Conditions on Surface Area and O/C and H/C Ratios of Biochar: Towards Understanding Performance of Biochar Using Simplified Approach. *Journal of Hazardous, Toxic, and Radioactive Waste* 24:04020048. [https://doi.org/10.1061/\(ASCE\)HZ.2153-5515.0000545](https://doi.org/10.1061/(ASCE)HZ.2153-5515.0000545)
2. **Wani I**, Kumar H, Rangappa SM, et al. (2021) Multiple Regression Model for Predicting Cracks in Soil Amended with Pig Manure Biochar and Wood Biochar. *Journal of Hazardous, Toxic, and Radioactive Waste* 25:04020061. [https://doi.org/10.1061/\(ASCE\)HZ.2153-5515.0000561](https://doi.org/10.1061/(ASCE)HZ.2153-5515.0000561)
3. Garg, A., **Wani, I.**, Zhu, H. *et al.* Exploring efficiency of biochar in enhancing water retention in soils with varying grain size distributions using ANN technique. *Acta Geotech.* **17**, 1315–1326 (2022). <https://doi.org/10.1007/s11440-021-01411-6>
4. Garg A, **Wani I**, Kushvaha V (2022) Application of Artificial Intelligence for Predicting Erosion of Biochar Amended Soils. *Sustainability* 14:684. <https://doi.org/10.3390/su14020684>

### Review papers and collaborative works

1. Garg, A., Huang, H., Kushvaha, V. *et al.* Mechanism of biochar soil pore–gas–water interaction: gas properties of biochar-amended sandy soil at different degrees of compaction using KNN modeling. *Acta Geophys.* **68**, 207–217 (2020). <https://doi.org/10.1007/s11600-019-00387-y>
2. **Wani, I.**, Ramola, S., Garg, A. *et al.* Critical review of biochar applications in geoengineering infrastructure: moving beyond agricultural and environmental perspectives. *Biomass Conv. Bioref.* (2021). <https://doi.org/10.1007/s13399-021-01346-8>
3. **Wani, I.**, Narde, S.R., Huang, X. *et al.* Reviewing role of biochar in controlling soil erosion and considering future aspect of production using microwave pyrolysis process for the same. *Biomass Conv. Bioref.* (2021). <https://doi.org/10.1007/s13399-021-02060-1>
4. **Wani, I.**, Kushvaha, V., Garg, A. *et al.* Review on effect of biochar on soil strength: Towards exploring usage of biochar in geo-engineering infrastructure. *Biomass Conv. Bioref.* (2022). <https://doi.org/10.1007/s13399-022-02795-5>